NEW OXIDOREDUCTASES FOR THE SYNTHESIS OF CHIRAL BUILDING BLOCKS

Nina Richter

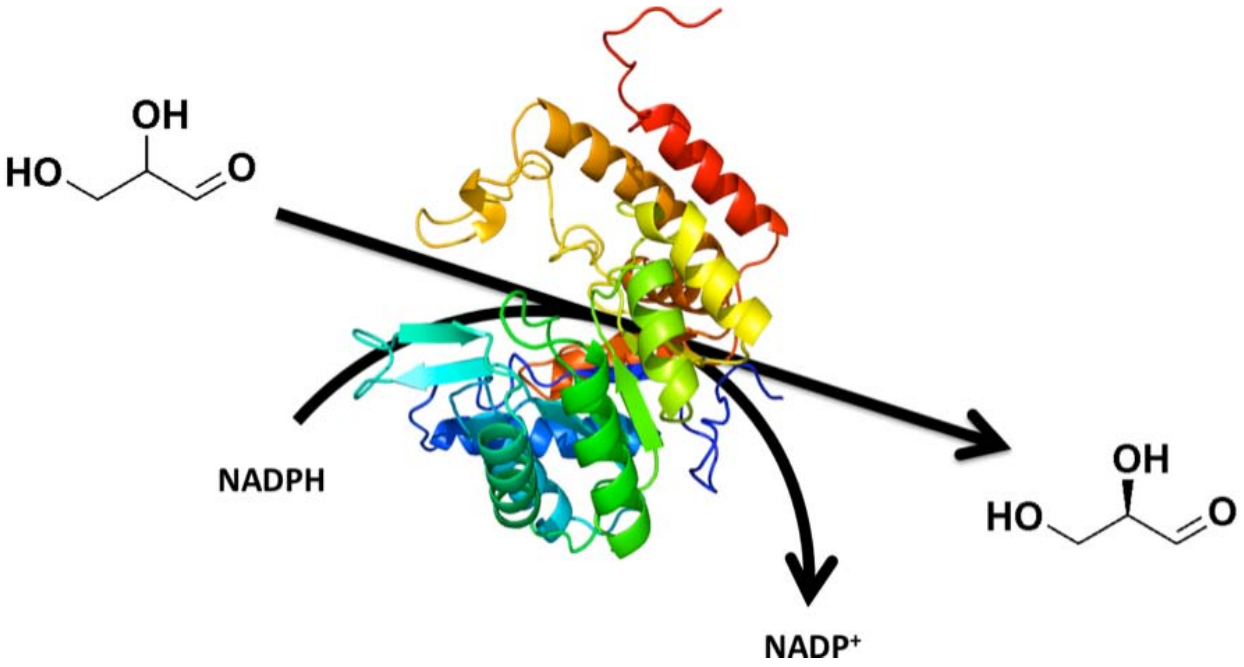

Thesis for doctoral degree (Dr. rer. nat.)

New oxidoreductases for the synthesis of chiral building blocks

Inaugural-Dissertation

zur Erlangung des Doktorgrades der
Mathematisch-Naturwissenschaftlichen Fakultät
der Heinrich-Heine-Universität Düsseldorf

vorgelegt von
Nina Richter
aus Essen

Mai 2010

Aus dem Institut für Molekulare Enzymtechnologie
der Heinrich-Heine-Universität Düsseldorf

Gedruckt mit der Genehmigung der
Mathematisch-Naturwissenschaftlichen Fakultät
der Heinrich-Heine-Universität Düsseldorf

Referent: Prof. Dr. W. Hummel
Koreferent: Prof. Dr. V. Urlacher

Tag der mündlichen Prüfung: 28. Juni 2010

ABSTRACT

Biocatalytic strategies for the synthesis of versatile chiral building blocks have gained increasing interest over the past few decades. Because of the high demand for new enzymes that are capable of catalysing reactions of biotechnological interest, the aim of this thesis was to identify new catalysts that facilitate biocatalytic access to valuable chiral synthons. Using a genome mining approach based on the sequence of the glycerol dehydrogenase GLD1 from *Hypocrea jecorina*, three interesting oxidoreductases were identified. These enzymes were characterised with respect to their ability to catalyse reactions of biotechnological interest.

Glycerol dehydrogenase from *Gluconobacter oxydans* (GlyDH): GlyDH catalyses the enantioselective reduction of aldehydes, as well as the asymmetric oxidation of different alcohols and sugar alcohols. According to the high enantioselectivity of GlyDH in the reduction of D-glyceraldehyde, this enzyme can be applied in the kinetic resolution of *rac*-glyceraldehyde to produce enantiopure L-glyceraldehyde on a preparative scale. For this purpose, two different systems have been constructed and studied comparatively: a cell free-system based on isolated enzymes (GlyDH and glucose dehydrogenase for cofactor regeneration) and a constructed recombinant whole-cell catalyst system. In addition, the application of GlyDH in the regio- and stereoselective oxidation was possible, facilitating the enantioselective production of different sugars from sugar alcohols.
Moreover, the structure of GlyDH was elucidated by X-ray-crystallography at 2.0 Å resolution. The crystal structure of GlyDH was used to understand the catalytic mechanism, the enantioselectivity and the substrate preference of GlyDH on a molecular level.

Carbonyl reductase from *Neurospora crassa* (NcCR): NcCR catalyses the reduction of different carbonyl compounds, in particular, α- and β-ketoesters, to produce the corresponding hydroxyesters. A feasible process using NcCR under standard conditions was not possible, but by applying methods of reaction engineering, a feasible process for the production of α- and β-hydroxyesters was established.

Enoate reductase from *G. oxydans* (EnR): EnR catalyses the chemo-, regio- and stereoselective reduction of C=C double bonds of various activated alkenes. By

applying EnR, different compounds with biotechnological interest, such as (*S*)-citronellal and (*R*)-levodione, were produced.

In summary, three enzymes that catalyse interesting reactions were identified, cloned, heterologously expressed and successfully applied in the biocatalytic synthesis of valuable chiral building blocks.

ZUSAMMENFASSUNG

Die biokatalytische Synthese wichtiger chiraler Schlüsselbausteinen hat in den letzten Jahren deutlich an Bedeutung gewonnen. Infolgedessen ist der Bedarf an neuen Enzymen, die die Synthese solcher Bausteine katalysieren hoch. Ziel dieser Doktorarbeit war es deshalb, neue Biokatalysatoren zu identifizieren und deren Potential in der Synthese chiraler Synthons aufzuzeigen.
Zu diesem Zweck wurde ein *in silico* Screening, ausgehend von der Sequenz der Glycerol-Dehydrogenase aus dem Pilz *Hypocrea jecorina,* durchgeführt. Mit Hilfe dieser Strategie gelang es, drei interessante Oxidoreduktasen zu identifizieren und hinsichtlich ihrer Anwendung in biotechnologisch relevanten Reaktionen zu untersuchen.

Glycerol Dehydrogenase aus *Gluconobacter oxydans* (GlyDH): Die GlyDH katalysiert die enantioselektive Reduktion einer Reihe von Aldehyden, sowie die asymmetrische Oxidation verschiedener Alkohole besonders Zuckeralkohole. Aufgrund der hohen Aktivität und Enantioselektivität in der Reduktion von D-Glyceraldehyd konnte die GlyDH erfolgreich in der kinetischen Racematspatlung von racemischen Glyceraldehyd eingesetzt werden. Darüber hinaus wurden für die Produktion von L-Glyceraldehyd zwei alternative Systeme vergleichend untersucht: Ein zellfreies Verfahren basierend auf isolierten Enzymen (GlyDH und Glucose-Dehydrogenase für die Coenzym-Regenerierung) und ein rekombinantes Ganzzellsystem. Im weiteren Verlauf der Arbeit konnte ebenfalls aufgezeigt werden, dass neben der Reduktion auch die Oxidation verschiedener Zuckeralkohole zu enantiomerenreinen Aldosen katalysiert wird.
Darüber hinaus, gelang es die Struktur der GlyDH röntgenkristallographisch mit einer Auflösung von 2.0 Å aufzuklären. Die resultierende Kristallstruktur ermöglicht Einblicke in molekulare Mechanismen, die für den katalytischen Mechanismus, die Enantioselektivität sowie die Substratspezifität der GlyDH verantwortlich sind.

Carbonyl Reduktase aus *Neurospora crassa* (NcCR): Die NcCR katalysiert die Reduktion verschiedener Carbonylverbindungen; besonders α- und β-Ketoester werden mit hohen Aktivitäten umgesetzt. Da jedoch ein geeigneter Prozess unter "Standardbedingungen" nicht möglich war, gelang es, mit Hilfe einfacher Methoden des Reaktionsengineering einen adäquaten Prozess zur Darstellung von α- und β-Hydroxyestern zu entwickeln.

Enoatreduktase aus *Gluconobacter oxydans* (EnR): Die EnR katalysiert die chemo-, regio- und stereoselektive Reduktion von C=C Doppelbindungen verschiedener aktivierter Alkene. Mit Hilfe der identifizierten EnR gelang es, verschiedene Verbindungen mit hoher

biotechnologischer Relevanz wie z.B. (*S*)-Citronellal und (*R*)-Levodion selektiv und enantiomerenrein zu synthetisieren.

Insgesamt lässt sich festhalten, dass im Rahmen dieser Arbeit, drei Enzyme mit biotechnologischer Bedeutung identifizieren, klonieren und heterolog exprimiert werden konnten. Des Weiteren konnten diese Enzyme erfolgreich in der Synthese hochwertiger Schlüsselbausteinen eingesetzt werden und somit deren Potential für eine Anwendung in biotechnologischen Prozessen demonstriert werden.

LIST OF PUBLICATIONS

Richter, N., Neumann, M., Liese, A., Wohlgemuth, R., Eggert, T., Hummel, W. (2009). Characterisation of a new recombinant NADP-dependent glycerol dehydrogenase from *Gluconobacter oxydans* and its application in the production of L-glyceraldehyde, *ChemBioChem* **10**, 1888-1896

Richter, N., Neumann, M., Liese, A., Wohlgemuth, R., Weckbecker, A., Eggert, T., Hummel, W. (2010). Characterization of a whole-cell catalyst co-expressing glycerol dehydrogenase and glucose dehydrogenase and its application in the synthesis of L-glyceraldehyde. *Biotechnol. Bioeng*. **106**, 541-552

Richter, N., Breicha, K., Hummel, W., Niefind, K. (2010) The three-dimensional structure of AKR11B4, a glycerol dehydrogenase from *Gluconobacter oxydans* reveals a tryptophan residue as an accelerator of the reaction turnover. *J. Mol. Biol.* **404**, 353-362

Richter, N., Gröger, H., Hummel, W., (2011) Asymmetric reduction of activated alkenes using an enoate reductase from *Gluconobacter oxydans*. *Appl. Microbiol. Biotechnol.* **89**, 79-89

Richter, N., Zienert, A., Hummel, W. (2011). A single point mutation enables lactate dehydrogenase from *Bacillus subtilis* to utilize NAD^+ and $NADP^+$ as Cofactor. *Eng. Life Sci*. **11**, 26-36

Kraußer, M., Winkler, T., **Richter, N.**, Dommer, S., Fingerhut, A., Hummel, W., Gröger, H. (2011) Combination of C=C bond formation *via* Wittig reaction and enzymatic C=C bond reduction in a one-pot process in water. *ChemCatChem* **3**, 293-296

Richter, N., Hummel, W. (2011). Enzyme-catalyzed enantioselective reduction of α- and β-ketoesters by NADP-dependent carbonyl reductase from *Neurospora crassa*. *Enzyme Microb. Tech. in press* (doi: 10.1016/j.enzimctec.2011.02.004)

Neumann, M., **Richter, N**., Eggert, T., Hummel, W., Wohlgemuth, R., Liese, A. (2011) Preparative enzymatic production and isolation of L-Glyceraldehyde. *Submitted*

PATENT APPLICATIONS

Richter, N., Hummel, W., Eggert, T., Liese, A., Neumann, M. (2009). Alkoholdehydrogenase aus *Gluconobacter* und deren Verwendung. Patent DE 10 2009 007 272.1 (evocatal GmbH)

POSTER PRESENTATIONS

Neumann, M., **Richter, N**., Hummel, W., Eggert, T., Wohlgemuth, R., Liese, A. (2008). Production of dihydroxyacetone and glyceraldehyde in enzymatic redoxreactions. Biocat 2008, Hamburg, Deutschland

Richter, N., Neumann, M., Liese,A., Wohlgemuth, R., Eggert, T., Hummel, W. (2009). Production of L-glyceraldehyde by a new NADP-dependent glycerol dehydrogenase from *Gluconobacter oxydans*. Biotrans 2009, Bern, Schweiz

Kraußer, M., **Richter, N**., Winkler, T., Hummel, W., Gröger, H., (2010). Combination of a Wittig reaction with an enzymatic C=C-reduction in an one-pot two-step synthesis of saturated ketones in aqueous media. EuChemMS 2010, Nürnberg, Deutschland

TABLE OF CONTENTS

ABBREVIATIONS

In the following a summary of all non-standard abbreviations used within this thesis is given. Standard abbreviations and SI unis are excluded, for amino acids the common one- or three letter code was used.

Abbreviations for enzymes

ADH	Alcohol dehydrogenase
AldDH	Aldehyde dehydrogenase
BsLDH	LDH from *Bacillus subtilis*
CR	Carbonyl reductase
EnR	Enoate reductase
FDH	Formate dehydrogenase
FSA	D-Fructose-6-phosphate aldolase
G-6-P-DH	Glucose-6-phosphate dehydrogenase
GDH	Glucose dehydrogenase
GLD1	GlyDH from *Hypocrea jecorina*
GluDH	Glutamate dehydrogenase
GlyDH	Glycerol dehydrogenase
GOase	Galactose oxidase
GsLDH	LDH from *Geobacillus stearothermophilus*
HLADH	ADH from horse liver
LbADH	ADH from *Lactobacillus brevis*
LDH	Lactate dehydrogenase
LeuDH	Leucine dehydrogenase
NcCR	CR from *Neurospora crassa*
NOX	NAD(P)H oxidase
TBADH	ADH from *Thermoanaerobacter brockii*
TtADH	ADH from *Thermus thermophilus*
TtLDH	LDH from *Thermus thermophilus*
BsLDH_V39R	Variant of the BsLDH

Further abbreviations

AKR	Aldo-keto reductase
C-terminal	Carboxy-terminal
CHBE	Ethyl 4-chloro-3-hydroxybutanoate
COBE	Ethyl 4-chloro-3-oxobutanoate
DHA	Dihydroxyacetone
DNA	Desoxyribonucleic acid
E.C.	Enzyme commission
ee	Enantiomeric excess
FAD	Flavin adenin dinucleotide
FMN	Flavin adenin mononucleotide
GA	Glyceraldehyde
GC	Gas chromatography
HPLC	High performance liquid chromatography
IPTG	Isopropyl-β-D-thiogaladopyranoside
KIP	Ketoisophorone
LB-medium	Lysogen broth
N-terminal	Amino-terminal
NAD(H)	Nicotinamide adenine dinucleotide
NADP(H)	Nicotinamide adenine phosphate dinucleotide
PDB	Protein data bank
PQQ	Pyrroloquinoline quinone
SDR	Short-chain dehydrogenase
TEA	Triethanolamine
BLAST	Basic local alignment search tool
NCBI	National center for biotechnology information
BRENDA	Braunschweig enzyme database
EMBL	European molecular biology laboratory
U	Unit

1 INTRODUCTION

1.1 CHIRAL BUILDING BLOCKS

Chirality has become a key issue in organic synthesis and biotransformation over the past few decades. The synthesis of chiral intermediates for the production of fine chemicals, agrochemicals, natural products and, in particular, pharmaceuticals is essential.

In the early 1990s, approximately 90% of all pharmaceutical were produced as racemic mixtures[1]. Enantiomers possess nearly identical chemical and physical properties, but their biological effects can differ immensely. Therefore, racemates of pharmaceutically active compounds must be regarded with suspicion[2]. One prominent example of unwanted side effects is thalidomide, a pharmaceutical used in the early 1960s that caused a multiplicity of fetal abnormalities. While the (*R*)-enantiomer has a sedative effect, the (*S*)-enantiomer is highly teratogenic and is responsible for severe side effects[3].

Consequently, in 1992, the US Food and Drug Administration (FDA) and the European Committee for Proprietary Medicinal Products increased the legalisation pressure for racemic mixtures by claiming a proof that the non-therapeutic isomer is non-toxic[4]. As a result, the production of chiral intermediates has become increasingly important, and since 1990, the development of chiral technologies has expanded considerably. In 2000, 35% of the produced intermediates were chiral, and this number was predicted to increased to 70% by the end of 2010[5]. The importance of chiral intermediates is circumstantiated by the fact that nine out of 10 of the top selling drugs have a chiral active ingredient[6]. As a result, no new racemic drugs have been placed on the market since 2001[7, 8].

Therefore, methods for asymmetric synthesis are required, including the use of chiral reagents or the use of naturally occurring chiral compounds (chiral pool) as starting materials to produce the needed enantiopure building blocks (Fig. 1.1). Due to the fact that only 10-20% of compounds are available from the chiral pool at an affordable price[1], enzymatic methods have gained increasing interest in the past few decades.

Moreover, based on the demand for complex molecules with a number of functional groups and chiral centres, the chemical synthesis without the use of auxiliaries and protection groups remains challenging. The high regio-, chemo- and enantioselectivity of enzymes are the primary reasons that they are utilised as an

alternative to asymmetric organic synthesis or reactions starting from the chiral pool[9].

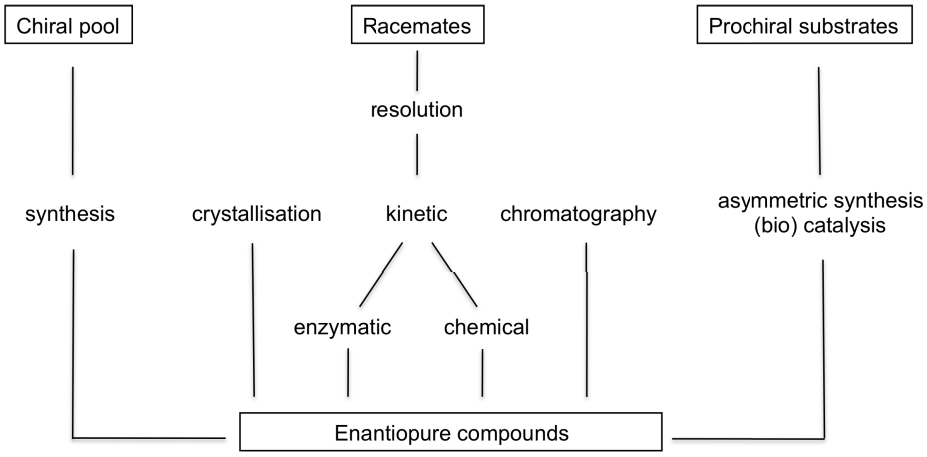

Fig. 1.1. Different methods to synthesise enantiopure compounds, according to Ghanem *et al.* (2005)[10]

These enzymatically derived chiral building blocks are ideally low-molecular compounds that exhibit several functional groups[11, 12]. Enantiopure glyceraldehyde is an example for a small chiral building block of great interest because of the wide applicability of its structural motif. Recently, enantiopure glyceraldehyde has been successfully used in the synthesis of enantiopure 4-(dihydroxyalkyl)-β-lactams (antibiotic)[13] and 8a-*epi*-swainsoine (anticancer drug)[14], as well as other pharmaceuticals[15, 16] (Fig. 1.2).

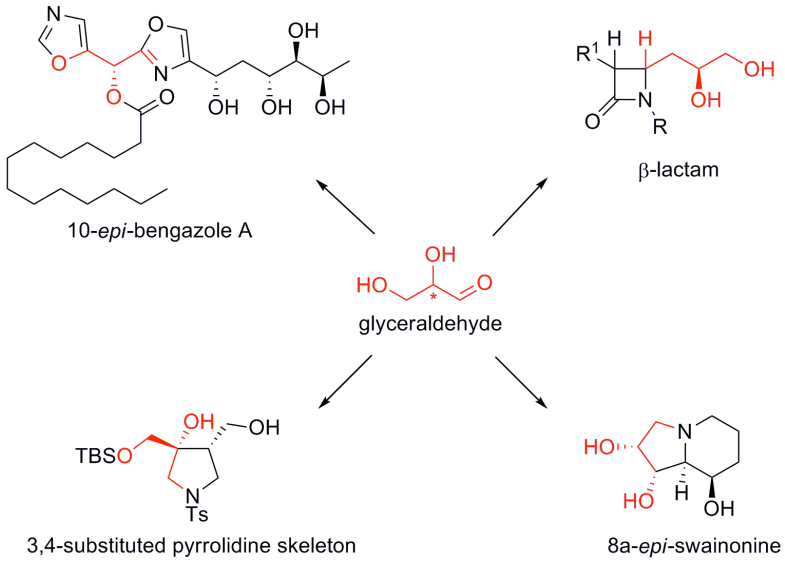

Fig. 1.2. Application of enantiopure glyceraldehyde. Scheme of the distribution of the structural motif (red) of glyceraldehyde in the following pharmaceuticals: β -lactams (antibiotic)[13], 8a-*epi*-swainsoine (anticancer drug)[14], 10-*epi*-bengazole A (antifungal activity)[15] and 3,5-substituted pyrrolodine skeletons (glycosidase inhibitor)[16].

Both glyceraldehyde enantiomers have been chemically synthesised by using different approaches starting from compounds from the chiral pool[17-22]. However, despite the achieved yields of the individual steps, the step economy and accumulated waste streams of the existing procedures are not very favourable for industrial applications. This is due to the synthetic designs that utilise protecting groups and requires many synthetic steps and large amounts of organic solvents, generating stoichiometric waste and toxic reagents. In regard to environmental improvements and cost reductions, new direct enzymatic routes for the preparation of enantiopure glyceraldehyde are attractive.

1.2 ENZYMATIC PRODUCTION OF CHIRAL BUILDING BLOCKS

Biocatalysis has become an important tool in organic synthesis for the production of fine chemicals, pharmaceuticals, agrochemicals and food ingredients. Therefore, the enzymatic production of chiral building blocks is a highly promising area of research for the development of sustainable processes[1, 9, 23-32].

The first application of enzymes in organic chemistry was the synthesis of (*R*)-mandelonitrile using a hydroxynitrile lyase-containing extract by Rosenthaler in 1908[33]. Since then, an increasing number of enzymes have been identified, and since the mid 1970 s, the reports of applications of enzymes in organic synthesis have substantially increased[32, 34]. Furthermore, another factor that facilitated the development of enzymes for synthesis was the progress in recombinant technologies, in particular, the finding of restriction enzymes that enabled the transfer of genes for large-scale protein expression in suitable organisms[35, 36]. Due to these developments, enzymes became easily accessible for commercialisation, leading to a reduction of time scales for industrial developments from 5-10 to 1-2 years[37, 38].

In general, enzymes can be classified into six categories according to the reaction they catalyse (Table 1.1).

These different enzymes can be used to catalyse reactions equivalent to almost every type of chemical reaction[1, 9, 23, 28, 29, 32, 39]. Further, a variety of different enzymes have already been used in chemoenzymatic synthesis[9, 26, 27, 31, 39-43].

In particular, due to high stereo-, regio- and chemoselectivity of enzymes, their application is often preferred over traditional chemical methods. Additionally, enzymes are very efficient catalysts, accelerating reaction rates by a factor of 10^8-10^{12} compared to the corresponding non-enzymatic reactions, leading to much higher acceleration rates than reactions mediated by chemical catalysts[44, 45].

Table 1.1. Enzyme classes and subclasses and their corresponding catalysed reaction[1].

Enzyme class	**Catalysed reaction** (examples of subclasses)
1. Oxidoreductases	Oxidation and reduction reactions (e.g. dehydrogenases, reductases, oxidases and monooxygenases)
2. Transferases	Transfer of functional groups (e.g. transketolases, transaminases and acetyltransferases)
3. Hydrolases	Hydrolysis and formation of e.g. esters, amides, lactams, lactones, epoxides, nitriles, anhydrides, glycosides and organohalides. (e.g. proteases, lipases, esterases, amidases, glycosidases and amylases)
4. Lyases	Addition or elimination of C=C, C=N, or C=O bonds (e.g. decarboxylases, carboxy-lyases, aldehyde-lyases and dehydratases)
5. Isomerases	Structural or geometrical rearrangement (e.g. racemases, epimerases, isomerases, tautomerases and mutases)
6. Ligases	Formation or cleavage of two substrates under simultaneous triphosphate cleavage (e.g. carboxylases)

Moreover, enzymes exhibit the ability to tolerate a wide range of structurally diverse substrates. Enzymatic reactions can be performed at ambient temperatures and atmospheric pressure, avoiding the use of extreme conditions that often cause problems with side reactions (e.g., isomerisation, racemisation, epimerisation and rearrangement). Considering environmental aspects, enzymes offer a safer and greener process in terms of organic solvents and workup procedures. Additionally, enzymes often reduce the number of individual steps required compared to chemical synthesis by their ability to catalyse reactions that are not even possible with conventional chemistry[46].

The application of enzymes also has some disadvantages, such as the process stability of the enzyme and the occurrence of inhibition by the substrate, product or any other compound in the reaction mixture. Furthermore, some enzymes require a cofactor, such as nicotinamide cofactors, that serves as carrier of redox equivalents that are too expensive to be used in stoichiometric amounts. To overcome this

limitation, a number of systems have been established to regenerate the cofactor[47, 48], which facilitates a sufficient use of cofactor-dependent enzymes in organic synthesis. Furthermore, methods of protein design can be used for the optimisation and adaption of the corresponding catalysts. For example, the requirement of lactate dehydrogenase from *Geobacillus stearothermophilus* for fructose 1,6-bisphosphate as an activator was eliminated by methods of directed evolution[30, 49].

Based on these establishments, a number of chemical routes in the pharmaceutical industry have already been replaced by biocatalytic steps[26]. For instance, the company DSM entirely redesigned the synthesis route for the antibiotic cephalexin. The traditional route, consisting of one fermentation followed by eight chemical steps, was replaced by a sequence of three biotransformations in series[11]. Another example is the chemical synthesis of cortisone, a steroidal drug, which traditionally consisted of 31 steps. With the introduction of a biocatalytic step, the synthesis was reduced to five steps. As a result of this decrease in the required reaction steps, the price of cortisone was reduced from 200$/g to 6$/g[50, 51].

Generally, there are two main reactions catalysed by enzymes: kinetic resolutions and asymmetric syntheses. The majority of kinetic resolutions are catalysed by hydrolases[1, 9, 29, 31, 32, 40, 46], while asymmetric synthesis is predominantly performed by oxidoreductases[1, 9, 11, 27, 29, 30, 32, 52-55] or by enzymes catalysing the formation of new carbon-carbon bonds, such as aldolases, hydroxynitrile lyases and transketolases[1, 56-58].

1.3 OXIDOREDUCTASES

Oxidoreductases are cofactor-dependent enzymes that are ubiquitously distributed and catalyse different reactions of biotechnological interest. Twenty-five percent of all presently known enzymes are members of this enzyme class consisting of dehydrogenases, oxygenases and oxidases[32]. Among the various groups of oxidoreductases, dehydrogenases are the most promising in terms of applicability in organic synthesis.

Dehydrogenases catalyse the NAD(P)H-dependent reduction of carbonyl groups, e.g., the reduction of aldehydes and ketones that produces the corresponding alcohol (Fig. 1.3a). However, there are also enzymes (reductases) that catalyse the reduction of activated C=C double bonds (Fig. 1.3b). Furthermore, the reverse reaction starting with the reduced compound is also catalysed by dehydrogenases (Fig. 1.3c).

Thus far, dehydrogenases have been successfully used in the reductive production of chiral hydroxyl acids[59], amino acids[60-62], α- and β-hydroxyesters[63-65] and especially alcohols[41-43, 52, 54, 66-71]. However, some examples of enzymatic oxidation in the kinetic resolution of chiral alcohols have also been published[72-83].

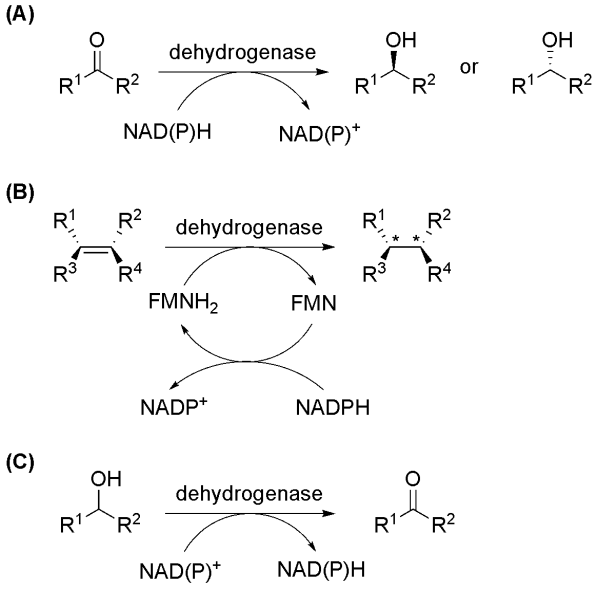

Fig. 1.3. Catalytic reaction of different dehydrogenases. The asymmetric reduction of carbonyl compounds (A), the reduction of a C=C double bond (B) and the enzymatic oxidation of an alcohol (C) are displayed.

1.3.1 Enzymatic reduction of carbonyl compounds

The asymmetric reduction of prochiral ketones is one of the most important reactions in organic synthesis for producing chiral alcohols. Therefore, alcohol dehydrogenases (ADHs) are of major interest.

A number of chemical methods are well-established for the asymmetric reduction of ketones by chemical means[84]. The disadvantage of these methods is the requirement of chiral catalysts to generate a chiral centre, starting from a prochiral compound. One of the best asymmetric reducing agents invented by chemists is the Corey-Bakishi-Shibata (CBS) reagent, which is a chiral borohydrin analogue leading to enantioselectivities of up to 97% using acetophenone as a substrate.

The drawback of using chemical methods is the fact that high enantioselectivities can only be obtained when the two substituents are sterically well-differentiated, while enzymes show high enantioselectivities with even aliphatic ketones such as ethyl propyl ketone[30]. This ability makes ADHs a versatile tool for the production of optically active secondary alcohols that are widely used as intermediates for the introduction of chiral information into compounds (Fig. 1.4)[30]. The produced chiral building blocks can act as key intermediates in the production of pharmaceuticals,

fine chemicals and natural products[23-26, 55]. Indeed, optically active 1,3-butanediol is such a key intermediate for the synthesis of various chiral compounds, much like azetidinone derivatives, which can be found in antibiotics, pheromones, fragrances and insecticides (Fig. 1.5)[73].

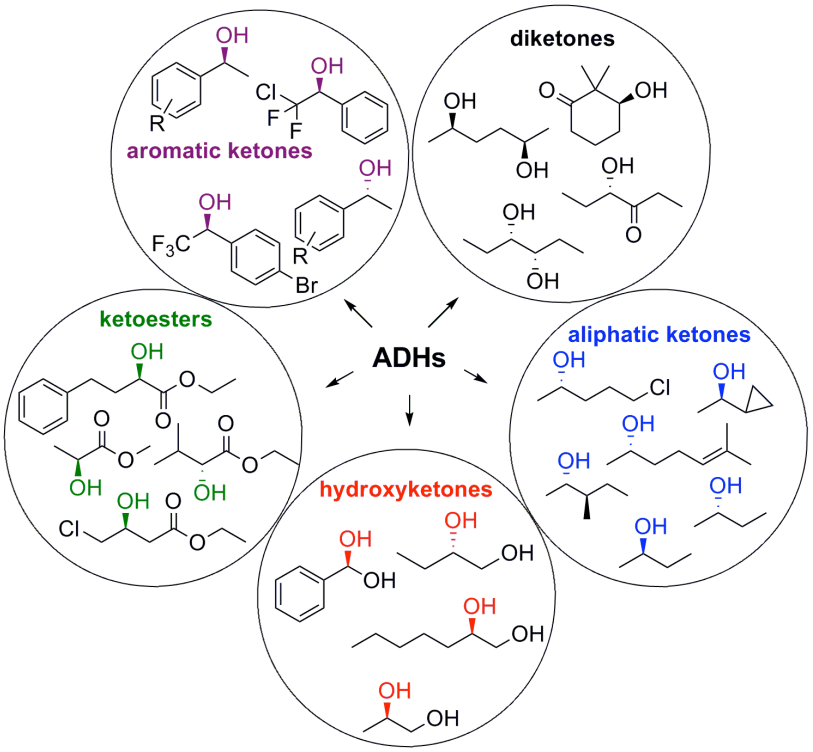

Fig. 1.4. Potential of ADHs in the asymmetric reduction of various ketones for the production of chiral alcohols.

Because the reduction catalysed by ADHs usually leads to the generation of a chiral centre, new catalysts with a broad substrate spectrum are of primary importance for various technical applications.

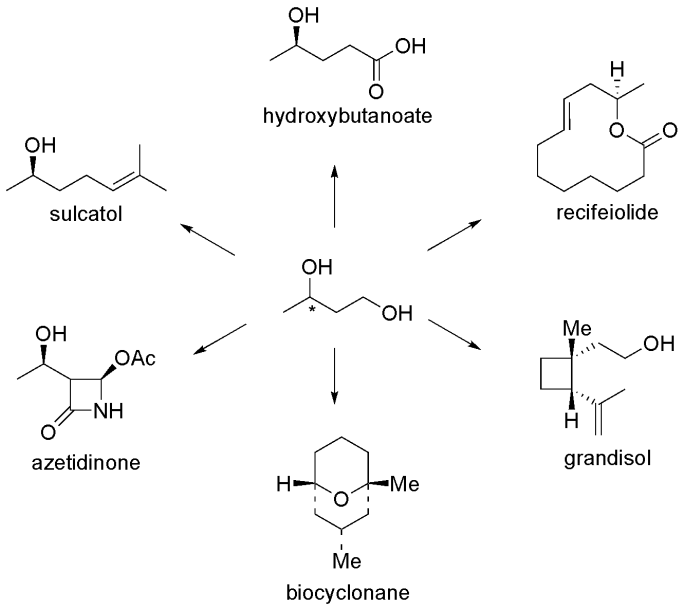

Fig. 1.5. 1,3-butanediol as a chiral building block for the synthesis of different chiral intermediates. Figure modified according to Matsuyama *et al.* (2001)[73]

In general, biotransformations are performed using either isolated enzymes or whole cells. A prominent example of a biocatalytic process that was developed to replace existing chemical routes is the enzymatic production of ethyl-(*R*)-cyano-3-hydroxybutanoate (HN). HN is a crucial intermediate for the production of atorvastatin (Lipitor®, a cholesterol-lowering drug).

The asymmetric reduction of ethyl-4-chloroacetoacetate is enzymatically catalysed by applying a ketoreductase to obtain ethyl-(*S*)-4-chloro-3-hydroxybutanoate. In a second enzymatic step, a halohydrin dehydrogenase is used for the subsequent conversion to ethyl-(*R*)-4-cyano-3-hydroxybutanoate. This sequence replaced a Claisen condensation carried out at -70°C and the application of chiral pool compounds (Fig. 1.6)[26].

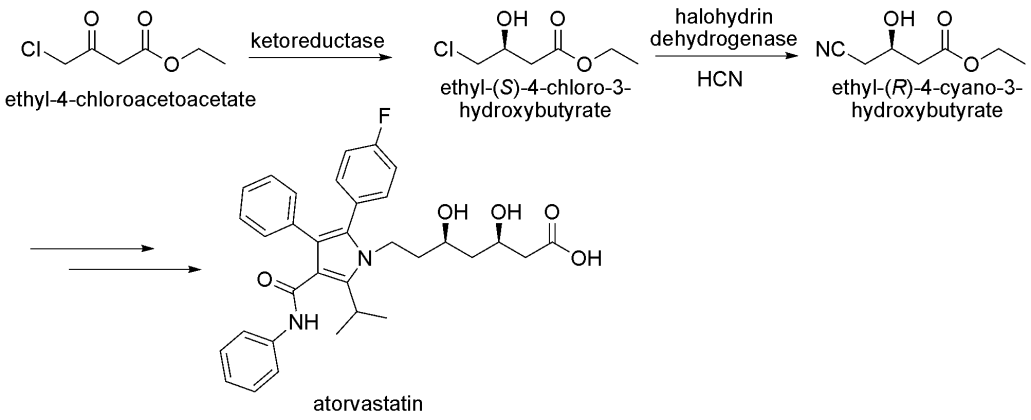

Fig. 1.6. Synthesis of atorvastatin. Two dehydrogenases, a ketoreductase and a halohydrin dehydrogenase, are applied to produce (*R*)-4-cyano-3-hydroxybutanoate, which is subsequently converted by several chemical steps to atorvastatin[26].

Another example is the enantioselective synthesis of (*R*)-2-bromo-1-(4-benzyloxyphenyl)ethanol and (*R*)-2-bromo-1-(4-benzyloxy-3-hydroxy-methylphenyl) ethanol using *Rhodotorula rubra* cells. The abovementioned compounds are chiral intermediates in the production of denopamine and salmeterol, two important β-adrenoreceptor agonists sold as racemates, of which the (*R*)-enantiomer is the active component (Fig. 1.7)[85]. The enantioselectivity introduced by the enzymatic step enables a direct route for the production of the enantiopure pharmaceutical.

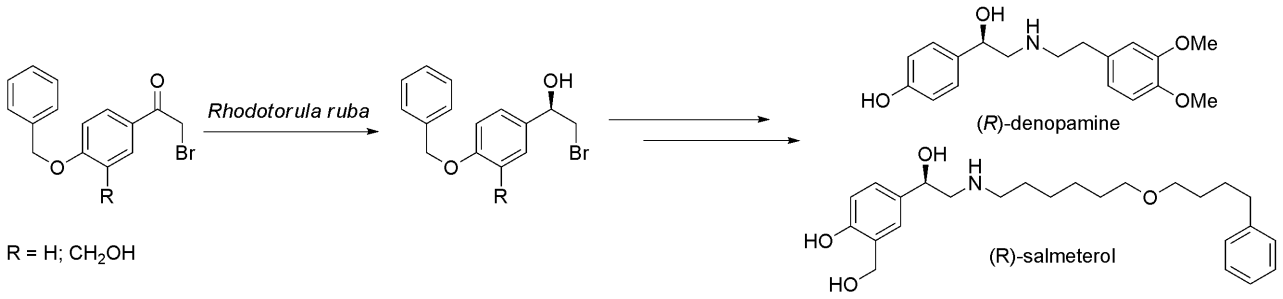

Fig. 1.7. Synthesis of (*R*)-denopamine and (*R*)-salmeterol. One key step in the reduction of the bromacetophenone derivative is stereoselectively catalysed by *R. rubra* cells[85].

1.3.2 Enzymatic reduction of C=C double bonds

In addition to the enzymatic reduction of carbonyl compounds, reductases are capable of catalysing the reduction of C=C double bonds. These enzymes are named enoate reductases based on the catalysed reaction. Enoate reductases are NAD(P)H-dependent flavoenzymes that catalyse the asymmetric reduction of olefinic double bonds by creating up to two chiral centres. For the equivalent chemical synthesis, a high number of alkene reductions are performed using asymmetric hydrogenation by chiral rhodium or ruthenium phosphines[86]. The major drawback is the limitation to highly polar functional groups (i.e., amides, acids and alcohols) as part of the structure. The chemical solutions also use complex ligands that require high pressure. The high regio- and enantioselectivity at ambient temperatures and pressure makes the biocatalytic counterpart a suitable alternative for the production of chiral building blocks.

In another example, *Candida macedoniensis* cells were applied to reduce the C=C double bond of 3,5,5-trimethyl-2-cyclohexene-1,4-dione (ketoisophorone, KIP) to produce (6*R*)-2,2,6-trimethylcyclohexane-1,4-dione (levidione), which is an important chiral intermediate for the synthesis of optically active compounds such as zeaxanthin (Fig. 1.8)[87, 88].

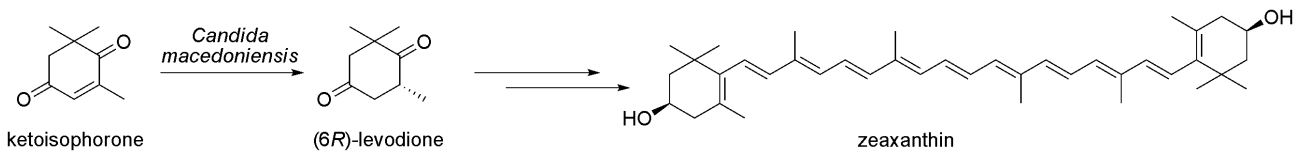

Fig. 1.8. Synthesis of zeaxanthin. The reduction of the C=C bond is catalysed by the enoate reductase from *C. macedoniensis* using whole cells[87].

Furthermore, citronellal, an important intermediate for the food and cosmetic industry, can be synthesised by the reduction of inexpensive prochiral citral using enoate reductases from different organisms[89-93]. Figure 1.9 shows the application of citronellal as an intermediate in the synthesis of menthol.

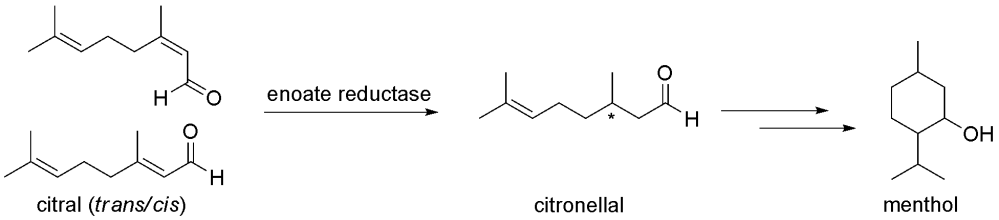

Fig. 1.9. Synthesis of menthols. Citronellal is synthesised by enoate reductases from different organisms (e.g., *G. oxidans, Candida parapsilosis, Pichia angusta, Rhodococcus ruber, Rhodococcus sp.* and *Botrytis cinerea*)[92].

1.3.3 Enzymatic alcohol oxidation

Oxidation of alcohols is one of the most fundamental and important reactions in organic chemistry. However, there are many disadvantages for performing oxidation reactions using traditional chemical methods. Many catalytic routes are based on toxic metal catalysts (e.g., chromium), which is unacceptable in terms of environmental issues, and the chemical methods used often lack chemoselectivity, leading to a number of side reactions. Moreover, the performance of a regio- and stereoselective oxidation is extremely difficult, especially when more than one hydroxyl group is present. This regioselective oxidation of polyols by chemical means requires a complicated protection and deprotection strategy to obtain the desired product[1, 72, 94-98].

According to the abovementioned difficulties, enzymatic oxidation has great potential with respect to environmental compatibility and catalytic efficiency, particularly when regio- and stereoselectivity is required[72, 99, 100]. In an overview on the current developments in biotransformation, Faber and Patel (2000) pointed out that novel catalysts are in great demand for catalysing reactions that are chemically difficult or impossible to perform by traditional methods (e.g., decarboxylation, stereoselective oxidation and asymmetric C-C bond formation)[101].

Most dehydrogenases are also capable of catalysing the oxidation of primary and secondary alcohols. The problem is that these oxidations are thermodynamically unfavourable. Therefore, the efficient regeneration of the required cofactor is a key issue for the successful application of dehydrogenases for enzymatic oxidation.

According to the fact that the oxidation of a secondary alcohol destroys a chiral centre, oxidations of secondary alcohols are of limited synthetic use. An exception for this application is when either the corresponding ketone is difficult to prepare or when there is no available enzyme to prepare the complementary enantiomer by reduction. A number of kinetic resolutions using ADHs can be found in literature[73, 76-79, 81, 83].

As an example, racemic 1,3-butanediol was resolved using strains with opposite enantiopreference (Fig. 1.10). This strategy provides access to both enantiomers because one enantiomer was reduced preferentially, while the other was untouched[73, 76]. As a second example, the L-leucine dehydrogenase from *Bacillus cereus* was successfully applied in the oxidative resolution of the racemic mixture of DL-*tert*-leucine for the preparation of enantiopure D-*tert*-leucine[83]. The major drawback of kinetic resolutions is that they only lead to a maximum yield of 50%, while the production of optically active compounds *via* asymmetric syntheses can result in up to a 100% yield.

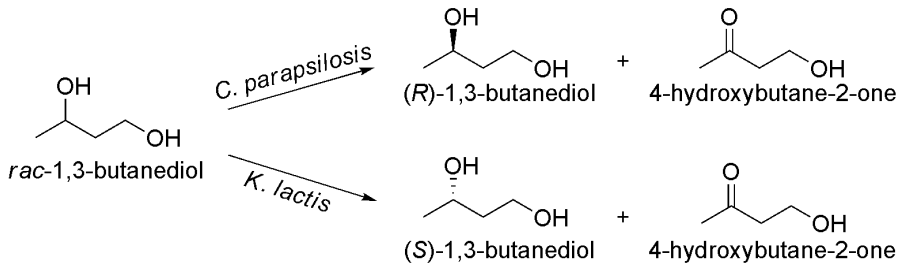

Fig. 1.10. Kinetic resolution of *rac*-1,3-butanediol. Both enantiomers can be prepared using different organisms with opposite enantiopreferences. *C. parapsilosis* oxidises the (*S*)-enantiomer, while the (*R*)-enantiomer is oxidised by *Kluyveromyces lactis*[73, 76].

Therefore, the asymmetric oxidation becomes considerably more interesting, particularly when complex molecules such as polyols are involved. In the selective oxidation of polyols, the application of a biocatalyst can significantly decrease the number of required steps due to the lack of protection and deprotection steps compared to the chemical synthesis.

Numerous sugars have been selectively oxidised in a single step using corresponding enzymes or microorganisms[74, 75]. The synthesis of L-ribulose by *Gluconobacter oxydans* is such an example, where ribitol is oxidised with high regio- and stereoselectivity in a single step (Fig. 1.11). Without the use of protection groups, this reaction is chemically impossible.

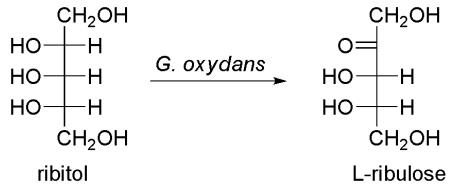

Fig. 1.11. Regio- and stereoselective microbial oxidation of ribitol to L-ribulose. *G. oxydans* has been applied to synthesise L-ribulose, a chiral intermediate[74].

A further example of the high regioselectivity of enzymes can be found in the production of 12-ketochenodeoxycholic acid from cholic acid catalysed by the 12α-hydroxysteroid dehydrogenase from *Clostridium* group P (Fig. 1.12). The compound 12-ketochenodeoxycholic acid is an essential intermediate in the synthesis of chenodeoxycholic acid, a drug with many therapeutic applications.

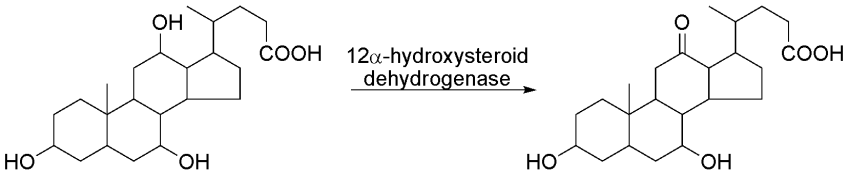

Fig. 1.12. Regioselective oxidative production of 12-ketochenodeoxycholic acid by 12α-hydroxysteroid dehydrogenase from *Clostridium* group P[75].

In summary, the application of oxidoreductases, particularly dehydrogenases, is a promising approach for the synthesis of chiral building blocks. The only drawback in terms of efficiency is the requirement for the addition of expensive cofactors, which can only be satisfied by the establishment and adaption of efficient and suitable regeneration systems for either the reduced or the oxidised cofactor.

1.4 IDENTIFICATION OF NEW OXIDOREDUCTASES

To expand the spectrum of enzymes that are capable of catalysing a variety of different reactions, the identification of novel biocatalysts is essential. There are two major routes to identify new enzymes for the application in organic synthesis. One is the screening of natural sources for new enzymes, and the other is the adaption and optimisation of enzymes by directed evolution or rational enzyme design.

1.4.1 Screening for new enzymes

The most established method to identify new enzymes is based on the screening of soil samples and strain collections by enrichment culturing[30, 35, 102, 103]. Enrichment

cultures enable the identification of microorganisms that display optimal growth under the experimental conditions. Often, media with limited nutrients or with the compound of interest as only carbon source are used. This approach enables the identification of microorganisms that contain enzymes that are capable of metabolising the corresponding compound. After selecting the suitable organisms, the enzymes responsible for the desired activity are identified in a second step. The advantage of this strategy is that the activity-based nature of the screening facilitates the identification of enzymes independent from sequence identities. However, if the gene sequence is required for the recombinant production of the biocatalyst, this method is rather time-consuming. In addition, this method is limited to the low number of culturable microorganisms[104]. Hence, new strategies have been applied more recently to include the "non-culturable" diversity. The metagenome approach is an example of such a culture-independent method, in which the entire genomic DNA from a soil sample is directly extracted, cloned, expressed and screened according to the desired activity[34, 105-107]. The benefit of applying this method is that the identified enzymes are already expressed in a recombinant form, and the DNA sequence can be easily analysed. One impressive example of the application of such an approach is the discovery of > 130 novel nitrilases from 600 environmental DNA libraries from different sources[106].
Another common method to identify novel catalysts is the so-called database mining approach[108]. This method is based upon the alignment of amino acid sequences with known activities and sequences of unknown function from databases using search tools such as BLAST[109]. Named tools can easily be used to identify sequences that potentially exhibit a similar or related activity. However, care must be taken because a similar sequence does not guarantee a similar activity. Therefore, this method can be used to provide first hints to novel enzymes. However, the biochemical properties and the substrate range must also be investigated.

1.4.2 Tailor-made enzymes

Rather than screening for an appropriate catalyst, the optimisation of the catalyst is often more efficient. Therefore, during the past few decades, much effort has been devoted to the development of capable methods to facilitate the adaption of biocatalysts according to the corresponding demands[110-118]. The intention of this approach is to improve catalytic properties, including higher catalytic turnover, altered substrate- or enantioselectivities, cofactor specificity, thermal and pH

stability and organic solvent tolerance. In principle, a distinction is drawn between two major strategies: directed evolution and rational protein design. However, both are used to improve an enzyme on the amino acid level.

Directed evolution

Directed evolution, also known as *in vitro* or molecular evolution, is a powerful tool, especially when no structural information for the enzyme is available or if it is uncertain which part of the catalyst must be changed to gain the desired ability. For a successful directed evolution approach, two steps are essential: 1) the random mutagenesis of the gene encoding the corresponding enzyme and 2) a reliable screening system for the identification of improved variants. Various techniques have been developed to effectively introduce mutations and screen the created libraries for the desired activity[35, 110, 112, 114, 119-121]. Furthermore, this approach has been successfully applied to adapt the properties of different catalysts, especially for industrial processes[35, 114, 117]. In addition, directed evolution has been used to improve oxidoreductases. For example, three rounds of random mutagenesis eliminated the required use of fructose 1,6-bisphosphate for the lactate dehydrogenase from *G. stearothermophilus*[49]. In a second example, six rounds of mutagenesis and sorting led to an improvement in catalytic activity and soluble expression of a phosphite dehydrogenase from *Pseudomonas stutzeri*[113].

Rational protein design

In contrast to directed evolution, rational protein design requires detailed knowledge of the three-dimensional structure of the protein or at least a homology model. Furthermore, information regarding the molecular principles, such as the reaction mechanism, is a prerequisite for identifying the positions for appropriate amino acid substitutions by site-directed mutagenesis. This technique is especially valuable in the understanding of structure-function relationships in combination with structural and biochemical investigations. According to the fact that most $NAD(P)^+$-dependent dehydrogenases exhibit a strong preference for either one of the cofactors, the attempt to alter the cofactor specificity of dehydrogenases by applying methods of rational protein design has become a major focus during the past few decades[122-133]. This interest is justified by the extensive knowledge of this enzyme class with respect to cofactor binding. The crucial amino acids were identified and consist of the highly conserved Rossmann-fold region $GXGXXG_{19}X$, exhibiting a negatively charged amino acid for NAD^+ preference, while a positively charged amino acid is responsible for $NADP^+$ binding (red X)[134-136].

In general, a combination of different techniques can be used to increase the scope of the enzyme of interest. A prominent example of such an approach is combinatorial active site mutagenesis (CAST) established by Reetz *et al.* (2005), which combines a single-site saturation mutagenesis and a simultaneous randomisation at multiple sites[115, 116, 118].

1.4.3 Identification of improved catalysts

The major challenge in enzyme evolution is the identification of improved variants within mutant libraries. In general, the numbers of generated variants differ remarkably when the methods of directed evolution and rational enzyme design are compared. However, if required, suitable screening or selection systems must be applied. Screening systems commonly use photometric- or fluorimetric-based assays on a microtitre plate scale or the formation of coloured products on agar plates to allow high-throughput strategies[119, 137-140]. One example is an on-plate activity assay based on the phenazinethosulfate-mediated reduction of nitrotetrazolium blue accompanied by the formation of a blue dye. This assay was applied to optimise formate dehydrogenase from *Candida boidinii*[141].

Highly efficient screening methods are based on selection strains, but the development of suitable selection strains is usually very time-consuming. Often, these strains are built upon complementation processes. This includes strains adapted for screening purposes by the deletion of essential enzymes or pathways. Such a strain is only able to grow if the essential metabolite is produced by a variant with the desired activity and drastically reduces the effort in screening large libraries[35, 142].

A variety of different screening and selection systems have been developed over the past few decades to identify successfully improved enzymes[118, 121, 143, 144].

1.5 COFACTOR REGENERATION

All redox enzymes require cofactors such as nicotinamide adenine dinucleotide [NAD(H)] and its respective phosphate [NADP(H)], flavins (FMN, FAD) and pyrroloquinoline quinone (PQQ), which serve as carrier of redox equivalents. Among the various cofactors, nicotinamides are the farthest distributed and most required by the majority of oxidoreductases[1]. These cofactors are not permanently bound to the enzyme and act as co-substrates. The successful use of dehydrogenases in synthetic applications requires either stoichiometric amounts of the cofactor or a

suitable regeneration system. Due to the high costs of the required nicotinamide cofactors, stoichiometric use is not feasible in terms of economical applicability. Therefore, the establishment of capable regeneration systems has been extensively studied over the past decade[47, 48]. There are different ways to regenerate either the reduced or oxidised cofactor, including enzymatic, chemical, photochemical and electrochemical strategies.

1.5.1 Electro- and photochemical cofactor regeneration

It is possible to regenerate nicotinamide cofactors with traditional chemical methods by applying reducing agents, such as sodium dithionite. However, due to very slow reaction rates and the common occurrence of side effects, such as enzyme inactivation, examples are scarce[145].

Photochemical cofactor regeneration is an environmentally friendly method that uses light energy to regenerate NAD(P)H with a photosynthetic biocatalyst such as *cyanobacterium*[30]. The light energy is converted through the electron transfer system into chemical energy in the form of NAD(P)H. Subsequently, the reduced cofactor can be used to enzymatically reduce ketones to chiral alcohols[146, 147].

Electrochemical methods are more common and flexible for the regeneration of the cofactor. One can differentiate between a direct electron transfer from the electrode and an indirect transfer where a mediator is interconnected, and several examples of electrochemical regeneration have been published[148-151].

1.5.2 Enzymatic regeneration of the reduced cofactor

Enzymatic regeneration systems have been extensively studied and used in combination with numerous dehydrogenases for different applications[1, 9, 27, 47, 54, 66, 68, 71, 152-158]. There are two possible strategies to regenerate the cofactor: 1) by the use of a second substrate and 2) the use of a second enzyme in combination with a second substrate.

Substrate-coupled cofactor regeneration

In substrate-coupled regeneration, the substrate is reduced by the dehydrogenase, and the required cofactor is regenerated by the addition of a co-substrate, which is oxidised by the same dehydrogenase. Requirements for this approach are the acceptance of high co-substrate and co-product concentrations (often 2-propanol and acetone) and the capability of the corresponding enzyme to oxidise the co-substrate.

The application of different dehydrogenases using the substrate-coupled strategy for cofactor regeneration has been published (Fig. 1.13)[47, 159-161].

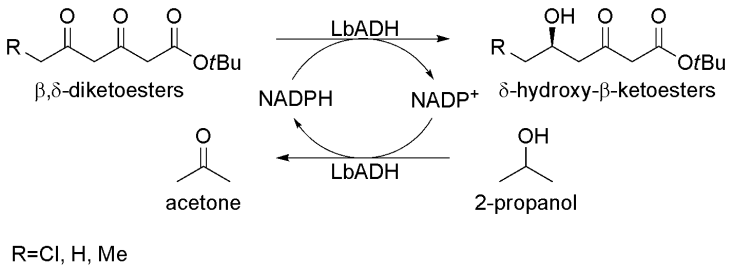

Fig. 1.13. Reduction of β,δ-diketo esters by the ADH from *Lacobacillus brevis* (LbADH). The same enzyme catalyses the simultaneous cofactor regeneration that oxidises 2-propanol as a co-substrate[159].

Although substrate-coupled regeneration appears elegant at first, there are some disadvantages encountered with this method. In general, not every dehydrogenase is able to catalyse the oxidation of the co-substrate, and additionally, inhibition of the enzyme by the co-substrate or the co-product is possible. Furthermore, due to the equilibrium reaction of the substrate-coupled mechanism, maximum reaction yields are not possible. Therefore, further strategies have been developed for the regeneration of the cofactor.

Enzyme-coupled cofactor regeneration

The second enzymatic strategy to regenerate the reduced cofactor is the use of two independent enzymes, which is often more advantageous than the substrate-coupled approach. In this case, two parallel redox reactions are performed simultaneously by two different enzymes (Fig. 1.14).

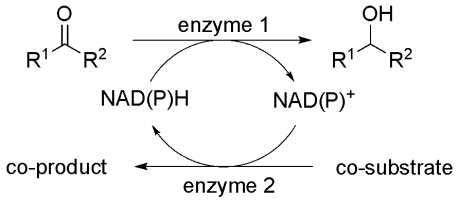

Fig. 1.14. Principle of the substrate-coupled cofactor regeneration approach using a second enzyme and a co-substrate.

Several enzymes are frequently used for the regeneration of reduced nicotinamide cofactors, such as formate dehydrogenase (FDH), glucose dehydrogenase (GDH) and glucose-6-phosphate dehydrogenase (G-6-P-DH).

Formate dehydrogenases (FDHs)

Based on the irreversible character of formate decarboxylation by the FDH and the formation of an easily removable product (CO_2), this strategy is preferentially used for the regeneration of NADH (Fig. 1.15).

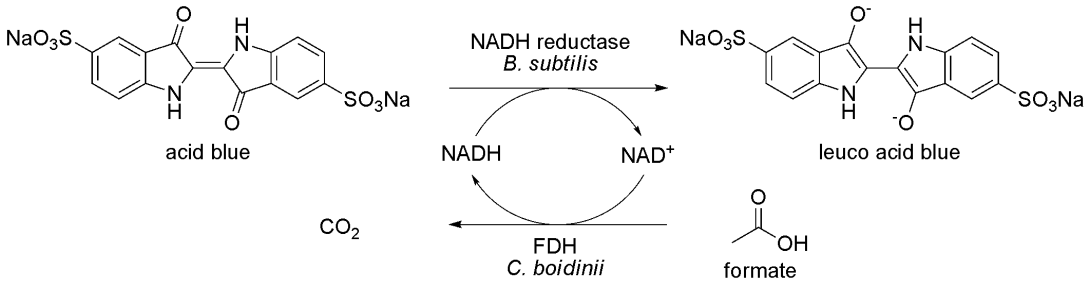

Fig. 1.15. Reduction of the dye acid blue by the NADH reductase from *Bacillus subtilis* coupled with FDH from *C. boidinii* for NADH regeneration[157].

Therefore, various examples of enzymatic reduction using FDH for cofactor regeneration are found in literature[47, 48, 66, 68, 71, 153, 157, 158]. However, due to the high cofactor specificity of FDH, its application is restricted to the regeneration of NADH. Furthermore, the specific activities of FDHs are very low compared to other enzymes.

Glucose dehydrogenases (GDHs)

GDHs can be used to regenerate NADH and NADPH. They catalyse the NAD(P)$^+$-dependent conversion of β-D-glucose to D-glucono-1,5-lactone. Due to the fact that the lactone formed can be quickly converted into the corresponding acid, this reaction is irreversible.

Thus far, GDHs have been successfully applied in NADH-dependent biotransformations [162, 163] and in a number of NADPH-dependent processes[153, 155, 156, 163-167].

Examples of such applications can be seen in the coupling of GDHs with an (*R*)-specific alcohol dehydrogenase in the production of different chiral alcohols[163, 167] or the production of 4-chloro-3-oxobutanoate, where GDH was used in combination with an aldehyde dehydrogenase[166].

Another interesting example is the application of the GDH from *Bacillus subtilis* in combination with ω-transaminase from *Vibrio fluvialis* and ADH from *Lactobacillus kefir*. These three enzymes were used for the simultaneous synthesis of enantiopure (*R*)-1-phenylethanol and (*R*)-α-methylbenzylamine from *rac*-α-methylbenzylamine (Fig. 1.16)[156]. These examples display the broad applicability of GDH in combination with various oxidoreductases.

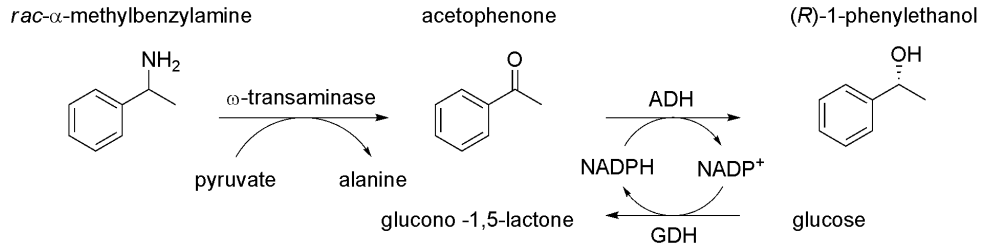

Fig. 1.16. Simultaneous synthesis of (*R*)-1-phenylethanol and (*R*)-α-methylbenzylamine from *rac*-α-methylbenzylamine, applying ω-transaminase from *V. fluvialis* and ADH from *L. kefir* in combination with GDH from *B. subtilis* for cofactor regeneration[156].

1.5.3 Enzymatic regeneration of the oxidised cofactor

The regeneration of the oxidised cofactor is also an essential area of research, especially in the environmentally benign enantioselective oxidation of alcohols using ADHs. Due to the fact that the equilibrium of dehydrogenase reactions lies heavily in favour of the reduction, the regeneration of the oxidised cofactor is more crucial than that of the reduced cofactor. In contrast to the variety of different regeneration systems for the reduced cofactor, suitable systems for the oxidised cofactor, particularly $NADP^+$, are rare.

The most widely used method for oxidised cofactor regeneration is the enzyme-coupled approach because shifting the equilibrium towards oxidation represents a serious challenge using the substrate-coupled approach. To apply such a strategy, the enzyme must be remarkably stable in high co-substrate concentrations, so the equilibrium can be shifted entirely. For example, Kosjek *et al.* (2003) used an acetone concentration of 25% (v/v) to catalyse the oxidation of *sec*-alcohols, employing whole cells of *R. ruber*[168-170]. Thus, the fact that only a few dehydrogenases can tolerate such high co-substrate concentrations demonstrates that the substrate-coupled approach has limitations.

Nevertheless, a number of useful enzyme-coupled regeneration systems exist, especially with regards to NAD^+, applying lactate dehydrogenases (LDHs), glutamate dehydrogenases (GluDHs) or water- and hydrogen peroxide-forming NAD(P)H oxidases (NOXs).

Lactate dehydrogenases (LDHs)

L-Lactate dehydrogenases are NAD^+-dependent dehydrogenases that catalyse the reduction of pyruvate to lactate. Based on their extraordinarily high specific activity and the high stability of the enzyme and substrate, LDHs have become a convenient system for enzymatic cofactor regeneration. For example, LDHs have been used to

regenerate NAD^+ in the oxidative resolution of 1-phenyl 1,2-ethanediol in combination with glycerol dehydrogenase (GlyDH)[78] and a number of other reactions[47, 78, 171-173]. However, the major drawback of using LDHs is their strict NAD^+-dependence. $NADP^+$-dependent enzymes have not yet been found in nature. Based on the advantages of LDHs, a $NADP^+$-dependent variant would be an interesting alternative in terms of economic aspects and the efficiency to facilitate the regeneration of $NADP^+$.

Therefore, according to the demand of a suitable regeneration system for $NADP^+$, protein engineering of the LDH from *G. stearothermophilus* has been investigated, particularly with the aim of altering its cofactor specificity[122-124]. Thus far, a number of LDH variants have been reported, and all show a shift in cofactor specificity[122, 123, 174]. However, with regards to activity, these variants were not significantly improved. Hence, none of the described variants have been used in the regeneration of the cofactor in combination with a second enzyme.

NAD(P)H oxidases (NOXs)

NOXs are O_2-dependent flavoenzymes that catalyse the NAD(P)H-dependent oxidation of molecular oxygen. They can be divided into water- and hydrogen peroxide-forming enzymes (Fig. 1.17). Water-forming enzymes are preferred over hydrogen peroxide-forming enzymes because the H_2O_2 produced leads to inactivation of the enzymes, and a third enzyme (catalase) is therefore required to decompose the H_2O_2.

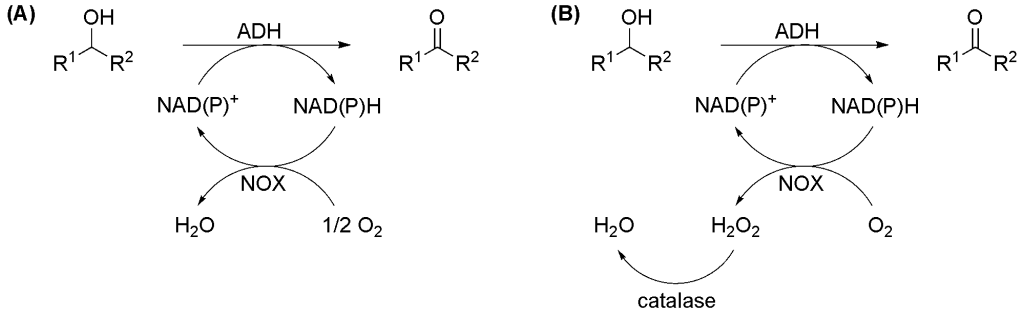

Fig. 1.17. Schematic diagram of $NAD(P)^+$-regeneration using either a water-forming (A) or a hydrogen peroxide-forming (B) NOX.

NOXs from different organisms are known and have been frequently used in the regeneration of NAD^+[47, 79, 83, 175, 176]. For example, NOX from *L. brevis* was applied in the kinetic resolution of DL-*tert*-leucine coupled with a leucine dehydrogenase[83].

However, the regeneration of $NADP^+$ using NOXs still remains challenging because many enzymes prefer NADH as a cofactor and show little to no activity with NADPH.

One exception is the water-forming NAD(P)H oxidase from *Lactobacillus sanfranciscensis,* which exhibits an adequate activity with NADPH (11 U/mg) in contrast to other oxidases[175].

Glutamate dehydrogenases (GluDHs)

GluDHs catalyse the synthesis of L-glutamate from ammonium and α-ketoglutarate. They prefer either NADH or NADPH or use both cofactors[81, 82, 177, 178] and show high specific activities. The only drawback for their biotechnological application is the relatively high price of the co-substrate used. Nevertheless, GluDH was applied in combination with GlyDH to regenerate NAD^+ during the oxidative resolution of 1,2-butanediol[81]. In addition, GluDH was used in combination with 12α-hydroxysteroid dehydrogenase from *Clostridium* group P for the regeneration of $NADP^+$ in the synthesis of ketochenodeoxycholic acid (Fig. 1.12).

1.6 WHOLE-CELL BIOCATALYSTS

Instead of using isolated dehydrogenases that require feasible cofactor recycling, whole microbial cells can be employed. The major advantage to this approach is that the addition of a cofactor is not necessary, and no regeneration system is required because the cofactor is regenerated by the metabolism of the cell. Therefore, whole wild-type cells are widely used in asymmetric synthesis, and numerous applications have been reported[11, 53, 73, 155, 167, 179-183]. However, the disadvantages are apparent concerning the variety of different dehydrogenases that occur in a microbial cell. The first drawback is that whole-cells often exhibit low stereoselectivities caused by the presence of multiple dehydrogenases with conflicting specificities. Furthermore, the produced compound can be metabolised by the cell, which leads to little to no yield. Aside from these disadvantages, the productivity of whole wild-type cells is generally low due to poor expression of the responsible enzymes compared to a recombinant expression system[184].

An alternative solution is the construction of so-called "designer cells" that enable the simultaneous expression of two or more enzymes in a single cell. This concept is based on a direct application of cells containing the desired enzymes in a sufficiently overexpressed form, using only the intracellular amount of the cofactor. The key benefit of this method is that side reactions can be avoided due to the high amount of recombinant enzyme. Furthermore, these renewable biocatalysts facilitate a process that does not require the recovery and purification of the enzymes.

A major issue for the successful creation of such catalysts is the optimisation of protein expression because activities of both enzymes are required in a similar range. Thus, there are different strategies available to generate an efficient "tailor-made" whole-cell catalyst.

In an indirect strategy, each enzyme is primarily produced in a different strain. Then for the subsequent biotransformation, cells from each strain are combined in various amounts, facilitating an adjustment in terms of activity[185]. The main drawback of this method is the required transfer of the corresponding cofactor between the cells.

However, other strategies that are strongly dependent on recombinant DNA technologies enable the simultaneous overexpression of the required enzymes in a single cell (Fig. 1.18).

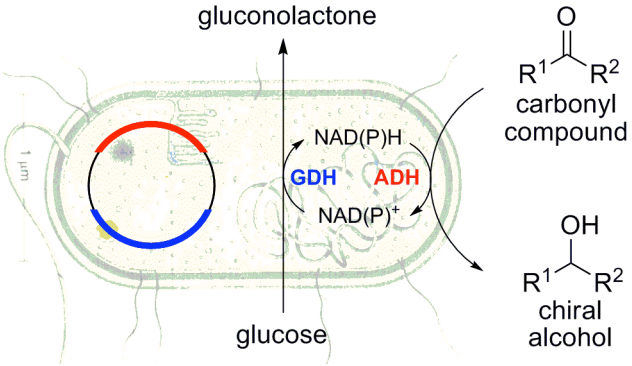

Fig. 1.18. Concept of a whole-cell catalyst using one plasmid for the simultaneous expression of the required ADH for carbonyl reduction and GDH for the regeneration of the cofactor.

In general, one can differentiate between a one- or two-plasmid strategy by integrating the genes of interest into one or two plasmids. By using such an approach, there are several options to adjust the activities of the enzymes such, as the copy number of the plasmids used or the strength of the selected promoters. According to the benefits offered by designer cells, their construction and application is very promising, particularly for technical applications. This interest can be seen in the growing number of processes using whole-cell catalysts [54, 62, 66, 166, 167, 185-192].

1.7 SCOPE AND OUTLINE OF THIS THESIS

As introduced, the biocatalytic synthesis of chiral building blocks has increasingly gained interest over the past few decades. The demand for biocatalytic strategies to produce these chiral synthons is high. Based on this requirement, the general aim of the thesis was the identification, recombinant expression and characterisation of novel oxidoreductases that can be applied in the synthesis of different chiral building

blocks (Chapters 2 and 3). Aside from the identification of oxidoreductases, a suitable biocatalytic process should be established to facilitate the production of chiral synthons on a preparative scale.

This goal should be achieved by database mining based on the protein sequences of enzymes that catalyse reactions related to the one that is desired. Moreover, recombinant access to the identified enzymes should be enabled. Additionally, the scope of these oxidoreductases should be examined with respect to reactions of biotechnological interest (Chapter 2). An application of the novel oxidoreductases requires a suitable and reliable cofactor regeneration system. Therefore, the adaption and establishment of cofactor regeneration systems was another focus of this work (Chapter 4). For this purpose, the cofactor specificity of lactate dehydrogenase from *B. subtilis* should be altered by applying methods of structure-guided saturation mutagenesis to broaden the applicability of lactate dehydrogenase in the cofactor regeneration.

Subsequently, a combination of the new oxidoreductases and a suitable regeneration system should facilitate biocatalytic strategies for the synthesis of different chiral building blocks on a preparative scale. If required, the process should be further optimised by reaction engineering.

Another aim of this thesis was to optimise and further simplify the established processes by the application of whole-cell catalysts. Such "designer cells" facilitate the expression of all required enzymes in a single cell and enable a reduction of time- and cost-consuming steps, as well as the addition of external cofactors (Chapter 5).

Finally, based on the newly established enzymatic routes, the production of a few selected chiral building blocks was demonstrated on preparative scale (Chapter 6).

2 IDENTIFICATION OF NEW OXIDOREDUCTASES

2.1 CHARACTERISATION OF A RECOMBINANT NADP-DEPENDENT GLYCEROL DEHYDROGENASE FROM *GLUCONOBACTER OXYDANS* AND ITS APPLICATION IN THE PRODUCTION OF L-GLYCERALDEHYDE

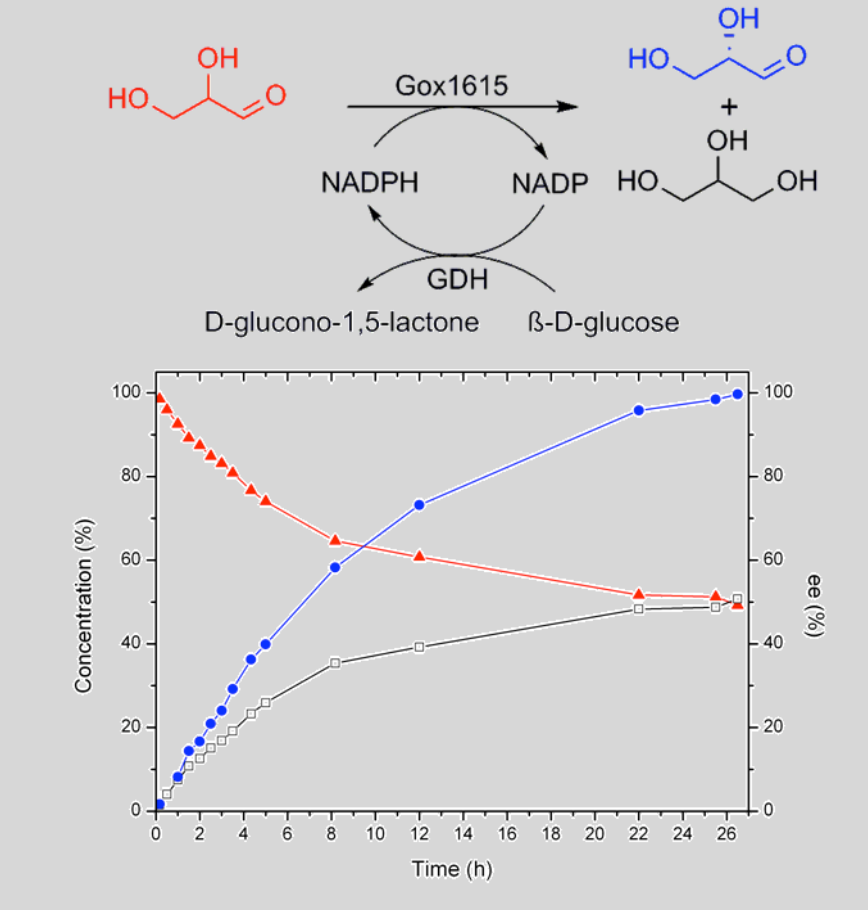

Nina Richter, Markus Neumann, Andreas Liese, Roland Wohlgemuth, Thorsten Eggert, and Werner Hummel (2009)

ChemBioChem 10, 1888-1896

(doi: 10.1002/cbic.200900193).

FULL PAPERS

Glycerol dehydrogenase from *Gluconobacter oxydans*

Characterisation of a recombinant NADP-dependent glycerol dehydrogenase from *Gluconobacter oxydans* and its application in the production of L-glyceraldehyde

Nina Richter,[a] Markus Neumann,[b] Andreas Liese[b], Roland Wohlgemuth,[c] Thorsten Eggert,[a] and Werner Hummel*[d]

The acetic acid bacterium Gluconobacter oxydans *has a high potential for oxidoreductases with a variety of different catalytic abilities. One putative oxidoreductase gene codes for an enzyme with a high similarity to the NADP$^+$-dependent glycerol dehydrogenase (GlyDH) from* Hypocrea jecorina. *Due to this homology, the GlyDH (Gox1615) has been cloned, overexpressed in* Escherichia coli*, purified and characterised. Gox1615 has shown an apparent native molecular mass of 39 kDa, which corresponds well to the mass of 37.213 kDa calculated from the primary structure. From HPLC measurements, a monomeric structure can be deduced. Kinetic parameters and the dependence of the activity on temperature and pH were determined. The enzyme has shown a broad substrate spectrum in the reduction of different aliphatic, branched and aromatic aldehydes. Additionally, the enzyme has been shown to oxidize a variety of different alcohols. The highest activities were observed for the conversion of* D*-glyceraldehyde in the reductive and for* L*-arabitol in the oxidative direction. Since high enantioselectivities were observed for the reduction of glyceraldehyde, a kinetic resolution of glyceraldehyde has been investigated yielding in enantiopure* L*-glyceraldehyde on preparative scale.*

Introduction

Oxidoreductases (E.C.1.1.1.x) are cofactor-dependent enzymes which are ubiquitously distributed and catalyse different reactions of biotechnological interest. Alcohol dehydrogenases (ADHs) are members of this enzyme class. Their ability to catalyse the chemo-, regio- and stereoselective reduction of ketones make them versatile tools for the production of chiral building blocks.[1, 2] These chiral building blocks act e.g. as key intermediates in the production of pharmaceuticals, fine chemicals and natural products.[3-5] Due to their stereochemical properties, including the high enantioselectivity, ADHs with a broad substrate spectrum are of primary importance for various technical applications.

Enantiopure glyceraldehyde is an example for a small chiral building block of great interest for further synthesis because of the wide applicability of its structural motive. It has been successfully used in the synthesis of for example enantiopure 4-(dihydroxyalkyl)-β-lactams (antibiotic)[6] or 8a-*epi*-swainsoine (anticancer drug).[7] Although the chemical synthesis of both glyceraldehyde enantiomers is possible on laboratory scale,[8, 9] the major drawbacks are the extensive and expensive procedures. The chemical synthesis of D-glyceraldehyde starts with D-mannitol, whereas the L-enantiomer is derived from L-arabinose. Up to now, only the synthesis of D-glyceraldehyde was realized in industrial scale. With regard to environmental aspects and cost factors new short enzymatic routes for the preparation to enantiopure glyceraldehyde are desirable. Therefore, enzymes catalysing either the selective oxidation of glycerol or the selective reduction of glyceraldehyde are of great interest. The class of enzymes which catalyse the NADPH-dependent reduction of glyceraldehyde to glycerol are called NADP$^+$ glycerol dehydrogenases (E.C.1.1.1.72) (Fig. 1). These enzymes are common in moulds and filamentous fungi

[a] *N. Richter, Dr. T. Eggert*
Evocatal GmbH
Merowingerplatz 1a
40225 Düsseldorf (Germany)

[b] *M. Neumann, Prof. Dr. A. Liese*
Institut für Technische Biokatalyse
Technische Universität Hamburg-Harburg
21073 Hamburg (Germany)

[c] *Dr. R. Wohlgemuth*
Research Specialties
Sigma-Aldrich Chemie GmbH, Industriestrasse 25
Buchs CH-9471 (Switzerland)

[d] *Prof. Dr. W. Hummel*
Institut für Molekulare Enzymtechnologie, Heinrich-Heine Universität Düsseldorf,Forschungszentrum Jülich, Stetternicher Forst
52426 Jülich (Germany)
Fax: (+49)2461-612490
E-mail: w.hummel@fz-juelich.de

and have been isolated from mammalian tissues.[10-14] So far different bacterial GlyDHs are reported to catalyse the reduction of dihydroxyacetone (DHA) to glycerol which can be classified as glycerol: $NADP^+$ 2-oxidoreductases (E.C. 1.1.1.156) or glycerol: NAD^+ 2-oxidoreductases (E.C. 1.1.1.6).[15-20] Among the GlyDHs catalysing the reduction of glyceraldehyde only the GlyDH from *H. jecorina*[12] has been heterologously expressed, purified and characterised whereas the others have been characterised using purified enzymes from wildtype stains.

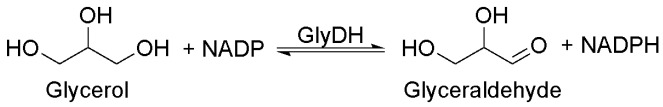

Figure 1: General reaction scheme of the NADP(H)-dependent oxidation and reduction catalysed by GlyDHs.

Acetic acid bacteria like *G. oxydans* show high activities in the oxidation of a wide range of substrates, such as alcohols, sugar, sugar acids, and sugar alcohols. For such oxidative reactions *G. oxydans* has numerous membrane-bound and cytosolic oxidoreductases which are of great biotechnological interest, due to their high stereo- and regioselectivity. *G. oxydans* is applied for example in the industrial production of 2-keto-L-gulonic acid, a vitamin C precursor, 6-amino- L-sorbose, a miglitol precursor and the production of DHA, an ingredient in tanning agents.[21] Because of this ability we selected *G. oxydans* for a homology search to identify oxidoreductases for the enzymatic production of enantiopure glyceraldehyde. Based on the sequence of GlyDH, GDL1 from *H. jecorina* known to catalyse the reduction of glyceraldehyde and DHA to glycerol, we identified by homology search an oxidoreductase with the ability to act specifically on glyceraldehyde.

Herein we report the cloning, heterologous expression and biochemical characterization of the GlyDH from *G. oxydans*. Furthermore, we show its applicability in the kinetic resolution of glyceraldehyde producing enantiopure L-glyceraldehyde on preparative scale.

Results

Identification of the alcohol GlyDH gene

The genome of *G. oxydans* 621H was recently sequenced by Prust and co-workers.[24] 75 genes were annotated to be putative oxidoreductases of unknown function. Therefore, *G. oxydans* was selected for a BLAST search using the sequence of GLD1 (DQ_422037), a NADPH-dependent glycerol dehydrogenase from the mould *H. jecorina*[12] as template. Named enzyme has previously been described by Liepins et al. [12] and found to catalyse the conversion of D- and L-glyceraldehyde to glycerol. The protein sequence of GLD1 was used to find homologies in the genome of *G. oxydans* 621H the putative oxidureductase Gox1615 (YP_192012), which showed a homology to GLD1 (Fig. 2), could be identified. A pairwise alignment between the protein sequences of both enzymes showed an identity of 17% and a similarity of 32% with 14% gaps. The corresponding gene *gox*1615 encodes for a protein with a calculated molecular mass of 37.213 kDa.

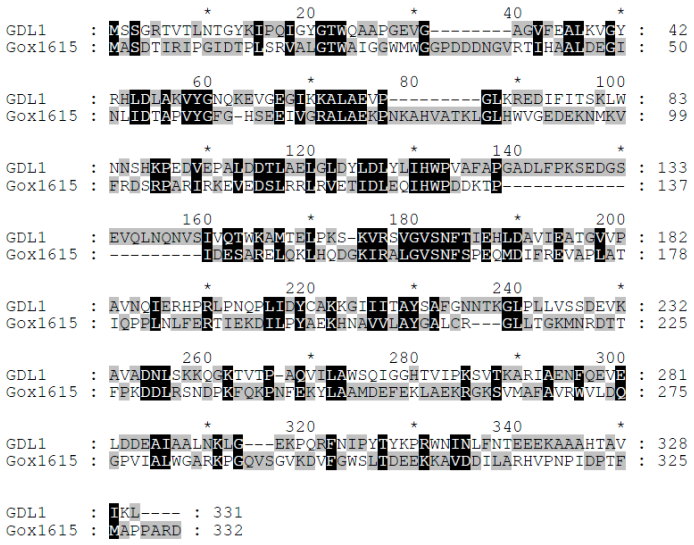

Figure 2: Comparison of amino acid sequences of the GlyDH from the mould *H. jecorina* (GDL1) and the α -proteobacterium *G. oxydans* (Gox1615). The alignment was created with the GeneDoc Software. Shaded boxes in black indicate conserved or similar amino acids. The two GlyDHs show a homoloy of 32%.

Cloning and heterologous overexpression of the GlyDH

In order to improve the expression and simplify the purification of the GlyDH standard cloning techniques were applied to create a recombinant plasmid containing the *glydh* gene with a hexahistidine affinity purification motif (his-tag) fused to the N-terminal protein. This recombinant plasmid was expressed in *E. coli* BL21(DE3) at different temperatures revealing best activities at 25°C. The protein with the N-terminal his-tag showed a specific activity of 9.2 U/mg in the crude extract for the reduction of glyceraldehyde. Soluble protein was expressed to a medium level (Fig.3, lane1). The his-tag allowed the purification of the protein *via* immobilized metal affinity chromatography (IMAC).

Table 1: Purification of the recombinant GlyDH from *E. coli* BL21(DE3) cells

Purification step	Total activity (U/ml)	Specific activity (U/mg)	Purification factor	Yield (%)
Crude extract	10323	9.0	1	100
Purified GlyDH	6867	36.4	4	66.5

Purification of the GlyDH

The recombinant enzyme with N-terminal his-tag was purified in one chromatographic step using IMAC with Ni-NTA resin material as shown in table 1. The purification resulted in a recovery of 67% of the activity measured in the crude extract. The specific activity of Gox1615 after the purification was 36.4 U/mg corresponding to a 4-fold improvement in activity compared to the crude extract. Samples of the crude extract and the target fraction after the purification were analyzed by SDS-PAGE (figure 3). A single band with an apparent molecular size of 39 kDa (Fig. 3, lane 4) corresponds to the enzyme protein confirming the calculated molecular mass of 37.213 kDa derived from the amino acid sequence. It has been possible to purify the recombinant

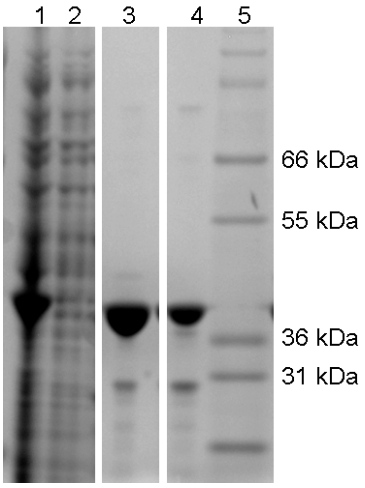

Figure 3: SDS-PAGE analysis of the purified GlyDH from *G. oxydans*. Lane 1: crude extract (25 µg), lane 2: flow through (25 µg), lane 3: purified Gox1615 (12.5 µg), lane 4: purified Gox1615 after desalting (6.25 µg), lane 5: molecular weight marker (Mark 12, Invitrogen). Lane 3 and 4 show a single major band at an apparent molecular weight of 39 kDa.

GlyDH almost to homogeneity (> 95%) applying a single purification step (Fig. 3).

Molecular characteristics of GlyDH

The calculated molecular mass of 37 kDa of one subunit of GlyDH was confirmed by SDS-PAGE (39 kDa, Fig. 3). Additionally, the native molecular mass was determined using size-exclusion chromatography. The apparent molecular mass of the GlyDH has been estimated to be 31 kDa, suggesting a monomeric structure.
Studies concerning the cofactor dependency have shown that Gox1615 preferred NADPH over NADH. Using NADPH, a 200-fold increase in activity was observed compared to the activity achieved with the same concentration of NADH (Data not shown).

Characterisation of the kinetic parameters

The kinetic properties of GlyDH during reduction and oxidation have been characterised based on the standard substrates glyceraldehyde and L-arabitol. Respective kinetic constants for the reduction of glyceraldehyde and the oxidation of L-arabitol were determined. Additionally, kinetic parameters for NADPH or rather $NADP^+$ were estimated using the purified enzyme. Michaelis-Menten constants determined during reduction of glyceraldehyde were 2.69 mM ± 0.35 (K_M) and 77.86 U/mg ± 3.53 (V_{max}). For the cofactor NADPH an inhibition at concentrations above 0.15 mM was observed. Therefore an equation for substrate-excess inhibition was used ($v=v_{max} * s / (K_M + s (1 + s / K_i))$ for fitting in the Michaelis Menten equation. The estimated kinetic constants are a K_M value of 0.04 mM ± 0.009, a V_{max} of 100.76 U/mg ± 12.8 and a K_i value of 0.4 mM ± 0.12. For the substrate L-arabitol the enzyme shows a hyperbolic reaction velocity versus substrate concentration plot with a K_M value of 192.87 mM ± 10.57 and a V_{max} of 8.67 U/mg ± 0.2. The oxidised cofactor $NADP^+$ follows a typical Michaelis Menten equation with a K_M value of 0.02 mM ± 0.001 and a V_{max} of 2.1 U/mg ± 0.02.

Dependence of the GlyDH activity on temperature and pH

Since the influence of temperature on the enzyme activity and stability is often a limiting parameter in technical applications,

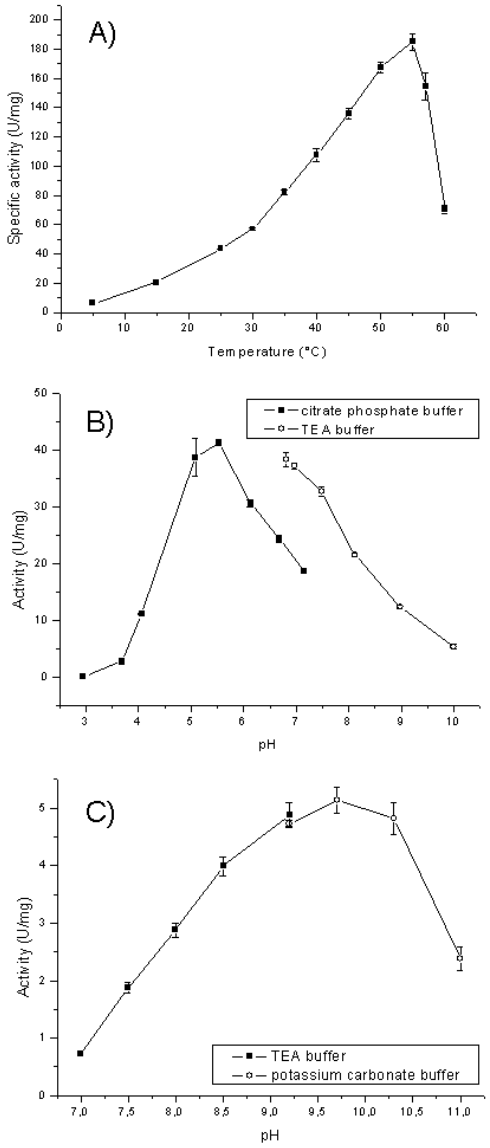

Figure 4: Determination of temperature (a) and pH optima for the reduction (b) and oxidation (c) of the GlyDH. The effects of temperature and pH on the enzyme activity were measured by using the standard specto-photometrical assays for reduction and oxidation. For the determination of the optimum pH in the reduction of glyceraldehyde two different buffers, (■) citrate phosphate buffer (pH 3.0 to 7.2) and (●) TEA (pH 6.8 to 10.0) were used. The determination of the pH optimum was examined using (■) TEA (pH 7.0 to pH 9.2) and (●) potassium carbonate buffer (pH 7.0 to 11.0).

studies concerning temperature optimum and stability were performed. Figure 4a illustrates that the purified enzyme shows its maximal activity at 55°C, whereas the activity decreases significantly to a residual activity of 50% at 57°C and 37°C, respectively. The pH dependence regarding the activity in the reduction of glyceraldehyde has been measured in a pH range from pH 3 to pH 10. As demonstrated in figure 4b the optimal activity has been found at pH 5.5. The pH dependence of the enzyme was examined using TEA buffer (pH 6.8 to 10.0) and

citrate phosphate buffer (pH 3 to 7.2). Best activities at same pH values (pH 7.0) were observed using citrate phosphate buffer.
For the determination of the pH optimum in the oxidation of L-arabitol, TEA buffer (pH 7.0 to pH 9.2) and potassium carbonate buffer (pH 9.2 to pH 11) were used. The optimum of activity is very broad with a maximum at pH 10.0 (Fig. 4c). At pH 9.2 the GlyDH shows an activity of 3.1 U/mg in TEA buffer and 3.2 U/mg

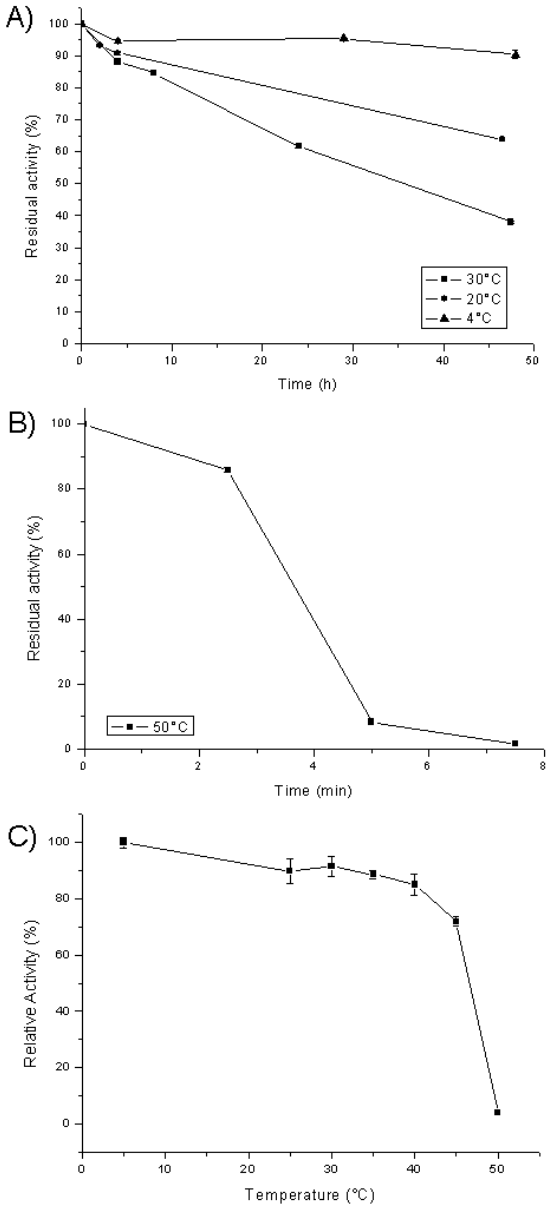

Figure 5: Thermal stability of the Gox1615. The effect of temperature over a period of 48 h at 4°C,20°C and 30°C (a) and 50°C (b) was investigated. For the determination of the residual activity the standard spectro-photometrical assay for reduction was used. (c) For the determination of the midpoint thermal inactivation T_m different temperatures were kept for 10 min before the samples were withdrawn to measure the residual activity in the soluble protein content. The standard deviation is shown in the diagram.

in potassium carbonate buffer. These results indicate a similar activity in both buffers.
Enzyme stability is also a very crucial parameter for technical applications and processes; hence the temperature-dependent inactivation over time and pH- and thermostability of GlyDH have been investigated. Studies concerning the thermostability of the purified enzyme were performed at different temperatures (4°C, 20°C and 30°C) over 48 h, and at 50°C over 8 min. As shown in figure 5a the enzyme is stable at 4°C, 20°C and 30°C during the investigated period, but at 50°C a rapid inactivation of the enzyme was found (Fig. 5b). After an incubation of 4 min only 50% and after 8 min no residual activity was detected. In a second study the midpoint thermal inactivation (T_m) of Gox1615 was determined as 47.2°C (Fig. 5c).

The pH-stability was investigated at three different pH-values (pH 5.5, pH 7.0 and pH 9.7) over a period of 43 h using the standard activity assay for the reduction to determine the residual activity. At all pH-values the enzyme was stable showing a residual activity of 93% (pH 7), 84% (pH 5.5) and 82% (pH 9.7), respectively indicating its applicability at these pH values.

Substrate specificity of the GlyDH

Substrate specificity of the enzyme was assessed using spectrophotometrical assays for either the reduction or oxidation reaction. The specific activities of the purified enzyme in the reduction of different aliphatic, branched and aromatic aldehydes and ketones and the oxidation of a variety of different alcohols were determined. For the reduction reaction the activities were compared to the standard substrate glyceraldehyde (entry 9) with a specific activity of 39.1 U/mg, while in the oxidation reaction L-arabitol (entry 44) was used as standard substrate (2.46 U/mg). Comparing both, the reduction and the oxidation, it becomes obvious that the GlyDH favours the reduction reaction; the observed specific activities are up to 19-fold higher than those observed for the oxidation. In the reduction the best activity was obtained with D-glyceraldehyde as substrate; activities towards other substrates are shown in table 2. In general, aliphatic, branched and aromatic aldehyde substrates are accepted by the GlyDH.

Table 2: Substrate spectrum in the reduction catalysed by the GlyDH from *G. oxydans*. The activity was obtained using the standard spectro-photometrical assay.

entry	Substrate	Specific activity [U/mg]
	Aldehydes	
1		0.1
2		1.1
3	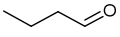	23.3
4	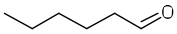	31.9
5	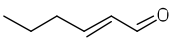	4.9
6	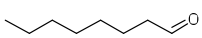	35.5
7	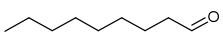	15.9
8	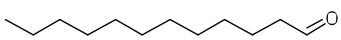	19.3
9	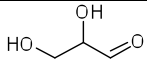	39.1
9a	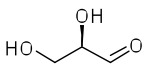	48.1
9b	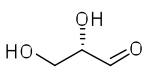	2.0
10		6.7

11	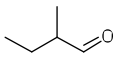	26.8
12	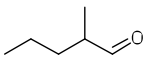	25.7
13	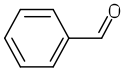	13.8
14	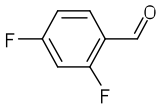	19.6
15	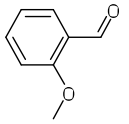	0
16	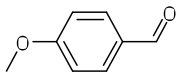	0.3
	Ketones	
17	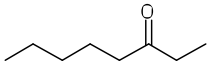	0.02
18	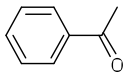	0.04
19	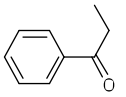	0.03
20	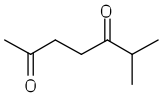	0.03
21	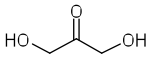	0.5

In the oxidation the highest activity was achieved using L-arabitol as substrate. Various other substrates with up to six alcohol groups where oxidised with different specific activities (table 3).

Table 3: Substrate spectrum in the oxidation catalysed by the GlyDH from *G. oxydans*. The activity was obtained using the standard spectro-photometrical assay.

entry	Substrate	Specific activity [U/mg]
22	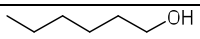	0.74
23	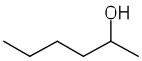	0.22
24	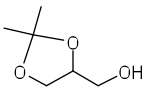	0.03
25	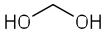	0.05
26		0.5
27	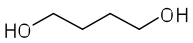	0.21
28	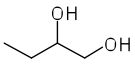	0.66
29	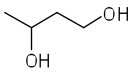	0.04
30	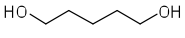	0.59
31	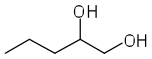	0.39
32	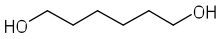	0.87
33	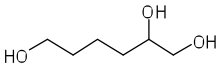	0.30
34	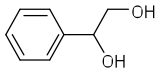	0.77
35	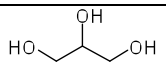	0.17
36	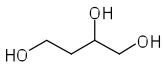	1.21
37	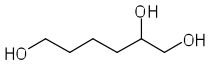	0.45
38	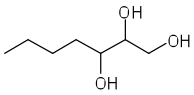	0.76
39	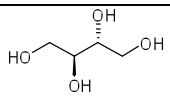	0.75
40	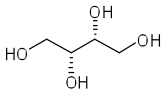	0
41	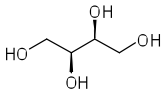	0.90
42	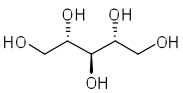	0.25
43	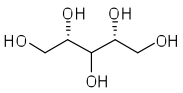	0
44	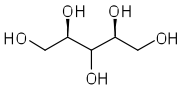	2.46
45	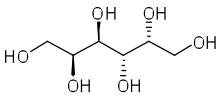	1.08

Kinetic resolution of glyceraldehyde

L-Glyceraldehyde is a versatile building block and has been successfully applied in a broad range of syntheses.[6, 7, 25, 26] Enantiopure glyceraldehyde can be obtained by regio- and stereoselective oxidation of glycerol or the stereoselective reduction of racemic glyceraldehyde. Thus, preparative-scale kinetic resolution of glyceraldehyde was performed with simultaneous regeneration of NADPH using glucose and glucose dehydrogenase (GDH) (Fig. 6). The conversion and enantiomeric excess (*ee*) were determined by means of HPLC and GC.

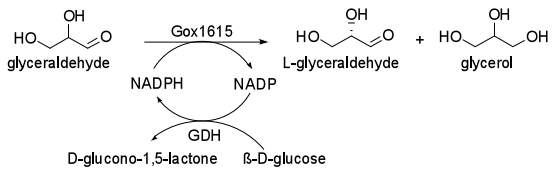

Figure 6: Scheme of the reduction of glyceraldehyde using Gox1615.

Figure 7 illustrates a typical time curve of the kinetic resolution of glyceraldehyde by the purified GlyDH from *G. oxydans*. The figure shows the development of glyceraldehyde and glycerol concentration and additionally the *ee* value of L-glyceraldehyde measured over a period of 26 h. A conversion of 50% and an *ee* > 99% has been achieved using Gox1615 in the kinetic resolution of glyceraldehyde on preparative scale.

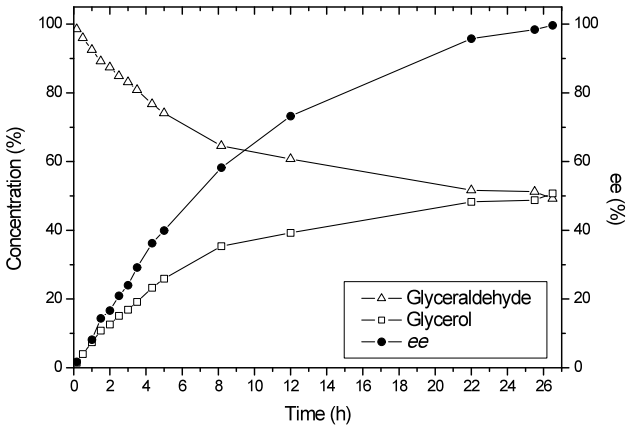

Figure 8: Kinetic resolution of glyceraldehyde by Gox1615. The figure shows the development of the glycerol (□) and rac-glyceraldehyde (Δ) concentration over a period of 26 h. Concentrations were determined by HPLC. The determination of the *ee* for L-glyceraldehyde (●) was done using GC.

Discussion

In the present study, a GlyDH from *G. oxydans* (Gox1615) was successfully cloned, expressed, purified, and biochemically characterised. Gox1615 was annotated as a putative oxidoreductase and showed 32% homology to the protein sequence of the GlyDH GLD1 from *H. jecorina*.[12] Both enzymes favour the reduction of glyceraldehyde compared to DHA. Therefore, Gox1615 belongs to the glycerol: $NADP^+$ oxidoreductases (EC 1.1.1.72). Other purified and characterised enzymes belonging to this class are e.g. the GlyDH from *N. crassa*[10] and the GlyDH from rabbit skeletal muscle.[13] Among these known members of this enzymes class Gox1615 is the only GlyDH of bacterial origin.

Moreover, a quarternary structure comparison of the different GlyDHs showed a considerable difference between Gox1615 and the GlyDH from *N. crassa* in the native conformation of these enzymes. Our results indicate that Gox1615, much like the GlyDH from rabbit muscle, has a monomeric structure whereas the GlyDH from *N. crassa* is a tetrameric protein. A biochemical comparison of the described GlyDHs and Gox1615 revealed a number of similarities with respect to substrate specificity but also a number of differences concerning selectivity.

Regarding substrate specificity, Gox1615 acts on a broad substrate range in the reduction as well as in the oxidation reaction, with the reduction being the favoured reaction as evident from a 19-fold higher activity for D-glyceraldehyde compared to L-arabitol, the best substrate in the oxidation.

With respect to the oxidative potential Gox1615 has shown a broad acceptance of alcohols with up to six alcohol groups. The best specific activity has been reached in the oxidation of L-arabitol, where Gox1615 has oxidized the L-enantiomer with a specific activity of 2.5 U/mg whereas no conversion has been detected for the D-enantiomer. These results lead to the suggestion that like in the reduction the enzyme shows a stereo- and regioselectivity in the oxidation.

This broad substrate range together with the assumed stereo- and regioselectivity in the oxidation makes Gox1615 a versatile tool for enzymatic oxidation to produce chiral hydroxy-aldehydes. The enzymatic oxidation opens an environmentally-friendly process of great interest[27, 28] in contrast to metal catalysed chemical oxidations. Additionally, the chemical alternatives often suffer from the lack of regio- and stereoselectivity in oxidative processes; a complicated protecting group strategy is neccesary to obtain the desired products.[29-32] Therefore, the oxidative potential of Gox1615 is currently under investigation.

Due to the named preference for the reduction the main focus of this work was the investigation of the substrate specificity and selectivity in this reaction. We could show that Gox1615 reduces different aliphatic aldehydes revealing best activities with a medium chain length of C_4 to C_8 (entries 3, 4, 6), similar to the GlyDH from rabbit skeletal muscle. A comparison of the activity of the unsaturated aldehyde *trans*-2-hexen-1-al (entry 5) with hexenal (entry 4) has shown significant variations in the activity, indicating the preference for saturated substrates. Branched-chained and aromatic aldehydes (entries 13+14) have also been accepted by the enzyme, emphasising the broad substrate range of Gox1615 in the reduction of different aldehydes.

Table 4: Comparisson of the biochemical properties of Gox1615, GLD1 and the GlyDHs from *N. crassa* and rabbit skeletal muscle.

	Gox1615 (*G. oxydans*)	GLD1 (*H. jecorina*)	GlyDH (*N. crassa)*	GlyDH (rabbit skeletal muscle)
DHA acceptance (D-Ga* : DHA)	100 : 1	100 : 20	100 : 43	100 : 4
Stereopreference (D-Ga* : L-Ga*)	D-specific 100 : 4	no preference 100 : 93	D-specific 100 : 36	D-specific 100 : 36
Molecular weight	39,000 (monomer)	/	43,000 (tetramer)	34,000 (monomer)
pH Optimum	Reduction: 5.5 Oxidation: 10	/	Reduction: 6.5 Oxidation: 9.5	Reduction: 5.0 – 7.0

* Ga = glyceraldehyde

Interestingly, Gox1615 showed almost no activity in the reduction of ketones. The other GlyDHs so far known from the literature show an inferior selectivity in the discrimination of ketones and aldehydes than those observed for Gox1615. All four compared enzymes show the highest activity in the reduction of glyceraldehyde (entry 9), but differ in the ability to reduce DHA (entry 21). The GlyDH from *N. crassa* reduces DHA with 43% related to the activity obtained for D-glyceraldehyde, GLD1 with 20%, the GlyDH from rabbit skeletal muscle with 4%, whereas Gox1615 showed the lowest side activity towards DHA in the range of 1%, meaning a quite high regioselective reaction and a good discrimination of aldehydes and ketones among the compared enzymes.

Comparisons of the enantiopreference of the different GlyDHs show that, whilst GLD1 showed no enantiopreference in the reduction of glyceraldehyde, the other GlyDHs showed a preference for reducing the D-enantiomer. As a result of a lower activity in the reduction of L-glyceraldehyde compared to the activity with the D-enantiomer. Gox1615 reduced L-glyceraldehyde with only 4% of the activity reached for the D-enantiomer, compared to a higher activity (36%) obtained for the GlyDH from *N. crassa* and rabbit skeletal muscle (Tab. 4). Therefore, Gox1615 showed the best stereoselectivity as evident from a 9-fold lower activity with L-glyceraldehyde compared to the other GlyDHs. The enantiopreference has been proven by GC analysis, where Gox1615 has shown an ee >99% for L-glyceraldehyde.

Due to this excellent enantioselectivity a kinetic resolution of racemic DL-glyceraldehyde has been the primary focus. Kinetic resolutions using oxidoreductases are not often mentioned in literature. Only few examples are described, like the kinetic resolution of 2-substituted 1-propanols to produce enantiomerically enriched 2-substituted propanoic acids (*Brevibacterium sp.* and *Arthrobacter sp.*),[28] and the kinetic resolution of racemic bicyclo[3.3.1]nonane-2,6-dione (*Saccharomyces cerevisiae*)[33] whole wild-type or genetically engineered cells as the catalyst. More common are kinetic resolutions with hydrolases[33-35] due to their easy applications without the need for coupled cofactor regeneration systems. The advantage of using oxidoreductases for kinetic resolutions are the excellent stereoselectivity of these enzymes for most of the substrates, compared to hydrolases which often show moderate stereoselectivity, especially towards primary alcohols.[36]

Additionally, L-glyceraldehyde is a valuable chiral building block which has to be synthesised using expensive L-arabinose as starting material. Consequently L-glyceraldehyde has not been easily accessible at industrial scale. Furthermore, our results show that using Gox1615 in the kinetic resolution of glyceraldehyde the optimal conversion of 50% was reached with an *ee* >99%.[35] The kinetic resolution was also performed on preparative scale (4.05 g, 45 mmol) with a high *ee* value. Therefore the present direct enzymatic one-step preparation of enantiopure L-glyceraldehyde represents an important milestone towards a viable industrial bioprocess.

Experimental Section

General: If not stated otherwise all chemicals were purchased from Sigma Aldrich. All columns and instruments for chromatography (FPLC, Äkta-Explorer) were purchased from GE Healthcare. Centrifugations were carried out using the centrifuges RC5BPlus (Sorvall), Mikro22 and Rotina 35 R (Hettich). For analytical methods GC-17A and LC-20AHT (both Shimadzu) were used. Restriction enzymes were purchased from Fermentas. The studied GlyDH is commercially available at evocatal (evo-1.1.190).

Molecular cloning of the GlyDH-gene: Genomic DNA from *G. oxydans* (DSM 2323) was used as template for the amplification of the *glydh* gene. For the following cloning steps primers with recognition sites for the restriction enzymes *Nde*I and *Sal*I were used for the construction of the enzyme with N-terminal his-tag in pET-28a (5'- ATA TAT ACA TAT GGC ATC CGA CAC CAT CCG CAT CCC C -3' and 5'- ATA TGT CGA CTC AGT CCC GTG CCG GGG GC -3'). The PCR product was cloned into pET-28b (Novagen) between the *Nde*I and *Sal*I restriction sites using standard techniques.

Heterologous expression of the GlyDH: *E. coli* BL21(DE3) cells carrying the recombinant plasmid were cultivated in 5 ml LB medium [22] containing 100 µg/ml ampicillin overnight at 37°C. These cultures were used to inoculate different amounts of LB medium containing 100 µg/ml ampicillin for expression in shaking flasks at a final concentration of 0.05 optical density at 600 nm (OD_{600}). The cultures were grown at 37°C. When the OD_{600} reached 0.5 to 0.7 the production of the recombinant GlyDH was induced by addition of isopropyl thio-β-D-galactoside (IPTG) to a final concentration of 0.3 mM. For the determination of the optimal growth conditions cultures were grown at 25, 30 and 37°C (after induction), and assayed after a period of 20 h.

Purification of the GlyDH: The bacterial culture was harvested by centrifugation at 17,000 x g for 20 min at 4°C. A cell suspension (10%) was prepared in 100 mM triethanolamine buffer (TEA) pH 7. Cells were disrupted by five sonification cycles of 5 min (40% power output) with cooling periods in-between. The lysed cells were centrifuged at 17,000 x g for 30 min at 4°C, and the supernatant was used for further purification steps. The enzyme was purified from the crude extract using immobilised metal affinity chromatography IMAC (Ni-NTA (Qiagen)). The column was equilibrated with TEA buffer (50 mM, pH 7). The GlyDH was eluted using a linear gradient of imidazole (0 to 500 mM) in TEA buffer. After a desalting step by gel-filtration on Sephadex G 25 (Pharmacia) the enzyme was stored freeze dried and kept at -20°C until use.

Activity assay: A continuous assay using UV absorbance at 340 nm was employed to monitor the NADPH concentration during reduction or oxidation catalysed by GlyDH. For the enzymatic reduction racemic glyceraldehyde was used as standard substrate. One unit of activity was defined as the amount of enzyme which catalyses the oxidation of 1 µmol NADPH per minute under standard conditions (30°C, pH 7). The reduction assay mixture contains 970 µl substrate solution (10 mM substrate in 100 mM TEA buffer pH 7), 20 µl NADPH (12.5 mM) in *A. dest.* and 10 µl enzyme solution. For the oxidation the standard conditions were 37°C and pH 9.7 using L-arabitol as standard substrate. The assay mixture contains 990 µl assay solution (1 mM NADP, 30 mM ammonium sulfate and 100 mM substrate in 100 mM potassium carbonate buffer pH 9.7) and 10 µl enzyme solution. Reactions were started by addition of the enzyme solution and measured over 1 min.

Protein analysis: Protein concentrations were determined according to Bradford using BSA as a standard.[23] SDS-PAGE was performed using 4–12% Bis-Tris gels in MOPS (3-(*N*-Morpholino) propanesulfonic acid) buffer (Invitrogen), Mark 12 Protein Standard (Invitrogen) was used for molecular weight estimation of proteins. The molecular mass of the GlyDH was determined using size-exclusion chromatography. Therefore, a BioSep SEC S2000-HPLC column (300 x 7.8 mm, Phenomenex) connected to a Shimadzu LC-20AHT system with 200 mM Tris-HCl buffer pH 7.5 as mobile phase (1 ml/min) was used. The lyophilized protein and the protein standard (AQUEOUS SEC 1, Phenomenex) were dissolved in 200 mM Tris-HCl buffer pH 7.5 and analysed by HPLC.

Determination of pH and temperature optima: In order to obtain the temperature optimum of the GlyDH the standard reduction enzyme assay was performed at different temperatures. The pH optimum was determined using both standard assays at different pH values (reduction and oxidation). For the investigation of the pH optimum of reduction the standard activity buffer TEA (pH 6.8 to 10.0) as well as citrate-phosphate buffer (pH 3.0 to 7.0) was used. For the oxidation potassium carbonate buffer (pH 9.2 to 11.0) and TEA buffer (pH 7.0 to 9.2) were used.

Stability investigations: For the investigation of temperature and pH stability the enzyme was incubated at different temperatures and pH values, respectively. At appropriate time intervals samples were taken and the residual activity was assayed using the standard reduction assay. For the determination of the midpoint of thermal inactivation (T_m) each temperature was kept for 10 min before samples were withdrawn to determine the residual activity.

Determination of kinetic constants: To determine the kinetic constants (K_M und V_{max}) the standard activity assays of reduction and oxidation were used. All parameters were kept constant, only the investigated parameter, cofactor- or substrate concentration was modified.

Preparative kinetic resolution of glyceraldehyde: The reaction mixture was prepared by dissolving racemic glyceraldehyde (4.05 g, 0.045 mol, 150 mM), glucose (8.92 g, 0.045 mol, 150 mM), ammonium sulfate (7.93 g ,0.06 mol, 200 mM) and $NADP^+$ (0.12 g, 0.15 mmol, 0.5 mM) in potassium phosphate buffer (250 mL, 100 mM, pH 7). The reaction was started by addition of GOX1615 crude extract (50 mL, 700 U) and glucose dehydrogenase from *Thermoplasma acidophilum* (300 µL, 460 U, Sigma G5909). Samples (50 µL) were taken periodically and diluted either with trifluoroacetic acid (300 µL, 0.5 M) for HPLC analysis or with ethyl acetate (300 µL) for GC analysis. GC samples were derivatized for 30 minutes with acetic anhydride (100 µL) and pyridine (10 µL). Concentrations of glyceraldehyde and glycerol were determined by using an Agilent 1100 HPLC equipped with a CS organic acid resin column (300 mm x 8 mm) with 5 mM trifluoroacetic acid (0.7 mL min^{-1}) at 5°C. The enantiomeric ratio for glyceraldehyde was determined by using a HP 6890 GC with a Varian CP-Chirasil-Dex CB column (25 m x 0.32 mm).

Acknowledgements

This project was supported by funds from the Deutsche Bundesstiftung Umwelt (DBU); project number Az13194

Keywords: $NADP^+$-dependent glycerol dehydrogenase · glycerol dehydrogenase · *Gluconobacter oxydans* · kinetic resolution · enantioselecitvity · L-glyceraldehyde

[1] M. Wills, J. Hannedouche, *Curr. Opin. Drug Discovery Dev.* **2002**, *5*, 881-891.
[2] M. Wills, M. Gamble, M. Palmer, A. Smith, J. Studley, J. Kenny, *J. Mol. Catal. A: Chem.* **1999**, *146*, 139-148.
[3] A. M. Rouhi, *Chem. Eng. News* **2004**, *82*, 47-62.
[4] J. A. Pesti, R. DiCosimo, *Curr. Opin. Drug Discovery Dev.* **2003**, *6*, 884-901.
[5] R. N. Patel, *Curr. Opin. Drug Discovery Dev.* **2006**, *9*, 741-764.
[6] P. Areces, E. Carrasco, M. E. Light, M. Santos, J. Plumet, *Synlett* **2007**, 3180-3182.
[7] J. Bi, V. K. Aggarwal, *Chem. Commun.* **2008**, 120-122.
[8] J. Jurczak, S. Pikul, T. Bauer, *Tetrahedron* **1986**, *42*, 447-488.
[9] E. Baer, H. O. L. Fischer, *J. Biol. Chem.* **1939**, *128*, 463-473.
[10] M. Viswanathreddy, J. E. Pyle, H. B. Howe, *J. Gen. Microbiol.* **1978**, *107*, 289-296.
[11] G. H. Sheys, W. J. Arnold, J. A. Watson, J. A. Hayashi, C. C. Doughty, *J. Biol. Chem.* **1971**, *246*, 3824-3827.
[12] J. Liepins, S. Kuorelahti, M. Penttila, P. Richard, *FEBS Journal* **2006**, *273*, 4229-4235.
[13] A. W. Kormann, R. O. Hurst, T. G. Flynn, *Biochim. Biophys. Acta* **1972**, *258*, 40-&.
[14] W. F. Bosron, R. L. Prairie, *J. Biol. Chem.* **1972**, *247*, 4480-4485.
[15] K. Yamada-Onodera, A. Nakajima, Y. Tani, *J. Biosci. Bioeng.* **2006**, *102*, 545-551.
[16] P. Spencer, K. J. Bown, M. D. Scawen, T. Atkinson, M. G. Gore, *Biochim. Biophys. Acta* **1989**, *994*, 270-279.
[17] A. Pandey, L. Iyengar, *J. Enzyme Inhib. Med. Chem.* **2002**, *17*, 49-53.
[18] H. Nishise, A. Nagao, Y. Tani, H. Yamada, *Agric. Biol. Chem.* **1984**, *48*, 1603-1609.
[19] R. E. Asnis, A. F. Brodie, *J. Biol. Chem.* **1953**, *203*, 153-159.
[20] R. Schuurink, R. Busink, D. H. A. Hondmann, C. F. B. Witteveen, J. Visser, *J. Gen. Microbiol.* **1990**, *136*, 1043-1050.
[21] U. Deppenmeier, M. Hoffmeister, C. Prust, *Appl. Microbiol. Biotechnol.* **2002**, *60*, 233-242.
[22] G. Bertani, *J. Bacteriol.* **1951**, *62*, 293-300.
[23] M. M. Bradford, *Anal. Biochem.* **1976**, *72*, 248-254.
[24] C. Prust, M. Hoffmeister, H. Liesegang, A. Wiezer, W. F. Fricke, A. Ehrenreich, G. Gottschalk, U. Deppenmeier, *Nat. Biotechnol.* **2005**, *23*, 195-200.
[25] I. Kumar, S. R. Bhide, C. V. Rode, *Tetrahedron: Asymmetry* **2007**, *18*, 1210-1216.
[26] J. A. Bull, E. P. Balskus, R. A. J. Horan, M. Langner, S. V. Ley, *Chemistry* **2007**, *13*, 5515-5538.
[27] A. Romano, R. Gandolfi, P. Nitti, M. Rollini, F. Molinari, *J. Mol. Catal. B: Enzym.* **2002**, *17*, 235-240.
[28] K. Miyamoto, K. Fujimori, J. I. Hirano, H. Ohta, *Biocatal. Biotransform.* **2009**, *27*, 66-70.
[29] C. J. Tang, Y. K. Wu, *Tetrahedron* **2007**, *63*, 4887-4906.
[30] T. Sambaiah, P. E. Fanwick, M. Cushman, *J. Org. Chem.* **2001**, *66*, 4405-4408.
[31] M. S. M. Pearson, R. Plantier-Royon, J. Szymoniak, P. Bertus, J. B. Behr, *Synthesis* **2007**, 3589-3594.
[32] M. G. Banwell, C. De Savi, D. C. R. Hockless, S. Pallich, K. G. Watson, *Synlett* **1999**, 885-888.
[33] M. Carlquist, C. J. Wallentin, K. Warnmark, M. F. Gorwa-Grauslund, *Tetrahedron: Asymmetry* **2008**, *19*, 2293-2295.
[34] C. Sanfilippo, G. Nicolosi, *Tetrahedron: Asymmetry* **2008**, *19*, 2171-2176.
[35] U. T. Bornscheuer, R. J. Kazlauskas, *Hydrolases in Organic Synthesis* 2nd ed., Wiley VCH, Weinheim, **2006**.
[36] T. Ohtani, H. Nakatsukasa, M. Kamezawa, H. Tachibana, Y. Naoshima, *J. Mol. Catal. B: Enzym.* **1998**, *4*, 53-60.

2.2 EXPLORING THE SCOPE OF GLYCEROL DEHYDROGENASE FROM *GLUCONOBACTER OXYDANS* IN THE OXIDATION OF SUGAR ALCOHOLS

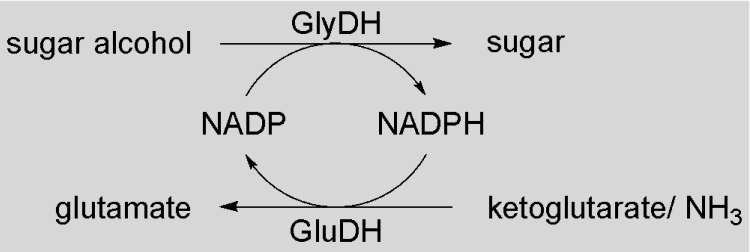

Nina Richter, Lothar Elling and Werner Hummel

Manuscript in preparation

Exploring the scope of glycerol dehydrogenase from *Gluconobacter oxydans* in the oxidation of sugar alcohols

Nina Richter[a], Lothar Elling[b], Werner Hummel[c*]

[a]evocatal GmbH, Merowingerplatz 1a, 40225 Düsseldorf, Germany
[b]Lehrstuhl für Biotechnologie und Helmholtz-Institut für Biomedizinische Technik, RWTH Aachen, Worringer Weg 1, 52056 Aachen, Germany
[c]Institut für Molekulare Enzymtechnologie, Heinrich-Heine-Universität Düsseldorf, Forschungzentrum Jülich, Stetternicher Forst
52426 Jülich, Germany

* corresponding author. Phone: (+49)2461-61-3790, fax: (+49)2461-61-2490
E mail: w.hummel@fz-juelich.de

The scope of glycerol dehydrogenase (GlyDH) from Gluconobacter oxydans in the oxidation of alcohols has been explored. With respect to substrate range of the enzyme a variety of different alcohols are accepted, whereas the best activity was observed in the oxidation of L-arabitol (2.5 U/mg). The biotransformation of glycerol revealed that a massive product inhibition was observed, caused by the produced aldehyde. Interestingly, this inhibition was not observed when sugar alcohols where used as substrate, because the formed straight-chain aldoses are able to form hemiacetal leading to cyclic pyranoses or furanoses. As case studies the conversions of two sugar alcohols (ribitol and L-arabitol) were investigated in terms of regio- and stereoselectivity of GlyDH. Because in general, GlyDH exhibits a high regio- as well as stereoselectivity. The enzyme only catalyses the oxidation of terminal hydroxy group, the only requirement is the L-cofiguration of the adjacent hydroxy group. The observed results make the GlyDH from G. oxydans a promising catalyst for applications in asymmetric enzymatic oxidation, for example in the production of rare sugars.

Introduction

The oxidation of alcohols is one of the most fundamental and important reactions in organic chemistry. Conventional chemical methods are often based on stochiometric amounts of toxic metal catalysts such as chromium, a major disadvantage in terms of environmental issues[1-5]. Therefore, catalytic aerobic methods have been developed recently, which are environmentally acceptable[1, 6-8]. Major drawbacks of these methods are that they lack selectivity, especially chemoselectivity leading to a common occurrence of side reactions. Moreover, a regio- and stereoselective oxidation is extremely difficult and requires a complex protection group strategy when more than one hydroxyl group is present. Therefore, biocatalytic methods offer a great potential with respect to environmental compatibility and catalytic efficiency. In addition, enzymes exhibit high chemo-, regio- and stereoselectivity without the need of protection groups[9-11].

Enzymes which are capable to catalyse the selective oxidation belonging to the oxidoreductase family, (E.C. 1.X.X.X), most frequently dehydrogenases or oxidases, have been applied[12].
Both are cofactor dependent enzymes, which need either nicotinamide or molecular oxygen as carrier for redox equivalents. Oxidases on the one hand do not require a regeneration of the cofactor, but based on the simultaneous production of hydrogen peroxide an addition of catalase is necessary to decompose the formed hydrogen peroxide. Dehydrogases on the other hand need a suitable regeneration system for the expensive oxidised cofactor and to shift the unfavourable equilibrium, but dehydrogenases do not form a harmful by-product.
Nevertheless, due to their high chemo-, regio- and stereospecificity dehydrogenases are interesting catalysts, and have been applied in the oxidation of different alcohols. During the last decades much work has been devoted to the oxidative application of dehydrogenases in the kinetic resolution of racemic

alcohols[13-18]. The use of dehydrogenases for the asymmetric oxidation is much more interesting according to the fact that in contrast to the kinetic resolution (max. 50%) 100% yield can be obtained. The selective enzymatic oxidation even becomes considerable more interesting when complex molecules such as polyols are used as substrates. Various examples of the oxidation of sugar alcohols using predominantly whole-cell systems can be found in literature[9-11,19-25]. The majority of the described processes employ acetic acid bacteria, which are well known for a long time for their oxidative potential. A prominent example is *Gluconobacter oxydans*, which is known to catalyse the oxidation of a wide range of substrates, such as alcohols, sugars, and sugar alcohols by numerous membrane-bound and cytosolic oxidoreductases[26-28]. *G. oxydans* is applied for example, in the industrial production of 2-keto-L-gulonic acid, a vitamin C precursor, or of 6-amino-L-sorbose, a miglitol precursor or for the production of DHA, an ingredient in tanning agents[28].

Furthermore, through the asymmetric enzymatic oxidation the production of different sugars is possible, especially rare sugars are of major interest[19-25, 29]. According to the fact that they are not abundant in nature they are one of the most worthy targets for various applications in the food, pharmaceutical and nutrition industries[20]. For instance, unnatural sugars can be applied as sweeteners to reduce calories or for diabetics. Moreover, they can be used as bulking agents, precursor compounds and nucleoside analogues. However, the use of dehydrogenases is limited by the fact that the unfavourable equilibrium has to be shifted by coupling of the primary reaction with an efficient cofactor regeneration system.

Recently, we described the cloning, expression, characterisation and application of a glycerol dehydrogenase (GlyDH) from *G. oxydans*[29]. GlyDH is a 39 kDa monomeric $NADP^+$-dependent dehydrogenase which catalyses the reduction of a variety of different aldehydes. Highest activity in the range of 46 U/mg was reached in the stereoselective reduction of D-glyceraldehyde. Although GlyDH strongly favours the reduction reaction, as evident from a 19-fold higher specific activity compared to the oxidation reaction, the oxidation of a variety of alcohols and polyols is possible with sufficient activity. Furthermore, the oxidation was presumed to be catalysed in a stereo- and regioselective manner. Optimal activity in the oxidation was observed at a pH of 10.0.

Herein, we report the investigation of the biocatalytic potential of the GlyDH in the oxidation of different alcohols and sugar alcohols. Furtheron, the regio- and stereoselectivity of the GlyDH was studied in detail.

Results and Discussion

Substrate specificity of the GlyDH in the oxidation

Preliminary tests revealed that GlyDH catalyses the oxidation of different alcohols, particularly sugar alcohols, with rather high activities (in the range of 0.1 – 2.5 U/mg). Table 1 summarises the substrate range of GlyDH in the oxidation. The comparison of the oxidation of primary and secondary alcohols revealed that GlyDH has a preference for primary alcohols. For example, 1-hexanol (**1**) was accepted with an activity of 0.74 U/mg, while 2-hexanol (**2**) proved to be a poor substrate, with an activity of 0.22 U/mg. Additionally, 1,2-diols were also reasonably good substrates, indicating that two adjacent hydroxyl groups at C1 and C2 are required for a good activity of GlyDH. For instance, 1,2-butandiol (**7**) was converted with an activity of 0.66 U/mg, an activity of only 0.21 U/mg was observed for the oxidation of 1,4-butandiol (**6**), and a very low activity of 0.04 U/mg was observed for the poor substrate 1,3-butandiol (**8**). In regards to the comparison of the different sugar alcohol substrates, GlyDH showed highest activity with L-arabitol (2.46 U/mg).

Due to the observation that GlyDH primarily acts on sugar alcohols, kinetic parameters for L-arabitol were determined: k_M=193 ±11 mM and v_{max}=8.67 ± 0.2U/mg[29]. These data indicate that oxidation is not the favoured reaction, as evident from a rather high k_M value and the 19-fold higher activity in the reduction of D-glyceraldehyde. However, the observation that only the terminal hydroxy group is oxidised, as well as the fact that only the L-enantiomer (arabitol (**23**) and threitol (**20**)) is converted by GlyDH, leads to the suggestion that the enzyme exhibits a regio- and stereospecificity in the oxidation of sugar alcohols. To obtain more insight into the oxidative potential of the enzyme, we investigated the conversion of L-arabitol (**23**) and ribitol (**21**) in detail.

Inhibition of the GlyDH by free aldehyde

To identify a suitable model reaction, different substrates were tested with simultaneous cofactor regeneration. Interestingly, product formation was only observed when sugar alcohols were used as substrate. For instance, when glycerol was used, strong product inhibition was observed (Fig. 1, -■-). The residual activity in the presence of 10 mM glyceraldehyde was 35%. In contrast, the oxidation of ribitol in the presence of 10 mM product (ribose) resulted in a residual activity of 85% (Fig. 1, -▲-). Addition of glyceraldehyde in the oxidation of ribitol yielded results similar to those observed with glycerol as the substrate (Fig. 1, -○-). These results clearly indicated that the presence of a free aldehyde group led to an inhibition of GlyDH. Otherwise, when a C5 or C6 sugar alcohol was oxidised, no inhibition occurred. This can be explained by the fact that in aqueous solution, the formation of a hemiacetal structure occurs, forming cyclic pyranose or furanose structures.

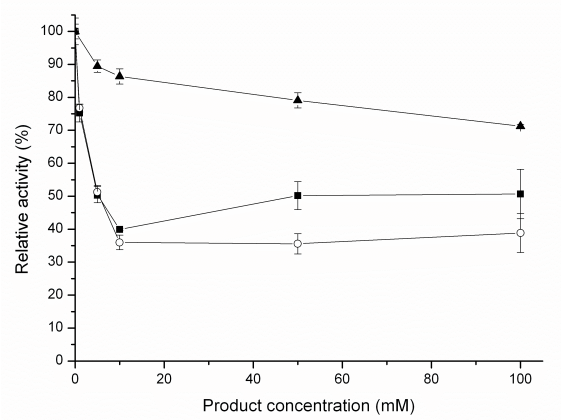

Fig. 1. Activity of GlyDH in the presence of different product concentrations. The residual activities of GlyDH during the oxidation of glycerol in the presence of glyceraldehyde (-■-) and the oxidation of ribitol in the presence of ribose (-▲-) and glyceraldehyde (-○-) are displayed.

Therefore, the observed inhibition was presumably caused by the produced free aldehyde. Explanations can be found by either product inhibition[14] or by an introduced modification of, for example, lysine residues involved in the catalytic mechanism by the produced aldehyde. The strong inhibition observed at even

Tab. 1: Substrate spectrum in the oxidation catalysed by the GlyDH from *G. oxydans*. The activity was determined using the standard spectrophotometric assay. 100% corresponds to 2.46 U/mg with L-arabitol.

	Substrate	Specific activity [U/mg]	Relative activity [%]
	Alcohols		
1	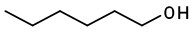	0.74	30.1
2	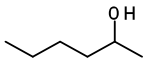	0.22	8.8
3	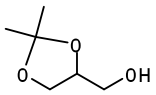	0.03	1.1
	diols		
4	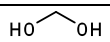	0.05	2.1
5		0.5	21.8
6	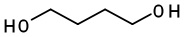	0.21	8.4
7	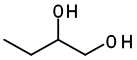	0.66	26.7
8	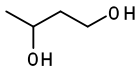	0.04	1.66
9		0.59	24.0
10	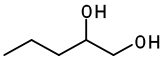	0.39	15.9
11	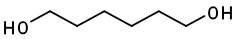	0.87	35.2
12	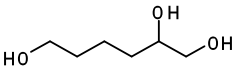	0.30	12.39
13	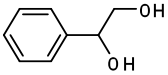	0.77	31.5
	triols		
14	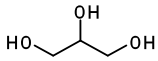	0.17	6.98
15	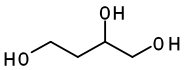	1.21	49.1
16	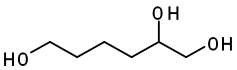	0.45	18.5
17	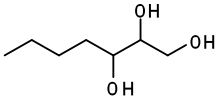	0.76	30.8
	sugar alcohols		
18	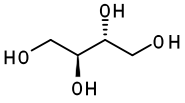	0.75	30.5
19	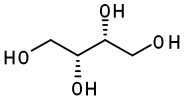	0	0
20	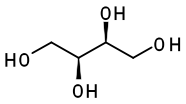	0.90	36.7
21	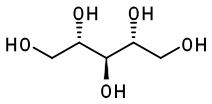	0.25	10.13
22	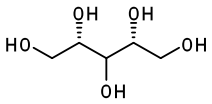	0	0
23	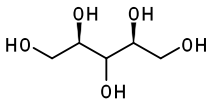	2.46	100
24	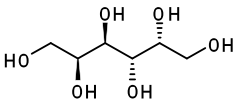	1.08	44.1

low aldehyde concentrations is rather uncommon for product inhibition. Therefore, an inactivation caused by a modification by lysine residues is more realistic. This modification can be caused by the Schiff base formation of an aldehyde and a lysine residue, which is common, especially at alkaline pH[30-32]. Unfortunately, a higher pH of approximately 10 is required for a feasible oxidation, whereas at a pH of 8, only 50% of residual activity is available.
Based on the three dimensional structure[33], two crucial lysine residues (Lys^{84} and Lys^{219}) were identified that may be involved in the observed inactivation. The inactivation seems to be a pH-dependent process based on the fact that there was no inhibition of the free aldehyde in the glyceraldehyde reduction at pH 7. Therefore, the oxidation reactions of substrates such as sugar alcohols are only possible if little or no free aldehyde is present. As a model reaction, the oxidation of L-arabitol and ribitol was performed.

GlyDH-catalysed oxidation of L-arabitol and ribitol

To facilitate a biotransformation of L-arabitol and ribitol, a suitable regeneration system is of major importance. Because the equilibrium of the reaction lies heavily in the reduction of aldehydes, it was essential to have a good regeneration system in the oxidation reaction to overcome this limitation.

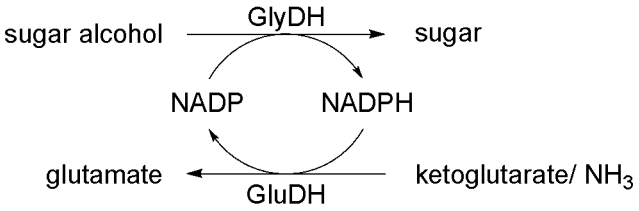

Fig. 2. Schematic overview of the oxidation of sugar alcohols by GlyDH with simultaneous cofactor regeneration of $NADP^+$, using GluDH and ketoglutarate as a co-substrate.

$NADP^+$-dependent glutamate dehydrogenase (GluDH) from *Escherichia coli* was applied to regenerate the oxidised cofactor using ketoglutarate as the co-substrate (Fig. 2). The conversion of L-arabitol and ribitol was possible by applying this strategy.

Figure 3 shows the result of the conversion of ribitol by GlyDH. The development of the ribose concentration over a period of 20 h was required for a full conversion.
In addition, the conversion of L-arabitol was studied (Fig. 4). After 41.5 h, a conversion of 100% was reached with an approximately 50% yield of arabinose.
Interestingly, the results of HPLC analysis revealed the formation of a second product with a rather similar retention time (Fig.5). When examining the structure of the substrate L-arabitol, it is interesting to observe that both terminal hydroxy groups are

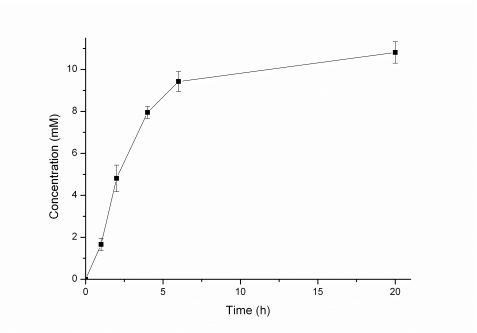

Fig. 3: Biotransformation of ribitol (10 mM) by GlyDH. The concentration of ribose was measured over a period of 20 h via HPLC.

located next to a hydroxy group with a L-configuration, indicating that an oxidation on both sides is possible. As a result, the formation of two different sugars, arabinose and lyxose, was observed (Fig. 6 (2)).

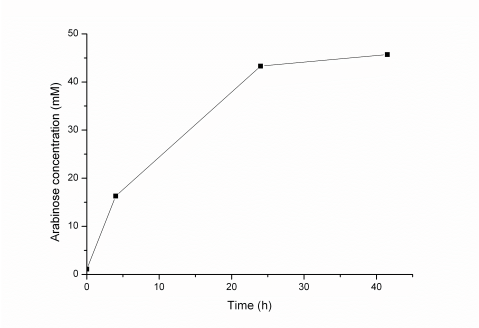

Fig. 4: Biotransformation of 100 mM L-arabitol catalysed by GlyDH. The conversion was followed over a period of 41.5 h, and concentrations were determined by HPLC.

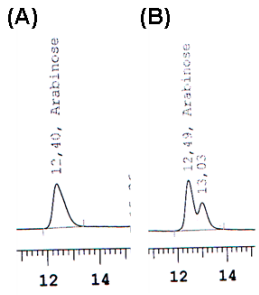

Fig. 5: HPLC-Chromatogram of arabinose reference (A) and the result of the GlyDH-catalysed conversion of L-arabinose (B).

According to the observed results using GlyDH, a number of other sugars can be synthesised by the oxidation of their corresponding sugar alcohols. The configuration of the product is based on the theoretical predictions, and the D-form is suggested in the case of ribose, while the L-form is suggested for arabinose and lyxose (Fig. 6).

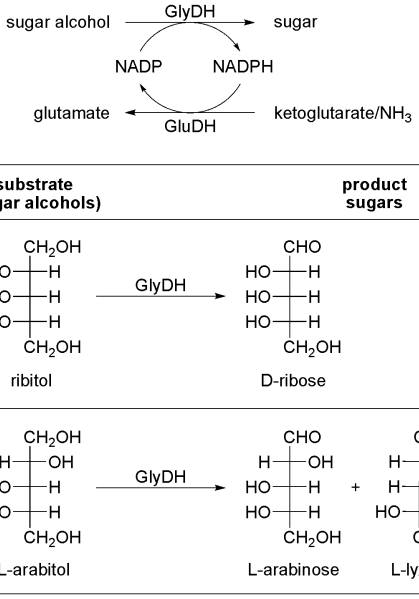

Fig. 6: Overview of the oxidation of ribitol (1) and L-arabitol (2) and the suggested products formed.

The fact that GlyDH accepts a variety of different sugar alcohols (Table 1) makes it an interesting catalyst in terms of enzymatic stereoselective oxidations.

Conclusion

In this paper, we discussed the oxidative potential of the GlyDH from *G. oxydans*. Although a massive product inhibition in the oxidation of different alcohols was observed, the oxidation of sugar alcohols was possible if the oxidation was coupled to the formation of a heterocyclic ring. The conversion of L-arabitol and ribitol were investigated in the case studies. Ribitol was fully converted to yield ribose, whereas L-arabitol was converted to arabinose and lyxose, based on the fact that both terminal hydroxy groups were oxidised by the enzyme. Theoretical predictions led to the assumption suggestion that the ribose is formed as the D-enantiomer while arabinose and lyxose are formed in the L-configuration. These results suggest that GlyDH is a promising catalyst for the application of a variety of different sugar alcohols in asymmetric oxidation.

Experimental Section

General: If not stated otherwise all chemicals were purchased from Sigma Aldich. Centrifugation was carried out using the centrifuges RC5BPlus (Sorvall), Mikro22 and Rotina 35 R (Hettich). For analytical methods HPLC equipped with a pumpe (PU-2080 plus) and autosampler (AS-2057 plus) (all Jasco, Groß-Umstadt, Germany) and a RI-detector LCD212 (Techlab GmbH, Erkerode, Germany) was used.

Expression and purification of the GlyDH: Glycerol dehydrogenase from *G. oxydans* was expressed fused to a N-terminal His-tag in *E. coli* BL21(DE3) and purified as described before[29].

Activity assay: A continuous assay using UV absorbance at 340 nm was employed to monitor the formation of NADPH during oxidation catalysed by GlyDH. One unit of activity was defined as the amount of enzyme which catalyses the reduction of 1 µmol $NADP^+$ per minute under standard conditions (37°C, pH 9.7). The assay mixture contained 990 µL assay solution (100 mM substrate, 1 mM $NADP^+$, 30 mM ammonium sulphate in 100 mM potassium phosphate buffer pH 9.7) and enzyme solution (10 µL). Reactions were started by addition of the enzyme solution and measured over 1 min. All measurements were carried out at least in triplicate.

Oxidation of glycerol and ribitol in the presence of glyceraldehyde: In order to investigate the effect of the formed produced aldehyde the standard activity assay was performed in the presence of 0 mM to 100 mM of the corresponding aldehyde.

Oxidation of ribitol: For the oxidation of ribitol the reaction mixture contained: 10 mM L-arabitol, 5 mM $NADP^+$, 1 U GlyDH, 20 U GluDH, 100 mM ammonium sulfate in 100 potassium carbonate buffer pH 9.7. The conversion was performed at 25ºC under continuous shaking. Samples were taken periodically and incubated at 85ºC for 5 min to denaturate the proteins followed by a separation *via* centrifugation (14,000 rpm, 5 min). The supernatant was analysed by HPLC equipped with a Nucleodur NH_2/NH_2-RP (Macherey Nagel, Düren, Germany) column using a mixture of acetonitril/water (80:20) as eluent at a flow rate of 0.6 ml/min and a temperature of 25ºC.

Oxidation of L-arabitol: For the oxidation of L-arabitol the reaction mixture contained: 100 mM L-arabitol, 5 mM $NADP^+$, 2 U GlyDH, 10 U GluDH, 150 mM ammonium sulfate in 100 potassium carbonate buffer pH 9.7. The conversion was performed at 25ºC under continuous shaking. Samples were taken periodically and incubated at 85ºC for 5 min to denaturate the proteins followed by a separation *via* centrifugation (14,000 rpm, 5 min). The supernatant was analysed by HPLC equipped with a Rezex 8% Ca column (Phenomenex, Aschaffenburg) using 0.085 N H_2SO_4 as eluent at a flow rate of 0.6 ml/min and a temperature of 80ºC.

Acknowledgements

We would like to thank Beatrix Paschold for great technical assistance, and Robert Simon for his ongoing support with respect to all chemical issues.

Keywords: glycerol dehydrogenase, asymmetric oxidation, Gluconobacter oxydans, rare sugars, sugar alcohols

References

[1] **Sheldon, R. A. and Arends, I.** Organocatalytic oxidations mediated by nitroxyl radicals. *Adv. Synth. Catal.* 2004. **346**: 1051-1071.

[2] **Sambaiah, T., Fanwick, P. E. and Cushman, M.** Investigation of an unexpected addition reaction that occurs when 2,3: 4,5-di-O-isopropylidene-D-ribose diethyl dithioacetal is treated with mercuric oxide and mercuric chloride. *J. Org. Chem.* 2001. **66**: 4405-4408.

[3] **Pearson, M. S. M., Plantier-Royon, R., Szymoniak, J., Bertus, P. and Behr, J. B.** Synthesis of a 5-spirocyclopropyl deoxyrhamnojirimycin as a constrained naringinase inhibitor. *Synthesis* 2007: 3589-3594.

[4] **Banwell, M. G., De Savi, C., Hockless, D. C. R., Pallich, S. and Watson, K. G.** Syntheses of the D-aldopentoses from non-carbohydrate sources. *Synlett* 1999: 885-888.

[5] **Tang, C. J. and Wu, Y. K.** On the synthesis of cepacin A. *Tetrahedron* 2007. **63**: 4887-4906.

[6] **Velusamy, S. and Punniyamurthy, T.** Novel vanadium-catalyzed oxidation of alcohols to aldehydes and ketones under atmospheric oxygen. *Org. Lett.* 2004. **6**: 217-219.

[7] **Okoro, H. K. and Odebunmi, E. O.** Kinetics and mechanism of oxidation of sugar and sugar alcohols by $KMnO_4$. *Int. J. Phys. Sci.* 2009. **4**: 471-476.

[8] **Zhan, B.-Z. and Thompson, A.** Recent developments in the aerobic oxidation of alcohols. *Tetrahedron* 2004. **60**: 2917-2935.

[9] **Burton, S. G.** Oxidizing enzymes as biocatalysts. *Trends Biotechnol.* 2003. **21**: 543-549.

[10] **Kroutil, W., Mang, H., Edegger, K. and Faber, K.** Recent advances in the biocatalytic reduction of ketones and oxidation of *sec*-alcohols. *Curr. Opini. Chem. Biol.* 2004. **8**: 120-126.

[11] **Kroutil, W., Mang, H., Edegger, K. and Faber, K.** Biocatalytic oxidation of primary and secondary alcohols. *Adv. Synth. Catal.* 2004. **346**: 125-142.

[12] **Schmid, R. D. and Urlacher, V. B.,** *Modern biooxidation*. Wiley-VCH, Weinheim: 2007.

[13] **Hummel, W., Kuzu, M. and Geueke, B.** An efficient and selective enzymatic oxidation system for the synthesis of enantiomerically pure D-tert-leucine. *Org. Lett.* 2003. **5**: 3649-3650.

[14] **Liese, A., Karutz, M., Kamphuis, J., Wandrey, C. and Kragl, U.** Enzymatic resolution of 1-phenyl-1,2-ethanediol by enantioselective oxidation: Overcoming product inhibition by continuous extraction. *Biotechnol. Bioeng.* 1996. **51**: 544-550.

[15] **Yamamoto, H., Kawada, K., Matsuyama, A. and Kobayashi, Y.** Cloning and expression in *Escherichia coli* of a gene coding for a secondary alcohol dehydrogenase from *Candida parapsilosis*. *Biosci. Biotechnol. Biochem.* 1999. **63**: 1051-1055.

[16] **Hummel, W. and Riebel, B.** Chiral alcohols by enantioselective enzymatic oxidation. *Enzyme Engin. XIII* 1996. **799**: 713-716.

[17] **Geueke, B., Riebel, B. and Hummel, W.** NADH oxidase from *Lactobacillus brevis*: a new catalyst for the regeneration of NAD. *Enzyme Microb. Technol.* 2003. **32**: 205-211.

[18] **Matsuyama, A., Yamamoto, H., Kawada, N. and Kobayashi, Y.** Industrial production of *(R)*-1,3-butanediol by new biocatalysts. *J. Mol. Catal. B-Enzym* 2001. **11**: 513-521.

[19] **Ahmed, Z., Shimonishi, T., Bhuiyan, S. H., Utamura, M., Takada, G. and Izumori, K.** Biochemical preparation of L-ribose and L-arabinose from ribitol: a new approach. *J. Biosci. Bioeng.* 1999. **88**: 444-448.

[20] **Ahmed, Z.** Production of natural and rare pentoses using microorganisms and their enzymes. *Electron. J. Biotechnol.* 2001. **4**: 1-9.

[21] **Jones, N. A., Rao, D., Yoshihara, A., Gullapalli, P., Morimoto, K., Takata, G., Hunter, S. J., Wormald, M. R., Dwek, R. A., Izumori, K. and Fleet, G. W. J.** Green syntheses of new 2-C-methyl aldohexoses and 5-C-methyl ketohexoses: D-tagatose-3-epimerase (DTE)-a promiscuous enzyme. *Tetrahedron Asymmetry* 2008. **19**: 1904-1918.

[22] **De Muynck, C., Pereira, C., Soetaert, W. and Vandamme, E.** Dehydrogenation of ribitol with *Gluconobacter oxydans*: Production and stability of L-ribulose. *J. Biotechnol.* 2006. **125**: 408-415.

[23] **Yun, M., Moon, H. R., Kim, H. O., Choi, W. J., Kim, Y. C., Park, C. S. and Jeong, L. S.** A highly efficient synthesis of unnatural L-sugars from D-ribose. *Tetrahedron Lett.* 2005. **46**: 5903-5905.

[24] **van Hellemond, E. W., Vermote, L., Koolen, W., Sonke, T., Zandvoort, E., Heuts, D., Janssen, D. B. and Fraaije, M. W.** Exploring the biocatalytic scope of alditol oxidase from *Streptomyces coelicolor*. *Adv. Synth. Catal.* 2009. **351**: 1523-1530.

[25] **Heuts, D. P. H. M., van Hellemond, E. W., Janssen, D. B. and Fraaije, M. W.** Discovery, characterization, and kinetic analysis of an alditol oxidase from *Streptomyces coelicolor*. *J. Biol. Chem.* 2007. **282**: 20283-20291.

[26] **Prust, C., Hoffmeister, M., Liesegang, H., Wiezer, A., Fricke, W. F., Ehrenreich, A., Gottschalk, G. and Deppenmeier, U.** Complete genome sequence of the acetic acid bacterium *Gluconobacter oxydans*. *Nat. Biotechnol.* 2005. **23**: 195-200.

[27] **Gupta, A., Singh, V. K., Qazi, G. N. and Kumar, A.** *Gluconobacter oxydans*: Its biotechnological applications. *J. Mol. Microbiol. Biotechnol.* 2001. **3**: 445-456.

[28] **Deppenmeier, U., Hoffmeister, M. and Prust, C.** Biochemistry and biotechnological applications of Gluconobacter strains. *App. Microbiol. Biotechnol.* 2002. **60**: 233-242.

[29] **Richter, N., Neumann, M., Liese, A., Wohlgemuth, R., Eggert, T. and Hummel, W.** Characterisation of a recombinant NADP-dependent glycerol dehydrogenase from *Gluconobacter oxydans* and its application in the production of L-glyceraldehyde. *ChemBioChem* 2009. **10**: 1888-1896.

[30] **Dax, C., Coincon, M., Sygusch, J. and Blonski, C.** Hydroxynaphthaldehyde phosphate derivatives as potent covalent Schiff base inhibitors of fructose-1,6-bisphosphate aldolase. *Biochemistry* 2005. **44**: 5430-5443.

[31] **Cho, S. W., Yoon, H. Y., Ahn, J. Y., Lee, E. Y. and Lee, J.** Cassette mutagenesis of lysine 130 of human glutamate dehydrogenase *Eur. J. Biochem.* 2001. **268**: 3205-3213.

[32] **Weber, H. K., Zuegg, J., Faber, K. and Pleiss, J.** Molecular reasons for lipase-sensitivity against acetaldehyde. *J. Mol. Catal. B Enzym.* 1997. **3**: 131-138.

[33] **Richter, N., Breicha, K., Hummel, W. and Niefind, K.** The three-dimensional structure of AKR11B4, a glycerol dehydrogenase from *Gluconobater oxydans* reveals a tryptophan residue as an accelerator of the reaction turnover. J. Mol. Biol. 2010. **404**: 353-362

2.3 BIOCHEMICAL CHARACTERISATION OF A NADPH-DEPENDENT CARBONYL REDUCTASE FROM *NEUROSPORA CRASSA* REDUCING α- AND β- KETO ESTERS

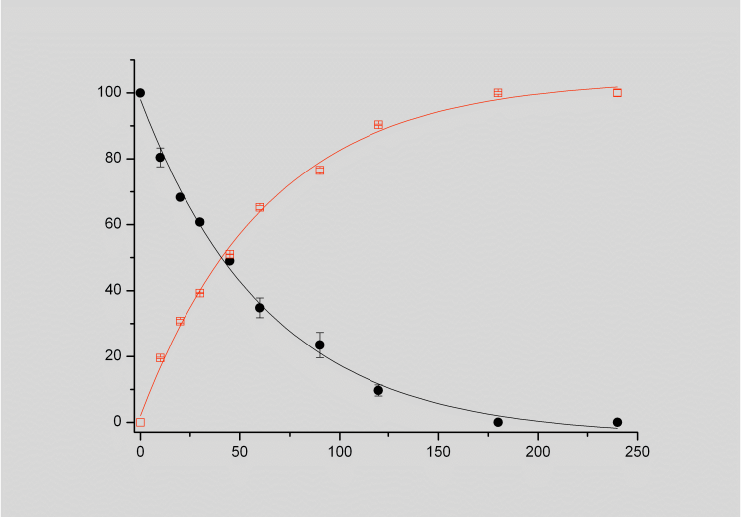

Nina Richter and Werner Hummel (2011)

Enzyme Microb. Tech. in press

(doi: 10.1016/j.enzmictec.2011.02.004)

FULL PAPERS

Biochemical characterisation of a NADPH-dependent Carbonyl Reductase from *Neurospora crassa* recucing α- and β- Keto esters

Nina Richter[a], Werner Hummel[b*]

A gene encoding an NADPH-dependent carbonyl reductase from Neurospora crassa (nccr) was cloned and heterologously expressed in Escherichia coli. The enzyme (NcCR) was purified and biochemically characterised. NcCR exhibited a restricted substrate spectrum towards various ketones, and the highest activity (468 U/mg) was observed with dihydroxyacetone. However, NcCR proved to be very selective in the reduction of different α- and β-keto esters. Several compounds were converted to the corresponding hydroxy ester in high enantiomeric excess (ee) at high conversion rates. The enantioselectivity of NcCR for the reduction of ethyl 4-chloro-3-oxobutanoate showed a strong dependence on temperature. This effect was studied in detail, revealing that the ee could be substantially increased by decreasing the temperature from 40 °C (78.8%) to -3 °C (98.0%). When the experimental conditions were optimised to improve the optical purity of the product, (S)-4-chloro-3-hydroxybutanoate (ee 98.0%) was successfully produced on a 300 mg (1.8 mmol) scale using NcCR at -3 °C.

1. Introduction

Oxidoreductases are cofactor-dependent enzymes that are ubiquitously distributed and known to catalyse a variety of biotechnologically interesting reactions. Members of this enzyme family include alcohol dehydrogenases (ADHs), which are excellent catalysts because of their ability to reduce prochiral ketones and α- and β-keto esters in a highly stereoselective manner. The resulting alcohols are often obtained with good chemo-, regio- and enantioselectivity. These features make them versatile tools for the production of chiral building blocks, which can act as key intermediates in the production of fine chemicals, pharmaceuticals and natural products [1-7].

Enantiomerically pure α- and β-hydroxy esters are of great interest as such building blocks. Consequently, significant effort has been devoted to the chemical and enzymatic production of these compounds [8-11].

One prominent example of a commonly used β-hydroxy ester is optically pure 4-chloro-3-hydroxybutanoate (CHBE); the (*R*)-enantiomer serves as an important precursor for L-carnitine [12, 13], whereas the (*S*)-enantiomer is a chiral building block for various pharmaceuticals [14, 15]. Because of its significance, a variety of chiral metal complexes have been developed to catalyse the asymmetric chemical reduction of prochiral ketones [16-19]. A significant number of processes have been reported with either isolated enzymes [20, 21], whole cell systems [8, 22-24] or even two-strain systems [25].

Due to the potential applications of such molecules, specifically in the field of pharmaceuticals, optical purity is important; the "wrong" enantiomer may be toxic or may have unpredictable side effects.

Unfortunately, even selective enzymes do not catalyse every reaction with the required enantioselectivity. The enantioselectivity of chemical and enzymatic reactions can be influenced by various factors [26-30]. Temperature has a significant impact on the stereochemistry of both chemical and enzymatic reactions [27, 28, 30, 31]. Phillips and co-workers extensively studied the effects of temperature on the enantioselectivity of enzymatic reactions using ADHs from horse liver and *Thermoanaerobacter ethanolicus* [27, 28, 31].

In this study, we describe the identification, cloning and heterologous expression of a novel carbonyl reductase gene from N. crassa (nccr). This NADPH-dependent carbonyl reductase reduces various α- and β-keto esters. Remarkably high activity was observed for the reduction of ethyl 4-chloro-3-oxobutanoate (COBE), but poor enantioselectivity of the corresponding alcohol

[a] *Nina Richter*
evocatal GmbH
Merowingerplatz 1a
40225 Düsseldorf (Germany)
[b] Prof. Dr. W. Hummel
Institut für Molekulare Enzymtechnologie, Heinrich-Heine Universität Düsseldorf,Forschungszentrum Jülich, Stetternicher Forst
52426 Jülich (Germany)
Fax: (+49)2461-612490
E-mail: w.hummel@fz-juelich.de

was obtained at room temperature with an ee of 89%. Similar enantioselectivities were observed for the other compounds under these conditions; therefore, the production of optically pure compounds was not possible. However, further investigations revealed a strong correlation between temperature and enantioselectivity for NcCR. We subsequently succeeded in establishing a process for the production of (S)-CHBE with an enantiomeric excess (ee) of 98.0% by adapting the reaction conditions to the requirements of the enzyme.

2. Materials and methods

2.1 General

If not stated, all chemicals were purchased from Sigma Aldrich, Buchs, Switzerland. All columns and instruments for chromatography (FPLC, Äkta-Explorer) were purchased from GE Healthcare, Freiburg, Germany. Centrifugations were carried out using RC5BPlus (Sorvall, Waltham, USA), Mikro22 and Rotina 35 R (Hettich, Tuttlingen, Germany) centrifuges. For analytical methods, GC-17A and LC-20AHT (both Shimadzu, Duisburg, Germany) and aan HPLC from Gynkotec equipped with a P580 pump and a UVD320S detector was used (Techlab, Erkerode, Germany). Restriction enzymes were purchased from Fermentas, St. Leon-Rot, Germany. The studied enzymes, NcCR and glucose dehydrogenase (GDH), were purchased from evocatal, Düsseldorf, Germany (evo-1.1.280 and evo-1.1.190, respectively).

2.2 Molecular cloning of the *nccd*-gene

Genomic DNA from *N. crassa* (DSM 894) was used as a template for amplification of the carbonyl reductase gene (XM_954278). For the following cloning steps, primers with recognition sites for the restriction enzymes *Nde*I and *Not*I were used for the construction of the gene fused with an N-terminal His-tag in pET-28a (Novagen (Merk), Darmstadt, Germany) (5'- ATATATACATATGACTGGATTCACTGCCGCCAACACCAC-3' and 5'- ATATGCGGCCGCTTACTCCTGCTTGAGCTGG-3'). The PCR product was cloned into the expression vector between the *Nde*I and *Not*I restriction sites using standard techniques.

2.3 Heterologous expression of NcCR

E. coli BL21(DE3) cells carrying the recombinant plasmid were cultivated in 5 mL LB medium [32] containing 50 µg/mL kanamycin overnight at 37 °C. These cultures were used to inoculate different amounts of LB medium containing 50 µg/mL kanamycin for expression in shaking flasks at a final optical density at 600 nm (OD_{600}) of 0.05. The cultures were grown at 37 °C. When the OD_{600} reached 0.5 to 0.7, production of the recombinant carbonyl reductase was induced by adding isopropyl thio-β-D-galactoside (IPTG) to a final concentration of 0.5 mM. For optimal enzyme expression cultures were grown at 25 ºC (after induction), and assayed after a period of 20 h.

2.4 Purification of NcCR

The bacterial culture was harvested by centrifugation at 17,000 x g for 20 min at 4 °C. A cell suspension (10% w/v) was prepared in 100 mM triethanolamine buffer (TEA), pH 7. Cells were disrupted by five sonication cycles of 5 min (40% power output) with cooling periods in-between cycles. The lysed cells were centrifuged at 17,000 x g for 30 min at 4 °C and the supernatant was used for further purification steps.
The enzyme was purified from the crude extract using an immobilised metal affinity chromatography IMAC (Ni-NTA (Qiagen, Hilden, Germany)). The column was equilibrated with TEA buffer (50 mM, pH 7). The carbonyl reductase was eluted using a linear gradient of imidazole (0 to 500 mM) in TEA buffer. After a desalting step by gel-filtration on Sephadex G 25 (Pharmacia (GE Healthcare), Freiburg, Germany), the enzyme was stored, freeze-dried at -20 °C until use.

2.5 Activity assay

A continuous assay using UV absorbance at 340 nm was employed to monitor the NADPH concentration during the reduction catalysed by carbonyl reductase.
Dihydroxyacetone was used as the standard substrate for the enzymatic reduction. One unit of activity was defined as the amount of enzyme that catalysed the oxidation of 1 µmol NADPH per minute under standard conditions (30 °C, pH 7). The reduction assay mixture contained 970 µL substrate solution (10 mM substrate in 100 mM TEA buffer, pH 7), 20 µL NADPH (12.5 mM) in distilled water and 10 µL enzyme solution. The reactions were initiated by adding the enzyme solution and were measured over 1 min.

2.6 Protein analysis

Protein concentrations were determined with a Bradford assay using BSA as a standard [33]. SDS-PAGE was performed using 4 to 12% Bis-Tris gels in MOPS (3-(*N*-morpholino) propanesulphonic acid) buffer (Invitrogen, Darmstadt, Germany). SeeBlue2 Protein Standard (Invitrogen) was used to estimate the molecular weight of proteins. The molecular mass of NcCR was determined using size-exclusion chromatography. A BioSep SEC S2000-HPLC column (300 x 7.8 mm, Phenomenex, Aschaffenburg, Germany) connected to a LC-20AHT system (Shimadzu, Duisburg, Germany) was used with 200 mM Tris-HCl buffer pH 7.5 as the mobile phase (1 mL/min). The lyophilised protein and protein standard (AQUEOUS SEC 1, Phenomenex, Aschaffenburg, Germany) were dissolved in 200 mM Tris-HCl buffer pH 7.5 and analysed by HPLC.

2.7 Determination of pH and temperature optima

In order to determine the temperature and pH optimum of NcCR, the standard reduction enzyme assay was performed at different temperatures as well as different pH values. The TEA (pH 6.8 to 10.0) standard activity buffer and citrate-phosphate buffer (pH 3.0 to 7.0) were used to determine the optimum pH.

2.8 Stability investigations

The enzyme was incubated at different temperatures to investigate temperature stability. At appropriate time intervals, samples were tested and the residual activity was assayed using the standard activity assay.

2.9 Biotransformation of different α- and β-ketoesters

The enantioselectivity of NcCR in the reduction of different α- and β-keto esters was examined using a simultaneous NADPH recycling system.

Table 1: Methods for chiral HPLC and GC.

Hydroxy compound	Methods	Retention time (min)
Ethyl 2-hydroxy-3-methylbutanoate[a]	GC, 60°C 2 min, 1°C/ min 90°C	*(R)*: 10.8 *(S)*: 12.4
Methyl lactate	GC, 40°C 3 min, 5°C/ min 90°C	*(R)*: 10.1 *(S)*: 10.9
Ethyl lactate	GC, 40°C 3 min, 5°C/ min 90°C	*(R)*: 12.0 *(S)*: 12.6
Ethyl 2-hydroxy-4-phenylbutanoate	HPLC, flow rate 0.4 ml/ min, hexane-isopropanol = 80 :20	*(R)*: 9.4 *(S)*: 8.9
Ethyl mandelate	HPLC, flow rate 1.0 ml/ min, hexane-isopropanol = 90 :10	*(R)*: 16.6 *(S)*: 17.9
Ethyl 4-chloro-3-hydroxybutanoate[a]	GC, 100ºC, 1°C/ min 113	*(R)*: 9.3 *(S)*: 9.0
Ethyl 2-chloro-3-hydroxybutanoate	GC, 60°C 5 min, 5°C/min 195°C	n.d.
Ethyl 3-hydroxybutanoate[a]	GC, 70°C, 5°C/ min 86°C, 0.1°C/ min 87°C	*(R)*: 6.7 *(S)*: 6.9
Ethyl 4,4,4-trifluoro-3-hydroxybutanoate	GC, 60°C 5 min, 5°C/min 195°C	*(R)*: 16.5 *(S)*: 16.8
Ethyl 3-hydroxy-3-phenylpropionate	GC, 60°C 5 min, 5°C/min 195°C	n.d.

[a] Hydroxyl group was acylated to a trifluoroacetate group as described; n.d.: not determined

The general composition was as follows: substrate (10 mM), D-glucose (100 mM), $NADP^+$ (0.5 mM), GDH (10 U) and NcCR (1 U when applicable) (when the activity was too low, an amount not exceeding 10% (v/v) of 10 mg/mL enzyme solution was used) in 70 mL TEA buffer (100 mM pH 7.0). Variations from the standard experimental setup are mentioned in the text. The mixture was stirred and incubated at 4 °C. Samples were tested periodically to follow product formation. After full conversion was reached, the mixture was extracted with ethyl acetate. When necessary, the produced hydroxy ester was purified by column chromatography on silica gel and analysed with chiral GC or HPLC to determine the *ee*. The absolute configuration of the product was identified by comparing the data with commercially available references. The corresponding compounds were prepared by reduction with $NaBH_4$, followed by identification of the absolute configuration by determining the specific rotation of the produced alcohol and comparing to published data.

2.10 Chiral GC and HPLC Analysis

Chiral HPLC analysis was performed using an HPLC from Gynkotec equipped with a P580 pump, a UVD320S detector (Techlab, Erkerode, Germany) and a Chirapak IC column (25 cm x 0.46 cm, Macherey Nagel, Düren, Germany). Chiral GC analysis was performed using a GC-17A (Shimadzu, Duisburg, Germany) equipped with a Varian CP-Chirasil-Dex CB column (25 m x 0.25 mm) using a flow of 200 mL/min and helium as the carrier gas. The applied methods are summarised in Table 1. When required, the hydroxyl group was acylated to trifluoroacetate. The reaction mixture (100 µl) was extracted with 200 µL diethyl ether and the organic solvent was evaporated. Acylation was performed by adding 10 µL trifluoroacetic anhydride for 15 min at 25 °C with continuous shaking. Subsequently, 200 µL ethyl acetate and 300 µL saturated sodium hydrogencarbonate were added and the organic phase was subjected to chiral GC.

Results and Discussion

3.1 Identification, cloning and heterologous overexpression of NcCR

A gene mining approach was performed to identify new oxidoreductases using the sequence of Gox1615 (YP_192012), an $NADP^+$-dependent glycerol dehydrogenase from *Gluconobacter oxydans* [34], as the template. Through the course of the *in silico* screening, a novel oxidoreductase (XM_954278) of unknown function was identified in the genome of *N. crassa*. The two enzymes showed 22% identity, 40% similarity and 27% gaps in a pairwise alignment between the protein sequences. The corresponding gene was predicted to be a member of the aldo-keto-reductase family (AKR), and it is 996 bp in length, contains no introns and codes for a protein with 331 amino acids.

Genomic DNA was used as the template for a PCR reaction, which was followed by cloning the amplified gene into the expression vector pET28a with standard techniques. The constructed recombinant plasmid contains the *nccr* gene with a hexahistidine affinity purification motif (His-tag) that was fused to the N-terminus of the protein.

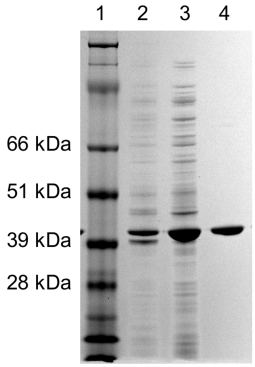

Fig. 1: SDS-PAGE analysis of purified NcCR. Lane 1: molecular weight marker (SeeBlue2, Invitrogen), lane 2: crude extract insoluble fraction (5 µg), lane 3: crude extract soluble (5 µg), lane 4: purified carbonyl reductase after desalting (1.25 µg). Lane 4 shows a single band at an apparent molecular weight of 40 kDa.

Table 2: Purification of recombinant NcCR from *E. coli* BL21(DE3) cells.

Purification step	Total activity (U/mL)	Specific activity (U/mg)	Purification factor	Yield (%)
Crude extract	513,000	149	1	100
Purified NcCR	180,000	468	3.1	35

This recombinant plasmid was expressed in *E. coli* BL21(DE3), and the highest activity was obtained after incubation at 25 °C. The protein showed a specific activity of 149 U/mg in the reduction of dihydroxyacetone (**1**). Soluble protein was expressed to approximately 82% of the total protein concentration (Fig. 1, lane 3), indicating that the eukaryotic origin of the gene causes no expression problems. The N-terminal His-tag allowed the purification of the protein using immobilised metal affinity chromatography (IMAC).

3.2 Purification of NcCR

The recombinant enzyme with a fused His-tag was purified in one chromatographic step using IMAC with Ni-NTA resin as shown in Table 2. After purification, 35% of the initial activity was recovered. The resulting specific activity was 468 U/mg, which was a 3.1-fold improvement in activity as compared to the crude extract. Samples of the crude extract and the target fraction after purification were analysed by SDS-PAGE (Fig. 1). A single band with an apparent molecular size of 40 kDa (Fig. 1, lane 4) was visible, confirming the calculated molecular mass of 37,533 Da derived from the amino acid sequence. Purification of the recombinant NcCR to homogeneity by applying a single purification step was possible.

3.3 Molecular characteristics of NcCR

In addition to analysing denatured carbonyl reductase, its native molecular mass was also determined by size-exclusion chromatography. The apparent molecular mass of NcCR was estimated to be 33.7 kDa, suggesting a monomeric structure of the native enzyme.
Investigations of the cofactor preference of NcCR revealed that the enzyme depended strictly on NADPH; NADH was not accepted (data not shown).

3.4 Dependence of NcCR activity on temperature and pH

Because the influences of temperature and pH on enzyme activity and stability are often crucial, investigations concerning the optimum temperature and pH and temperature stability were performed.
The optimum temperature for the reduction of dihydroxyacetone (**1**) by NcCR was determined to be 40 °C, and the activity decreased sharply at temperatures higher than 45 °C. The pH dependence of the enzyme was examined in the pH range between 3.0 and 10.0, and the optimal enzymatic activity observed was at pH 7.0.
Additionally, the temperature stability of NcCR under storage conditions at 30 ºC, 4 °C and -20 °C was measured over a period of 21 days. The observed residual activity was 83% at 4 °C and 92% at -20 °C, indicating sufficient stability of the enzyme under these conditions. When the enzyme was stored at 30 °C for 21 days, it showed only moderate stability; the residual activity was 25% of the initial activity. Thus, NcCR can be stored at 4 °C and -20 °C for at least 21 days without a notable loss of activity, but it can only be stored for a shorter period of time at elevated temperatures (30 °C).

3.5 Substrate specificity of NcCR

The substrate specificity of NcCR towards a variety of different substrates was investigated by applying aldehydes, ketones and α- and β -keto esters (Table 3-5). The enzyme prefers the reduction of α - and β -keto esters over a range of accepted substrates.
Among the tested aliphatic and aromatic ketones and aldehydes, only a few were converted by the enzyme (Table 3). For example, dihydroxyacetone (**1**) was found to be the best substrate among these compounds, whereas hydroxyacetone (**2**) was reduced with only 0.2% of the activity achieved with **1**.

Table 3: Photometric activities for the reduction of ketones and diketones by NcCR. In addition to the displayed compounds, glyceraldehyde, hexanal, benzaldehyde, acetophenone, 4'-chloro-acetophenone, 2-chloroacetophenone, 2'-hydroxyacetophenone, 2-octanone, 3-octanone, propiophenone, 2-cyclohexen-1-one, cyclohexanone, 2-methylcyclohexanone, 2-pentanone, 4-phenyl-2-butanone, cyclopropyl methyl ketone, trans-3-nonen-2-one, 2-butanone, 2-methyl-2-cyclopenten-1-one, β-ionone were also tested. NcCR showed no detectable activity applying the spectrophotometrical activity assay to these substrates.

Entry	Substrate	Specific activity [U/mg]	Relative activity [%]
1	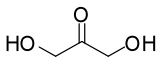	468	100
2	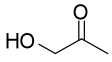	1.0	0.2
3	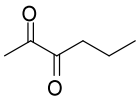	80.9	17.3
4	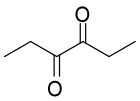	3.5	0.7
5	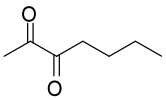	88.0	18.8

Table 4: Reduction of α-ketoesters by carbonyl reductase NcCR from *N. crassa*. The standard spectrophotometrical activity assay was used for the determination of specific activity. Conversion and *ee* were determined by chiral GC or HPLC.

Entry	Substrate	Specific activity [U/mg]	Conversion [%]	ee [%]
6	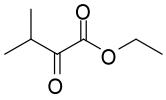	31.9	95	98.3 *(R)*
7	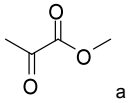 a	12.9	67	>99,9 *(S)*
8	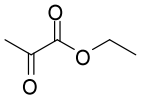 a	8.0	70	94.6 *(S)*
9	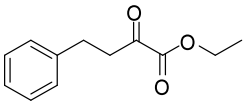	1.6	100	80 *(R)*
10	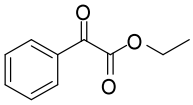	0.3	75	80 *(R)*

[a] Biotransformation was performed at 30 °C

Notably, diketones were also accepted by the enzyme. The highest activities were obtained with α, β-diketones carrying the two ketogroups near the end of the aliphatic chain: 2,3-hexandione (**3**) and 2,3-heptandione (**5**) were reduced with high activities of 80 and 89 U/mg, respectively, whereas 3,4-substituted hexandione (**4**) was converted with low activity (3.5 U/mg) and 2,5-hexandione was not converted at all.

Because NcCR showed a more pronounced acceptance of α- and β-keto esters, and because they are important in the synthesis of fine chemicals and pharmaceuticals [21, 35-37], the reduction of these compounds was studied in detail.

In order to explore substrate specificity, different substituted α-keto esters were used as substrates (Table 4). Among the tested compounds, NcCR showed the highest specific activity for the reduction of ethyl 3-methyl-2-oxobutanoate (**6**). However, low activity was observed with α-keto esters carrying an aromatic side chain (0.3 U/mg for ethyl 2-oxo-4-phenylbutanoate (**9**) and 1.6 U/mg for ethyl 2-oxophenylacetate (**10**)). These observations led to the hypothesis that NcCR activity increases with increasing distance between the keto group and the aromatic ring.

Yield and enantioselectivity were determined using GDH from *Bacillus subtilis* [38] to regenerate NADPH (Fig. 2). In the reduction of α-keto esters, NcCR converted all the tested compounds into their corresponding α-hydroxy esters at high rates. Concerning stereoselectivity, this carbonyl reductase displayed high enantioselectivity with all tested aliphatic compounds (**6**, **7**, **8**) and diminished selectivity in the reduction of aromatic α-keto esters (**9**, **10**). These results, in combination with the specific activity of NcCR regarding this substrate class, indicate that an aromatic substitution affects both the activity and selectivity of NcCR.

In addition to α-keto esters, the biotransformation of various β-keto esters was also investigated (Table 5). Due to their applicability as precursors for various chiral building blocks, the selected substrates are of great interest. The conversion and enantioselectivity for each β-keto ester were determined as described previously.

Remarkably high specific activity was observed with COBE as the substrate (325 U/mg) when compared to the activity of 21 U/mg with ethyl 2-chloro-3-oxobutanoate (**12**) and 1.8 U/mg with ethyl 3-oxobutanoate (**13**).

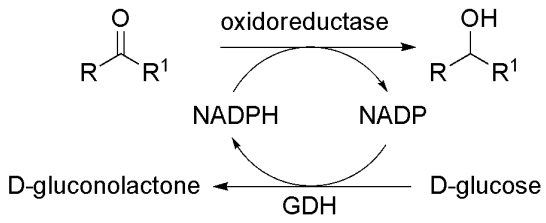

Fig. 2: Schematic diagram of the reduction of carbonyl compounds by NcCR with a simultaneous regeneration of NADPH by GDH using D-glucose as substrate.

This experiment indicated the importance of the substitution pattern. Substrates **11**, **12** and **13** were converted efficiently and high *ee* values were obtained for **11** and **13**. Two additional substrates were tested, ethyl 4,4,4-trifluoro-3-oxobutanoate (**14**) and ethyl 3-oxo-3-phenylpropionate (**15**), and satisfactory conversion was difficult to achieve due to low activity; furthermore, long incubation times were required to produce appropriate amounts of the corresponding hydroxy ester.

When comparing these low productivities to the results with the α-keto esters, the low specific activity was not the only reason for low productivity. In the reduction of **9**, which showed a photometric activity in a similar range, such low productivity did not occur. Although the incubation time for the conversion of **9** was longer (24 h) than for the other tested α-keto esters, efficient conversion was possible. Substrate **14** required up to 7 days (168 h) for full conversion and compound **15** showed insufficient conversion. In the assay with substrate **14**, supplementation with additional enzyme (NcCR and GDH) was necessary to reach full conversion. The reason for the insufficient conversion of substrate **15** can be assumed to be low activity, but other factors may be involved such as the inhibition of one or both enzymes. The fluoro substitution in **14** might be the cause of the observed inhibition occurring in its reduction; therefore, the stabilities of

Table 5: Reduction of β-ketoesters by NcCR from *N. crassa*. No activity in the spectrophotometrical test was observed using the following compounds as substrate: ethyl 3-oxohexanoate, methyl 4,4-dimetoxy-3-oxovalerate, methyl 4,4-dimethyl-3-oxopentanoate, methyl 3-oxopentanoate, ethyl 2-oxocyclohexanecarboxylate, ethyl 2-oxocyclopentanecarboxylate. Chiral GC or HPLC were used to determine *ee* and conversion.

Entry	Substrate	Specific activity [U/mg]	Conversion [%]	*ee* [%]
11	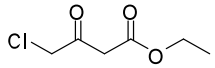	325	100	96.5 *(S)*
12	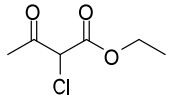	20.9	77	n.d
13	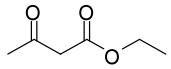	1.8	95	91 *(R)*
14	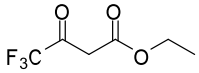	0.8	100	56 *(S)*
15	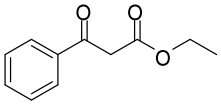	0.1	-[a]	-[a]

[a] The conversion was not sufficient for determining yield or *ee*; n.d.: not determined

NcCR and GDH in the presence of **14** were investigated separately. The corresponding studies over 72 h revealed that **14** had no negative effect on the activity of neither GDH nor NcCR.

NcCR exhibited high activity with dihydroxyacetone (**1**) and with α,β-diketones such as **3** and **4**. A variety of different aliphatic and aromatic ketones and aldehydes were not converted by this carbonyl reductase. Additionally, α - and β -keto esters were converted by the enzyme with high activity and the substitution pattern had a significant effect. Substrates bearing chlorine (**11**, **12**) were converted much faster than substrates without chlorine (**13**).

Notably, other enzymes described in the literature show similarly limited substrate specificity, such as the carbonyl reductases PsCR from *Pichia stipitis* [39] and KaCRI from *Kluyeromyces aestuarri* [24]. Both enzymes are members of the SDR superfamily, whereas NcCR belongs to the AKR superfamily. In addition to similar substrate acceptance, all three enzymes were found to prefer the (*S*)-isomer in the reduction of COBE. This stereoselectivity does not correlate with the hypothesis by Ye and co-workers that carbonyl reductases from the AKR family produce the (*R*)-isomer, whereas members of the SDR family yield the (*S*)-isomer [39] due to differences in conserved residues responsible for substrate binding. Therefore, the amino acid residues involved in substrate binding were compared between NcCR and other members from the SDR- and AKR-superfamilies. Surprisingly, the alignment revealed that NcCR showed low to medium identity with carbonyl reductases from the SDR and AKR families, with maximal identities of 22% with SDRs (PsCR) and 55% with AKRs. The crystal structure of SSCR (carbonyl reductase from *Sporobolomyces salmonicolor)*, which is a member of the SDR family, has been solved and the residues involved in substrate binding are known [11, 40]. A comparison revealed that NcCR shows no similarity to the relevant residues. The BLAST alignment tool was used to compare the amino acid sequence of NcCR with those of several other proteins; NcCR showed up to 86% identity with glycerol dehydrogenases belonging to the AKR-superfamily. Apart from similar substrate profiles, PsCR, KaCRI and NcCR share no common structural features. Therefore, based on its high homology to glycerol dehydrogenases and high activity towards dihydroxyacetone, the classification of NcCR as a glycerol dehydrogenase appears to be appropriate.

When considering the observed stereoselectivity in the reduction of α- and β -keto esters, the enzyme appeared to deliver the hydride ion from the same side of the prochiral keto esters, with the exception of **7** and **8**. This behaviour can be explained by a model postulating a large and a small pocket in the active site. The small pocket only accepts small alkyl groups, such as a methyl group, but an isopropyl side chain results in an inversion of the orientation of the substrate and an inverted stereospecificity. This result corresponds to observations from other enzymes, such as alcohol dehydrogenases from *Thermoanaerobacter ethanolicus* (TEADH) [31] and *T. brockii* (TBADH) [41] and carbonyl reductase from *Sporobolomyces salmonicolor* (SSCR) [11]. TEADH and TBADH reduce small substrates such as 2-butanone and 3-methyl-2-butanone to the corresponding (*R*)-alcohol, whereas ketones with a longer side chain yield (*S*)-alcohols. SSCR catalyses the reduction of aromatic α -keto esters to give the (*S*)-enantiomer, and the reduction of aliphatic α-keto esters yields the (*R*)-enantiomer.

3.6 Temperature and substrate effect on the selectivity of NcCR

Initial studies revealed that the enantioselectivity of NcCR in the reduction of COBE is strongly influenced by temperature and substrate concentration. Therefore, further studies were performed to investigate the influences of these two factors on stereoselectivity. It is well known that temperature is connected to enantioselectivity in both chemical and enzymatic reactions [26-28, 30], and this was also confirmed for NcCR in the present study. In an initial experiment, the reduction of COBE was performed at different temperatures (Fig. 3). Complete conversion of COBE to CHBE was possible at all the investigated temperatures, and the enantioselectivity increased with decreasing temperature. At 40 °C, the *ee* of the product was only 78.8%, but the *ee* could be enhanced to 98.0% by shifting the reaction temperature to -3 °C. Due to the high specific activity of the enzyme in the reduction of COBE, the reaction velocity was still sufficient at this low temperature and full conversion could be reached after 3 h using 300 mg COBE (10 mM) and 50 mg of NcCR (corresponding to 1270 U as determined photometrically with COBE at 4 °C). Another important parameter influencing the enantioselectivity of the enzyme was the substrate concentration.

This effect was studied and further enhancements were obtained at low substrate concentrations. When converting 100 mM COBE, NcCR showed an *ee* of 90.2%, whereas the enantioselectivity could be increased to 97.4% at a concentration of 10 mM (Fig. 3).

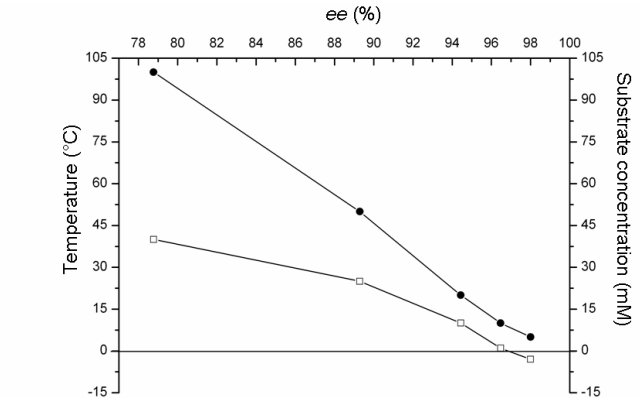

Fig. 3: Influence of temperature and substrate concentration on the stereoselectivity of NcCR. Development of *ee* value for the reduction of COBE in response temperature (-□-) and substrate concentration (-●-) are shown. The *ee* was determined by chiral gas chromatography. Temperature dependence was assessed using a substrate concentration of 10 mM, and investigation of the influence of substrate concentration was conduced at 1ºC.

The influence of physical parameters such as the temperature on enantio- and stereoselectivity has been described for other enzymes [41, 42], whereas the effect of different substrate concentrations has only been observed for cyclohexanone monooxygenase from *Acinetobacter calcoaceticus* [43]. For example, pig liver esterase shows the highest enantioselectivity in 20% aqueous methanol at -10 °C [42]. ADH from *Thermoanaerobium brockii* (TBADH) catalyses the reduction of 2-pentanone with the highest enantioselectivity at 7 °C [41]. Keinan and co-workers investigated the correlation between temperature and the selectivity of TBADH in detail. Their study revealed that the enzyme showed a strong dependence on temperature, as demonstrated by a drastic enhancement of its selectivity by shifting the temperature from 50 °C to 7 °C.

These are examples of correlations between temperature and enantioselectivity. The enantioselectivity of an enzymatic reaction is defined by the ratios of the specificity constants, the k_{cat}/K_m ratios, for the two enantiomeric products [26, 44]. Using transition state kinetic theory, the ratio is related to the difference in activation free energy (ΔΔG) for the enantiomeric products. The activation free energy can be regarded as a contribution from enthalpy and entropy, and both are temperature-sensitive terms.

In general, these results demonstrate how simple methods of reaction engineering may lead to a significant enhancement of optical purity. In this study, a process for the production of several interesting chiral building blocks at high enantiomeric purity was successfully established.

3.7 Bioreduction of COBE

The activity of the enzyme was tested at different temperatures to assess the use of NcCR at lower temperatures (Figure 4). Optimal activity was observed at 40 °C, whereas at 4 °C the activity was significantly reduced to 6.1% of the optimal activity. Therefore, the amount of enzyme used for bioreduction at -3 °C was adjusted to account for the reduced activity of NcCR.

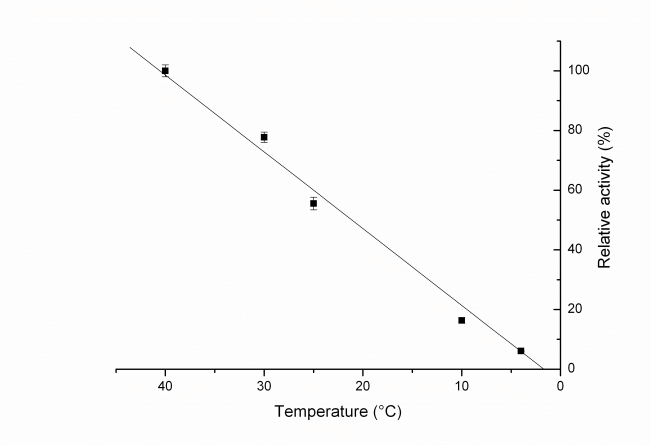

Fig. 4: Temperature dependence on enzyme activity. Enzyme activity was determined using the standard spectrophotometrical assay at different temperatures. The standard deviation from triplicates is shown in the diagram.

In order to prove the applicability of the enzyme, a conversion of COBE was subsequently performed on a 300 mg scale (10 mM COBE in 200 mL TEA buffer (100 mM, pH 7.0)). At this scale, 1.8 mmol of COBE was completely converted to 1.8 mmol CHBE at -3ºC under constant vigorous stirring and simultaneous regeneration of the cofactor by GDH (Fig. 2). Freezing of the aqueous solution was prevented by adding 100 mM buffer salts to reduce the melting point and by intensive stirring. Figure 5 illustrates the results, concentrations of COBE and CHBE as monitored over a 4 h period.

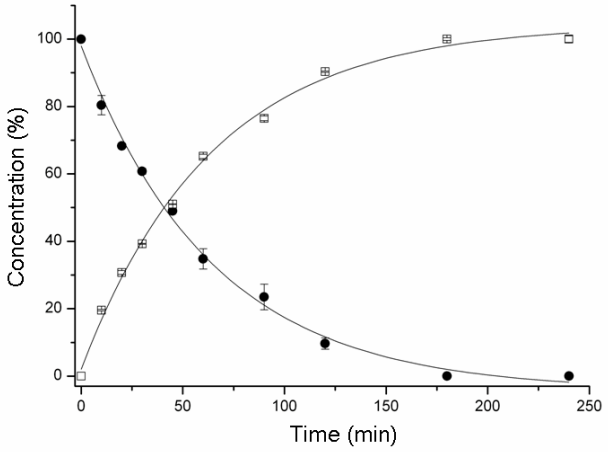

Fig. 5: Conversion of COBE by NcCR. The concentrations of COBE (-●-) and (*S*)-CHBE (-□-) were measured over a period of 240 min; concentrations were determined by chiral GC. The conversion was performed using 40 mg NcCR, 300 mg (10 mM) COBE, 20 mM D-glucose, 800µl GDH (crude extract) and 0.5 mM $NADP^+$ in 200 mL 100 mM TEA pH 7.0 at -3ºC.

After a 3 h reaction, the complete conversion of COBE to (*S*)-CHBE was reached, and the product was obtained at 98.0% *ee*. However, numerous processes exist to produce both enantiomers of CHBE using different enzymatic routes, and they are far more feasible in terms of selectivity, productivity and milder reaction conditions [20-25, 45, 46]. In the present study, we demonstrate that with reaction engineering, it was possible to establish a suitable process using an enzyme that initially did not seem feasible. In summary, 300 mg of (*S*)-CHBE was produced using a carbonyl reductase from *N. crassa*.

4. Conclusion

A novel recombinant carbonyl reductase from *N. crassa* was purified and biochemically characterised. NcCR exhibited high activity, high conversion and pronounced stereoselectivity in the reduction of several α - and β -keto esters, which makes this enzyme a promising biocatalyst for the production of enantiopure hydroxy esters. Moreover, the dependence of NcCr's enantioselectivity on temperature was investigated, and an efficient process was established that yielded (*S*)-CHBE on a 300-mg scale.

Acknowledgements

We would like to thank Robert Simon for helpful discussions and support regarding all chemical issues. In addition we would like to thank Benita Kopka and Martin Diener for preliminary work.

References

[1] T. Daußmann, H. G. Hennemann, T. C. Rosen and P. Dünkelmann, Enzymatic technologies for the synthesis of chiral alcohol derivatives, Chem. Ing. Tech. *78* (2006), 249-255.

[2] K. Nakamura, R. Yamanaka, T. Matsuda and T. Harada, Recent developments in asymmetric reduction of ketones with biocatalysts, Tetrahedron Asymmetry *14* (2003), 2659-2681.

[3] R. N. Patel, Biocatalysis: Synthesis of chiral intermediates for drugs, Curr. Opin. Drug. Discov. Devel. *9* (2006), 741-764.

[4] J. A. Pesti and R. DiCosimo, Recent progress in enzymatic resolution and desymmetrization of pharmaceuticals and their intermediates, Curr. Opin. Drug. Discov. Devel. *6* (2003), 884-901.

[5] A. M. Rouhi, Chiral chemistry, Chem. Eng. News *82* (2004), 47-62.

[6] M. Wills, M. Gamble, M. Palmer, A. Smith, J. Studley and J. Kenny, Novel catalysts for asymmetric reduction of carbonyl groups, J. Mol. Catal., A Chem. *146* (1999), 139-148.

[7] M. Wills and J. Hannedouche, New methodology for the asymmetric reduction of ketones, Curr. Opin. Drug. Discov. Devel. *5* (2002), 881-891.

[8] C. M. He, D. L. Chang and J. Zhang, Asymmetric reduction of substituted α- and β-ketoesters by *Bacillus pumilus* Phe-C3, Tetrahedron Asymmetry *19* (2008), 1347-1351.

[9] Y. Yang, D. Zhu, T. J. Piegat and L. Hua, Enzymatic ketone reduction: mapping the substrate profile of a short-chain alcohol dehydrogenase (YMR226c) from *Saccharomyces cerevisiae*, Tetrahedron Asymmetry *18* (2007), 1799-1803.

[10] D. M. Zhu, J. E. Stearns, M. Ramirez and L. Hua, Enzymatic enantioselective reduction of α-ketoesters by a thermostable 7 α-hydroxysteroid dehydrogenase from *Bacteroides fragilis*, Tetrahedron *62* (2006), 4535-4539.

[11] D. M. Zhu, Y. Yang, J. D. Buynak and L. Hua, Stereoselective ketone reduction by a carbonyl reductase from *Sporobolomyces salmonicolor*. Substrate specificity, enantioselectivity and enzyme-substrate docking studies, Org. Biomol. Chem. *4* (2006), 2690-2695.

[12] G. J. Wang and R. I. Hollingsworth, Synthetic routes to L-carnitine and L-gamma-amino-beta-hydroxybutyric acid from (*S*)-3-hydroxybutyrolactone by functional group priority switching, Tetrahedron Asymmetry *10* (1999), 1895-1901.

[13] B. N. Zhou, A. S. Gopalan, F. Vanmiddlesworth, W. R. Shieh and C. J. Sih, Stereochemical control of yeast reductions .1. Asymmetric-synthesis of L-carnitine, J. Am. Chem. Soc. *105* (1983), 5925-5926.

[14] D. S. Karanewsky, M. C. Badia, C. P. Ciosek, J. A. Robl, M. J. Sofia, L. M. Simpkins, B. Delange, T. W. Harrity, S. A. Biller and E. M. Gordon, Phosphorus-containing inhibitors of Hmg-CoA reductase .1. 4-[(2-arylethyl)hydroxyphosphinyl]-3-hydroxybutanoic acids - a new class of cell-selective inhibitors of cholesterol-biosynthesis, J. Med. Chem. *33* (1990), 2952-2956.

[15] E. Santaniello, R. Casati and F. Milani, Chiral synthesis of a component of amanita-muscaria, (-)-4-hydroxypyrrolidin-2-one, and assessment of its absolute-configuration, J. Chem. Res. (1984), 132-133.

[16] Y. X. Liang, Z. Wang and K. L. Ding, Generation of self-supported noyori-type catalysts using achiral bridged-BIPHEP for heterogeneous asymmetric hydrogenation of ketones, Adv. Synth. Catal. *348* (2006), 1533-1538.

[17] D. S. Matharu, D. J. Morris, A. M. Kawamoto, G. J. Clarkson and M. Wills, A stereochemically well-defined rhodium(III) catalyst for asymmetric transfer hydrogenation of ketones, Org. Lett. *7* (2005), 5489-5491.

[18] T. Ohkuma, N. Utsumi, K. Tsutsumi, K. Murata, C. Sandoval and R. Noyori, The hydrogenation/transfer hydrogenation network: Asymmetric hydrogenation of ketones with chiral η^6-arene/N-tosylethylenediamine-ruthenium(II) catalysts, J. Am. Chem. Soc. *128* (2006), 8724-8725.

[19] M. T. Reetz and X. G. Li, An efficient catalyst system for the asymmetric transfer hydrogenation of ketones: Remarkably broad substrate scope, J. Am. Chem. Soc. *128* (2006), 1044-1045.

[20] Y. Yasohara, N. Kizaki, J. Hasegawa, M. Wada, M. Kataoka and S. Shimizu, Molecular cloning and overexpression of the gene encoding an NADPH-dependent carbonyl reductase from *Candida magnoliae*, involved in stereoselective reduction of ethyl 4-chloro-3-oxobutanoate, Biosci. Biotechnol. Biochem. *64* (2000), 1430-1436.

[21] Q. Ye, M. Yan, L. Xu, H. Cao, Z. Li, Y. Chen, S. Li and H. Ying, A novel carbonyl reductase from *Pichia stipitis* for the production of ethyl (*S*)-4-chloro-3-hydroxybutanoate, Biotechnol. Lett. *31* (2009), 537-542.

[22] M. Kataoka, K. Yamamoto, H. Kawabata, M. Wada, K. Kita, H. Yanase and S. Shimizu, Stereoselective reduction of ethyl 4-chloro-3-oxobutanoate by *Escherichia coli* transformant cells coexpressing the aldehyde reductase and glucose dehydrogenase genes, Appl. Microbiol. Biotechnol. *51* (1999), 486-490.

[23] N. Kizaki, Y. Yasohara, J. Hasegawa, M. Wada, M. Kataoka and S. Shimizu, Synthesis of optically pure ethyl (*S*)-4-chloro-3-hydroxybutanoate by *Escherichia coli* transformant cells coexpressing the carbonyl reductase and glucose dehydrogenase genes, Appl. Microbiol. Biotechnol. *55* (2001), 590-595.

[24] H. Yamamoto, K. Mitsuhashi, N. Kimoto, A. Matsuyama, N. Esaki and Y. Kobayashi, A novel NADH-dependent carbonyl reductase from *Kluyveromyces aestuarii* and comparison of NADH-regeneration system for the synthesis of ethyl (*S*)-4-chloro-3-hydroxybutanoate, Biosci. Biotechnol. Biochem. *68* (2004), 638-649.

[25] Z. N. Xu, Y. Liu, L. M. Fang, X. X. Jiang, K. J. Jing and P. L. Cen, Construction of a two-strain system for asymmetric reduction of ethyl 4-chloro-3-oxobutanoate to (*S*)-4-chloro-3-hydroxybutanoate ethyl ester, Appl. Microbiol. Biotechnol. *70* (2006), 40-46.

[26] H. Buschmann, H. D. Scharf, N. Hoffmann and P. Esser, The Isoinversion principle - a general-model of chemical selectivity, Angew. Chem. Int. Ed. Engl *30* (1991), 477-515.

[27] R. S. Phillips, Temperature modulation of the stereochemistry of enzymatic catalysis: Prospects for exploitation, Trends Biotechnol. *14* (1996), 13-16.

[28] R. S. Phillips, C. Zheng, V. T. Pham, F. A. C. Andrade and M. A. C. Andrade, Effects of temperature on stereochemistry of enzymatic-reactions, Biocatalysis *10* (1994), 77-86.

[29] F. Secundo and R. S. Phillips, Effects of pH on enantiospecificity of alcohol dehydrogenases from *Thermoanaerobacter ethanolicus* and horse liver, Enzyme Microb. Technol. *19* (1996), 487-492.

[30] A. Wiegers and H. D. Scharf, The influence of electronic effects and temperature on the enantioselective reductions of acetophenone derivatives with (-)-diisopinocampheylchloroborane - A dynamic model of enantioselection, Tetrahedron Asymmetry *7* (1996), 2303-2312.

[31] V. T. Pham and R. S. Phillips, Effects of substrate structure and temperature on the stereospecificity of secondary alcohol-dehydrogenase from *Thermoanaerobacter ethanolicus*, J. Am. Chem. Soc. *112* (1990), 3629-3632.

[32] G. Bertani, Studies on lysogenesis .1. the mode of phage liberation by lysogenic *Escherichia coli*, J. Bacteriol. *62* (1951), 293-300.

[33] M. M. Bradford, Rapid and sensitive method for quantitation of microgram quantities of protein utilizing principle of protein-dye binding, Anal. Biochem. *72* (1976), 248-254.

[34] N. Richter, M. Neumann, A. Liese, R. Wohlgemuth, T. Eggert and W. Hummel, Characterisation of a Recombinant NADP-dependent glycerol

dehydrogenase from *Gluconobacter oxydans* and its application in the production of L-glyceraldehyde, ChemBioChem *10* (2009), 1888-1896.

[35] H. Asako, M. Shimizu and N. Itoh, Biocatalytic production of (*S*)-4-bromo-3-hydroxybutyrate and structurally related chemicals and their applications, Appl. Microbiol. Biotechnol. *84* (2009), 397-405.

[36] I. Kaluzna, A. A. Andrew, M. Bonilla, M. R. Martzen and J. D. Stewart, Enantioselective reductions of ethyl 2-oxo-4-phenylbutyrate by *Saccharomyces cerevisiae* dehydrogenases, J. Mol. Catal., B Enzym. *17* (2002), 101-105.

[37] I. A. Kaluzna, B. D. Feske, W. Wittayanan, I. Ghiviriga and J. D. Stewart, Stereoselective, biocatalytic reductions of α-chloro-β-keto esters, J. Org. Chem. *70* (2005), 342-345.

[38] A. Weckbecker and W. Hummel, Glucose dehydrogenase for the regeneration of NADPH and NADH, Adv. Biochem. Engin. / Biotechnol. *17* (2005), 225-237.

[39] Q. Ye, M. Yan, Z. Yao, L. Xu, H. Cao, Z. J. Li, Y. Chen, S. Y. Li, J. X. Bai, J. Xiong, H. J. Ying and P. K. Ouyang, A new member of the short-chain dehydrogenases/reductases superfamily: Purification, characterization and substrate specificity of a recombinant carbonyl reductase from *Pichia stipitis*, Bioresour. Technol. *100* (2009), 6022-6027.

[40] S. Kamitori, A. Iguchi, A. Ohtaki, M. Yamada and K. Kita, X-ray structures of NADPH-dependent carbonyl reductase from *Sporobolomyces salmonicolor* provide insights into stereoselective reductions of carbonyl compounds, J. Mol. Biol. *352* (2005), 551-558.

[41] E. Keinan, E. K. Hafeli, K. K. Seth and R. Lamed, Thermostable enzymes in organic-synthesis .2. asymmetric reduction of ketones with alcohol-dehydrogenase from *Thermoanaerobium brockii*, J. Am. Chem. Soc. *108* (1986), 162-169.

[42] L. K. P. Lam, R. Hui and J. B. Jones, Enzymes in organic-synthesis .35. stereoselective pig-liver esterase catalyzed hydrolyzes of 3-substituted glutarate diesters - optimization of enantiomeric excess via reaction conditions control, J. Org. Chem. *51* (1986), 2047-2050.

[43] F. Zambianchi, P. Pasta, G. Ottolina, G. Carrea, S. Colonna, N. Gaggero and J. M. Ward, Effect of substrate concentration on the enantioselectivity of cyclohexanone monooxygenase from *Acinetobacter calcoaceticus* and its rationalization, Tetrahedron-Asymmetry *11* (2000), 3653-3657.

[44] A. R. Fersht, *Enzyme structure and mechanism*, San Francisco, CA: 1985.

[45] M. Kataoka, A. Hoshino-Hasegawa, R. Thiwthong, N. Higuchi, T. Ishige and S. Shimizu, Gene cloning of an NADPH-dependent menadione reductase from *Candida macedoniensis*, and its application to chiral alcohol production, Enzyme Microb. Technol. *38* (2006), 944-951.

[46] M. A. Yu, Y. M. Wei, L. Zhao, L. Jiang, X. B. Zhu and W. Qi, Bioconversion of ethyl 4-chloro-3-oxobutanoate by permeabilized fresh brewer's yeast cells in the presence of allyl bromide, J. Ind. Microbiol. Biotechnol. *34* (2007), 151-156.

Keywords: Carbonyl reductase, *Neurospora crassa*, NADPH, (*S*)-4-chloro-3-hydroxybutanoate, dependence of temperature on enantioselectivity

2.4 ASYMMETRIC REDUCTION OF ACTIVATED ALKENS USING AN ENOATE REDUCTASE FROM *GLUCONOBACTER OXYDANS*

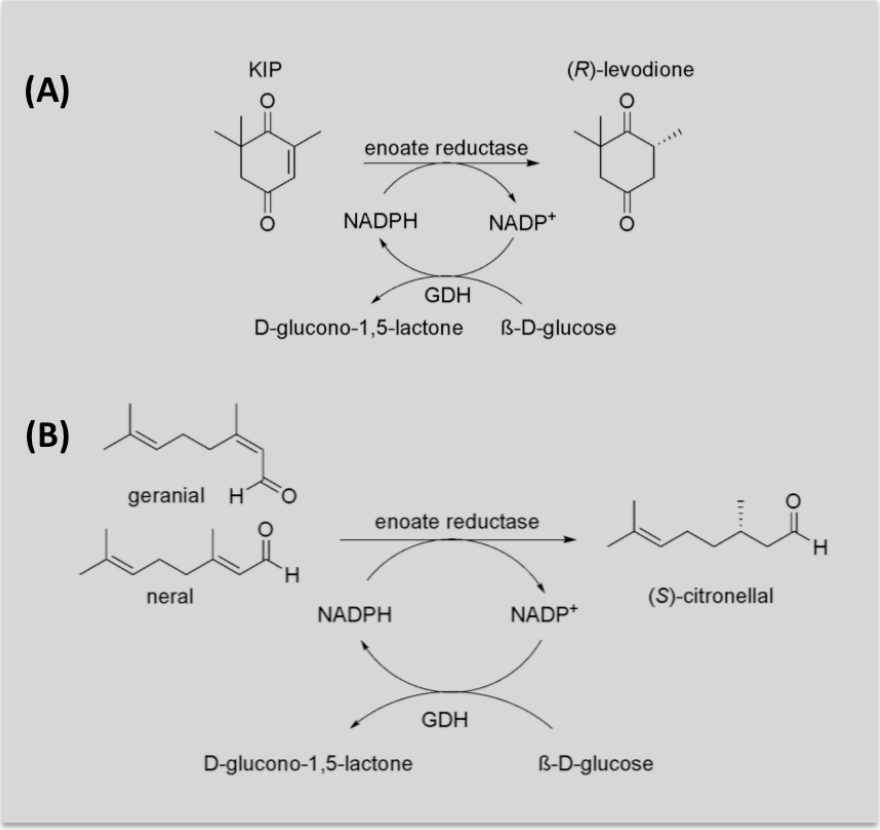

N. Richter, H. Gröger and W. Hummel (2011)

Appl. Microbiol. Biotechnol. 89, 79-89

(doi: 10.1007/s00253-10-2793-y)

Asymmetric reduction of activated alkenes using an enoate reductase from *Gluconobacter oxydans*

Nina Richter[a], Harald Gröger[b], Werner Hummel[c*]

[a] evocatal GmbH, Merowingerplatz 1a, 40225 Düsseldorf, Germany
[b] Department Chemie und Pharmazie, Universität Erlangen-Nürnberg, Henkelstr. 42, 91054 Erlangen, Germany
[c] Institut für Molekulare Enzymtechnologie, Heinrich-Heine Universität Düsseldorf, Forschungszentrum Jülich, Stetternicher Forst, 52426 Jülich, Germany

* corresponding author,
phone: +49 2461-61-3790, fax: (+49)2461-61-2490, email: w.hummel@fz-juelich.de

A recombinant enoate reductase from Gluconobacter oxydans was heterologously expressed purified, characterised and applied in the asymmetric reduction of activated alkenes. In addition to the determination of the kinetic properties the major focus of this work was to utilise the enzyme in the biotransformation of different interesting compounds such as 3,5,5-trimethyl-2-cyclohexen-1,4-dione (ketoisophorone, KIP) and (E/Z)-3,7-dimethyl-2,6-octadienal (citral). The reaction proceeded with excellent stereoselectivities (> 99% ee) as well as absolute chemo- and regioselectivity, only the activated C=C bond of citral was reduced by the enoate reductase, while non-activated C=C bond and carbonyl moiety remained untouched. The described strategy can be used for the production of enantiomerically pure building blocks, which are difficult to prepare by chemical means. In general the results show that the investigated enoate reductase is a promising catalyst for the use in asymmetric C=C bond reductions.

Introduction

Enoate reductases [E.C. 1.3.1.31] are members of the "old yellow enzyme family" (Stuermer et al. 2007; Williams and Bruce 2002). The name derives from the flavin cofactor of its first representative, the old yellow enzyme isolated from *Saccharomyces carlsbergensis* by Warburg and Christian in 1932 (Warburg and Christian 1932). Until now many homologous enzymes of this class of flavoproteins have been found in yeasts, bacteria and plants (Adalbjörnsson et al. 2010; Burda et al. 2009; Hall et al. 2008b; Hirata et al. 2009; Kitzing et al. 2005; Miranda et al. 1995; Rohdich et al. 2001; Strassner et al. 1999; Yanto et al. 2010).

In general, enoate reductases are flavin dependent oxidoreductases which catalyse the asymmetric reduction of olefinic double bonds by creating up to two stereogenic centres (Fig. 1). The catalytic mechanism has been solved and studied in detail (Hult and Berglund 2007; Vaz et al. 1995). A hydride derived from the flavin cofactor is transferred stereoselectively onto a carbon atom of the double bond. A tyrosine residue being part of the active site of the enoate reductase hydrogenates the other carbon with a solvent-proton from the opposite side. Finally the oxidised FMN is reduced at the expense of NADPH, whose regeneration is coupled to another independent redox reaction.

The enzymatic transformation described is a promising alternative to the respective chemical process, where a high number of enantioselective alkene reduction reactions are performed using asymmetric hydrogenation by chiral rhodium or ruthenium phosphines (Knowles 2002, Noyori 2002). One major drawback of the chemical processes is the limitation to highly polar functional groups (amides, acids and alcohols) as part of the structure. With less polar groups like aldehydes, ketones, esters or nitrogroups these methods are less successful, except for few reported examples (Dobbs et al. 2000; Lipshutz and Servesko 2003; Lipshutz et al. 2004; Ohta et al. 1995). Further issues are the disposal of complex heavy metal ligands and the requirement of high pressure. The high regio- and enantioselectivity at ambient temperature and pressure make the biocatalytic counterpart a suitable alternative for the production of chiral building blocks.

In the area of enzymatic hydrogenation, research efforts were mainly focussed on whole-cell systems with wild-type microorganisms (e.g. baker's yeast), due to the instability of the available isolated enzymes (Fuganti 1990; Hogberg et al. 1994; Servi 1990). Besides the drawback of high (bio-)catalyst loading required in these syntheses (due to low expression of the desired enzymes), this strategy exhibits a further major disadvantage, namely a high number of side reactions occurring. These side reactions are leading to the formation of by-products, caused by various enzymes abundant in the cell. Among these are for example NAD(P)H-dependent dehydrogenases catalysing the reduction of the carbonyl moiety.

Therefore, stable isolated enoate reductases with a broad substrate range are demanded for technical applications, for example the reduction of 3,5,5-trimethyl-2-cyclohexen-1,4-dione (ketoisophorone, KIP) to (*R*)-3,5,5-trimethyl-2-cyclohexan-1,4-dione (levodione), an important chiral intermediate for optically active compounds like zeaxanthin (Kataoka et al. 2002; Leuenberger et al. 1976b). Another example is (*R*)-citronellal, applied in the food and cosmetic industry (Goussevskaia et al. 2007; Scott et al. 2008; Wegner et al. 2008) that can be synthesised by the reduction of the non-chiral inexpensive (E/Z)-3,7-dimethyl-2,6-octadienal (citral).

Based on the great potential of this enzyme class, a number of enzymes have been studied and applied in organic synthesis during the last decades (Adalbjörnsson et al. 2010; Burda et al. 2009; Fuganti 1990; Hall et al. 2006; Hall et al. 2008a; Hall et al. 2008b; Hall et al. 2007; Hirata et al. 2009; Hogberg et al. 1994; Müller et al. 2006; Müller et al. 2007; Servi 1990; Stuermer et al. 2007; Yanto et al. 2010). Among them is an enoate reductase from *Gluconobacter oxydans* (Schweiger et al. 2008; Shinagawa et al. 2008; Yin et al. 2008). Herein we report its application in the asymmetric reduction of citral and ketoisophorone (KIP) as well as the impact of an N- or C-terminal hexahistidine tag (His-tag) on the biological activity.

Experimental Section

General: If not stated otherwise all chemicals were purchased from Sigma Aldrich (Buchs, Switzerland). All columns and instruments for chromatography (Äkta-Explorer) were purchased from GE Healthcare, Freiburg, Germany. Centrifugation was carried out using the centrifuges RC5BPlus (Sorvall, Waltham, USA), Mikro22 and Rotina 35 R (Hettich, Tuttlingen, Germany). For analytical methods GC-17A and LC10Ai (both Shimadzu, Duisburg, Germany) were used. Restriction enzymes were purchased from Fermentas, St. Leon Roth, Germany.

Molecular cloning of the enoate reductase gene: Genomic DNA isolated from *G. oxydans* (DSM: 2343) was used as template for amplification of the enoate reductase (YP_190936) with the following primers containing: a) construct with N-terminal His-tag (cloned in pET28a, Novagen (Merk), Darmstadt, Germany) and without modification (pET22b, Novagen (Merk), Darmstadt, Germany) (5'-ATATGTCGACTCAGTTGGGGCCGGAGGTGGCGG-3' and 5'- TA TCTCGAGGTTGGGGCCGGAGGTGGCGGAC-3'), with recognition sites for *Nde*I and *Sal*I respectively. b) construct with C-terminal His-tag (pET22b) (5'- ATATGTCGACTCAGTTGGGGCCGGAGGTGG CGG-3' and 5'- TATCTCGAGGTTGGGGCCGGAGGTGGCGGAC-3') with recognition sites for the restriction enzymes *Nde*I and *Xho*I. The PCR product was cloned into pET22b and pET28a (Novagen) between the *Nde*I and *Sal*I / *Xho*I restriction sites using standard techniques.

Heterologous expression of the enoate reductase: For recombinant protein expression, *E. coli* BL21(DE3) cells carrying the recombinant plasmid were cultivated overnight at 37°C in 5 mL LB medium (Bertani 1951) containing either 100 µg/mL ampicillin or 50 µg/mL kanamycin. For expression in conical flasks, a final concentration of 0.05 optical density at 600 nm (OD_{600}) was used to inoculate different amounts of LB medium containing the corresponding antibiotic for selection. The cultures were cultivated at 37°C. At an OD_{600} of 0.5 to 0.7 the production of the recombinant enoate reductase was induced by addition of isopropyl thio-β-D-galactoside (IPTG) to a final concentration of 0.5 mM. For the determination of the optimal conditions cultures were grown after induction at 25, 30 and 37°C, and assayed after a period of 20 h.

Purification of the enoate reductase: The bacterial culture was harvested by centrifugation (17000 x g, 20 min, 4°C). A cell suspension (10%) was prepared in 100 mM triethanolamine buffer (TEA) pH 7.0 and disrupted by sonication on ice (5 min (40% power output), 5 min cooling, 5 cycles in total). After a centrifugation step (17000 x g, 30 min, 4°C), the cleared crude extract was used for protein purification using immobilised metal affinity chromatography IMAC (Ni-NTA (QIAgen, Hilden, Germany). The column was equilibrated with TEA buffer (50 mM, pH 7.0). After loading, the sample and elution of non-bound proteins with equilibration buffer a linear gradient of imidazol (0 to 500 mM, 150 min) in TEA buffer was performed. The enoate reductase elutes at 130 mM imidazol. After a desalting step (Sephadex G 25 (Pharmacia), [10 mM TEA buffer pH 7.0]) the enzyme was stored at -20ºC prior to use.

Activity assay: A continuous assay using UV absorbance at 340 nm was employed to monitor the decrease in NADPH concentration during reduction catalysed by the enoate reductase. Trans-2-hexenal was used as standard substrate. One unit of activity was defined as the amount of enzyme catalysing the oxidation of 1 µmol NADPH per minute under standard conditions (30°C, pH 7.0). The reduction assay mixture contained 970 µL substrate solution (10 mM substrate in 100 mM TEA buffer pH 7.0), 20 µL NADPH (12.5 mM) in distilled water and 10 µL enzyme solution. Reactions were started by addition of the enzyme solution and measured over 1 min.

Determination of pH and temperature optima: In order to obtain the pH and temperature optimum of the enoate reductase activity the standard enzyme assay was performed at different temperatures or pH values. For the determination of the pH optimum, two buffers with overlapping pH ranges were applied (TEA (pH 6.6 to 10.0) and citrate-phosphate buffer (pH 3.5 to 7.0)).

Stability investigations: For investigation of temperature stability the enzyme was incubated under standard assay conditions at different temperatures. After different incubation times the residual activity was assayed.

Determination of kinetic parameters: To determine the kinetic parameters (K_M und V_{max}) the standard activity assay for reduction was used. All parameters were kept constant, only the investigated parameter (cofactor or substrate concentration) was modified. Kinetic parameters were calculated using a non-linear fitting algorithm (Origin Software).

Protein analysis: Protein determination was performed according to Bradford using BSA as a standard (Bradford 1976). SDS-PAGE was performed using 4–12% Bis-Tris gels running in MOPS buffer, SeeBlue Plus2 Protein standard (both Invitrogen, Darmstadt, Germany) was used for molecular weight estimation of proteins.

Determination of the flavin species: The separation of protein bound flavin species was carried out by HPLC. For the separation and quantification of flavin adenine dinucleotide (FAD), flavin mononucleotide (FMN) and riboflavin, a reverse phase C_{18}- HPLC column (250/4 Nucleodur, Macherey&Nagel, fitted with an 8/4 pre-column containing the same material) connected to a Shimadzu LC10Ai HPLC system was used. As mobile phases 50 mM ammonium acetate buffer pH 6.0 (eluent B) and 70% acetonitrile in B (eluent A) were used. The enzyme sample was incubated for 10 min at 99°C to release the cofactor, denatured protein was removed by centrifugation at 21,900 x g for 20 min. The supernatant was spun through a Microcon YM3 (Millipore, MWCO 3000 Da) centrifugal concentrator device (18,900 x g, 20 min) to remove residual protein. The resulting sample was analysed by HPLC, the protocol used for the separation is shown in Table 1.

Biotransformation of citral and ketoisophorone (KIP): For the different biotransformations (1 mL) 10 mM substrate in 100 mM TEA buffer, pH 7.0,

Table 1 HPLC protocol used for the separation of different flavin species

Time [min]	Flow rate [mL/min]	Eluent A [%]	Eluent B [%]
0	0.63	5	95
20	0.63	40	60
22	0.8	40	60
29	0.63	5	95

A: 70% acetonitrile in B, B: 50 mM NH_4Ac pH 6.0

3.5 U bacterial glucose dehydrogenase (GDH) (evo-1.1.060, evocatal, Düsseldorf, Germany), 0.5 mM $NADP^+$ and 0.05 U (citral) and 0.16 U (KIP) enoate reductase, respectively were incubated at 30°C. Samples (50 µL) were taken periodically and diluted with ethyl acetate (300 µL) for GC analysis. Concentrations and enantiomeric excess (*ee*) were determined using a GC-17A (Shimadzu, Duisburg, Germany) equipped with a β -cyclodextrin column (CP-Chirasil-Dex CB column, 25 m x 0.25 mm, Varian, Darmstadt, Germany). For separation the following method was applied: 100°C; 5°C/min to 150°C; 40°C to 195°C, the corresponding retention times were: KIP 7.8 min, (R)-levidione 8.4 min, neral (citral) 8.1 min, geranial (citral) 8.8 min, cironellal 6.1 min. The *ee*-value of citronellal was determined using a modified β-cycolodextrin column (Hydrodex-β-TBDAc, 25 m x 0.25 mm). Temperature program: 80°C hold 2 min, 1 °C/min 95°C; 0.5°C/min 100°C. Retention times: (*S*)- and (*R*)-citronellal 19.8 and 20.3, respectively. The absolute configuration of citral was identified by comparing the data with the commercially available reference. The determination of the absolute configuration of levodione, which was synthesised by the reduction of ketoisophorone using the enoate reductase from *G. oxydans*, has been done via measurement of the optical rotation of the purified product and comparison with literature data (Leuenberger et al. 1976a). For the purification of (*R*)-levodione a biotransformation as described was performed on 300 mg scale (20 ml). After 24 h the reaction mixture was extracted two times against ethyl acetate and tert-butyl methyl ether, and three times against tert-butyl methyl ether. The combined organic layer was dried with $MgSO_4$, filtered and concentrated under reduced pressure. Flash column chromatography on silica (Merk silica gel 60; eluent petroleum ether/ethyl acetate, 90:10) gave the desired (*R*)-levodione.

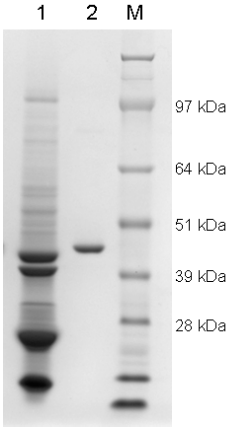

Fig. 1 SDS-PAGE analysis of the purified enoate reductase from *G. oxydans*. Lane M, molecular weight marker, lane 1 crude extract, lane 2 purified enoate reductase.

Results

Cloning and heterologous overexpression of the enoate reductase

In order to improve and simplify the expression and the purification of the enoate reductase, standard cloning techniques were used to create three different recombinant plasmids. All of them contain the enoate reductase gene. In two constructs a hexahistidine affinity purification motif (His-tag) was either fused to the C- or N-terminus of the protein. The third construct contains the enoate reductase without any modification (wild-type). According to the fact that the best activity was observed using the enoate reductase with the N-terminal His-tag, this variant was purified and used for all further investigations.

Purification of the enoate reductase

The N-terminal His-tag of the protein enables purification via IMAC with Ni-NTA resin material. An overview of the protein purification is shown in Table 2 and Fig. 1. The accomplished purification achieved a recovery of 58%. The resulting specific activity of the enoate reductase after the purification was 0.83 U/mg, corresponding to a threefold improvement in specific activity compared to the crude extract. A single band with an apparent molecular size of 44 kDa (Fig. 1, lane 2) corresponds to the enzyme, confirming the calculated molecular mass (39.24 kDa) derived from the amino acid sequence. In summary, a purification of the recombinant enoate reductase to homogeneity (>95%) was achieved by a single purification step (Fig. 1).

Classification of the enoate reductase

A sequence alignment of the amino acid of three yeast enzymes, OYE 1 and 2 (*Saccharomyces pastorianus (carlsbergensis)/ cerevisiae*) (Saito et al. 1991; Stott et al. 1993), KYE1 (*Kluyveromyces lactis*) (Miranda et al. 1995), one plant enzyme OPR1 (*Lycopersicon esculentum*) (Strassner et al. 1999), and two bacterial enzymes Yqjm (*Bacillus subtilis*) (Mizuno et al. 1996) and the studied enoate reductase from *G. oxydans* was performed using the Clustal W alignment tool (Larkin et al. 2007). Considerable sequence identity was observed over the entire sequence with respect to the different origins of the investigated enzymes. Furthermore, several highly conserved regions like the catalytic tyrosine, the residues for substrate binding, and FMN binding are present. Indeed, the enoate reductase from *G. oxydans* exhibits 6 out of 10 residues which are crucial for FMN binding and therefore are highly conserved (Fig. 2) (Breithaupt et al. 2001; Fox and Karplus 1994).

Table 2 Purification of the enoate reductase from *E. coli* BL21 (DE3) cells

Purification step	Total activity [U]	Specific activity [U/mg]	Purification factor	Yield [%]
Crude extract	293	0.26	1	100
Ni-NTA	239	0.67	2.6	81.5
Gelfiltration	340	0.83	3.2	58

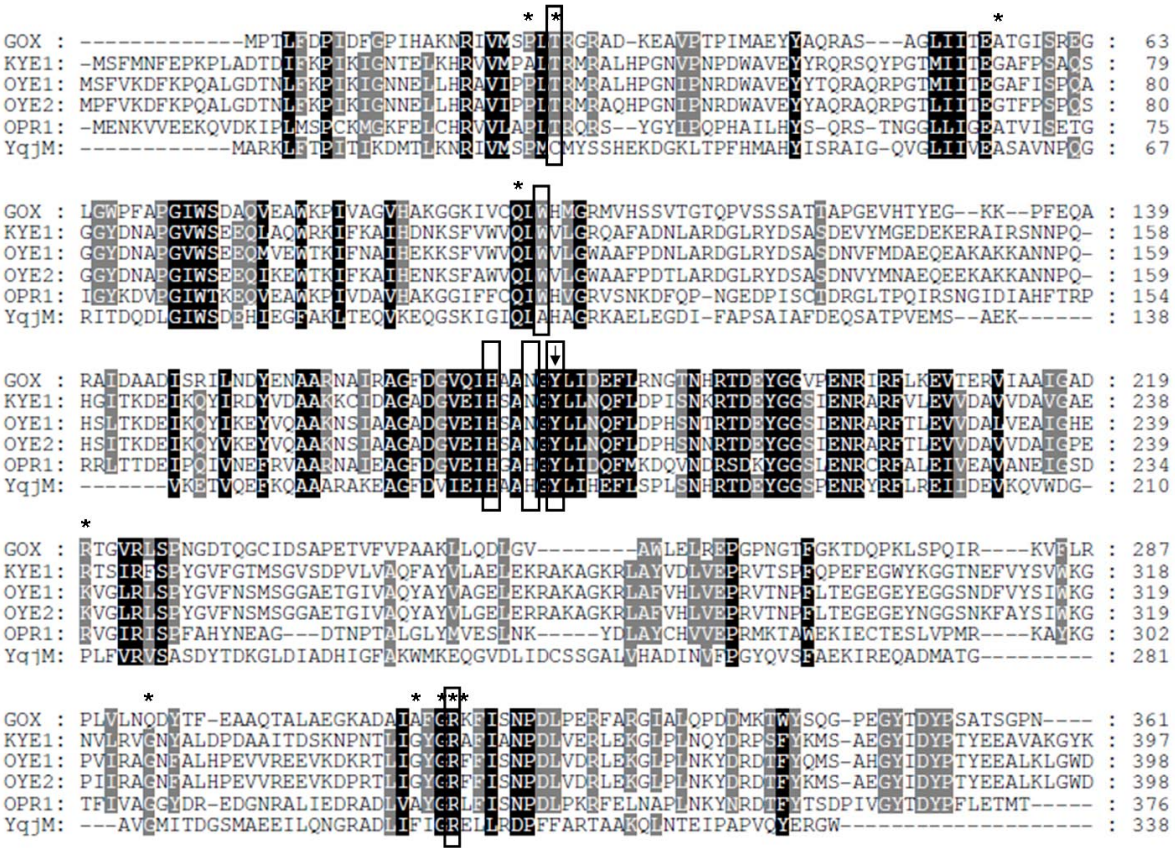

Fig 2 Amino acid sequence alignment of the enoate reductase from *G. oxydans* with several published OYE. The sequences of *S. pastorianus* (carlsbergensis) OYE1, S. cerevisiae OYE2, *K. lactis* KYE1, *L. esculentum* OPR1 and *B. subtilis* Yqjm are compared with the protein sequence of the enoate reductase from *G. oxydans*. The alignment was created using the Clustal W alignment tool. Shaded boxes in black indicate conserved amino acids, grey ones highlight similar amino acids. The amino acid residues involved in substrate binding (black frames), FMN-binding (*) and the catalytic tyrosine (↓) are indicated.

Based on these results the enoate reductase could be classified as a member of the TIM barrel protein superfamily, showing the typical characteristics of the "old yellow enzyme-like FMN" family.

Molecular characteristics of enoate reductase

Studies concerning cofactor dependency of the enoate reductase revealed that both nicotinamide cofactors are accepted by the enzyme. In comparison to NADH the phosphorylated cofactor NADPH is preferred, showing an 8-fold higher specific activity (Data not shown).

In addition the requirement of the enoate reductase for a flavin coenzyme was investigated. To determine which flavin species is bound to the protein the coenzyme was extracted from the enzyme by heat denaturation and analysed by HPLC alongside with authentic FAD, FMN and riboflavin as standards. Since only FMN was detected we could demonstrate that the enoate reductase requires FMN as coenzyme.

Characterisation of the kinetic parameters

The kinetic parameters for the substrate *trans*-2-hexenal and the cofactor NADPH were estimated using purified enoate reductase. For *trans*-2-hexenal the Michaelis-Menten constant (K_M) was determined to be 0.82 ±0.02 mM and the maximal specific activity (V_{max}) was 0.95 ±0.01 U/mg. For the cofactor NADPH an inhibition at concentrations above 0.3 mM was observed. This limits the cofactor concentrations that can be used to estimate the apparent kinetic constants. Therefore, cofactor concentrations up to 0.3 mM were used for fitting with the Michaelis-Menten equation. The estimated kinetic constants were: K_M = 0.16 mM ±0.06 and V_{max} = 0.62 U/mg ±0.03.

Dependence of the enoate reductase activity on temperature and pH

The influence of temperature and pH on the enzyme activity and stability is a crucial parameter especially for technical applications. Therefore, temperature- and pH-optimum as well as temperature stability were investigated. The purified enzyme exhibits an optimum activity at 45°C, while only 25% residual activity was observed above 53°C or below 30°C (Fig. 3A). The pH dependency of the enoate reductase was measured in a range of 3.5 to 10.0 using citrate phosphate buffer (pH 3.5 to 7.0) and TEA puffer (pH 6.6 to 10.0), respectively. As demonstrated in Fig. 3B the optimum activity in the reduction of *trans*-2-hexenal was measured at a pH of 5.5. Best activities at same pH values (pH 7.0) were observed in citrate-phosphate buffer.

Enzyme stability is also a crucial parameter for technical applications and processes. Hence the temperature-dependent inactivation over time and the thermostability of the enoate reductase were investigated. Studies concerning the thermostability were performed at different temperatures (4°C, 20°C and 30°C) over 24 h. The enzyme is stable under these

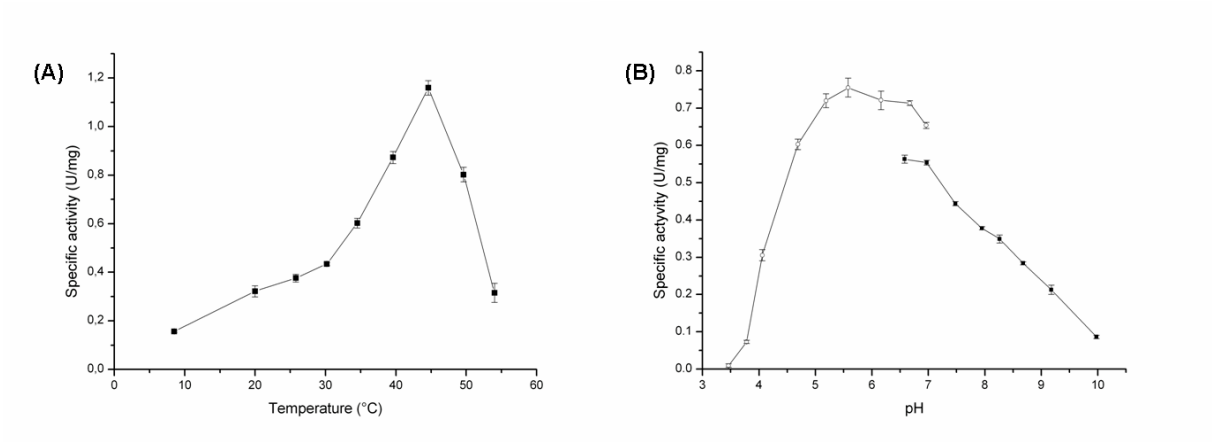

Fig 3 Determination of temperature (A) and pH optima (B). The effect of temperature and pH on the enzyme activity of the purified enoate reductase was measured by using the standard spectrophotometrical assay. For the determination of the optimum pH two different buffers, citrate phosphate buffer (pH 3.5 to 7.0) (-○-) and TEA (pH 6.6 to 10.0) (-■-) were used. The standard deviation of triplicates is shown in each diagram.

conditions during the investigated period, as evident from an unchanged activity after 24 h compared to the beginning of the experiment within this temperature range (data not shown). In a second study the midpoint thermal inactivation (T_m) of enoate reductase (crude extract) was determined to be 59°C (Fig. 4).

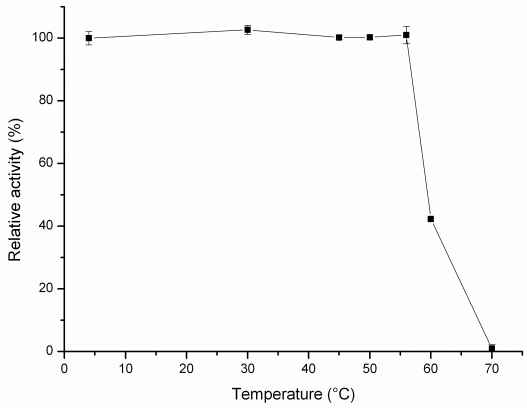

Fig 4 Midpoint thermal inactivation (T_m) of the enoate reductase. For the determination of the T_m different temperatures were kept for 10 min before the samples were withdrawn to measure the residual activity in the soluble protein content.

Substrate specificity of the enoate reductase

The substrate specificity of the enzyme was assessed using the spectrophotometrical standard assay as described. The specific activities of the crude extract against different aliphatic and cyclic olefins were determined comparatively to the standard substrate *trans*-2-hexenal (0.24 U/mg). The best activity was obtained in the reduction of KIP, Table 3 summarises the activities towards different substrates.

Biotransformation of citral

Due to the presence of multiple C=C and C=O bonds, the asymmetric synthesis of citral is a challenging task in terms of chemo-, regio- and stereoselectivity. Therefore, this reaction was chosen to investigate the potential of the enoate reductase. Citral, a mixture of the isomers geranial (*trans*) and neral (*cis*), is converted by the enoate reductase into citronellal, which is an

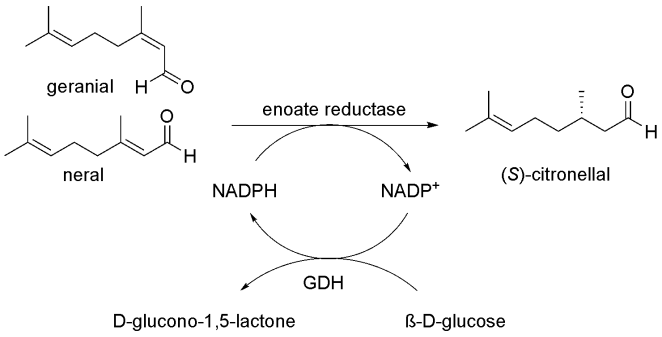

Fig 5 The asymmetric enzymatic reduction of the isomers neral and geranial (citral) to (*S*)-citronellal by the enoate reductase from *G. oxydans*. The reduced cofactor NADPH was simultaneously regenerated by glucose dehydrogenase and β-D-glucose as co-substrate.

important chiral building block useful for example for the cosmetic and food industry (Scott et al. 2008; Trasarti et al. 2004) (Fig. 5). Preliminary experiments showed that the use of purified enzyme is essential to obtain chiral citronellal, because the application of crude extract led to the formation of unidentified side products (data not shown).

The production of (*S*)-citronellal using purified enzyme was monitored over a period of 2 h; the result is shown in Fig. 6. For the regeneration of the reduced cofactor, glucose dehydrogenase in combination with glucose as co-substrate was used. The enoate reductase showed a diastereoselectivity for the reduction of the *cis*-isomer neral, because in the first 60 min geranial is preferentially reduced. When the concentration of neral falls below 1.25 mM the *trans*-isomer geranial is converted as well. Interestingly, the reaction rate of the geranial reduction is significantly reduced but full conversion was reached. Nevertheless, the reduction was performed with high regio- and chemoselectivity, the second double bound and the carbonyl moiety stayed untouched. Regarding the stereoselectivity of the product the enzyme produced the (*S*)-enantiomer with an *ee* of >99%.

Table 3 Relative activity of the enoate reductase towards different substrates. The activity was obtained using the standard spectrophotometrical assay; 100% corresponds to 0.24 U/mg (crude extract)

Substrate	Structure	Relative activity [%]
trans-2-hexenal	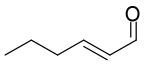	100
2,6.6-trimethyl-2-cyclohexen-1,4-dione (KIP)*	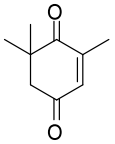	103.0
trans-3-nonen-2-one	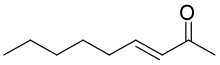	61.6
2-cyclohexen-1-one	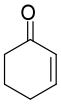	56.7
citral	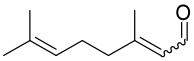	34.0
2-methyl-cyclopenten-1-one		12.4

* 5 mM of KIP were used in the assay

Biotransformation of ketoisophorone (KIP)

As a further example the chemo- and stereoselective reduction of KIP to levodione was investigated using the enoate reductase from *G. oxydans*. The resulting product (*R*)-levodione represents an interesting chiral building block, which is used for the synthesis of zeaxanthin (Leuenberger et al. 1976b). Thus, a small-scale reduction of KIP to levodione (1,5 mg, Fig. 7) was performed with a simultaneous regeneration of NADPH using glucose and glucose dehydrogenase. The substrate and product concentrations were measured by chiral GC.

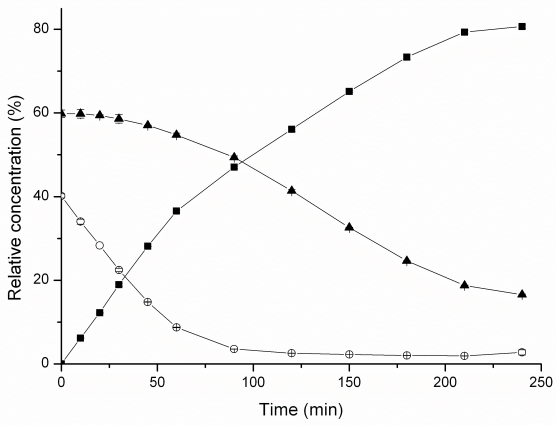

Fig 6 Citral biotransformation by the purified enoate reductase. The concentrations of neral (-○-), geranial (-▲-) and (*S*)-citronellal (-■-) were determined by chiral GC over a period of 240 min. Average values from three replicates with error bars are given.

Fig. 8 illustrates the time course of the asymmetric reduction of KIP applying purified enoate reductase. The reaction was monitored over a period of 2 h. During the first 60 min a linear

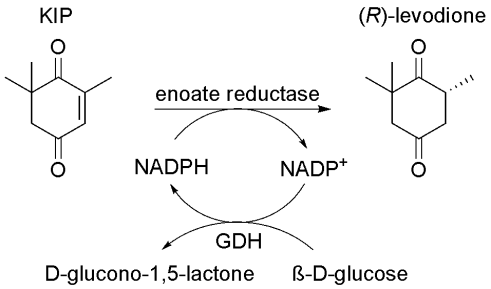

Fig 7 The asymmetric enzymatic reduction of KIP to (*R*)-levodione by the enoate reductase from *G. oxydans*. The reduced cofactor NADPH was simultaneously regenerated by the glucose dehydrogenase and β-D-glucose as co-substrate.

decrease of KIP combined with a linear increase of (*R*)-levodione was determined. Moreover, the enzyme showed a high preference for the formation of the (*R*)-enantiomer yielding an *ee* of >99%. The absolute configuration of the product was determined by optical rotation according to literature (Leuenberger et al. 1976a).

Discussion

In the present study, the enoate reductase from *G. oxydans* was successfully cloned, expressed, purified, biochemically characterised, and identified to be a member of the “old yellow enzyme family”. The enzyme and its heterologous expression and purification has been described previously (Schweiger et al. 2008; Yin et al. 2008). However, the published data differ especially concerning cofactor dependency, pH optimum and the selectivity in the biotransformation of citral (Table 4).

With regard to cofactor specificity, the different studies generally reveal a NADPH preference of the enzyme, only Yin and co-workers reported a NADH dependence of the enzyme. The

Table 4 Comparison of measured kinetic properties of the enoate reductase from *G. oxydans* with published data

	cofactor dependency	pH-optimum	temperature-optimum	biotransformation of citral
Yin *et al.* (Yin et al. 2008)	NADH	-	-	diastereoselective (*cis)*-isomer
Shinagawa *et al.* (Shinagawa et al. 2008)	NADPH	5.0	-	-
Schweiger *et al.* (Schweiger et al. 2008)	NADPH	7.0	RT	-
this study	NADPH	5.5	45°C	diastereoselective (*cis)*-isomer

pH- and temperature optimum differ significantly from the values reported by Schweiger *et al.* while the pH-optimum reported by Shinagawa *et al.* could be confirmed in the present study. According to the fact that the same enzyme was characterised the deviations of the parameter are remarkable. The different pH optimum reported by Schweiger *et al*. might be caused by the use of different buffers, sodium acetate (pH 4.5-6.5) compared to citrate phosphate in our study. The significantly different temperature optimum published by Schweiger *et al*. remains questionable.

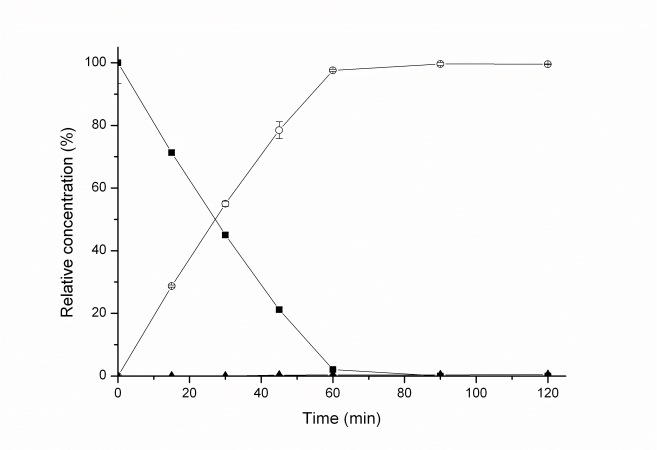

Fig 8 Biotransformation of KIP by the enoate reductase over 120 min. Concentrations of KIP (-■-), (*R*)-and (*S*)-levodione (-▲-/-○-) were determined by chiral GC. Error bars of triplicate measurements are given.

Apart from the cofactor specificity, another considerable difference in comparison to the work of Yin *et al.* is the reported observation that only the *cis*-isomer neral is reduced by the enzyme. Our study confirmed that indeed neral is the preferred substrate by the enzyme but geranial, the *trans*-isomer, is reduced, too, when the neral concentration is reduced significantly. This points out that the two *cis-trans* isomers neral and geranial isomerize easily which is well known for compounds with an enal structure. For example, Wolken *et al.* describe that such an isomerisation occur catalysed by a common amino acid (Wolken et al. 2000).

In addition to the biochemical properties of the enoate reductase the main focus of this study was to investigate its potential for chemo-, regio- and stereoselective asymmetric reductions of olefinic double bonds. Therefore, two reductions which lead to interesting chiral building blocks were chosen as model reactions. Both substrates were reduced in a stereoselective manner, producing (*S*)-citronellal and (*R*)-levidione. Moreover, in the reduction of citral the enoate reductase exhibits additionally a high regio- and chemoselectivity and a high diastereoselectivity by reducing preferentially the *cis*-isomer neral. First experiments using crude extract in the reduction of citral revealed the formation of side products. Side product formation is a common problem occurring when whole cells or crude extracts, in particular in the conversion of compounds with more than one functional group, are used. These by-products are often the result of alcohol dehydrogenases (ADH) which catalyse the NAD(P)H-dependent reduction of the carbonyl moiety (Hall et al. 2006; Müller et al. 2006; Müller et al. 2007; Servi 1990; Stuermer et al. 2007). Therefore, for some transformations the application of purified enzyme is required to attain the desired product. Hall *et al.* recently reported that the use of commercial formate dehydrogenase (FDH) for cofactor regeneration led to the formation of by-products, produced by contaminations of the FDH preparation by ADHs catalysing reductions at carbonyl moieties (Hall et al. 2008a). Therefore, an easy access to purified protein like described here is of major importance to overcome these limitations.

The asymmetric reduction of citral and KIP has already been investigated using other enoate reductases for example two isoenzymes from the plant *L. esculentum* (OPR1 and OPR3) (Hall et al. 2008a; Hall et al. 2007), YqiM from *B. subtilis* (Hall et al. 2008a) and other enoate reductases from bacteria, yeast and fungi (Müller et al. 2006) (Table 5). All these enzymes have in common that they can be applied for a variety of different substrates. Therefore, and with regard to the excellent stereo-, regio-, chemo- and diastereoselectivity shown in model reaction in this work the enoate reductase from *G. oxydans* is a promising catalyst and has a great potential to be applied in the preparative asymmetric reductions of carbonyl double bonds.

Acknowledgements

We would like to thank Thomas Eschemann and Astrid Wirtz for their excellent assistance and Robert Simon helpful discussions and for his chemical support. Furthermore, we would like to thank Jenifer Andexer for critical reading.

Keywords: enoate reductase, asymmetric reduction, ketoisophorone, enantioselectivity, biocatalysis

Adalbjörnsson BV, Toogood HS, Fryszkowska A, Pudney CR, Jowitt TA, Leys D, Scrutton NS (2010) Biocatalysis with thermostable enzymes: structure and properties of a thermophilic 'ene'-reductase related to old yellow enzyme. ChemBioChem 11:197-207.

Table 5 Overview of different enoate reductases and their ability in the reduction of ketoisophorone and citral. Applying either whole cells or isolated enzymes from *Aspergillus niger, Gluconobater oxydans, Lycopersicon esculentum B. subtilis, Salmonella typhimurium, Zymomonas mobilis, Thermoanaerobacter pseudethanolicus* and *Candida macedoniensis*.

		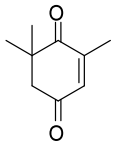 ketoisophorone		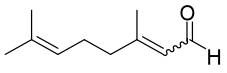 citral	
enzyme	origin	selectivity [*ee*]	conversion [%]	selectivity [*ee*]	conversion [%]
whole cells (Yamazaki et al. 1988)	*A. niger*	(*R*)	6 products	-	-
GYE1 (Yin et al. 2008)	*G. oxydans*	-	-	n.d.	40
OPR1 (Hall et al 2008a)	*L. esculentum*	(*R*) > 51	> 98	(*S*) > 95	> 99
OPR3 (Hall et al 2008a)	*L. esculentum*	(*R*) >43	> 85	(*S*) >95	> 90
YqiM (Hall et al 2008a)	*B. subtilis*	(*R*) >42	> 95	(*S*) >95	> 70
NRSal (Yanto et al. 2010)	*S. typhimurium*	(*R*) 87	12	-	no conversion
NCR-EnR (Hall et al. 2008b)	*Z. mobilis*	(*R*) >95	>99	(*S*) >95	> 99
TOYE (Adalbjörnsson et al. 2010)	*T. pseudethanolicus E39*	(*R*) 26	74	-	-
EnR (Kataoka et al. 2002)	*C. macedoniensis*	(*R*)	n.d	-	-
EnR (this study)	*G. oxydans*	(*R*) >99	>99	(*S*) >99	> 99

Bertani G (1951) Studies on lysogenesis .1. the mode of phage liberation by lysogenic *Escherichia coli*. J Bacteriol 62:293-300.

Bradford MM (1976) Rapid and sensitive method for quantitation of microgram quantities of protein utilizing principle of protein dye binding. Anal Biochem 72:248-254.

Breithaupt C, Strassner J, Breitinger U, Huber R, Macheroux P, Schaller A, Clausen T (2001) X-ray structure of 12-oxophytodienoate reductase 1 provides structural insight into substrate binding and specificity within the family of OYE. Structure 9:419-429.

Burda E, Kraußer M, Fischer G, Hummel W, Müller-Uri F, Kreis W, Gröger H (2009) Recombinant $\Delta^{4,5}$-steroid 5 β-reductases as biocatalysts for the reduction of activated C=C-double bonds in monocyclic and acyclic molecules. Adv Synth Catal 351:2787-2790.

Dobbs DA, Vanhessche KPM, Brazi E, Rautenstrauch V, Lenoir JY, Genet JP, Wiles J, Bergens SH (2000) Industrial synthesis of (+)-*cis*-methyl dihydrojasmonate by enantioselective catalytic hydrogenation; Identification of the precatalyst [Ru((-)-Me-DuPHOS)(H)-(η^6-1,3,5-cyclooctatriene)] (BF_4). Angew Chem Int Ed 39:1992-1995.

Fox KM, Karplus PA (1994) Old yellow enzyme at 2-A resolution: Overall structure, ligand binding, and comparison with related flavoproteins. Structure 2:1089-1105.

Fuganti C (1990) Bakers yeast mediated synthesis of natural products. Pure Appl Chem 62:1449-1452.

Goussevskaia EV, Robles Dutenhfner PA, Da Silva Rocha KA; Univ Federal Minas Gerais, assignee. 2007. Catalytic production of isopulegol by cyclizing of citronelal comprises application of hetero polyacid as catalyst in menthol precursor preparation patent BR200502489-A.

Hall M, Hauer B, Stuermer R, Kroutil W, Faber K (2006) Asymmetric whole-cell bioreduction of an α,β-unsaturated aldehyde (citral): competing prim-alcohol dehydrogenase and C-C lyase activities. Tetrahedron Asymmetry 17:3058-3062.

Hall M, Stueckler C, Ehammer H, Pointner E, Oberdorfer G, Gruber K, Hauer B, Stuermer R, Kroutil W, Macheroux P and others (2008a) Asymmetric bioreduction of C=C bonds using enoate reductases OPR1, OPR3 and YqjM: Enzyme-based stereocontrol. Adv Synth Catal 350:411-418.

Hall M, Stueckler C, Hauer B, Stuermer R, Friedrich T, Breuer M, Kroutil W, Faber K (2008b) Asymmetric bioreduction of activated C = C bonds using *Zymomonas mobilis* NCR enoate reductase and old yellow enzymes OYE 1-3 from yeasts. Eur J Org Chem:1511-1516.

Hall M, Stueckler C, Kroutil W, Macheroux P, Faber K (2007) Asymmetric bioreduction of activated alkenes using cloned 12-oxophytodienoate reductase isoenzymes OPR-1 and OPR-3 from *Lycopersicon*

esculentum (Tomato): A striking change of stereoselectivity. Angew Chem Int Ed 46:3934-3937.

Hirata T, Matsushima A, Sato Y, Iwasaki T, Nomura H, Watanabe T, Toyoda S, Izumi S (2009) Stereospecific hydrogenation of the C=C double bond of enones by *Escherichia coli* overexpressing an enone reductase of *Nicotiana tabacum*. J Mol Catal B Enzym 59:158-162.

Hogberg HE, Berglund P, Edlund H, Fagerhag J, Hedenstrom E, Lundh M, Nordin O, Servi S, Vorde C (1994) Biocatalysis as a useful tool in pheromone synthesis: Enantiomerically pure building blocks from bakers yeast reductions and enzyme-catalyzed resolutions. Catal Today 22:591-606.

Hult K, Berglund P (2007) Enzyme promiscuity: mechanism and applications. Trends Biotechnol 25:231-238.

Kataoka M, Kotaka A, Hasegawa A, Wada M, Yoshizumi A, Nakamori S, Shimizu S (2002) Old yellow enzyme from *Candida macedoniensis* catalyzes the stereospecific reduction of the C=Cbond of ketoisophorone. Biosci Biotechnol Biochem 66:2651-2657.

Kenig M, Peternel S, Gaberc-Porekar V, Menart V (2006) Influence of the protein oligomericity on final yield after affinity tag removal in purification of recombinant proteins. J Chromatogr A 1101:293-306.

Kitzing K, Fitzpatrick TB, Wilken C, Sawa J, Bourenkov GP, Macheroux P, Clausen T (2005) The 1.3 A crystal structure of the flavoprotein YqjM reveals a novel class of old yellow enzymes. J Biol Chem 280:27904-27913.

Knowles WS (2002) Asymmetric hydrogenations Angew Chem Int Ed 41:1998-2007

Larkin MA, Blackshields G, Brown NP, Chenna R, McGettigan PA, McWilliam H, Valentin F, Wallace IM, Wilm A, Lopez R and others (2007) Clustal W and clustal X version 2.0. Bioinformatics 23:2947-2948.

Leuenberger HGW, Boguth W, Widmer E, Zell R (1976a) Synthesis of Optically-Active Natural Carotenoids and Structurally Related Compounds .1. Synthesis of Chiral Key Compound (4r,6r)-4-Hydroxy-2,2,6-Trimethylcyclohexanone. Helvetica Chimica Acta 59:1832-1849.

Leuenberger HGW, Boguth W, Widmer E, Zell R (1976b) Synthesis of optically active natural carotenoids and structurally related compounds 1. Synthesis of chiral key compound (4*R*,6*R*)-4-hydroxy-2,2,6-trimethylcyclohexanone. Helv Chim Acta 59:1832-1849.

Lipshutz BH, Servesko JM (2003) CuH-catalyzed asymmetric conjugate reductions of acyclic enones. Angew Chem Int Ed 42:4789-4792.

Lipshutz BH, Servesko JM, Petersen TB, Papa PP, Lover AA (2004) Asymmetric 1,4-reductions of hindered β-substituted cycloalkenones using catalytic SEGPHOS-ligated CuH. Org Lett 6:1273-1275.

Miranda M, Ramirez J, Guevara S, Ongaylarios L, Pena A, Coria R (1995) Nucleotide sequence and chromosomal localization of the gene encoding the old yellow enzyme from *Kluyveromyces lactis*. Yeast 11:459-465.

Mizuno M, Masuda S, Takemaru K, Hosono S, Sato I, Takeuchi M, Kobayashi Y (1996) Systematic sequencing of the 283 kb 210 degrees-232 degrees region of the *Bacillus subtilis* genome containing the skin element and many sporulation genes. Microbiol 142:3103-3111.

Müller A, Hauer B, Rosche B (2006) Enzymatic reduction of the α,β-unsaturated carbon bond in citral. J Mol Catal B Enzym 38:126-130.

Müller A, Sturmer R, Hauer B, Rosche B (2007) Stereospecific alkyne reduction: Novel activity of old yellow enzymes. Angew Chem Int Ed 46:3316-3318.

Noyori R (2002) Asymmetric catalysis: Science and Opportunities Angew Chem Int Ed 41:2008-2022.

Ohta T, Miyake T, Seido N, Kumobayashi H, Takaya H (1995) Asymmetric hydrogenation of olefins with aprotic oxygen functionalities catalyzed by BINAP-Ru(II) complexes. J Org Chem 60:357-363.

Pietzsch M, Wiese A, Ragnitz K, Wilms B, Altenbuchner J, Mattes R, Syldatk C (2000) Purification of recombinant hydantoinase and L-N-carbamoylase from *Arthrobacter aurescens* expressed in *Escherichia coli*: comparison of wild-type and genetically modified proteins. J Chromatogr B 737:179-186.

Rohdich F, Wiese A, Feicht R, Simon H, Bacher A (2001) Enoate reductases of *Clostridia* J Biol Chem 276:5779-5787.

Rumlova M, Benedikova J, Cubinkova R, Pichova I, Ruml T (2001) Comparison of classical and affinity purification techniques of mason-pfizer monkey virus capsid protein: The alteration of the product by an affinity tag. Protein Expr Purif 23:75-83.

Saito K, Thiele DJ, Davio M, Lockridge O, Massey V (1991) The cloning and expression of a gene encoding old yellow enzyme from *Saccharomyces carlsbergensis*. J Biol Chem 266:20720-20724.

Schweiger P, Gross H, Wesener S, Deppenmeier U (2008) Vinyl ketone reduction by three distinct *Gluconobacter oxydans* 621H enzymes. Appl Microbiol Biotechnol 80:995-1006.

Scott DC, Sanker LA, Goulbourne EA; Scott D C; Sanker L a; Goulbourne E a; Procter & Gamble Co, assignee. 2008. Blend of essential oil components useful in personal care products e.g. skin lotion, and in oral care compositions e.g. chewable tablet for treating caries, comprises acyclic components e.g. citral, and cyclic components e.g. eugenol patent US2008253976-A1; WO2008126057-A2.

Servi S (1990) Baker yeast as a reagent in organic synthesis. Synthesis 1-25.

Shinagawa E, Ano Y, Adachi O, Matsushita K (2008) The occurrence of a novel NADH dehydrogenase, distinct from the old yellow enzyme, in *Gluconobacter* strains. Biosci Biotechnol Biochem 72:260-264.

Stott K, Saito K, Thiele DJ, Massey V (1993) Old yellow enzyme - the discovery of multiple isozymes and a family of related proteins. J Biol Chem 268:6097-6106.

Strassner J, Furholz A, Macheroux P, Amrhein N, Schaller A (1999) A homolog of old yellow enzyme in tomato - Spectral properties and substrate specificity of the recombinant protein. J Biol Chem 274:35067-35073.

Stuermer R, Hauer B, Hall M, Faber K (2007) Asymmetric bioreduction of activated C=C bonds using enoate reductases from the old yellow enzyme family. Curr Opin Chem Biol 11:203-213.

Trasarti AF, Marchi AJ, Apesteguia CR (2004) Highly selective synthesis of menthols from citral in a one-step process. J Catal 224:484-488.

Vaz ADN, Chakraborty S, Massey V (1995) Old yellow enzyme - aromatization of cyclic enones and the mechanism of a novel dismutation reaction. Biochemistry 34:4246-4256.

Warburg O, Christian W (1932) On a new oxidation enzyme. Naturwissenschaften 20:980-981.

Wegner G, Kaibel G, Therre J, Aquila W, Fuchs H; Basf Ag, assignee. 2008. Citral preparation in high yield, for use e.g. as intermediate for perfumes or vitamins, by 6-stage process from isobutene and formaldehyde via isoprenol, prenal and prenol patent WO2008037693-A1.

Williams RE, Bruce NC (2002) 'New uses for an old enzyme' - the old yellow enzyme family of flavoenzymes. Microbiology 148:1607-1614.

Wolken WAM, ten Have R, van der Werf MJ (2000) Amino acid-catalyzed conversion of citral: Cis-trans isomerization and its conversion into 6-methyl-5-hepten-2-one and acetaldehyde. J. Agric. Food Chem 48: 5401-5405.

Yamazaki Y, Hayashi Y., Hori N, Mikami Y (1988) Microbial conversion of 4-oxoisophorone by *Aspergillus niger*. Agric. Biol. Chem 52: 2919-2920.

Yanto Y, Hall M, Bommarius AS (2010) Nitroreductase from *Salmonella typhimurium*: characterization and catalytic activity. Org Biomol Chem 8:1826-1832.

Yin B, Yang XP, Wei GD, Ma YS, Wei DZ (2008) Expression of two old yellow enzyme homologues from *Gluconobacter oxydans* and identification of their citral hydrogenation abilities. Mol Biotechnol 38:241-245.

3 THE CRYSTAL STRUCTURE OF THE GLYCEROL DEHYDROGENASE FROM *GLUCONOBACTER OXYDANS*

3. 1 THE THREE-DIMENSIONAL STRUCTURE OF AKR11B4, A GLYCEROL DEHYDROGENASE FROM *GLUCONOBACTER OXYDANS*, REVEALS A TRYPTOPHAN RESIDUE AS AN ACCELERATOR OF REACTION TURNOVER

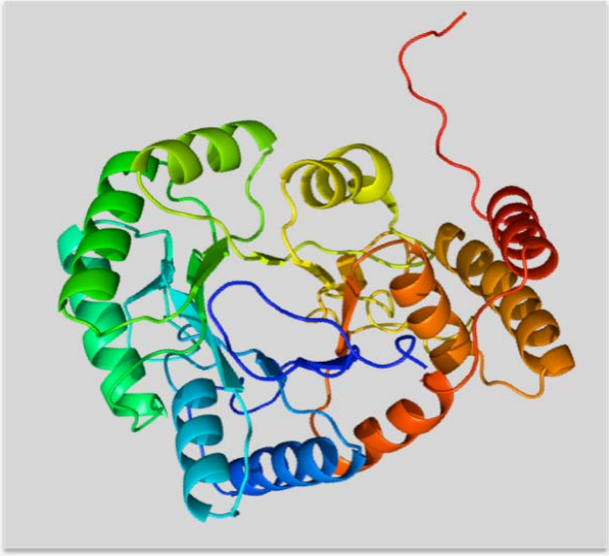

N. Richter, K. Breicha, W. Hummel and K. Niefind (2010)

J. Mol. Biol. 404, 353-362

(doi: 10.1016/j.jmb.2010.09.049)

Structure of glycerol dehydrogenase from *G.oxydans*

The Three-dimensional structure of AKR11B4, a glycerol dehydrogenase from *Gluconobacter oxydans*, reveals a tryptophan residue as an accelerator of the reaction turnover

Nina Richter[1#], Klaus Breicha[2#], Werner Hummel[3] and Karsten Niefind[2*]

This paper is dedicated to Professor Dr Dietmar Schomburg on the occasion of his 60th birthday.

[1] evocatal GmbH, Merowingerplatz 1A, D-40225 Düsseldorf, Germany
[2] Universität zu Köln, Institut für Biochemie, Zülpicher Straße 47, D-50674 Köln, Germany
[3] Institut für Molekulare Enzymtechnologie der Heinrich-Heine-Universität Düsseldorf, Forschungszentrum Jülich, Stetternicher Forst, D-52426 Jülich, Germany

[#]*Common first authors* / **Corresponding author*

E-mail address of the corresponding author:
Karsten.Niefind@uni-koeln.de

The NADP-dependent glycerol dehydrogenase (EC 1.1.1.72) from Gluconobacter oxydans is a member of family 11 of the aldo-keto reductase (AKR) enzyme superfamily; according to the systematic nomenclature within the AKR superfamily the abbreviation AKR11B4 has been assigned to the enzyme. AKR11B4 is a biotechnologically attractive enzyme because of its broad substrate spectrum combined with a distinctive regio- and stereoselectivity. These features can be partially rationalized on the basis of a 2-Å-crystal structure of apo-AKR11B4 which we describe and interprete here against the background of functional complex structures of other members of the AKR family 11. The structure of AKR11B4 shows the AKR-typical $(\beta/\alpha)_8$ TIM-barrel fold with three loops and the C-terminal tail determining the particular enzymatic properties. In comparison to AKR11B1 - its closest AKR relative - AKR11B4 has a relatively broad substrate and cosubstrate binding cleft. In the crystalline environment it is completely blocked by the C-terminal segment of a neighbouring protomer. The structure reveals a conspicuous tryptophane residue (Trp23) that has to adopt an unconventional and strained side chain conformation to permit cosubstrate binding. We predict and confirm by site-directed mutagenesis that Trp23 is an accelerator of (co-)substrate turnover. Further, we show that simultaneously this tryptophane residue is a critical determinant for substrate binding by the enzyme, while the enantio selectivity is probably governed by a methionine residue within the C-terminal tail. We present structural reasons for these notions on the basis of ternary complex models of AKR11B4, $NADP^+$ and either octanal, D-glyceraldehyde or L-glyceraldehyde.

Introduction

The subject of this study - glycerol dehydrogenase (EC1.1.1.72) from *Gluconobacter oxydans* was - discovered in an effort to find biotechnologically interesting oxidoreductases disposing of a high regio and stereoselectivity[1]. The particular objective of that work[1] was the identification of an enzyme that can be applied for the production of enantiopure L-glyceraldeyde which is a valuable synthon for organic synthesis. In fact, the glycerol dehydrogenase from *G. oxydans* catalyzes the following equillibrium between glycerol and D-glyceraldehyde:

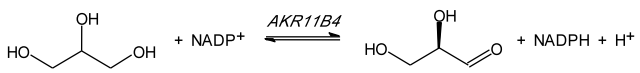

As a consequence the enzyme can be used to kineticly resolve a racemic mixture of D- and L-glyceraldehyde so that the L-enantiomer is left.

The glycerol dehydrogenase from *G. oxydans* is a monomeric protein of 332 residues and a calculated molecular mass of 37213 g/mole. Its amino acid sequence identifies the enzyme as a member of the aldo-keto reductases (AKR), a superfamily of enzymes, catalysing the reversible NADPH-dependent reduction of carbonyl compounds[2,3]. AKRs are ubiquitously distributed and can be found in plants, animals and prokaryotes. They are characterized by a $(\beta/\alpha)_8$ TIM-barrel fold that occurs very

frequently in enzymes[4] and by a common reaction mechanism based on a conserved catalytic tetrad[5]. As found for the glycerol dehydrogenase from *G. oxydans*[1] AKR enzymes are typically monomers with an approximate mass of 35 kDa. The substrate spectrum of AKRs is very broad: activities with different alcohols, steroids and also aromatic ketones have been observed[3].

Table 1: Sequence identities after pairwise sequence alignments of GlyDH and all three family 11 AKRs structurally characterized so far. The sequence alignments were calculated with the program GAP of the GCG package (Accelrys, Inc., San Diego, USA).

	GlyDH (this work)	AKR11B (1PZ1)	AKR11A (1PZ0)	AKR11C (1YNP)
GlyDH (this work)	**100**	**57.2**	33.2	30.4
AKR11B (1PZ1)	**57.2**	**100**	37.1	30.7
AKR11A (1PZ0)	33.2	37.1	100	32.9
AKR11C (1YNP)	30.4	30.7	32.9	100

According to sequence homology the known AKR sequences have been clustered into 15 families[2], the glycerol dehydrogenase from *G. oxydans* belongs to family 11 comprising so far only bacterial enzymes three of which (AKR11A1, AKA11B1 from *Bacillus subtilis* and AKR11C1 from *Bacillus halodurans*) have been structurally characterized[6,7]. Pairwise sequence alignment between the novel glycerol dehydrogenase and those three AKR11 enzymes (Tab. 1) reveal that its closest relative is AKR11B1 while the sequence identities to AKR11A1 and to AKR11C1 are significantly below the 40% identity level which normally constitutes AKR families[2,3]. Accordingly, after submission of the sequence of the *G. oxydans* glycerol dehydrogenase to the AKR superfamily data base[2] the designation “AKR11B4” was assigned that we use from here on.

We report here a crystal structure of AKR11B4; it will supplement the knowledge about AKR family 11 structures and – since AKR11B4 is enzymatically better characterized[1] than the other enzymes of Tab. 1 – about structure/function relationships.

Results and Discussion

Overview of the AKR11B4 structure

We performed crystallization experiments with AKR11B4 both as an apo-enzyme and in the presence of $NADP^+$ and D-glyceraldehyde, but in spite of many efforts high-quality crystals could be obtained only with the apo-enzyme. Our failure to grow and optimize binary and ternary complex crystals may be caused by the enzyme’s tendency to block the $NADP^+$ binding site in the crystalline environment by the C-terminal segment of a neighbouring protomer (Fig. 2b).

The structure of apo-AKR11B4 was solved by molecular replacement and refined to a resolution of 2 Å (Tab. 2). Like all members of the AKR family AKR11B4 folds into a $(\beta/\alpha)_8$ barrel motif (Figs. 1 and 2a). In addition to the core α-helices (α1-α8) and β-strands (β1-β8) the structure of AKR11B4 exhibits three secondary structure elements that are common to the AKR superfamily, namely the two α-helices H1 and H2 (magenta in Fig. 2a) and a two-stranded antiparallel β-sheet next to the N-terminus (B1 and B2; black in Fig. 2a). Finally a further β-hairpin (B3 and B4; blue in Fig. 2a) that is embedded in the interconnection between strand β3 and helix α3 (loop 3) is unusual for AKRs in general but a typical feature of the bacterial enzymes of AKR family 11. As described for AKR11B1 and AKR11A1[6] loop 3 takes over a region in space that in AKRs is normally occupied by the extended loop 4 which consequently in AKR11B4 (and other AKR11 family members) is reduced to a short interconnection.

```
                1        10         20  Trp23  30         40         50
                |        |          |   ↓    |          |          |
AKR11B4         MASDTIRIPG IDTPLSRVAL GTWAIggwmw ggpDDDNGVR TIHAALDEGI
AKR11B1         ~~MEYTSIAD TGIEASRIGL GTWAIggtmw ggtDEKTSIE TIRAALDQGI
sec. struct.       <B1>       <B2> <β1>           <-------α1------>
                |N-terminal hairpin|   |--loop 1--|

                Asp54 Tyr59 62      70         78 80  Lys84  90      98
                  ↓     ↓   |       |          |  |   ↓     |       |
AKR11B4         NLIDTAPVYG FGHSEEIVGR ALAEKPD..K AHVATKLGLH WVGedeknMK
AKR11B1         TLIDTAPAYG FGQSEEIVGK AIKEYMKrdQ VILATKTALD WKN.....NQ
sec. struct. <-β2>       <-----α2----->        <--β3-><-B3->
                                                      |---loop 3---

                 100        110        120      His130        140      148
                  |          |          |          ↓          |        |
AKR11B4         VFRDSRPARI RKEVEDSLRR LRVETIDLEQ IHWPDDKTPI DESARELQKL
AKR11B1         LFRHANRARI VEEVENSLKR LQTDYIDLYQ VHWPDPLVPI EETAEVMKEL
sec. struct.<-B4>  <------α3-------->     <-β4->       <-----α4----
                loop 3|

                 150        160        170        180        190      198
                  |          |          |          |          |        |
AKR11B4         HEDGKIRALG VSNFSPEQMD IFREVAPLAT IQPPLNLFER TIEKDILPYA
AKR11B1         YDAGKIRAIG VSNFSIEQMD TFRAVAPLHT IQPPYNLFER EMEESVLPYA
sec. struct. α4->   <-β5->   <----α5--->    <β6>          <---α6---

                 200        210        220        Arg232     240      248
                  |          |          |          ↓          |        |
AKR11B4         EKHNAVVLAY GALCRGLLTG KMNRDTTFPK DDLRSNDPKF EKPNFEKYLA
AKR11B1         KDNKITTLLY GSLCRGLLTG KMTEEYTFEG DDLRNHDPKF QKPRFKEYLS
sec. struct. α6-> <--β7->                                  <----αH1-
                          |--------------loop 7------------|

                 250        260        270        280 Arg285 290    296
                  |          |          |          |    ↓     |      |
AKR11B4         AMDEFEKLAE .KRGKSVMAF AVRWVLDQGP .VIALWGARK PGQVSGVKDV
AKR11B1         AVNQLDKLAK TRYGKSVIHL AVRWILDQPG ADIALWGARK PGQLEALSEI
sec. struct. ------H1-----> <-----α7----->    <-β8->    <---α8--->

                   300        310        320 Met326   332
                    |          |          |   ↓      |
AKR11B4         FGWSLTDEEK KAVDDILARH VPDPIDPTFM Appard~~
AKR11B1         TGWTLNSEDQ KDINTILENT ISDPVGPEFM Apptreei
sec. struct.       <------H1----->
```

Fig. 1: Structure-based sequence alignment between AKR11B4 and AKR11B. AKR11B1 is the nearest relative of AKR11B4 with a known structure[6]. The two structures were loaded in BRAGI[13] that was used to calculate a 3D-alignment according to a procedure developed by Lessel & Schomburg[14]. Important residues mentioned in the text were highlighted by colours.

The most conspicuous features of the AKR11B4 structure are an extended C-terminal segment pointing away from the core of the molecule (Figs. 2a/c) and an open active site cleft best visible in the centre of Fig. 2d. These two elements are not independent of each other; rather – as mentioned above - the C-terminal region is embedded in the active site cleft of a neighbouring symmetry mate (Fig. 2b).

Structural comparison of AKR11B4 and AKR11B1

It is well established that in the AKR superfamily the structurally highly conserved TIM barrel core is accompanyied by a large

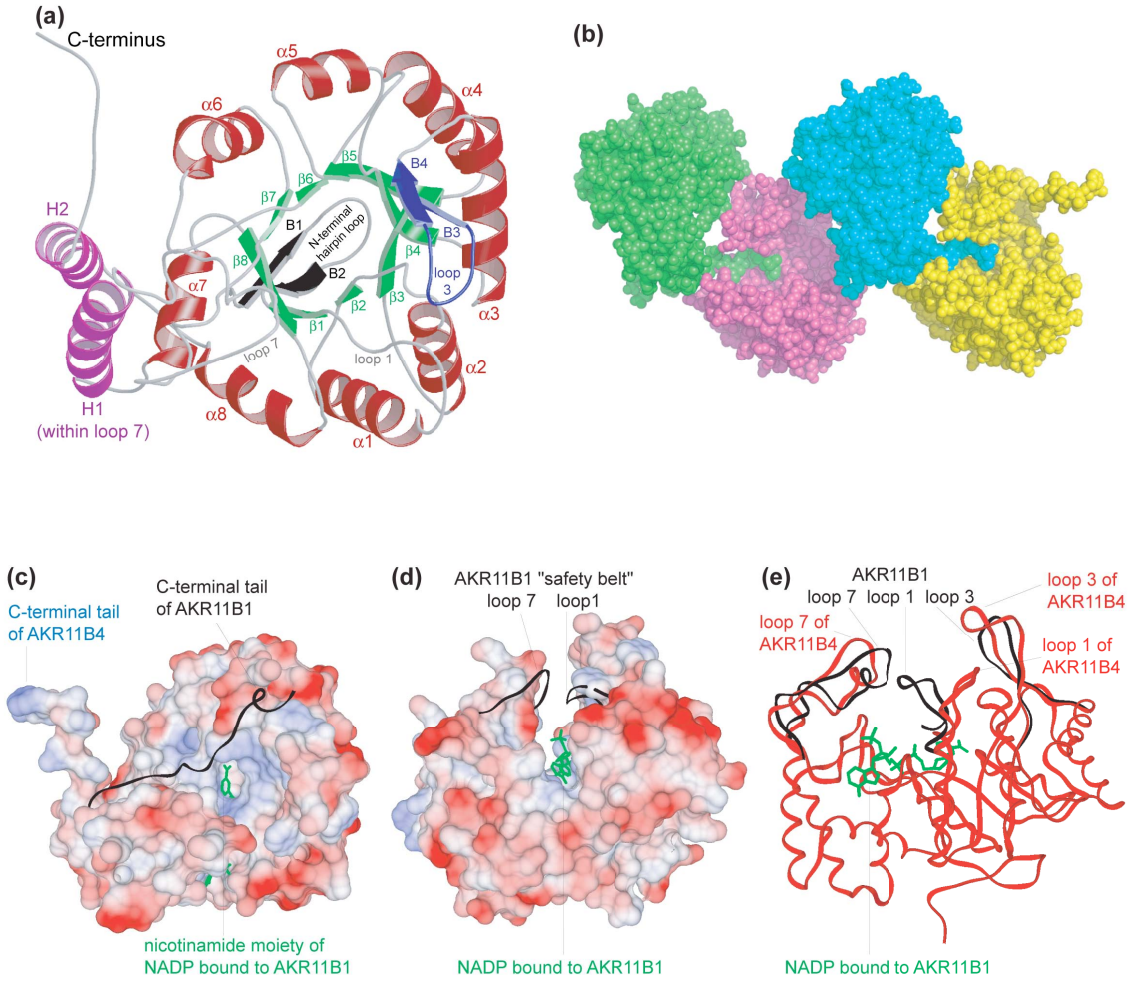

Fig. 2: Overview of the GlyDH structure. **(a)** View on the $(\beta/\alpha)_8$ TIM-barrel from the top prepared with BOBSCRIPT[15] and Raster3D[16]. **(b)** A chain of four AKR11B4 molecules from the crystal packing illustrating that the C-terminal segment extends into a neighbouring symmetry mate. The figure was drawn with PyMol[17]. **(c-e)** A sequence of three views on a structural overlay of AKR11B4 (this work) and AKR11B1[6] prepared with BRAGI[13] The $NADP^+$ molecule from the AKR11B1/$NADP^+$ complex was drawn in green to illustrate the location of the active site. The black ribbons indicate the backbone course of AKR11B1, the red ones of AKR11B4. In the parts (c) and (d) of the figure the AKR11B4 molecule was covered with a surface indicating the hydrophobicity in blue (strongly hydrophobic) over white to red (strongly hydrophilic).

adaptability in the loop regions at the C-terminal side of the barrel. This is true in the sense of the phylogenetic evolution as revealed by comparison of different AKR superfamily members but it is also valid for the conformational plasticity of a specific AKR with respect to different functional situations. In the case of AKR11B4 we currently dispose only of an apo-structure, but AKR11B1, its closest relative in sequence (Tab. 1, Fig. 1), provides a good supplement since for this enyme only a binary complex structure with $NADP^+$ is available[6]. In the following we take the AKR11B1/$NADP^+$ structure (PDB 1PZ1[6]) as a matrix to derive reasonable models of binary and ternary complexes of AKR11B4.

The most obvious differences between the two structures concern the C-terminal segment and the active site cleft. In contrast to the above-mentioned neighbour-anchoring conformation in AKR11B4 (Fig. 2b) the C-terminus in AKR11B1 adopts a conformation common for catalytically active AKRs: locked by hydrophobic interactions, it is swung over the active site cleft like a handle (black ribbon in Fig. 2c) and is thus prepared to play a role in substrate binding as demonstrated for the first time for human aldose reductase[8]. In addition – and again in contrast to AKR11B4 - the active site cleft of AKR11B1 is closed from the other side in a way that is typical for AKRs, too: the two loops 1 and 7 are in direct atomic contact (black ribbons in Fig. 2d) and thus cross the cleft. This a characteristic arrangement that has been refered to as “safety belt” in the AKR literature[6] since it contributes to the fixation of $NADP^+$, in particular of the phospho group (Fig. 3b).

The question arises whether these structural differences are consequences of the different functional states of the two enzymes – AKR11B1: binary complex with $NADP^+$; AKR11B4: apo-enzyme – or whether they are inherent features of the protein molecules arising from their specific sequences. In the case of the C-terminal segment of AKR11B4 it is clear that an alternative conformation must exist. The C-terminal segment has a largely hydrophobic surface (Fig. 2c) and adopts the extended conformation only because it is embedded in the $NADP^+$ binding cleft of a crystalline neighbour which is rendered inaccessible in this way. In solution, however, AKR11B1 is monomeric and requires – since it is active – an accessible $NADP^+$ binding site. It is possible that under this condition the C-terminal tail swings over the top of the barrel as found in AKR11B1 (see black coil in

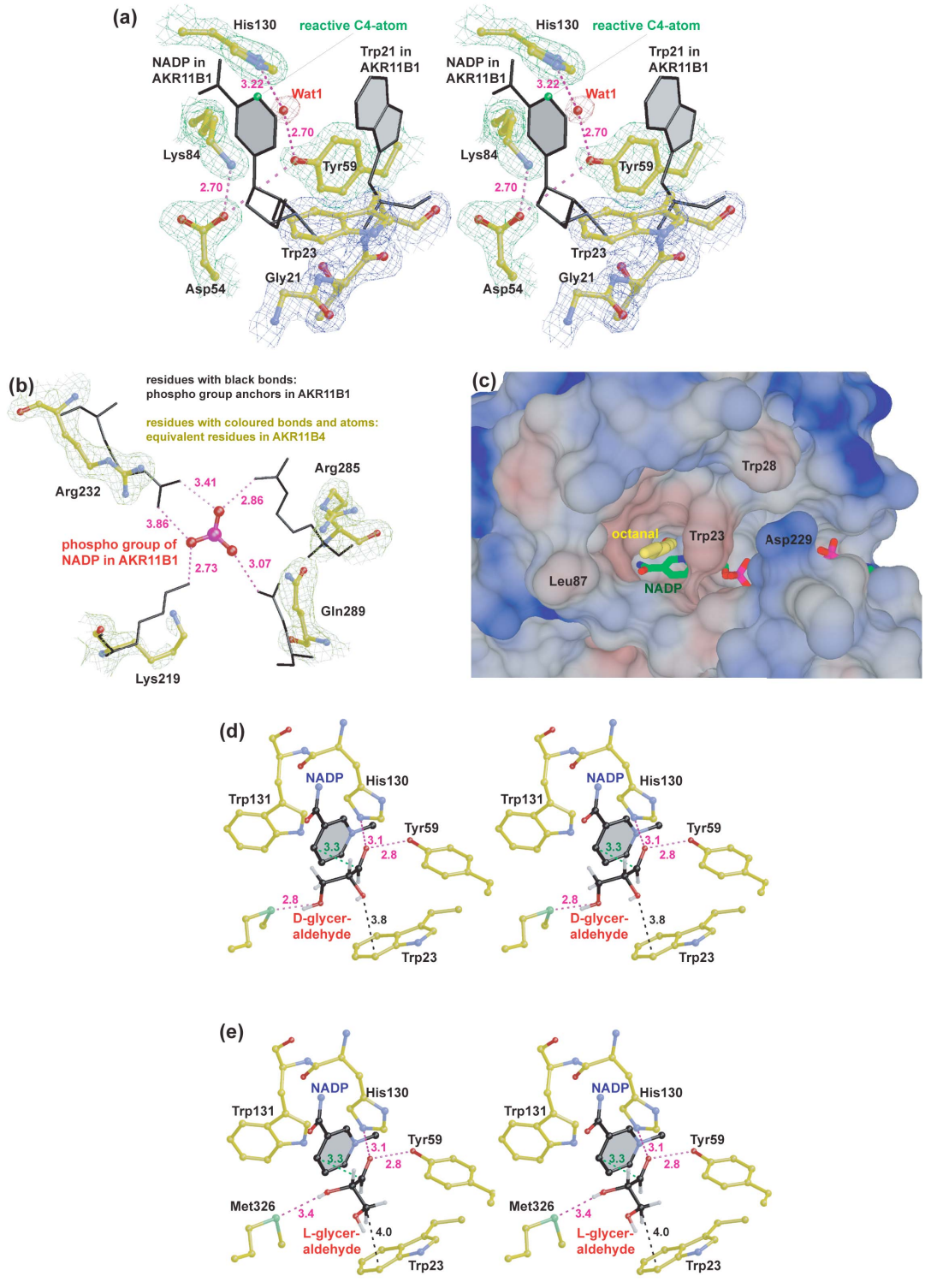

Fig. 3: Details of NADP$^+$ and substrate binding to AKR11B4 **(a)** Stereo figure to illustrate the active site and the role of Trp23: the four members of the catalytic tetrad (Tyr59, His130, Lys84, Asp54) are drawn and covered with green electron density. The water molecule Wat1 (red electron density) marks the position of the carbonyl oxygen of a substrate molecule. Trp23 (blue electron density) is shown in its relaxed conformation as found in apo-AKR11B4. To illustrate the strained conformation the equivalent tryptophane residue from the AKR11B1/NADP$^+$ complex was drawn in black. The contouring level for the electron density illustration was 1.5 σ. Atomic distances are given in Å. The figure was prepared with BOBSCRIPT[15] and Raster3D[16].**(b)** Fixation of the phospho group of NADP$^+$ by components of loop 7: in the AKR11B1/NADP$^+$ complex[6] a "safety belt" of loop 7 and loop 1 is formed (Fig. 2d) which correlates with the fixation of the NADP$^+$-phospho group by two arginine, a lysine and a glutamine side chain from loop 7. These side chains of AKR11B1 are illustrated with black bonds. The equivalents in apo-AKR11B4 (this work) are drawn with coloured bonds and atoms and are covered by the final electron density (contouring level 1 σ above the mean). Atomic distances are given in Å. The figure was prepared with BOBSCRIPT[13] and Raster3D[16]. **(c)** The entrance channel to the active site occupied with a modelled octanal molecule (yellow): the underlying ternary complex was modelled as a combination of the enzyme part (apo-AKR11B4), NADP$^+$ from the AKR11B1/NADP$^+$ complex[6] and octanal as a typical substrate molecule of AKR11B4. The Trp23 side chain was turned out of the NADP$^+$ binding area as illustrated in Fig. 3a. The carbonyl oxygen of octanal was placed at the Wat1 position shown in Fig. 3a. The hydrocarbon chain of octanal was placed in such a way that it overlapped largely with the cortisone molecule in the AKR1D1/NADP$^+$/cortisone complex structure (PDB 3CMF)[11]. Interfering water molecules of the apo-AKR11B4 structure were deleted. Finally the complex was refined with 5 cycles of REFMAC[19] leading to an optimization of the atomic contacts. The parametrization of the octanal molecule was calculated with LIBCHECK[19]. In the picture the enzyme part is covered with a molecular surface coloured according to hydrophobicity (red: hydrophobic, blue: hydrophilic). The figure was drawn with BRAGI[13]. **(d/e)** Stereo pictures of ternary complex models of AKR11B4, NADP$^+$ and either D-glyceraldehyde (d) or L-glyceraldehyde (e). The models were built with the equivalent procedure described above (legend of Fig. 3c) for the AKR11B4/NADP$^+$/octanal complex. Atomic distances are given in Å and coloured in three different ways (magenta: hydrogen bonds; green: hydride ion transfer route between NADPH and the aldehyde substrate; black: smallest interatomic distance between the substrate and the Trp23 side chain. The figures were prepared with BOBSCRIPT[15] and Raster3D[16].

Fig. 2c). In general such a conformation is regarded as a prerequisite for an AKR enzyme with significant activity (although AKR11C1 is a counter-example[7]). Further - as explained below in more detail - an AKR11B1-similar conformation of the C-terminal segment of AKR11B4 is even very likely because only then and under inclusion of parts of the C-terminal segment as critical

determinants a plausible rationalization of the enzyme's substrate profile is possible.

With respect to the loops 1 and 7 the comparison with the AKR11B1/NADP$^+$ complex (Fig. 2d) suggests that NADP$^+$ binding to AKR11B4 closes the "safety belt". However, again AKR11C7 provides a counter-example that NADP$^+$ binding to an AKR enzyme can happen without a closed safety belt of the loops 1 and 7. The notion that in AKR11B4 no safety belt closure occurs would fit to the observation that the loop 1 is conspicuously hooked up by the loop 3 (Fig. 2e). As mentioned above this loop is generally longer in the bacterial AKRs of family 11 than in other AKRs and contains a non-consensus β -sheet (strands B3 and B4). In AKR11B4, however, loop 3 is particularly large and significantly longer than in AKR11B1 (Fig. 1) suggesting that its intense contact to loop 1 might prevent the latter from approaching loop 7 and forming the canonical safety belt after NADP$^+$ binding.

Since so far we have no AKR11B4/NADP$^+$ complex structure to reveal the potential loop1/loop7 safety belt directly we performed a mutational study with AKR11B4. In AKR11B1 one consequence of the tight contact of the loops 1 and 7 over the NADP$^+$ molecule is that two positively charged arginine residues (the equivalents of Arg232 and Arg285 in AKRB4; Fig. 3b) approach the phospho group of the cosubstrate. To probe the role of the equivalent residues in AKR11B4 (Arg232 and Arg285) we changed each of them both to aspartate and to glutamate. The resulting mutants AKR11B4-^{Arg232Asp}, AKR11B4-^{Arg232Glu}, AKR11B4-^{Arg285Asp} and AKR11B4-^{Arg285Glu} were inactive, a result that supports the idea of a saftety belt closure correlated with NADP$^+$ binding.

Trp23 is a key residue for NADP$^+$/NADPH and substrate turnover

A subtle, but functionally important structural difference between AKR11B1 and AKR11B4 refers to Trp23 in loop 1 which in the folded enzyme is located close to the catalytic tetrad of Tyr59, His130, Lys84 and Asp54 (Fig. 3a): in the apo-structure of AKR11B4 the side chain of this residue adopts a conformation which is not very frequent (6% according to the rotamer data base of COOT[9]) but nevertheless a preferred rotamere of tryptophane. In this conformation the side chain is packed against the small and side chain-lacking residue Gly21 (Fig. 3a) and overlaps with the binding region of the ribose moiety on the nicotinamide side of NADP$^+$ which becomes obvious after an overlay of the AKR11B1/ NADP$^+$ complex structure (Fig. 3a). This finding means that NADP$^+$ binding to AKR11B4 can only happen after a large conformational change of the Trp23 side chain.

We took this observation into account when we modelled an AKR11B4/ NADP$^+$ complex: we merged the NADP$^+$ molecule of the superimposed AKR11B1/ NADP$^+$ complex with the AKR11B4 structure, removed some interfering water molecules, turned the χ-angles of the Trp23 side chain to values found for the equivalent tryptophane residue in the AKR11B1/ NADP$^+$ complex (black Trp21 residue in Fig. 3a) and finally calculated a few refinement cycles to optimize the atomic distances. Interestingly the resulting Trp23 side chain conformation is – like that of Trp21 in AKR11B1 - not a preferred tryptophane rotamere, but has an unfavourable χ_2 angle. Thus, binding of NADP$^+$ to AKR11B4 (and to AKR11B1) leads to local structural tension which supports the release of the cosubstrate after the reaction and is thus a driving force of the catalytic cycle.

To test this hypothesis we generated and kinetically characterized the two point mutations AKR11B4^{Trp23Met} and AKR11B4^{Trp23Ala} (Fig. 4; supplementary Fig. 1). Methionine is present at the equivalent position in AKR11C1[7]; yet the primary rationale to choose this amino acid here was that it disposes like tryptophane of a large hydrophobic side chain which is, however, more variable so that a structural tension is less probable. Eventually the exchange of Trp23 by alanine should completely avoid any side chain tension at this position. In summary, we expected a significant reduction of the turnover number for the cosubstrate and – since NAD(P)-dependent dehydrogenases typically follow a ternary complex mechanism of compulsory order in which the converted cosubstrate is only released after liberation of the product – also of the substrate.

(a)

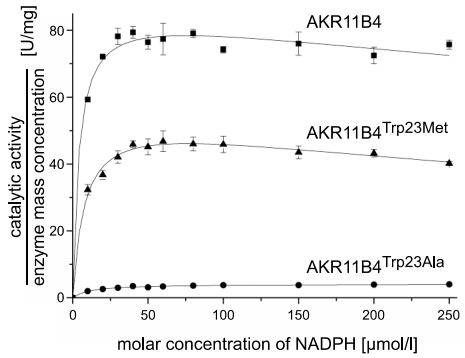

(b)

NADPH			
enzyme variant*	**V_{max} [U/mg]**	**K_M [µM]**	**k_{cat} [s^{-1}]**
AKR11B4	87.1	4.1	57.2
AKR11B4^{Trp23Met}	54.0	6.2	35.4
AKR11B4^{Trp23Ala}	4.2	6.2	2.7
D/L-glyceraldehyde			
enzyme variant*	**V_{max} [U/mg]**	**K_M [mM]**	**k_{cat} [s^{-1}]**
AKR11B4	80.5	2.4	52.8
AKR11B4^{Trp23Met}	37.0	49.4	24.2
AKR11B4^{Trp23Ala}	4.9	118.0	3.2

* plus N-terminal $(His)_6$-tag

Fig. 4: Kinetic characterization of the point mutants AKR11B4^{Trp23Met} and AKR11B4^{Trp23Ala} in comparison to the wildtype enzyme. Two point mutants of His-tagged AKR11B4 at position 23 were generated following the quick change PCR strategy[18]. The two mutants were prepared and purified as described previously for the wildtyp enzyme[1]. Subsequently the mutants and the wildtype were kinetically characterized at 30°C and with D/L-glyceraldehyde as a substrate and NADPH as a cosubstrate. Activities were determined by measuring the initial absorbance change at 340 nm under variable start concentrations of either NADPH (a) or D/L-glyceraldehyde (supplementary Fig.1). One unit of activity was defined as the amount of enzyme that catalyzes the oxidation of 1 µmol NADPH per minute. The principal composition of the enzyme assay was 970 µl substrate solution in 100 mM triethanolamine buffer, pH 7.0, mixed with 20 µl NADPH in distilled water and 10 µl enzyme solution. The detailed concentrations of D/L-glyceraldehyde, NADPH and the enzyme in the assay were dependent on the purpose of the specific experiment and on the results of preliminary tests in which we determined for each of the three AKR11B4 variants the saturation concentrations of D/L-glyceraldehyde and of NADPH. For example, to obtain the curves in part (a) we used a D/L-glyceraldehyde stock solution of 10 mM for assays with the wildtype enzyme and 250 mM in case of the mutants. Each point in the curves indicates the average of four independent measurements. The Michaelis-Menten parameters K_M and v_{max} were extracted by curve fitting using the ORIGIN software (version 7G). In all but one cases [(a), lower graph] a significant substrate inhibition was detectable so that the following variant of the Michaelis-Menten equation was applied: $v = v_{max} * c_S / [K_M + c_S + c_S^2/K_i]$. In this equation c_S is the molar concentration of either the substrate or the cosubstrate, and K_i is the (co-)substrate inhibition constant. The determined values for K_M, v_{max} and k_{cat} are summarized in part (b) of the figure.

Moreover, we predicted that the K_M value for NADPH should be largely unaffected because in the AKR11B1/$NADP^+$ complex the critical tryptophane side chain (Trp21; Fig. 3a) does not make any specific contacts to the bound $NADP^+$ molecule and thus does not contribute to the affinity between enzyme and cosubstrate.
The kinetic data we determined with the two AKR11B4 mutants and for comparison with the wildtype (Fig. 4) are in full agreement with the structure-based predictions outlined above. While the K_M-value of NADPH is nearly the same with all three variants (Fig. 4b), the turnover number (k_{cat}) is significantly reduced from 52.8 s^{-1} (wildtype) over 35.4 s^{-1} ($AKR11B4^{Trp23Met}$) to 2.7 s^{-1} ($AKR11B4^{Trp23Ala}$). The k_{cat}-value for the substrate is reduced in the same succession and order of magnitude (Fig. 4b). Hence, the kinetic data clearly support a critical role of Trp23 for the reaction turnover. The residue provides an intriguing example how an enzyme systematically establishes local tension during (co-)substrate binding and exploits it as a driving force of the catalytic cycle.

Substrate specitrum of AKR11B4

The data of Fig. 4b further demonstrate that - in contrast to the K_M-value for NADPH – the K_M-value for racemic glyceraldehyde is strongly affected by the mutagenesis. This observation leads over to the substrate binding and recognition properties of AKR11B4 the principles of which we will try to rationalize on the basis of ternary complex models of AKR11B4 with $NADP^+$ and substrate molecules. Beforehand, it makes sense to recapitulate shortly some of the results obtained by the extensive enzymological studies described by Richter *et al.*[1]:
(i) AKR11B4 catalyses the reduction of keto compounds much more effectively than the oxidation of alcohols. Accordingly the substrate specificity profile is significantly more pronounced in the reduction direction.
(ii) Aldehyds are distinctly better substrates than ketons. Hence, it can be concluded that the enzyme provides only very limited space on one side of the carbonyl group.
(iii) With glyceraldehyde - a standard substrate of AKRs – AKR11B4 shows a significant enantio selectivity: the D-form of glyceraldehyde is a more than 20 times better substrate than the L-form[1].
(iv) Very short aldehydes like ethanal and propanal are nearly no substrates of AKR11B4. However, butanal and further aldehydes with long aliphatic chains up to at least dodecanal (laurinaldehyde) are well accepted substrates. Richter *et al.*[1] also tested trans-2-hexen-1-al with a less flexible carbon chain and found it to be a much weaker substrate than hexenal.

Ternary complex of AKR11B4 with $NADP^+$ and octanal

Among all AKR11B4 substrates tested by Richter *et al.*[1] octanal and D-glyceraldehyde have the highest specific activities. Therefore, we modelled ternary complexes of AKR11B4 and $NADP^+$ together with either of these two compounds as well as L-glyceraldehyde (Fig. 3b-e), respectively, in order to generate hypotheses about the structural bases of the enzyme's enantio specificity and its preference for aldehydes with long aliphatic chains.
In this context we did not model the loops 1 and 7 to a safety belt since this region was not crucial for substrate binding. However, because of the well-known substrate recognition function of the C-terminal segment we modelled this region over the $(\beta/\alpha)_8$ TIM-barrel according to the equivalent region in AKR11B1[6] (Fig. 2c).
As many apo- and $NADP^+$-complex structures of AKR enzymes the AKR11B4 structure contains a water molecule[10] (Wat1 in Fig. 3a) in hydrogen-bonding distance (2.7 Å) to the catalytic tyrosine (Tyr59 in Fig. 3a). This water molecule mimics the carbonyl oxygen of the keto group to be reduced and thus, it is an important anchor point for modelling. Accordingly we placed an octanal molecule in a stretched conformation and orientated it such that (i) the *re*-plane of the aldehyde group faces the pyridinium ring of $NADP^+$, (ii) that the distance between the two critical partner atoms of the hydride transfer (the C4-atom of the nicotinamide moiety and the carbonyl C-atom of octanal) is below 3.5 Å and (iii) that the aliphatic chain overlaps largely with cortisone after superimposition of the AKR1D1/$NADP^+$/cortisone complex structure (PDB 3CMF)[11].
The resulting AKR11B4/$NADP^+$/octanal complex is visible in Fig. 3c in surface representation coloured according to hydrophobicity. It is plausible both with respect to the orientation of the reactive carbonyl group to the catalytic key components of the enzyme and the cosubstrate and with respect to the environment of the aliphatic hydrocarbon chain. The latter is embedded in a hydrophobic channel (Fig. 3c) formed by several side chains among them primarily Trp23 in its non-apo-conformation. Further Met326 and Pro328 from the remodelled C-terminal segment contribute to this channel as well as Val58, Tyr59, Leu87, Val99 and Trp131. The channel is broader and longer than required for octanal fitting to the observation[1] that also benzaldehyde, dodecanal or branched-chain aldehydes like 2-methyl-butanal or 2-methyl-pentanal are good substrates of AKR11B4.
The prominent function of Trp23 for substrate binding coincides with the similar role of the equivalent residue Met21 in the context of AKR11C1[7]. Further, it is supported by the kinetic data in Fig. 4b (lower half) whereupon an exchange of the tryptophane side chain lowers the affinity of the enzyme even to a smaller substrate than octanal significantly as reflected in increasing K_M-values for racemic glyceraldehyde.

A methionine residue of the C-terminal segment is the most probable candidate to determine enantio selectivity

With the hydrophobic channel visible in Fig. 3b it can be plausibly explained that aldehydes with long alkyl chains are favourite substrates of AKR11B4, whereas it is more difficult to understand the asymmetric induction that leads to the enzyme's biotechnologically interesting preference for D-glyceraldehyde over L-glyceraldehyde[1]. Glyceraldehyde is a relatively small substrate suggesting that residues in the direct neighbourhood of the active site are the critical determinants of the enantio specificity. For precise inspection we built ternary complex models of AKR11B4, $NADP^+$ and either D- or L-glyceraldehyde in preferred conformations and optimized atomic distances to the neighbouring enzyme and $NADP^+$ molecules (Fig. 3d/e). In these models the orientations of the aldehyde moiety, of the C2-H2-bond and – as a consequence – also of the two other substituents of the C2-atom were unambiguous.
The two models show the substrate molecules surrounded by the nicotinamide moiety of $NADP^+$ and further by Trp23, Tyr59, His130, Trp131 and Met326 (Fig. 3d/e). Except the latter all of these residues are equivalently present in GLD1, i.e. in an alternative glycerol dehydrogenase from *Hypocrea jecorina*[12], which accepts L- and D-glyceraldehyde as substrates, too, but does not prefer either of them[1]. Hence, Met326 - which in GLD1 is exchanged against a valine residue - is the most probable candidate to cause the asymmetric induction in AKR11B4. In fact,

the ternary complex with D-glyceraldehyde shows that a hydrogen bond should be possible between the sulphur atom of Met326 and the oxygen atom of the terminal hydroxy methyl group of D-glyceraldehyde (Fig. 3d).

With L-glyceraldehyde as a substrate the terminal hydroxy methyl group is in contact with Trp23, while it is the hydroxy group in 2-position that points towards Met326 (Fig. 3e). Only a weak hydrogen bond with the sulphur atom of Met326 seems to be possible in this case. Hence, in coincidence with the enzymological data[1] it is probably the better hydrogen bonding potential with Met326 that favours D-glyceraldehyde as a substrate of AKR11B4 compared to its enantiomer without excluding the latter entirely.

In summary, bearing in mind the limits of structure-based modelling work we suggest that Met326 is the most important determinant of the enantiospecificity of AKR11B4 concerning glyceraldehydes, a hypothesis, that can be easily tested in the future by site-directed mutagenesis.

Accession code

The atomic coordinates and structure factor amplitudes of the AKR11B4 structure are available from the PDB under the accession code 3N2T.

Experimental

AKR11B4 provided with an N-terminal $(His)_6$-tag was prepared as described[1]. The purified protein was concentrated and rebuffered in 10 mM Tris/HCl, pH 8.5. The first crystallization trials with this preparation led to heavy precipitation problems. Therefore we applied the enzyme to a gelfiltration column equilibration in 10 mM Tris/HCl, 150 mM NaCl, 0.5 mM EDTA, pH 8.5. A significant amount of high-molecular aggregates could be separated in this way. The final AKR11B4 stock solution used for successful crystallization had the following composition: 10 mg/ml AKR11B4 protein, 10 mM Tris/HCl, 150 mM NaCl, 0.5 mM EDTA, pH 8.5. Crystals of AKR11B4 were grown with the sitting drop variant of the vapour diffusion method. The reservoir composition was 35% (w/v) polyethylen glycol 3350 (PEG 3350), 200 mM KNO_3; the crystallization drop contained equal volumes of the reservoir and the protein stock solution before equilibration. AKR11B4 crystals were prepared for cryo-crystallography by exchanging the reservoir against 45% (w/v) PEG 3350, 200 mM KNO3, and subsequent re-equllibration. The crystals were frozen in liquid nitrogen directly from the resulting drops. X-ray diffraction data were collected at the beamline X11 of the EMBL outstation in Hamburg. The wavelength of the X-rays was 0.9537 Å. The data collection temperature was 100 K. All diffraction data were processed with XDS[18]. The GlyDH structure was determined by molecular replacement using MOLREP from the CCP4 suite[19] and the structure of AKR11B (PDB file 1PZ1[6]) as a search model. For the refinement we used PHENIX[20]. Manual corrections were performed with COOT[21].

Table 2: X-ray diffraction data collection and refinement statistics.

Diffraction data collection	
Temperature [K]	100
Space group	$P2_1$
Cell dimensions	
a, b, c [Å]	41.25, 62.39, 59.82
α, β, γ [°]	90.00, 90.47, 90.00
Resolution [Å]	34.50-2.00 (2.05-2.00)[1]
R_{sym} [2]	13.3 (69.9)[1]
Signal to noise ratio (I/σ_I)	10.10 (2.99)[1]
No. of unique reflections	26999
Completeness [%]	99.8 (99.9)[1]
Redundancy	5.4 (5.1)[1]
B-factor from Wilson plot [$Å^2$]	29.1
Refinement	
Resolution [Å]	34.5 - 2.0
No. of refl. in working set/test set	25746/1253
R_{work} / R_{free}	17.0/23.3
No. of atoms	
Protein	5634
Ligand/ion	28
Water	204
B-factors	
Protein	41.4
Ligand/ion	46.3
Water	33.2
R.m.s deviations	
Bond lengths [Å]	0.006
Bond angles [°]	0.885

[1]values in parentheses are for highest resolution shell

[2]$R_{sym} = \Sigma_h\Sigma_j|I_{h,j} - \langle I_{ch}\rangle| / \Sigma_h\Sigma_j I_{h,j}$, where $I_{h,j}$ is the intensity of the jth observation of unique reflection h, and $\langle I_h\rangle$ is the mean intensity of that reflection. Friedel mates were merged.

Acknowledgements

We are grateful to the staff of the EMBL outstation at DESY in Hamburg for assistence X-ray diffraction data collection.

Keywords: Aldo-keto reductases (AKR); AKR11B4; $NADP^+$-dependent glycerol dehydrogenase; enantio selectivity; X-ray crystallography; conformational tension to accelerate reaction turnover

References

1 Richter, N., Neumann, M., Liese, A., Wohlgemuth, R., Eggert, T. & Hummel, W. (2009). Characterization of a recombinant NADP-dependent glycerol dehydrogenase from Gluconobacter oxydans and its application in the production of L-glyceraldehyde. *ChemBioChem* **10**, 1888-1896.

2 Hyndman, D., Bauman, D. R., Heredia, V. V. & Penning, T. M. (2003). The aldo-keto reductase superfamily homepage. *Chem. Biol. Interact.* **143-144**, 621-631.

3 Mindnich, R. D. & Penning, T. M. (2009). Aldo-keto reductase (AKR) superfamily: genomics and annotation. *Hum. Genomics* **3**, 362-370

4 Brändén, C. I. (1991). The TIM barrel-the most frequently occuring folding motif in proteins. *Curr. Opin. Struct. Biol.* **1**, 978-983.

5 Tarle, I., Borhani, D. W., Wilson, D. K., Quiocho, F. A. & Petrach, J. M. (1993). Probing the active site of human aldose reductase. Site-directed mutagenesis of Asp-43, Tyr48, Lys-77, and His-110. *J. Biol. Chem.* **268**, 25687-25693.

6 Ehrensberger, A. H. & Wilson, D. K. (2004). Structural and catalytic diversity in the two family 11 aldo-keto reductases. *J. Mol. Biol.* **337**, 661-673.

7 Marquardt, T., Kostrewa, D., Balakrishnan, R., Gasperina, A., Kambach, C., Podjarny, A., Winkler, F. K., Balendiran, G. K. & Li, X. D. (2005). High-resolution crystal structure of AKR11C1 from *Bacillus halodurans*: an NADPH-dependent 4-hydroxy-2,3-trans-nonenal reductase. *J. Mol. Biol.* **354**, 304-316.

8 Bohren, K. M., Grimshaw, C. E. & Gabbay, K. H. (1992). Catalytic effectiveness of human aldose reductase: critical role of C-terminal domain. *J. Biol. Chem.* **267**, 20965-20970.

9 Emsley, P. & Cowtan, K. (2004). Coot: model-building tools for molecular graphics. *Acta Crystallogr.* **D60**, 2126-2132.

10 Jez, J. M., Bennett, M. J., Schlegel, B. P., Lewis, M. & Penning, T. M. (1997). Comparative anatomy of the aldo-keto reductase superfamily. *Biochem J.* **326**, 625-636.

11 Di Costanzo, L., Drury, J. E., Penning, T. M. & Christianson, D. W. (2008). Crystal structure of human liver Δ^4-3-ketosteroid 5β-reductase (AKR1D1) and implications for substrate binding and catalysis. *J. Biol. Chem.* **283,** 16830-16839.

12 Liepins, J., Kuorelahti, S., Penttilä, M. & Richard, P. (2006) Enzymes for the NADPH-dependent reduction of dihydroxyacetone and D-glyceraldehyde and L-glyceraldehyde in the mould *Hypocrea jecorina*. *FEBS J.* **273**, 4229-4235.

13 Schomburg, D. & Reichelt, J. (1988). BRAGI: a comprehensive protein modeling program system. *J. Mol. Graph.* **6**, 161 - 165.

14 Lessel, U. & Schomburg, D. (1994). Similarities between protein 3-D structures. *Protein Eng.* **7**, 1175-1187.

15 Esnouf, R. M. (1997). An extensively modified version of MolScript that includes greatly enhanced coloring capabilities. *J. Mol. Graphics* **15**, 132–134.

16 Merritt, E. A. & Bacon, D. J. (1997). Raster3D: photorealistic molecular graphics. *Methods Enzymol.* **277**, 505-524.

17 DeLano, W. L. "The PyMOL Molecular Graphics System." DeLano Scientific LLC, San Carlos, CA, USA.

18. Kunkel, T. A. (1985). Rapid and efficient site-specific mutagenesis without phenotypic selection. *Proc. Natl. Acad. Sci. U. S. A.* **82**, 488-492.

19 Kabsch, W. (2010). XDS. *Acta Crystallogr.* **D66**, 125-132.

20 Collaborative Computational Project, Number 4 (1994). The CCP4 suite: programs for protein crystallography. *Acta Crystallogr.* **D50**, 760-763.

21 Adams, P. D., Afonine, P. V., Bunkóczi, G., Chen, V. B., Davis, I. W., Echols, N., Headd, J. J., Hung, L. W., Kapral, G. J., Grosse-Kunstleve, R. W., McCoy, A. J., Moriarty, N. W., Oeffner, R., Read, R. J., Richardson, D. C., Richardson, J. S., Terwilliger, T. C. & Zwart, P. H. (2010). PHENIX: a comprehensive Python-based system for macromolecular structure solution. *Acta Crystallogr.* **D66**, 213-221.

Supporting information

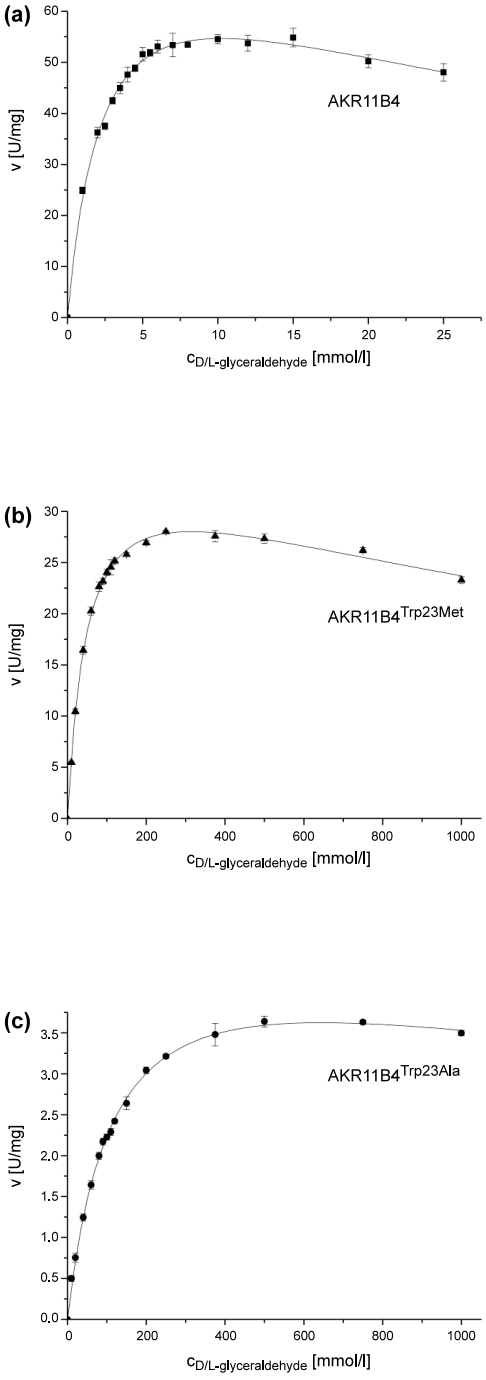

Supplementary Fig. 1. Michaelis–Menten graphs with respect to the racemic substrate D/L-glyceraldehyde: (a) AKR11B4, (b) AKR11B4^{Trp23Met}, and (c) AKR11B4^{Trp23Ala}. The experimental approach and data processing were equivalent to the procedures described in the legend to Fig. 4. The K_m and V_{max} values extracted are summarized in Fig. 4b. It should be noted that the scales of the three *y*-axes, as well the scales of the *x*-axis of (a) compared to the *x*-axes of (b) and (c), are different.

4 ESTABLISHMENT OF A SUITABLE REGENERATION SYSTEM FOR THE OXIDISED COFACTOR

4.1 A SINGLE POINT MUTATION ENABLES LACTATE DEHYDROGENASE FROM *BACILLUS SUBTILIS* TO UTILIZE NAD^+ AND $NADP^+$ AS COFACTOR

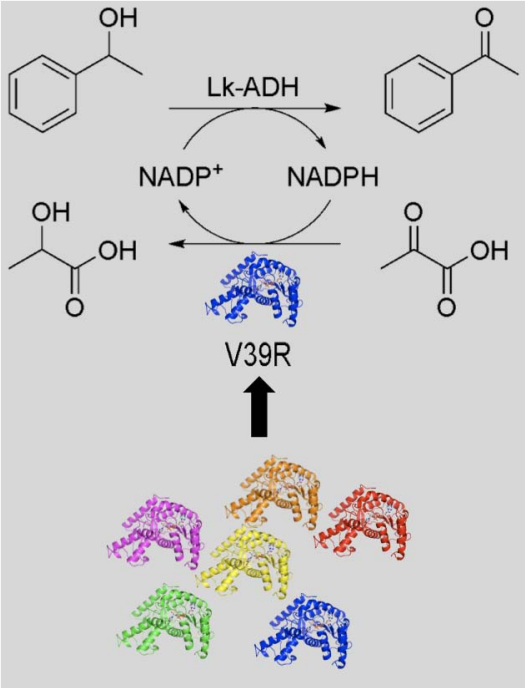

N. Richter, A. Zienert and W. Hummel (2011)

Eng. Life Sci. 11, 26-36

(doi: 10.1002/elsc.201000151)

Construction of a $NADP^+$-dependent lactate dehydrogenase

A Single Point Mutation Enables Lactate Dehydrogenase from *Bacillus subtilis* to utilize NAD^+ and $NADP^+$ as Cofactor

Nina Richter,[a] Anke Zienert,[b] Werner Hummel*[b]

The NAD^+-dependent lactate dehydrogenase from Bacillus subtilis (BsLDH) catalyzes the enantioselective reduction of pyruvate to lactate. BsLDH is highly specific to NAD^+ and exhibits only a low activity with $NADP^+$ as cofactor. Based on the high activity and good stability of LDHs, these enzymes have been frequently used for the regeneration of NAD^+. While an application in the regeneration of $NADP^+$ is not sufficient due to the cofactor preference of the BsLDH; additionally $NADP^+$-dependent LDHs have not yet been found in nature. Therefore, based on the extensive structural knowledge of LDHs, particularly in the field of cofactor binding, a structure-based approach was performed to predict amino acids involved in cofactor specificity. Methods of site-saturation mutagenesis were applied to vary these amino acids, with the aim to alter the cofactor specificity of the BsLDH. Five constructed libraries where screened for improved $NADP^+$ acceptance. Within the screening, the mutant V39R was identified, which showed increased activity with $NADP^+$ relative to the wild-type. Therefore, V39R was purified and biochemically characterized in comparison to the wild-type BsLDH. V39R showed excellent kinetic properties with NADP(H) and NAD(H), for instance the maximal specific activity with NADPH was enhanced 100-fold to 90.8 U/mg. Furthermore, a 249-fold increased catalytic efficiency was observed. Surprisingly, the activity with NADH was also improved significantly. Overall, we were able to successfully apply V39R in the regeneration of $NADP^+$ in an enzyme-coupled approach combined with the $NADP^+$-dependent alcohol dehydrogenase from Lactobacillus kefir. Thereby, we demonstrated for the first time an application of a LDH in the regeneration of $NADP^+$.

1 Introduction

L-Lactate dehydrogenases (LDH, EC 1.1.1.27) are NAD^+-dependent dehydrogenases which catalyze the reduction of pyruvate to lactate. LDHs are ubiquitously distributed and have been isolated from many different prokaryotic [1, 2] and eukaryotic sources [3]. In general, the different LDHs can be classified as allosteric enzymes, which are activated by fructose 1,6-bisphosphate (FBP) and FBP-independent enzymes [2].

A common feature of this enzyme class is their high specificity for NAD^+ as cofactor, $NADP^+$-dependent LDHs have not yet found in nature. Among the different LDHs, the LDH from *Geobacillus stearothermophilus* (GsLDH) has been studied most extensively [4-8] and its three-dimensional structure has been solved [9]. In general, the members of the LDH family show a high degree of structural similarity, especially the nucleotide binding domain is highly conserved. They exhibit like numerous $NAD(P)^+$-dependent dehydrogenases the extensively studied Rossmann-fold motif for cofactor binding [10].

Detailed studies of LDHs are justified by the considerable biotechnological potential of this enzyme class. According to their ability to produce optically pure α-hydroxy acids by reducing the corresponding pro-chiral α-oxo acids, LDHs can be applied in the production of pharmaceutically active compounds [8, 11, 12]. Furthermore, due to the extraordinary high specific activity in the reduction of pyruvate [1] and the high stability of enzyme and substrate, LDHs have become a convenient system for enzymatic cofactor regeneration. The great interest in enzymatic cofactor regeneration systems is founded in the growing number of industrial synthetic applications using $NAD(P)^+$-dependent oxidoreductases [13-19]. Especially the use of alcohol dehydrogenases in the environmental benign enantioselective oxidation of alcohols is of major interest. In contrast to the variety of different regeneration systems for the reduced cofactor, suitable systems for the oxidized cofactor, particularly $NADP^+$ are rare.

With regard to NAD^+, a number of useful enzymatic regeneration systems exist, applying LDH [16], glutamate dehydrogenase [20] or water- and hydrogen peroxide-forming NAD(P)H oxidase [21, 22]. For example, LDHs have been used to

[a] *N. Richter*
Evocatal GmbH , Merowingerplatz 1A
40225 Düsseldorf (Germany)

[b] A. Zienert, Prof. Dr. W. Hummel
Institut für Molekulare Enzymtechnologie
Heinrich-Heine Universität Düsseldorf, Forschungszentrum Jülich
Stetternicher Forst, 52426 Jülich (Germany)
Fax: (+49) 2461-612490
E-mail: w.hummel@fz-juelich.de

regenerate NAD^+ in the oxidative resolution of 1-phenyl-1,2-ethandiol in combination with glycerol dehydrogenase [16], and a number of other reactions [23-27]. However, the regeneration of $NADP^+$ remains challenging, due to the fact that many NAD(P)H oxidases prefer NADH as cofactor and show no or just a low activity with NADPH [21, 28, 29]. One exception is the water-forming NAD(P)H oxidase from *Lactobacillus sanfranciscensis* which in contrast to other oxidases exhibits a high activity with NADPH (11 U/mg) [30]. Compared to for example the specific activity of LDHs with NAD^+ the observed activity is still low. Better activities with NADPH are observed with glutamate dehydrogenases which prefer either one cofactor or accept both [31-33]. For the biotechnological applications of glutamate dehydrogenase, a drawback is the price of the used co-substrate. Therefore, a $NADP^+$-dependent LDH would be a good alternative enzymatic system for the regeneration of the oxidized phosphorylated cofactor.

Due to the fact that most $NAD(P)^+$-dependent dehydrogenases in general exhibit a strong preference for either one of the cofactors, the attempt to alter the cofactor specificity of dehydrogenases applying methods of directed evolution has become one major focus during the last decades [5-7, 34-42]. In summary the studies revealed, that a negatively charged amino acid at the highly conserved sequence $GXGXXG_{19}D(E)$ in the Rossmann-fold region is crucial for NAD^+ preference of dehydrogenases [26, 27].

According to the demand of a suitable regeneration system for $NADP^+$, protein engineering of particularly the LDH from *G. stearothermophilus* with the aim of altering the cofactor specificity has been applied [5-7, 43-45]. Previous attempts have yielded in LDH variants, which show a shift in cofactor specificity, whereas this shift toward NADPH was caused by a declined NADH acceptance, while the catalytic efficiency with NADPH was only slightly enhanced [5, 7]. Beyond that, none of the described variants has been used in the regeneration of the cofactor in combination with a second enzyme.

In the present study, we describe the structure guided alteration of the cofactor specificity of the LDH from *Bacillus subtilis* (BsLDH). BsLDH is an enzyme which has been the topic of a number of studies [46-48]. Therefore, biochemical features are already known, and based on the observed homology with the LDH from *G. stearothermophilus* the calculation of a structure model was possible.

With the help of this modeled structure, saturation libraries have been created and screened for their ability to utilize $NADP^+$ as cofactor. Suitable variants have been purified and biochemically characterized in terms of applicability for regeneration of $NADP^+$. Furthermore, the oxidation of (*R*)-1-phenylethanol of *rac*-1-phenylethanol using the $NADP^+$-dependent alcohol dehydrogenase from *Lactobacillus kefir* (LkADH) with simultaneous cofactor regeneration was performed in order to demonstrate the applicability of new LDH variants.

2 Materials and Methods

2.1 General: If not stated otherwise, all chemicals were purchased from Sigma Aldrich. Centrifugations were carried out using the centrifuges RC5BPlus (Sorvall), Mikro22 and Rotina 35 R (Hettich). For analytical methods GC-17A (Shimadzu) was used. Restriction enzymes were purchased from Fermentas. The studied BsLDH (evo-1.1.150), V39R (evo-1.1.151) and LkADH (evo-1.1.220) are commercially available at evocatal GmbH.

2.2 Molecular modelling: The three dimensional structure of BsLDH was modelled using the structure of the LDH from *G. stearothermophilus* (1LDN) as template. The alignment was done with tools available in the SwissPdbViewer [49]. Due to the fact that both enzymes are highly conserved with respect to the cofactor binding domain no further refinement was necessary.

2.3 Saturation mutagenesis and library creation: The five mutant libraries Val36, Ile37, Asp38, Val39 and Asn40 were constructed by Quick change PCR [50] using *Pfu* DNA polymerase. Preliminary the wild-type *bsldh* was cloned into the commercial expression vector pET21a between the restriction sites *Nhe*I and *Hind*III using standard techniques (pLDH). The created vector contained the wild-type *bsldh* fused to a C-terminal hexahistidine affinity purification motif (his-tag). The primers used for the introduction of the mutations are shown in Table 1. The PCR was performed according to standard procedures using pLDH as template, and applying the following temperature program: Initial denaturation 95°C, 0.5 min; 20 x (95°C, 0.5; 55°C, 1 min; 68°C 24 min), final elongation 68°C 24 min. After the PCR reaction, the remaining template was digested by the restriction enzyme *Dpn*I (10 U, 37°C, 2 h). The *Dpn*I digested PCR product was transformed into *E. coli* BL21(DE3). The cells were spread onto auto-induction media plates to accomplish the first round of screening.

2.4 Screening assay: *E. coli* BL21(DE3) cells carrying the BsLDH library were plated onto auto induction agar plates (TB medium (24 g/L yeast extract, 12 g/L casein hydrolysate, 5 g/L glycerol in 100 mM KP_i buffer pH 7), 2 g/L lactose, 0.5 g/L glucose, 15 g/L agar), supplemented with ampicillin (100 µg/ml). Plates were incubated at 25°C for two days, followed by an on plate activity assay. The corresponding assay was done as described previously [51], based on a phenazinethosulfate mediated reduction of nitotetrazolium blue accompanied by the formation of a blue dye. Positive colonies were selected by the formation of purple halos. Subsequently the plasmids were isolated and the sequence was analyzed.

2.5 Activity assays: In order to determine the activity in crude extracts, a continuous assay using UV absorbance at 340 nm was employed to monitor the NAD(P)H concentration during either the reduction or oxidation catalyzed by LDH. For the enzymatic reduction, pyruvate was used as standard substrate, while lactate was used as standard substrate monitoring the enzymatic oxidation of the enzyme. One unit of activity was defined as the amount of enzyme which catalyses the oxidation of 1 µmol NAD(P)H per minute under standard conditions (30°C, pH 7). For the determination of the enzyme activity in the reduction reaction, the assay mixture contained 970 µL substrate solution (4.5 mM pyruvate in 100 mM triethanolamine buffer buffer (TEA) pH 7), 20 µL NAD(P)H (12.5 mM) in distilled water and 10 µL enzyme solution. For the determination of the enzyme activity in the oxidation of L-lactate, the assay mixture contains 970 µL substrate solution (100 mM L-lactate in 100 mM TEA buffer pH 7), 20 µL $NAD(P)^+$ (125 mM) in distilled water and 10 µL enzyme solution. Reactions were started by addition of the enzyme solution and measured over a period of 1 min.

2.6 Expression and purification of V39R and wild-type BsLDH: *E. coli* BL21(DE3) cells carrying the recombinant plasmid were cultivated in 5 mL LB medium [52] containing 100 µg/mL ampicillin overnight at 37°C. These cultures were used to inoculate different amounts of LB medium containing 100 µg/mL ampicillin for expression in shaking flasks at a final concentration of 0.05 optical density at 600 nm (OD_{600}). The cultures were grown at 37°C. When the OD_{600} reached 0.5 to 0.7, the production of the recombinant LDH was induced by addition of isopropyl thio-β-D-galactoside (IPTG) to a final concentration of 0.2 mM. For optimal enzyme expression, cultures were grown at 25ºC (after induction), and assayed after a period of 20 h.

Table 1: Overview over the primers used for the creation of the libraries position 36 to 40. NNS codes for ATGC/ATGC/GC

Primer	Sequence (5'-3')
Val36	GGGATCACAGATGAGCTTGTGNNSATTGATGTAAATAAAGAAAAAAG
Val36_anti	CTTTTTCTTTATTTACATCAATSNNCACAAGCTCATCTGTGATCCC
Ile37	GGGATCACAGATGAGCTTGTGGTCNNSGATGTAAATAAAGAAAAAAGCAATG
Ile37_anti	CATTGCTTTTTCTTTATTTACATCSNNGACCACAAGCTCATCTGTGATCCC
Asp38	ATCACAGATGAGCTTGTGGTCATTNNSGTAAATAAAGAAAAAGCAA
Asp38_anti	TTGCTTTTTCTTTATTTACSNNAATGACCACAAGCTCATCTGTGAT
Val39	GATGAGCTTGTGGTCATTGATNNSAATAAAGAAAAAGCAATGGGC
Val39_anti	GCCCATTGCTTTTTCTTTATTSNNATCAATGACCACAAGCTCATC
Asn40	ATGAGCTTGTGGTCATTGATGTANNSAAAGAAAAAGCAATGGGCGATG
Asn40_anti	CATCGCCCATTGCTTTTTCTTTSNNTACATCAATGACCACAAGCTCAT

For the following purification procedure, the bacterial culture was harvested by centrifugation at 17,000 x g for 20 min at 4°C. A cell suspension (20%) was prepared in 50 mM TEA pH 7.5. Cells were disrupted by three sonification cycles of 3 min (40% power output) with cooling periods in-between. The lysed cells were centrifuged at 17,000 x g for 30 min at 4°C, and the supernatant was used for further purification steps. First, an initial heat precipitation was performed by incubating the crude extract for 10 min at a temperature of 50°C, followed by separation of denaturated protein via centrifugation. The enzyme was purified from the crude extract using immobilized metal affinity chromatography IMAC (Ni-NTA (Qiagen)). The column was equilibrated with TEA buffer (50 mM, pH 7.5), and the crude extract was applied to the column. Subsequently, the column was washed using TEA buffer (50 mM, pH 7.5 with 20 mM imidazole). The LDH was eluted using a concentration of 200 mM imidazole in 50 mM TEA buffer pH 7.5. After a desalting step using PD-10 desalting columns (GE Healthcare), the enzyme was stored in 50 mM TEA pH 7.5 at 4°C until use.

2.7 Protein analysis: Protein concentrations were determined according to Bradford using BSA as a standard [53]. SDS-PAGE was performed using 4–12% Bis-Tris gels in MOPS (3-(N-Morpholino) propanesulfonic acid) buffer (Invitrogen), SeeBlue2 Protein Standard (Invitrogen) was used for molecular weight estimation of proteins.

2.8 Determination of kinetic parameters: For the determination of the kinetic parameters for both, oxidized and reduced cofactors, the described standard activity assay for the oxidation or reduction was used. The resulting kinetic parameters were calculated from multiple measurements (at least as triplicates) using the Michaelis-Menten equation for the oxidized cofactor ($NAD(P)^+$). While for the reduced cofactor, due to a strong substrate inhibition a reliable fit using either Michaelis-Menten or substrate excess inhibition was not possible. Therefore the kinetic parameters were calculated using the apparent v_{max}.

2.9 Temperature and pH dependence: The temperature and pH dependency were determined using the standard activity assay for the reduction and oxidation as described above. All parameters were kept constant, only the investigated parameter like temperature and pH were changed. In order to obtain the pH optimum of the LDH variants the standard activity buffer TEA (pH 6.7 to 10.0) as well as MES (2-(N-morpholino) ethanesulfonic acid) (pH 5.2 to 7.1) was used. The resulting values are at least the result of three independent measurements.

2.10 Application of V39R and wild-type LDH in the regeneration of $NADP^+$: To determine the applicability of V39R in the enzyme coupled cofactor regeneration, the oxidation of (*R*)-1-phenylethanol from *rac*-1-phenylethanol by the $NADP^+$-dependent LkADH was used as model reaction. For the determination of the optimal ratio 10 mM *rac*-1-phenylethanol, 0.5 mM $NADP^+$, 50 mM pyruvate, 0.5 to 10 U V39R and 1 U LkADH in 100 mM TEA buffer pH 7 were used. While for the comparison of the V39R and the wild-type BsLDH the same amount of enzyme was used (7.4 mg equals, 1 U V39R). In both cases the reaction mixture was incubated at 30°C under continuous shaking (800 rpm). Samples (100 µL) were taken periodically and extracted with ethyl acetate (400 µL) for GC analysis. Concentrations of acetophenone, (*R*)- and (*S*)-1-phenylethanol were determined using a GC-17A (Shimadzu) equipped with the chiral CP-Chirasil-Dex CB column (Varian). The used temperature program was as follows: 100°C 3 min, 5°C/min 140°C, 55°C/min 195°C. The retention times are: 7.1 min acetophenone, 10.4 min (*R*)-1-phenylethanol and 10.7 min (*S*)-1-phenylethanol, respectively.

3 Results

3.1 Structure modelling and identification of residues for mutagenesis

For the identification of the crucial amino acids involved in cofactor binding, an alignment of different members of the LDH family from different organisms was performed (Fig. 1). The alignment revealed that the cofactor binding site is highly conserved showing the typical $GXGXXG_{19}D$ motif (Fig. 1 grey box), followed by the strictly conserved negatively charged Asp38 (Fig. 1, star), responsible for the NAD^+ preference.

In addition to the alignment, a homology model of the LDH from *B. subtilis* was constructed based on the three-dimensional structure of the LDH from *G. stearothermophilus*. Both enzymes show an identity of 67% and a similarity of 80% with regard to their amino acid sequence. Therefore, the calculated model of the BsLDH was excellent with a root mean square (RMS) between model and template below 0.005 for all atoms according to WHAT IF server [54].

Figure 2 demonstrates that the presumable function of Asp38 in the discrimination of $NADP^+$-binding by either unfavorable interactions due to charge repulsion or sterical hindrance effects could be possible. For example, Val39 might also sterical hinder the $NADP^+$ binding (Fig. 2).

```
                                    1          10   GXGXXG 20          30        * 40
B. subtilis (LDH)             : MMNKHVNKVALIGAGFVGSSYAFALINQGITDELVVIDVNKEKA
G. stearothermophilus (LDH)   : MKNDGGTRVVVIGTGFVGASYAFALMNQGITDEIVLIDANESKA
S. aureus (MDH)               : MNKFKGNKVVLIGNGAVGSSYAFSLVNQSIVDELVIIDLDTEKV
C. sp. (LDH)                  : M*KHDNRKIALIGTGMVGMSYAYSLLNQNVCDELVLIDVNKKRA
S. carnosus (LDH)             : MKNIKANKVVLVGDGAVGSSYAFAMVAQGVADEFVIVDIAVDKV
```

Figure 1. Amino acid sequence alignment of the NAD^+-binding region of LDHs from different organisms. Displayed are the LDHs from *B. subtilis* (BAA08939), *G. stearothermophilus* (BAA85589), *Clostridium sp.* (ZP_05130364) and *Staphylococcus carnosus* (YP_002634458). Additionally, the sequence from a malate dehydrogenase (MDH) from *Staphylococcus aureus* (ZP_05680931) was used. The conserved NAD^+-binding motif GXGXXG is marked in grey, the important negatively charged residue 19 amino acids downstream is indicated by asterisks (*). The numbers correspond to the *B. subtilis* LDH. The alignment was produced using the GeneDoc software.

Therefore, in addition to Asp38 the adjacent amino acids (36-40) were selected for saturation mutagenesis.

3.2 Site saturation mutagenesis at position 36 to 40

Saturation mutagenesis was used due to the ability of this method to create diversity at certain positions without the screening of large libraries. The first round of screening was performed using the describrd agar plate based activity test. Figure 3 shows the halo formation of a positive variant (A) in comparison to the wild-type BsLDH (B). Active variants identified within the first round of screening were sequenced and additionally expressed in shaking flasks. The crude extract of the variants was tested spectophotometrically in a second round of screening for activity using $NADP^+$ as cofactor. The initial sreening resulted in one improved variant (library Val39)

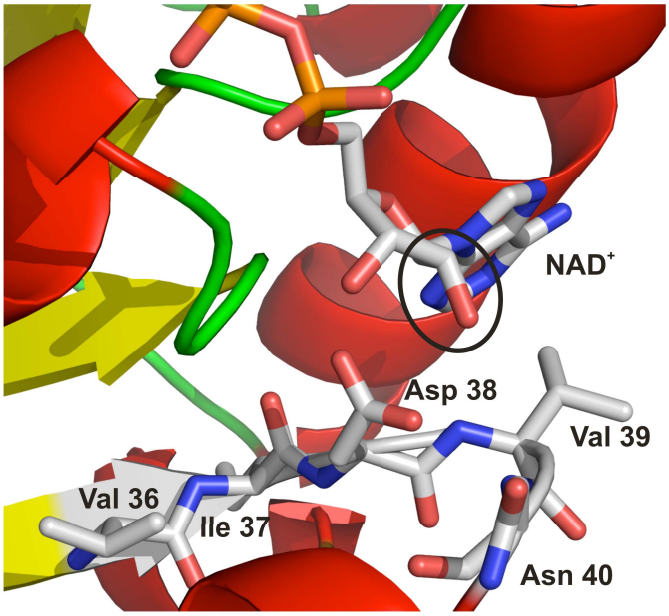

Figure 2. Structure of the wild-type LDH/NAD^+ complex, modelled using the LDH from *G. stearothermophilus* as template (1LDN). The protein backbone is colored by secondary structure elements: α -helices red, β -sheets yellow and single strands green. The atoms are colored according to type: oxygen red, nitrogen blue, carbon grey and phosphorus orange. Displayed is the part of the NAD^+-binding region responsible for $NADP^+$ discrimination, including NAD^+ and the selected amino acids for mutagenesis. The location of the additional phosphate group is encircled.

showing an activity of 179 U/mL with NAD^+ and 35.8 U/mL with $NADP^+$ in the crude extract. Sequence analysis confirmed that the mutant contained a single point mutation at position Val39 which was changed to Arg. Based on the observed results the variant Val39Arg (V39R) was purified and biochemically characterized in comparison to the wild-type BsLDH.

3.3 Expression and purification of V39R and wild-type LDH

Since the *ldh* gene is fused with a hexahistidine affinity purification motif (his-tag) at the C-terminus, a simple purification procedure was possible.
Preliminary, based on the good thermal stability of the BsLDH an initial heat treatment was performed (10 min, 50°C). Subsequently, both V39R and the wild-type BsLDH were purified in one chromatographic step using IMAC with Ni-NTA resin material. The results of the V39R purification are shown in Table 2. The purification yielded in a recovery of 29% of the primary activity.

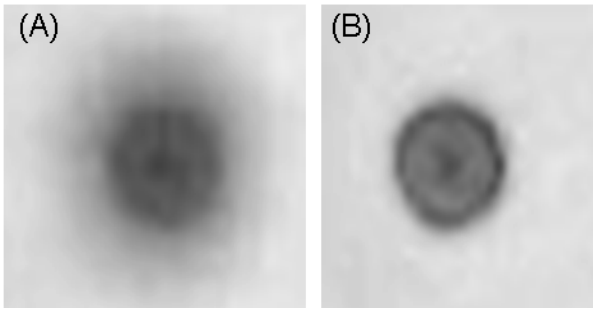

Figure 3. Activity screening assay on agar plates. Displayed is a colony of V39R (A) and the wild-type BsLDH (B). The mutant V39R clearly shows the formation of a halo around the colony compared to the wild-type enzyme.

The resulting specific activity of V39R in the oxidation of L-lactate using NAD^+ as cofactor after the purification was 7.8 U/mg. A single band with an apparent molecular size of 39 kDa (Figure 4, lane 6) is visible confirming the calculated molecular mass of 34.918 kDa derived from the amino acid sequence of one subunit.
In summary, a purification of the recombinant wild-type BsLDH (data not shown) and the mutant V39R to homogeneity after a single chromatographic step was possible.

3.4 Kinetic parameters

For further characterization of the mutant in comparison to the wild-type BsLDH, the kinetic properties of both enzymes were determined for the cofactors NAD(H) and NADP(H), using L-lactate and pyruvate, respectively as substrate.

Table 1. Purification of the recombinant V39R from *E. coli* BL21(DE3) cells. Specific activities were determined in the oxidation of L-lactate using NAD^+ as cofactor.

Purification step	Total activity [U mL^{-1}]	Specific activity [U mg^{-1}]	Purification factor	Yield [%]
Crude extract	1090	8.5	1	100
Heat precipitation	963	10.6	1.2	88
NiNTA	430	13.6	1.6	39
Desalting (Purified GlyDH)	312	7.8	0.9	29

The corresponding kinetic parameters were calculated according to the Michaelis-Menten equation. Due to a strong substrate excess inhibition of both variants with the reduced cofactors (NAD(P)H), a fit with standard Michaelis-Menten equation and even with the substrate excess inhibition equation was not possible.

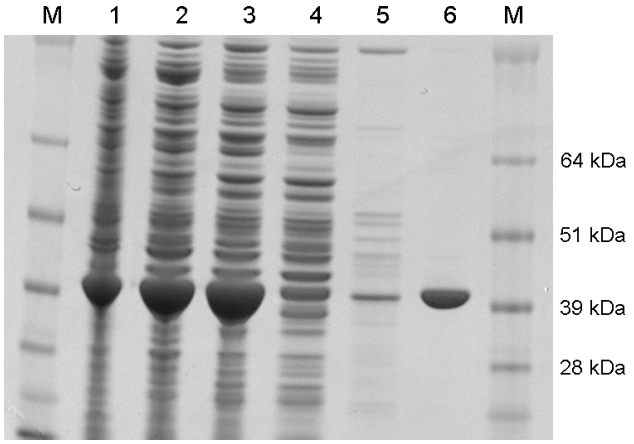

Figure 4. SDS-PAGE analysis of the purification of V39R. The lanes marked with M show the molecular weight marker (SeeBlue2, Invitrogen). Lane 1: crude extract unsoluble (14 µg), lane 2: crude extract soluble (14 µg), lane 3: crude extract after heat treatment (14 µg), lane 4: flow-through (8 µg) lane 5: wash fraction (5 µg), lane 6: purified V39R (1.2 µg). Lane 6 shows a single band at an apparent molecular weight of 39 kDa.

Therefore, we used the apparent v_{max} for the calculation of the kinetic parameters (Table 3 and Supporting Information).

This decision was justified by the fact that for a sufficient cofactor regeneration an approximate concentration of maximal 0.5 mM cofactor (sum of $NAD(P)^+$ and NAD(P)H) is accessible to the enzyme. Therefore, high cofactor concentrations were not of major interest.

The results of the kinetic characterization of the wild-type BsLDH and the mutant V39R are shown in Table 3. V39R shows a higher affinity to $NADP^+$ and NADPH (K_M = 2.3 mM and 0.11 mM, respectively), whereas the wild-type BsLDH has only an affinity of 10.4 mM with $NADP^+$ and 0.4 mM with NADPH. The maximal specific activity of the mutant V39R was improved for all investigated cofactors, particularly a 100-fold enhancement in the specific activity with NADPH could be reached. Surprisingly, the activity with NADH was improved as well (3.6-fold).

Moreover, turnover numbers turnover number (k_{cat}) and the catalytic efficiency (k_{cat}/K_M) of the mutant compared to the wild-type BsLDH could be enhanced significantly (Table 3).

Moreover, the pH optima for the wild-type BsLDH and V39R in the reduction of pyruvate using the reduced cofactor were investigated (Figure 5 C/D).

Table 2. Overview of the kinetic constants in the reduction and oxidation using V39R with NAD^+ or $NADP^+$, respectively, in reduced and oxidized form.

	Wild-type BsLDH				V39R			
Cofactor	K_M [mM]	v_{max} [U mg^{-1}]	K_{cat} [S^{-1}]	K_{cat}/K_M [μM^{-1} s^{-1}]	K_M [mM]	v_{max} [U mg^{-1}]	K_{cat} [S^{-1}]	K_{cat}/K_M [μM^{-1} s^{-1}]
NAD^+	0.5 ± 0.08	1.6 ± 0.05	3.8	8×10^{-3}	1.4 ± 0.2	16.2 ± 0.5	25.0	0.02
$NADP^+$	10.4 ± 4.2	0.1 ± 0.02	0.15	0.01×10^{-3}	2.3 ± 0.4	2.0 ± 0.1	3.1	0.001
NADH[a)]	0.05 (0.05)[b)]	52.8 (59.6)[b)]	77.5 (87.1)[b)]	1.5 (1.7)[b)]	0.06	188.7	291.6	4.9
NADPH[a)]	0.14	0.9	1.3	9.4×10^{-3}	0.06	90.8	140.4	2.3

[a)] According to a strong substrate excess inhibition at higher NAD(P)H concentrations the apparent v_{max} was used to determine the kinetic parameters.

[b)] In the case of wild-type BsLDH in addition to the apparent kinetic parameters the Michaelis-Menten equation was used for the calculation of the kinetic parameters.

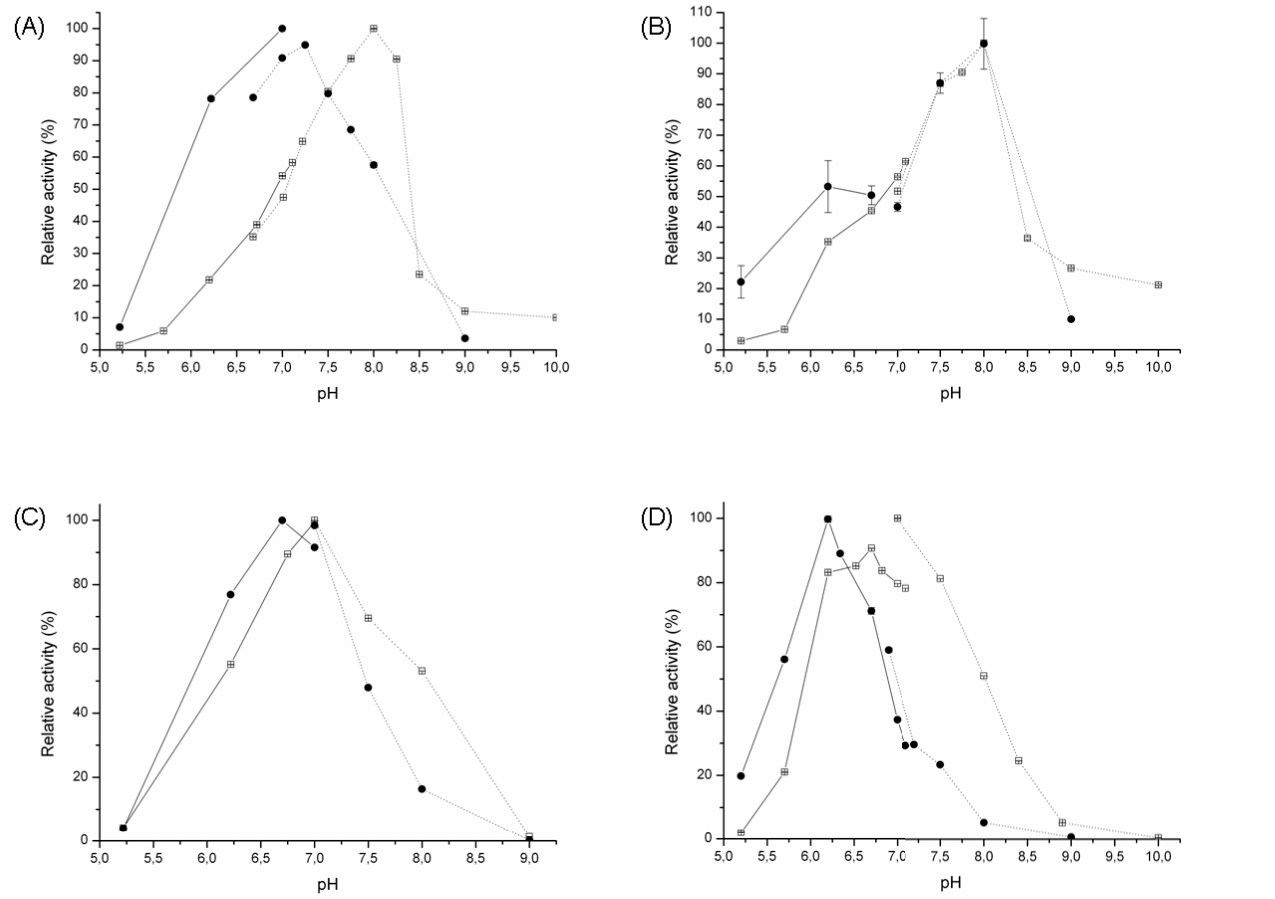

Figure 6. The pH dependence of the wild-type BsLDH and the mutant V39R using either the oxidized (A and B) or the reduced cofactor (C and D).The optimal activity of V39R (A) and wild-type BsLDH (B) in the oxidation of L-lactate with NAD^+ (□) or $NADP^+$ (●), respectively. For a better comparability the measured optimal activities were set as 100%. The corresponding specific activities were as follows: V39R: NAD^+ 12.7 U/mg; $NADP^+$ 1.0 U/mg; wild-type BsLDH: NAD^+ 2.0 U/mg; $NADP^+$ 0.02 U/mg. For the determination of the pH optimum 100 mM L-lactate with 2.5 mM cofactor was used and the pH was varied from 5.2 to 10.0. For the pH values from 5.2 to 7.1 100 mM MES buffer (—) and from 6.7 to 10.0 100 mM TEA buffer (····) was used. Additionally displayed are the pH optima of the V39R (C) and the wild-type BsLDH (D) in the reduction of pyruvate using NADH (□) or NADPH (●). The optimal specific activities of V39R and the wild-type BsLDH were: 163.3 U/mg with NADH and 76.1 U/mg with NADPH for V39R while the determined activities for the wild-type BsLDH were 44.1 U/mg with NADH and 1.8 U/mg with NADPH. The pH optimum was determined using 4.5 mM pyruvate and 0.25 mM cofactor in 100 mM MES buffer (pH 5.2 to 7.1)(····) and 100 mM TEA (pH 6.7 to 10) (—) were used.

With NADH as cofactor the wild-type BsLDH and V39R showed pH optima of 7, whereas with NADPH the pH optimum is shifted to a more acidic pH; pH 6.7 (V39R) and 6.2 (wild-type BsLDH).

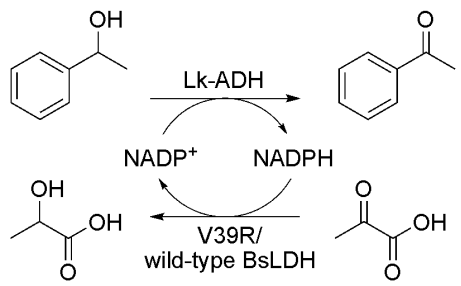

Figure 6. Scheme of the oxidation of rac-1-phenylethanol to acetophenone catalyzed by the alcohol dehydrogenase from *L. kefir* (LkADH). The cofactor $NADP^+$ is simultaneously regenerated using the reduction of pyruvate to L-lactate applying V39R or the wild-type BsLDH respectively.

In summary, the pH profiles of both enzymes are rather similar with optimal activities for reduction and oxidation for all cofactors in a range from 6.2 to 8. The determined biochemical parameters have been used to develop a suitable application of V39R in the regeneration of $NADP^+$ coupled with a second enzyme.

3.6 Application of V39R in the regeneration of $NADP^+$

According to the fact, that LDHs are often used for the regeneration of the oxidized cofactor, the biotransformation of *rac*-1-phenylethanol to acetophenone was investigated using the alcohol dehydrogenase from *L. kefir* (LkADH). This enzyme is a (*R*)-selective $NADP^+$-dependent dehydrogenase which has already been applied in a variety of different biotransformations [55, 56].

For the investigated biotransformation, the wild-type BsLDH and the variant V39R were used for the regeneration of $NADP^+$ (Figure 6). A preliminary experiment was performed to find an optimal ratio of both used enzymes (V39R and LkADH). Different ratios were used in cell-free biotransformation reactions, starting from 0.5:1 (V39R:LkADH) up to a 10-fold excess of V39R. The

results of this experiment are shown in Figure 7, indicating, that the reaction rate could be slightly enhanced by using V39R in excess. The figure also illustrates that a full conversion after 120 min could be reached with all chosen enzyme ratios.

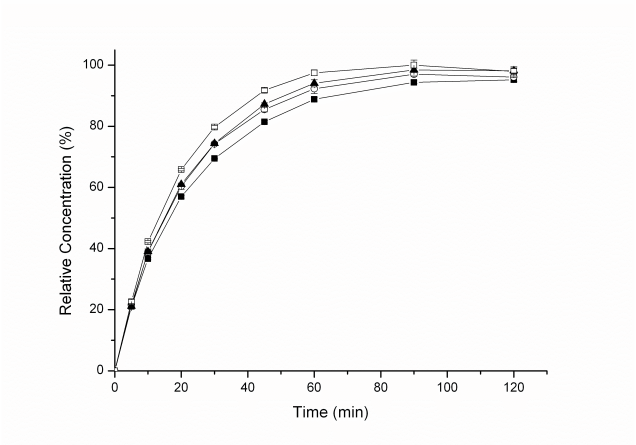

Figure 7. Determination of the optimal activity ratio of LkADH and V39R for feasible cofactor regeneration. Investigated were different ratios of V39R to LkADH: 0.5:1 (■); 1:1 (○); 2:1 (▲) and 10:1 (□). Displayed is the acetophenone concentration over a period of 120 min. The concentration was determined using gas chromatography. The reaction mixture contained 0.5 to 10 U V39R, 1 U LkADH, 0.5 mM $NADP^+$, 50 mM pyruvate and 10 mM rac-1-phenylethanol in 100 mM TEA buffer pH 7.

In a second experiment, the oxidation of (*R*)-1-phenylethanol of *rac*-1-phenylethanol by the LkADH with a simultaneous regeneration of $NADP^+$ was investigated using the same amount (mg) of V39R or the wild-type BsLDH. Figure 8 illustrates that using V39R for the regeneration of $NADP^+$ an efficient conversion of *rac*-1-phenylethanol to acetophenone catalyzed by the LkADH was possible. The study also shows that the wild-type BsLDH has a slight side-reaction with $NADP^+$. Applying wild-type BsLDH for $NADP^+$-regeneration, a conversion of 18% was reached after 210 min whereas a similar conversion was reached after a reaction time of only 5 min using V39R.

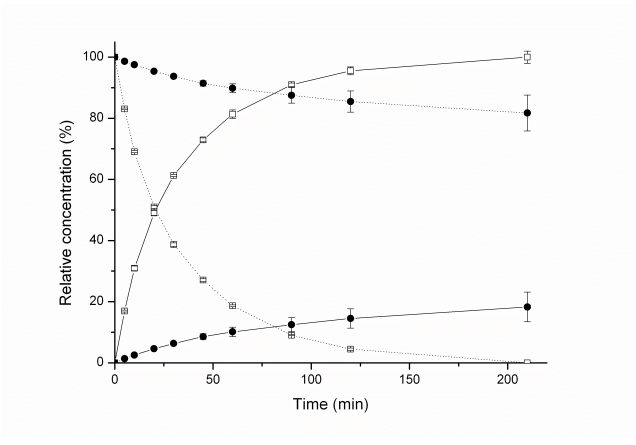

Figure 8. Oxidation of (*R*)-1-phenylethanol of the racemic mixture to acetophenone catalyzed by the LkADH using V39R or wild-type LDH for the regeneration of $NADP^+$. Outlined are the relative acetophenone (__) and (*R*)-1-phenylethanol (….) concentrations for V39R (□) and the wild-type LDH (●) over a period of 210 min. 7.4 mg V39R or wild-type BsLDH, 10 mM rac-1-phenylethanol, 0.5 mM $NADP^+$ and 50 mM pyruvate in 100 mM TEA buffer pH 7.

In conclusion the observed results emphasize the feasibility of V39R in the regeneration of $NADP^+$.

4 Discussion

The structural basis of dehydrogenases in terms of cofactor acceptance is an issue of major interest, in particular the tailoring of enzymes to alter their cofactor specificity has been investigated extensively [5-7, 34-42].

Based on the demand for suitable cofactor regeneration systems for either the reduced or the oxidized cofactor a number of approaches to alter the specificity of enzymes involved in cofactor regeneration have been published [5-7, 34, 37, 42, 57]. In the present study, we were able to construct a BsLDH variant with an altered cofactor specificity as the result of a structure guided approach using site-saturation mutagenesis. The identified variant V39R was characterized with respect to its biochemical properties and applied in the regeneration of $NADP^+$.

Examining the introduced mutation of the identified BsLDH variant in detail, it arises that the amino acid next to the conserved aspartic acid (Asp38), valine (Val39) was replaced by an arginine (Arg). This means that a neutral small amino acid was replaced by a strongly positively charged bulky one. Asp38 is presumably responsible for the preference for NAD(H) due to the ability to form hydrogen bonds with the 2'- and 3'-hydroxyl groups of the adenosine ribose part of the cofactor [45]. Furthermore, due to its negative charge it is responsible for the repulsion of the phosphorylated cofactor. While another crucial factor influencing cofactor specificity are amino acids which sterically avoid the cofactor binding. In the case of the constructed mutant V39R, obviously, the sterical effect does not affect the binding of the cofactor. This statement can be emphasized by the observed mutation, which introduces a bulkier amino acid at a position where the additional phosphate group of NADP(H) is located.

Moreover, we could show that a strong positively charged amino acid (Arg) next to a negatively charged one (Asp) enables the mutant to accept both cofactors, whereas an introduction of two positively charged amino acids (D38R:V39R) led to a dramatic decrease in activity combined with a rejection of NADH (data not shown).

These observations led to the suggestion that the amino acid Asp38 might be crucial for cofactor acceptance. Moreover, if a positively charged amino acid is located near the negatively charged Asp38 the charge repulsion can be overcome, maybe by stabilizing interactions between the Arg39 and the negatively charged phosphate group of $NADP^+$.

Besides these interesting structural observations, in our study the biochemical characterization and application of V39R was from fundamental interest. Previously, the cofactor specificity of the LDH from *G. stearothermophilus* (GsLDH) has been investigated and the corresponding mutants D38S and I37K:D38S have been characterized with regard to the acceptance of NADP(H) [5, 7]. In another study Tomita *et al*. introduced the loop region of a $NADP^+$-dependent malate dehydrogenase into the cofactor binding site of the LDH from *Thermus thermophilus* (TtLDH) [57]. Although these mutants show a shift towards NADP(H), only moderate improvements in the catalytic efficiency with NADPH were observed.

A comparison of the published results with the present study demonstrates that the improvements with regard to affinity, specific activity and catalytic efficiency make V39R a promising candidate for the application in the regeneration of $NADP^+$. Table 4 summarizes comparatively the kinetic parameters of

Table 3. Comparison of the biochemical properties of V39R and the wild-type BsLDH with literature data

	K_M (mM)		K_{cat} (s^{-1})		K_{cat} /K_M (μM s^{-1})		Alteration compared to wild-type [a)]
	NADH	NADPH	NADH	NADPH	NADH	NADPH	
Wild-type BsLDH	0.05	0.14	77.5	1.3	1.5	9.4×10^{-3}	-
V39R	0.06	0.06	291.6	140.4	4.9	2.2	249
BsLDH [16c]	0.06	-	-	-	-	-	-
G. stearothermophilus D38S [3c]	0.04	0.1	145	55	3.63	0.55	1.1
G. stearothermophilus I37K:D38S [3b]	1.0	0.7	160	160	0.16	0.23	1.6
T. thermophilus Tt27LDH-EX7[20]	1.19	0.35	11.2	127	0.03	0.11	2.4

[a)] For NADPH compared to the wild-type values published together with the corresponding mutants

V39R, the wild-type BsLDH, literature data of the wild-type BsLDH [47], and the mutants D38S [5], I37K:D38S [7] of GsLDH and Tt27LDH-EX7 of TtLDH [57]. With regard to the wild-type BsLDH the published data could be confirmed [47], while the three LDH mutants show a number of differences in their kinetic properties. For instance the affinity for NADPH (K_M), where V39R and D38S show with 0.1 mM high affinities, while I37K:D38S shows a 7-fold lower affinity for NADPH. For NADH only D53S shows a comparable affinity to the wild-type BsLDH, V39R shows a 3-fold increased K_M -value, and the affinity of I37K:D38S is with 1 mM significantly decreased (20-fold).

The highest turnover numbers (k_{cat}-values) for NADPH and NADH were observed with V39R (411.9 s^{-1} and 203.5 s^{-1}, respectively). Furthermore, with a 249-fold improved catalytic efficiency with NADPH compared to the wild-type BsLDH, V39R shows the best kinetic properties among the different mutants. In comparison the observed enhancements in catalytic efficiency of the two GsLDH mutants, were 1.6-fold with I37K:D38S and 1.1-fold with D53S and 2.4-fold with Tt27LDH-EX7. These observations make V39R the most promising mutant for a sufficient regeneration of $NADP^+$ among the four variants.

In addition to these three mutants another GsLDH variant has been published [6]. The Mutant Mut31 (F16Q:C81S: N85:R) I37K:D38S contains five mutations which lead to an alteration of the cofactor specificity in the presents of FBP as activator. Under these conditions the specific activity of the mutant was 36-fold improved compared to the wild-type BsLDH, while V39R showed a 100-fold improvement compared to the wild-type BsLDH. However, the good improvements exhibited by Mut31 I37K:D38S with $NADP^+$ as cofactor are strictly dependent on an addition of FBP, which in terms of feasibility exhibits according to stability and price a major drawback.

Based on the demand of feasible systems for the regeneration of the oxidized cofactors, particularly $NADP^+$, a $NADP^+$-dependent LDH would be very useful. According to this biotechnological interest and due to the significantly increased performance with NADP(H), we applied the mutant in the regeneration of $NADP^+$. For this purpose, the oxidation of (*R*)-1-phenylethanol out of its racemic mixture catalyzed by the $NADP^+$-dependent LkADH was performed with a continuous regeneration of $NADP^+$ using V39R. In comparison to the wild-type BsLDH, excellent conversions were observed. Furthermore, the reaction rate of the process was significantly increased by applying V39R, a conversion of 18% was reached after 210 min whereas a similar conversion was reached already after a reaction time of 5 min using the mutant enzyme V39R.

A comparison with established $NADP^+$ regeneration systems and the investigated BsLDH variant reveals, that due to a higher specific activity compared to $NAD(P)^+$ oxidases, the use of a favorable co-substrate in comparison to the glutamate dehydrogenase and no need for FBP addition, the studied LDH variant is an attractive alternative for the regeneration of $NADP^+$.

In addition to the excellent applicability, the created BsLDH mutant show comparable properties to the wild-type BsLDH (temperature and pH-dependency) and even significantly increased catalytic efficiencies for NADP(H) and NAD(H).

In conclusion, we were able to construct a mutant of the BsLDH, which is capable to accept NAD(H) and NADP(H), both with better efficiencies than the wild-type BsLDH.

Moreover, we were able to demonstrate the first $NADP^+$ regeneration system applying a lactate dehydrogenase and pyruvate as the co-substrate.

Acknowledgements

We thank Dr. Andrea Weckbecker, Prof. Dr. Martina Pohl and Dr. Antje Spieß for the critical reading and helpful discussions.

Conflict of Interest Statement

The authors have declared no conflict of interest.

Keywords: Alteration of cofactor specificity, $NAD(P)^+$-dependent lactate dehydrogenase, *Bacillus subtilis*, saturation mutagenesis, structure guided mutagenesis

References

[1] Garvie, E. I., Bacterial lactate dehydrogenases. *Microbiol. Rev.* **1980**. *44*, (1), 106-139.

[2] Hensel, R., Mayr, U., Fujiki, H. and Kandler, O., Comparative studies of lactate dehydrogenases in lactic-acid bacteria *Eur. J. Biochem.* **1977**. *80*, (1), 83-92.

[3] Taylor, S. S. and Oxley, S. S., Homologies in active site regions of lactate dehydrogenases. *Arch. Biochem. Biophys.* **1976**. *175*, (2), 373-383.

[4] Binay, B. and Karaguler, N. G., Attempting to remove the substrate inhibition of L-lactate dehydrogenase from *Bacillus stearothermophilus* by site-directed mutagenesis. *Appl. Biochem. Biotechnol.* **2007**. *141*, 265-272.

[5] Feeney, R., Clarke, A. R. and Holbrook, J. J., A single amino acid substitution in lactate dehydrogenase improves the catalytic efficiency with an alternative coenzyme. *Biochem. Biophys. Res. Commun.* **1990**. *166*, (2), 667-672.

[6] Flores, H. and Ellington, A. D., A modified consensus approach to mutagenesis inverts the cofactor specificity of Bacillus stearothermophilus lactate dehydrogenase. *Protein Engineering Design & Selection* **2005**. *18*, (8), 369-377.

[7] Holmberg, N., Ryde, U. and Bülow, L., Redesign of the coenzyme specificity in L-lactate dehydrogenase from *Bacillus stearothermophilus* using site-directed mutagenesis and media engineering. *Protein Eng.* **1999**. *12*, (10), 851-856.

[8] Karagüler, N. G., Sessions, R. B., Binay, B., Ordu, E. B. and Clarke, A. R., Protein engineering applications of industrially exploitable enzymes: *Geobacillus stearothermophilus* LDH and *Candida methylica* FDH. *Biochem. Soc. Trans.* **2007**. *35*, 1610-1615.

[9] Wigley, D. B., Gamblin, S. J., Turkenburg, J. P., Dodson, E. J., Piontek, K., Muirhead, H. and Holbrook, J. J., Structure of a ternary complex of an allosteric lactate dehydrogenase from *Bacillus stearothermophilus* at 2.5 A resolution. *J. Mol. Biol.* **1992**. *223*, (1), 317-335.

[10] Rao, S. T. and Rossmann, M. G., Comparison of super-secondary structures in proteins. *J. Mol. Biol.* **1973**. *76*, (2), 241-256.

[11] Kim, M.-J. and Whitesides, G. M., L-Lactate dehydrogenase: Substrate specificity and use as a catalyst in the synthesis of homochiral 2-hydroxy acids. *J. Am. Chem. Soc.* **1988**. *110*, (9), 2959-2964.

[12] Schmidt, E., Ghisalba, O., Gygax, D. and Sedelmeier, G., Optimization of a process for the production of (*R*)-2-hydroxy-4-phenylbutyric acid - an intermediate for inhibitors of angiotensin converting Enzyme. *J. Biotechnol.* **1992**. *24*, (3), 315-327.

[13] Baer, K., Krausser, M., Burda, E., Hummel, W., Berkessel, A. and Gröger, H., Sequential and modular synthesis of chiral 1,3-diols with two stereogenic centers: access to all four stereoisomers by combination of organo- and biocatalysis. *Angew. Chem. Int. Ed.* **2009**. *48*, (49), 9355-9358.

[14] Daußmann, T., Hennemann, H. G., Rosen, T. C. and Dünkelmann, P., Enzymatic technologies for the synthesis of chiral alcohol derivatives. *Chem Ing Tech* **2006**. *78*, (3), 249-255.

[15] Goldberg, K., Schroer, K., Lütz, S. and Liese, A., Biocatalytic ketone reduction - a powerful tool for the production of chiral alcohols - part I: processes with isolated enzymes. *Appl. Microbiol. Biotechnol.* **2007**. *76*, (2), 237-248.

[16] Liese, A., Karutz, M., Kamphuis, J., Wandrey, C. and Kragl, U., Enzymatic resolution of 1-phenyl-1,2-ethanediol by enantioselective oxidation: Overcoming product inhibition by continuous extraction. *Biotechnol. Bioeng.* **1996**. *51*, (5), 544-550.

[17] Müller, M., Wolberg, M., Schubert, T. and Hummel, W., Enzyme-catalyzed regio- and enantioselective ketone reductions. *Adv. Biochem. Engin. / Biotechnol.* **2005**. *92*, 261-287.

[18] Patel, R. N., Biocatalysis: Synthesis of chiral intermediates for drugs. *Curr Opin Drug Discov Dev* **2006**. *9*, (6), 741-764.

[19] Wolberg, M., Filho, M. V., Bode, S., Geilenkirchen, P., Feldmann, R., Liese, A., Hummel, W. and Müller, M., Chemoenzymatic synthesis of the chiral side-chain of statins: application of an alcohol dehydrogenase catalysed ketone reduction on a large scale. *Bioprocess Biosyst. Eng.* **2008**. *31*, (3), 183-191.

[20] Lee, L. G. and Whitesides, G. M., Preparation of optically active 1,2-diols and a-hydroxy ketones using glycerol dehydrogenase as catalyst: Limits to enzyme-catalyzed synthesis due to noncompetitive and mixed inhibition by product. *J. Org. Chem.* **1986**. *51*, (1), 25-36.

[21] Geueke, B., Riebel, B. and Hummel, W., NADH oxidase from *Lactobacillus brevis*: a new catalyst for the regeneration of NAD. *Enzyme Microb. Technol.* **2003**. *32*, (2), 205-211.

[22] Hummel, W., Kuzu, M. and Geueke, B., An efficient and selective enzymatic oxidation system for the synthesis of enantiomerically pure D-tert-leucine. *Org. Lett.* **2003**. *5*, (20), 3649-3650.

[23] Chenault, H. K. and Whitesides, G. M., Lactate dehydrogenase-catalyzed regeneration of NAD from NADH for use in enzyme-catalyzed synthesis. *Bioorg. Chem.* **1989**. *17*, (4), 400-409.

[24] Weckbecker, A., Gröger, H. and Hummel, W., Regeneration of nicotinamide coenzymes: Principles and applications for the synthesis of chiral compounds. *Adv. Biochem. Engin./ Biotechnol.* **2010**(In press).

[25] Wong, C.-H. and Whitesides, G. M., Enzyme-catalyzed organicsynthesis: NAD(P)H cofactor regeneration using ethanol alcohol dehydrogenase/ aldehyde dehydrogenase and methanol/ alcohol dehydrogenase/ aldehyde dehydrogenase/ formate dehydrogenase. *J. Org. Chem.* **1982**. *47*, (14), 2816-2818.

[26] Monti, D., Ferrandi, E. E., Zanellato, I., Hua, L., Polentini, F., Carrea, G. and Riva, S., One-pot multienzymatic synthesis of 12-ketoursodeoxycholic acid: subtle cofactor specificities rule the reaction equilibria of five biocatalysts working in a row. *Adv. Synth. Catal.* **2009**. *351*, (9), 1303-1311.

[27] Riva, S., Bovara, R., Zetta, L., Pasta, P., Ottolina, G. and Carrea, G., Enzymatic α/β inversion of C-3 hydroxyl of bile acids and study of the effects of organic solvents on reaction rates. *J. Org. Chem.* **1988**. *53*, (1), 88-92.

[28] Hirano, J., Miyamoto, K. and Ohta, H., Purification and characterization of thermostable H_2O_2-forming NADH oxidase from 2-phenylethanol-assimilating *Brevibacterium* sp KU1309. *Appl. Microbiol. Biotechnol.* **2008**. *80*, (1), 71-78.

[29] Park, H. J., Reiser, C. O. A., Kondruweit, S., Erdmann, H., Schmid, R. D. and Sprinzl, M., Purification and characterization of a NADH oxidase from the thermophile *Thermus thermophilus* Hb8. *Eur. J. Biochem.* **1992**. *205*, (3), 881-885.

[30] Riebel, B. R., Gibbs, P. R., Wellborn, W. B. and Bommarius, A. S., Cofactor regeneration of NAD^+ from NADH: Novel water-forming NADH oxidases. *Adv. Synth. Catal.* **2002**. *344*, (10), 1156-1168.

[31] Carrea, G., Bovara, R., Cremonesi, P. and Lodi, R., Enzymatic Preparation of 12-Ketochenodeoxycholic Acid with Nadp Regeneration. *Biotechnology and Bioengineering* **1984**. *26*, (5), 560-563.

[32] Sakamoto, N., Kotre, A. M. and Savageau, M. A., Glutamate Dehydrogenase from *Escherichia coli* - Purification and Properties. *J. Bacteriol.* **1975**. *124*, (2), 775-783.

[33] Veronese, F. M., Nyc, J. F., Degani, Y., Brown, D. M. and Smith, E. L., Nicotinamide Adenine Dinucleotide-Specific Glutamate-Dehydrogenase of Neurospora .1. Purification and Molecular-Properties. *Journal of Biological Chemistry* **1974**. *249*, (24), 7922-7928.

[34] Andreadeli, A., Platis, D., Tishkov, V., Popov, V. and Labrou, N. E., Structure-guided alteration of coenzyme specificity of formate dehydrogenase by saturation mutagenesis to enable efficient utilization of $NADP^+$. *Eur. J. Biochem.* **2008**. *275*, (15), 3859-3869.

[35] Bubner, P., Klimacek, M. and Nidetzky, B., Structure-guided engineering of the coenzyme specificity of *Pseudomonas fluorescens* mannitol 2-dehydrogenase to enable efficient utilization of NAD(H) and NADP(H). *FEBS Lett.* **2008**. *582*, (2), 230-234.

[36] Chen, R. D., Greer, A. and Dean, A. M., Redesigning secondary structure to invert coenzyme specificity in isopropylmalate dehydrogenase. *Proc. Natl. Acad. Sci. USA* **1996**. *93*, (22), 12171-12176.

[37] Gul-Karaguler, N., Sessions, R. B., Clarke, A. R. and Holbrook, J. J., A single mutation in the NAD-specific formate dehydrogenase from *Candida methylica* allows the enzyme to use NADP. *Biotechnol. Lett.* **2001**. *23*, (4), 283-287.

[38] Leitgeb, S., Petschacher, B., Wilson, D. K. and Nidetzky, B., Fine tuning of coenzyme specificity in family 2 aldo-keto reductases revealed by crystal structures of the Lys-274 -> Arg mutant of *Candida tenuis* xylose reductase (AKR2B5) bound to NAD^+ and $NADP^+$. *FEBS Lett.* **2005**. *579*, (3), 763-767.

[39] Machielsen, R., Looger, L. L., Raedts, J., Dijkhuizen, S., Hummel, W., Hennemann, H. G., Daussmann, T. and Van der Oost, J., Cofactor engineering of *Lactobacillus brevis* alcohol dehydrogenase by computational design. *Eng. Life Sci.* **2009**. *9*, (1), 38-44.

[40] Rosell, A., Valencia, E., Ochoa, W. F., Fita, I., Pares, X. and Farres, J., Complete reversal of coenzyme specificity by concerted mutation of three consecutive residues in alcohol dehydrogenase. *J. Biol. Chem.* **2003**. *278*, (42), 40573-40580.

[41] Scrutton, N. S., Berry, A. and Perham, R. N., Redesign of the coenzyme specificity of a dehydrogenase by protein engineering. *Nature* **1990**. *343*, (6253), 38-43.

[42] Wu, W. H., Zhu, D. M. and Hua, L., Site-saturation mutagenesis of formate dehydrogenase from *Candida bodinii* creating effective $NADP^+$-

dependent FDH enzymes. *J. Mol. Catal. B-Enzymatic* **2009**. *61*, (3-4), 157-161.

[43] Carugo, O. and Argos, P., NADP-dependent enzymes .I: Conserved stereochemistry of cofactor binding. *Proteins* **1997**. *28*, (1), 10-28.

[44] Carugo, O. and Argos, P., NADP-dependent enzymes .2. Evolution of the mono- and dinucleotide binding domains. *Proteins-Structure Function and Genetics* **1997**. *28*, (1), 29-40.

[45] Clermont, S., Corbier, C., Mely, Y., Gerard, D., Wonacott, A. and Branlant, G., Determinants of coenzyme specificity in glyceraldehyde-3-phosphate dehydrogenase: Role of the acidic residue in the fingerprint region of the nucleotide binding fold. *Biochemistry* **1993**. *32*, (38), 10178-10184.

[46] Hediger, M. A., Frank, G. and Zuber, H., Structure and function of L-lactate dehydrogenases from thermophilic and mesophilic bacteria .IV. The primary structure of the mesophilic lactate dehydrogenase from *Bacillus subtilis*. *Biol.l Chem. Hoppe-Seyler* **1986**. *367*, (9), 891-903.

[47] Yoshida, A., Enzymic properties of lactate dehydrogenase of *Bacillus subtilis*. *Biochim. Biophys. Acta* **1965**. *99*, (1), 66-77.

[48] Yoshida, A. and Freese, E., Purification and chemical characterization of lactate dehydrogenase of *Bacillus subtilis*. *Biochim. Biophys. Acta* **1965**. *99*, (1), 56-65.

[49] Guex, N. and Peitsch, M. C., SWISS-MODEL and the Swiss-PdbViewer: An environment for comparative protein modeling. *Electrophoresis* **1997**. *18*, (15), 2714-2723.

[50] Kunkel, T. A., Rapid and efficient site-specific mutagenesis without phenotypic selection. *Proc. Natl.Acad. Sci. USA* **1985**. *82*, (2), 488-492.

[51] **Felber, S.,** Optimierung der NAD-abhängigen Formiatdehydrogenase aus *Candida boidinii* für den Einsatz in der Biokatalyse. Heinrich Heine-Universität Düsseldorf 2001.

[52] Bertani, G., Studies on lysogenesis :1. the mode of phage liberation by lysogenic *Escherichia coli*. *J Bacteriol* **1951**. *62*, (3), 293-300.

[53] Bradford, M. M., Rapid and sensitive method for quantitation of microgram quantities of protein utilizing principle of protein-dye binding. *Anal Biochem* **1976**. *72*, (1-2), 248-254.

[54] Hooft, R. W. W., Vriend, G., Sander, C. and Abola, E. E., Errors in protein structures. *Nature* **1996**. *381*, (6580), 272-272.

[55] Weckbecker, A. and Hummel, W., Improved synthesis of chiral alcohols with *Escherichia coli* cells co-expressing pyridine nucleotide transhydrogenase, $NADP^+$-dependent alcohol dehydrogenase and NAD^+-dependent formate dehydrogenase. *Biotechnol. Lett.* **2004**. *26*, (22), 1739-1744.

[56] Weckbecker, A. and Hummel, W., Cloning, expression, and characterization of an (*R*)-specific alcohol dehydrogenase from *Lactobacillus kefir*. *Biocatal. Biotransformation* **2006**. *24*, (5), 380-389.

[57] Tomita, T., Kuzuyama, T. and Nishiyama, M., Alteration of coenzyme specificity of lactate dehydrogenase from *Thermus thermophilus* by introducing the loop region of NADP(H)-dependent malate dehydrogenase. *Biosci. Biotechnol. Biochem*. **2006**. *70*, (9), 2230-2235.

Supporting information

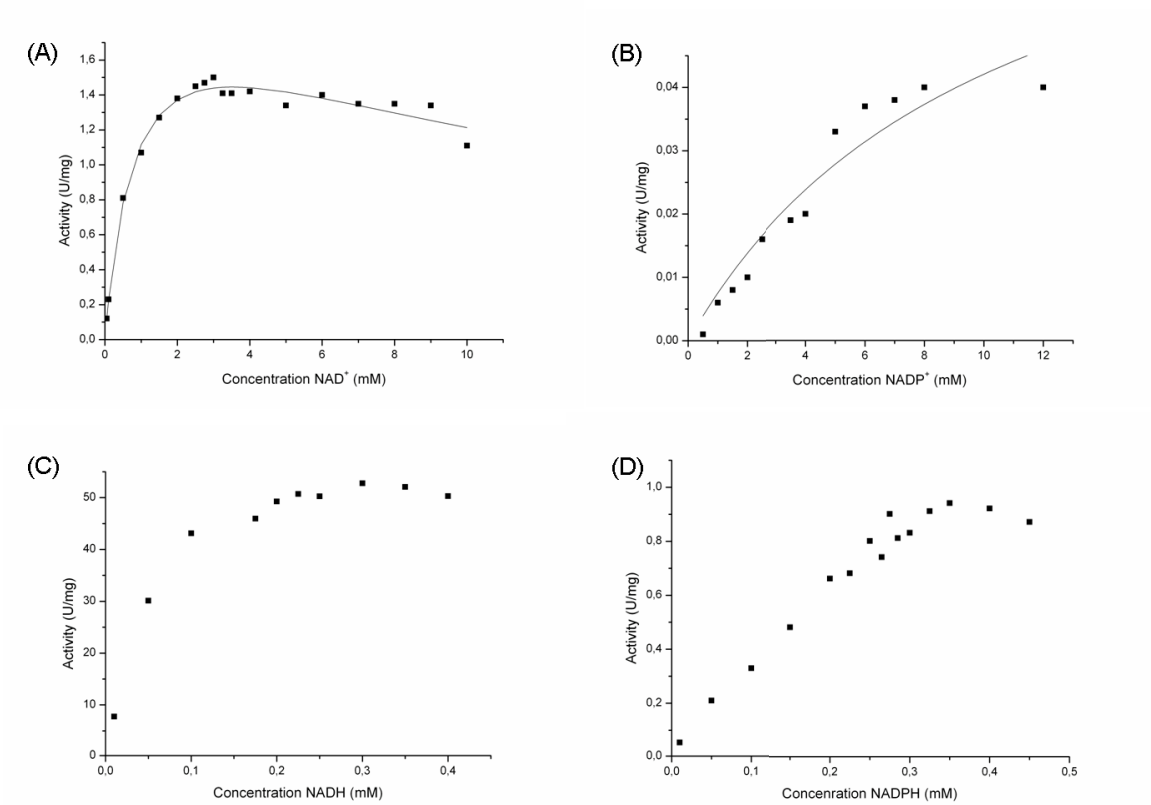

Figure I. Displayed are the measurements of the kinetic parameters for the wild-type BsLDH, for NAD^+ (A), $NADP^+$ (B), NADH (C) and NADPH (D). The corresponding kinetic parameters are shown in Table 2.

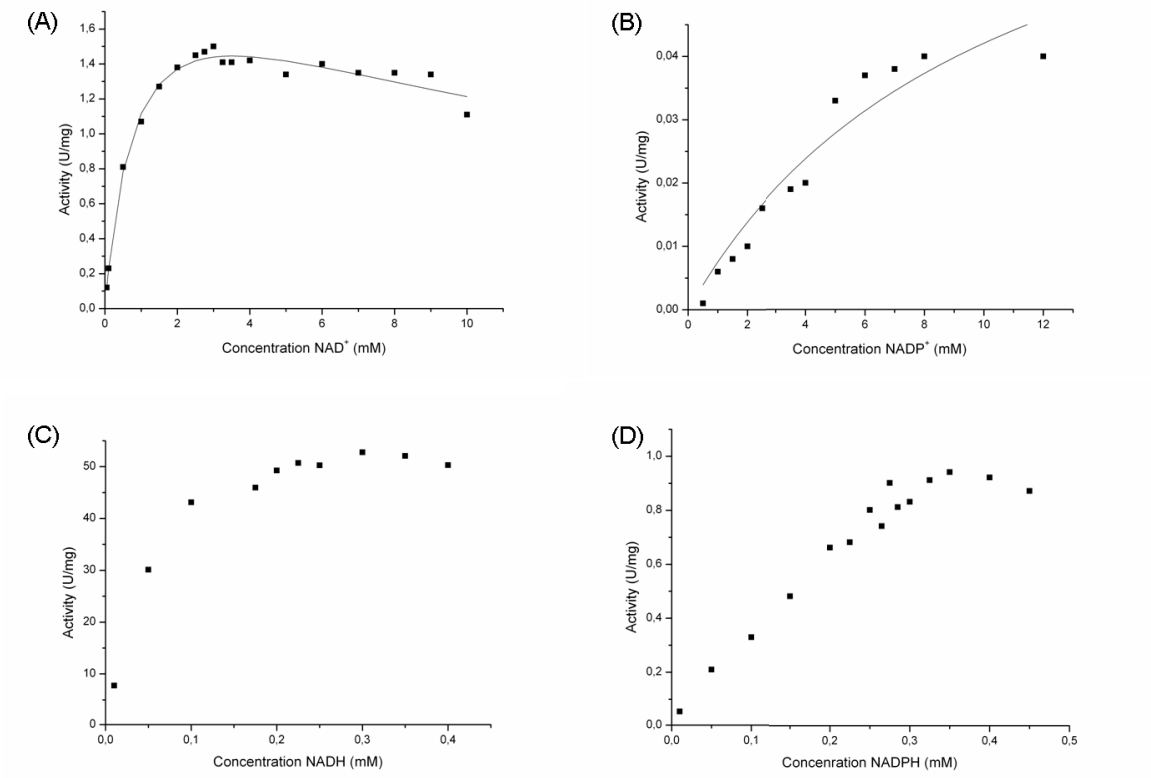

Figure I. Displayed are the measurements of the kinetic parameters for the wild-type BsLDH, for NAD^+ (A), $NADP^+$ (B), NADH (C) and NADPH (D). The corresponding kinetic parameters are shown in Table 2.

5 CONSTRUCTION OF A WHOLE-CELL CATALYST FOR THE PRODUCTION OF L-GLYCERALDEHYDE

5.1 CHARACTERIZATION OF A WHOLE-CELL CATALYST CO-EXPRESSING GLYCEROL DEHYDROGENASE AND GLUCOSE DEHYDROGENASE AND ITS APPLICATION IN THE SYNTHESIS OF L-GLYCERALDEHYDE

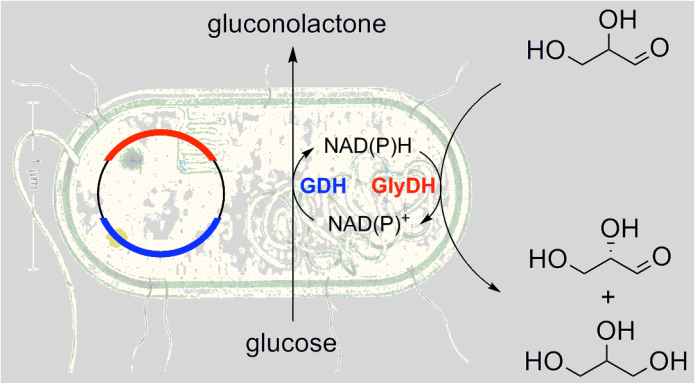

N. Richter, M. Neumann, A. Liese, R. Wohlgemuth, A. Weckbecker, T. Eggert, W. Hummel (2010)

Biotechnol. Bioeng. 106, 541-552

(doi: 10.1002/bit.22714)

FULL PAPER

Characterization of a whole-cell catalyst co-expressing glycerol dehydrogenase and glucose dehydrogenase and its application in the synthesis of L-glyceraldehyde

Nina Richter,[1] Markus Neumann,[2] Andreas Liese,[2] Roland Wohlgemuth,[3] Andrea Weckbecker,[1] Thorsten Eggert,[1] Werner Hummel[4*]

[1] evocatal GmbH, Merowingerplatz 1a, 40225 Düsseldorf, Germany
[2] Institut für Technische Biokatalyse, Technische Universität Hamburg-Harburg, 21073 Hamburg, Germany
[3] Research Specialties, Sigma-Aldrich Chemie GmbH, Industriestrasse 25, Buchs CH-9470, Switzerland
[4] Institut für Molekulare Enzymtechnologie, Heinrich-Heine Universität Düsseldorf,
Forschungszentrum Jülich, Stetternicher Forst
52426 Jülich, Germany
* corresponding author. Phone: (+49)2461-61-3790, fax: (+49)2461-61-2490
E-mail: w.hummel@fz-juelich.de

Abstract. A whole-cell catalyst using *E. coli* BL21(DE3) as a host, co-expressing glycerol dehydrogenase (GlyDH) from *Gluconobacter oxydans* and glucose dehydrogenase (GDH) from *Bacillus subtilis* for cofactor regeneration, has been successfully constructed and used for the reduction of aliphatic aldehydes such as hexenal or glyceraldehyde to the corresponding alcohols. This catalyst was characterized in terms of growth conditions, temperature and pH dependency and regarding the influence of external cofactor and permeabilization. In the case of external cofactor addition we found a 4.6-fold increase in reaction rate caused by the addition of 1 mM $NADP^+$. Due to the fact that pH and temperature are also factors which may affect the reaction rate, their effect on the whole-cell catalyst was studied as well. Comparative studies between the whole-cell catalyst and the cell-free system were investigated. Furthermore, the successful application of the whole-cell catalyst in repetitive batch conversions could be demonstrated in the present study. Since the GlyDH was recently characterized and successfully applied in the kinetic resolution of racemic glyceraldehyde we were now able to transfer and establish the process to a whole-cell system, which facilitated the access to L-glyceraldehyde in high enantioselectivity at 54% conversion. All in all, the whole-cell catalyst shows several advantages over the cell-free system like a higher thermal, a similar operational stability and the ability to recycle the catalyst without any loss of activity. The results obtained making the described whole-cell catalyst an improved catalyst for a more efficient production of enantiopure L-glyceraldehyde.

Keywords: whole-cell catalyst, designer cells, $NADP^+$-dependent glycerol dehydrogenase, kinetic resolution, enantioselectivity, L-glyceraldehyde

Introduction

During the last decades much attention has been payed to the enzymatic production of chiral building blocks, like for example hydroxy esters, hydroxy acids or chiral alcohols (Ghisalba et al. 2009). Oxidoreductases are high-potential biocatalysts because of their use in asymmetric oxidations as well as their ability to catalyze the stereo- and regioselective reduction of a variety of carbonyl compounds. Particularly, these enzymes have been used successfully in the production of chiral hydroxy acids (Vasic-Racki et al. 1989), amino acids (Bommarius et al. 1998; Galkin et al. 1997; Menzel et al. 2004), steroids (Crocq et al. 1997) and alcohols (Goldberg et al. 2007; Gröger et al. 2004; Liese et al. 1998; Pollard et al. 2006; Röthig et al. 1990; Schubert et al. 2001; Wills and Hannedouche 2002). The produced chiral building blocks can act as key intermediates in the production of pharmaceuticals, fine chemicals or natural products (Breuer et al. 2004; Patel 2006; Pesti and DiCosimo 2003; Rouhi 2004).

Enantiopure glyceraldehyde is an example for a small chiral building block of great interest because of the wide applicability of its structural motif. Recently, it has been successfully used in the synthesis of e.g. enantiopure 4-(dihydroxyalkyl)-β-lactams (antibiotic) (Areces et al. 2007) or 8a-*epi*-swainsoine (anticancer drug) (Bi and Aggarwal 2008). Both glyceraldehyde enantiomers have been synthesised chemically by different approaches starting from chiral pool compounds (Andrews et al. 1981; Baer and Fischer 1939; Hubschwerlen 1986; Hubschwerlen et al. 1995; Jurczak et al. 1986; Schmid and Bryant 1995). The step economy and accumulated waste streams of the existing procedures are however not very favourable for

industrial applications despite the achieved yields of the individual steps. This is due to the synthesis design using protecting groups which generate stoichiometric waste, toxic reagents, many synthetic steps and organic solvents. With regard to environmental improvements and cost reductions, new direct enzymatic routes for the preparation of enantiopure glyceraldehyde are attractive. In a previous paper we could successfully report such an enzymatic route (Richter et al. 2009) by applying the glycerol dehydrogenase (GlyDH) from *Gluconobacter oxydans* in the kinetic resolution of racemic glyceraldehyde, producing enantiopure L-glyceraldehyde on preparative scale.

However, in terms of efficiency, the need for isolated enzymes and as well the requirement for addition of expensive cofactor $NADP^+$ is disadvantageous. Therefore, a regeneration of the reduced cofactor is necessary by either a second substrate or a second enzyme together with a second substrate (Chenault and Whitesides 1987; Geueke et al. 2003; Hummel 1999; Weckbecker et al. 2010). To overcome the problem of cofactor regeneration and to improve and simplify the process, a simultaneous expression of two or more enzymes in a single cell is a promising approach, which has been shown by numerous literature known processes using whole-cell catalyst (Goldberg et al. 2007; Gröger et al. 2006a; Gröger et al. 2004; Gröger et al. 2006b; Kataoka et al. 1999; Kosjek et al. 2008; Patel et al. 2004; Schroer et al. 2007; Uzura et al. 2009; Weckbecker and Hummel 2004).

Different enzymes have already been applied in the regeneration of either the reduced or the oxidized cofactor in cell-free or whole-cell systems (Ernst et al. 2005; Hummel 1999; Kosjek et al. 2008; Moore et al. 2007; Weckbecker and Hummel 2004). For the regeneration of the oxidized cofactor we used glucose dehydrogenase (GDH) from *Bacillus subtilis*, an enzyme which can regenerate both NADH and NADPH (Fujita et al. 1977; Hilt et al. 1991; Weckbecker and Hummel 2004; Weckbecker and Hummel 2005). So far, it has been successfully applied in NADH-dependent biotransformations (Hanson et al. 1999) as well as in a number of NADPH-dependent processes. Examples are given by coupling with a (*R*)-specific alcohol dehydrogenase in the production of different chiral alcohols (Gröger et al. 2006a; Weckbecker and Hummel 2005), or the production of 4-chloro-3-oxobutanoate where it was used in combination with an aldehyde dehydrogenase (Kataoka et al. 1999). These examples display the broad applicability of the GDH in combination with various oxidoreductases.

Based on the process established for the cell-free biotransformation using GlyDH and GDH in the production of L-glyceraldehyde we constructed a whole-cell catalyst expressing both enzymes in parallel. Furthermore, we characterized the catalyst in terms of pH, temperature, storage and operational stability and other parameters and compared the whole-cell catalyst to the cell-free system. We were able to demonstrate that like the cell-free system, the whole-cell catalyst can also be applied successfully in the kinetic resolution of racemic glyceraldehyde producing enantiopure L-glyceraldehyde.

Results

Construction of recombinant *E. coli* cells co-expressing GlyDH and GDH

For co-expression of the *glydh* and *gdh* genes in *E. coli* BL21(DE3) the plasmid pNR-2 has been constructed (figure 1). The different specific activities of the pure investigated enzymes (GlyDH 39 U/mg and GDH 295 U/mg (Richter et al. 2009; Weckbecker and Hummel 2005)) led to the chosen arrangement of the genes in the commercial vector pETDuet-1. Based on the fact that no transcription terminator is located between the two MCS, *gdh* was cloned into MCS-1 and *glydh* into the MCS-2.

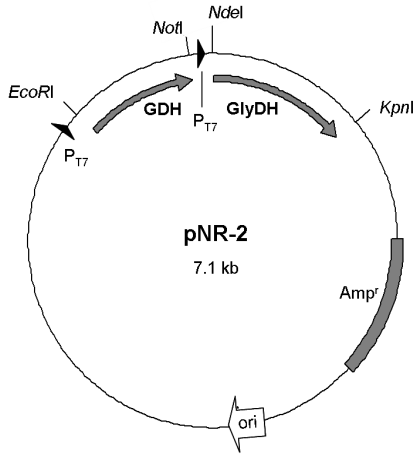

Figure 1. Structure of the plasmid pNR-2 derived from pETDuet-1 containing the genes for GlyDH and GDH. Additionally the plasmid contains an amp^r and two T7 promoters.

As next step the efficient co-expression of the whole-cell catalyst cultivated in LB medium at 25°C (standard conditions) was investigated in detail using both RT-PCR and spectrophotometric activity assays. Since it was the aim to regulate the activity of the GlyDH and GDH by controlling the transcripts of the corresponding genes, transcript levels of the *glydh* and *gdh* gene were analysed by RT-PCR. The studies revealed that the amount of *glydh* gene transcript is ten-fold higher compared to the *gdh* gene. Due to the 7.6-fold higher specific activity of the GDH on transcript level the difference could be adjusted. Therefore further experiments concerning the enzyme activity were performed additionally.

The functional expression of both enzymes was determined by measuring the activities in cell-free extracts. The GlyDH activity was found to be 22.3 U/mg of crude protein which was 3.1-fold higher than the activity determined for the GDH (7.18 U/mg of crude protein). Accordingly, the results of transcription levels could be confirmed by the analysis of the expression level, demonstrating that a co-expression with activities in a similar range could be successfully performed expressing pNR-2 in *E. coli* BL21(DE3). In the recent study the constructed whole-cell catalyst has been characterized regarding different parameters

Biotransformation of hexanal

In order to study the influence of different factors on the activity of the whole-cell catalyst the reduction of hexanal to hexanol has been selected as standard reaction (figure 2). This reaction was selected as model due to a better applicability and a more reliable GC analysis for hexanal and hexanol.

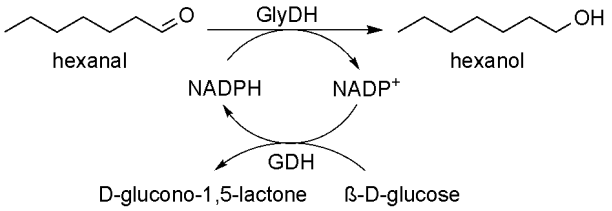

Figure 2. Scheme of the reaction catalyzed by the whole-cell catalyst. Hexanal is reduced by the GlyDH while the GDH simultaneously regenerates the cofactor catalyzing the oxidation of β-D-glucose.

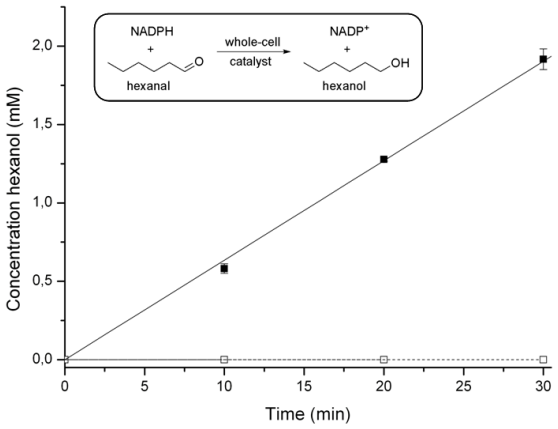

Figure 3. Determination of the initial rates in the conversion of 20 mM hexanal. The figure shows a typical time curve for the production of hexanol over a period of 30 min using per mL either 2.5 mg whole-cell catalyst (-■-) or 2.5 mg of cells expressing the empty vector (¨□¨). Standard deviations are given in the diagram, hexanol concentrations were measured by means of gas chromatoraphy

Initial rates have been determined measuring the production of hexanol over 30 min at 30°C without cofactor addition. Figure 3 illustrates a typical time course for the determination of the initial rate under standard conditions. The slope has been used for the calculation of the activity of the whole-cell catalyst (U/g). The control (empty vector) showed no activity at all, whereas the whole-cell catalyst on the contrary showed an activity of 27.2 ± 7.3 U/g (figure 3).
For a better comparison of the whole-cell and the cell-free systems, initial rates for both systems were determined using the same amount cell-free extract obtained by disrupting the whole-cell catalyst by sonification. The activity of the cell-free system was 1.5-fold higher than using the whole-cell system, indicating a better access for substrate and cofactor to the enzymes involved in the reaction (data not shown).
Using these standard conditions different parameters and their influence on the whole-cell catalyst have been investigated.

Effect of growth conditions and media on the expression level of the GlyDH and GDH

Based on economical reasons an optimal expression and especially an ideal ratio of the two co-expressed genes is of major importance. In addition to molecular methods, variation of growth conditions and media is a way to influence the expression levels of the corresponding enzymes. Therefore different growth conditions and a variety of media have been tested to optimize the expression levels of the two co-expressed enzymes. The corresponding results are summarized in table I, showing that best GlyDH activities were observed expressing the whole-cell catalyst at 25°C in LB, AI and M9 medium. In contrast to the GlyDH, the GDH activity increased with higher incubation temperatures. In general, a retarded expression caused by suboptimal growth conditions such as reduced temperature and minimal medium (M9) led to an increased GlyDH activity whereas better GDH activities were reached at optimal growth conditions like 37°C. instance the best GlyDH activity was reached with cells cultivated at 25°C in minimal medium (M9). This crude extract showed a 1.5-fold higher activity in the reduction of *rac*-glyceraldehyde compared to LB medium. For the GDH, the best activity was reached at an expression at 37°C in LB medium for 4 h, where a 1.5-fold enhancement of activity, compared to 25°C and 20 h, could be achieved.
Regarding the activity and ratio of both enzymes involved, LB medium at different temperatures and the HDF showed best results. Based on the observed spectrophotometrical results the initial rates of the whole-cell catalyst cultivated under these four different conditions in the reduction of hexanal have been comparatively studied.
The results are shown in figure 4 (diamond). Best conversions were reached with the cells cultivated at 25°C in LB medium (standard conditions, black) where the activity ratio of GlyDH and GDH was 3.1. A cultivation at 30°C for 4 h lead to an activity ration of 1.6 and an initial rate of 58.0% in the reduction of hexanal compared to standard conditions. The GDH activity of the whole-cell catalyst cultivated at 37°C is higher than the GlyDH activity under same condition resulting in a ratio of 0.7. Cells cultivated under these conditions reached an initial rate of 96.5% compared to the conversion velocity under standard conditions. A cultivation of the whole-cell catalyst under high density conditions led to a ratio of 1.3 in activity levels of GlyDH and GDH. These cells showed an initial rate of 84.1% of the rate determined after an expression at 25°C.
Thus, by the use of different growth conditions and media, the ratio of the two co-expressed enzymes could be varied from 0.7 (LB medium, 37ºC, 4 h) to 18.1 (TB medium, 25ºC, 20 h). However, the total activity of the involved enzymes is also a crucial parameter. The observed results regarding total performance of the catalyst in the reduction of hexanal indicates that a good ratio combined with high activities of GlyDH and GDH is necessary for the construction of an efficient catalyst. This point is emphasized by the fact that a good ratio of 1.3 and a medium GlyDH activity (HDF) led to a comparable

Table I. Effect of growth conditions and media on the expression levels of GlyDH and GDH. Activities are given in relation to LB medium at 25°C (100%), 100% equates to 22.3 U/mg crude protein for the GlyDH and 7.18 U/mg crude protein for the GDH. All activities have been measured with *rac*-glyceraldehyde (GlyDH) and D-glucose (GDH) as substrates using the described spectrophotometrical assays with cell-free extract of the whole-cell catalyst.

Medium	Temperature/ Incubation time	Relative GlyDH activity [%]	Relative GDH activity [%]	Ratio [GlyDH/GDH]
LB medium	25°C/20 h	100	100	3.1*
LB medium	30°C/4h 30°C/20 h	46.2 80.7	91.1 105.8	1.6* 2.4
LB medium	37°C/4h 37°C/20 h	35.0 30.9	150.4 62.7	0.7* 1.5
TB medium	25°C/20 h	14.8	2.8	18.1
Autoinduction medium	25°C/20 h	143.9	66.9	6.7
M9 medium	25°C/20 h	147.1	114.2	4.0
High density fermentation (HDF)	25°C/41 h	43.5	105.8	1.3*

* Cells cultivated under these conditions were used for further investigations regarding initial rates in the reduction of hexanal to hexanol (figure 4).

performance of the whole-cell catalyst that a medium ratio 3.1 and a high GlyDH activity (LB medium, 25ºC).

Influence of external cofactor on whole-cell biotransformation

The cofactor concentration has a major impact on enzyme activity. By using whole-cell systems, the intracellular cofactor level can be a limiting factor. Under normal growth conditions, the $NADP^+$ and NADPH level of *E. coli* is in the range of 3.62 and 2.42 nmol/mg dry weight (Lilius et al. 1979), meaning that the sum of the intracellular concentration of $NADP^+$ and NADPH is approximately 0.4 mM (Walton and Stewart 2004). In consideration of the fact that the investigated enzymes show K_m values for NADPH of 0.04 mM (GlyDH, determined with *rac*-glyceraldehyde as substrate (Richter et al. 2009)) and 0.025 mM for $NADP^+$ (GDH, determined with D-glucose as substrate (Weckbecker 2005)) optimal activities should be obtainable. However, due to differences in growth conditions and an often noticeable loss of internal cofactor by permeabilization effects, optimal activities are difficult to achieve. Therefore, experiments concerning the influence of the addition of different amounts of $NADP^+$ (1 mM and 5 mM) on the initial rates were studied. The results indicate that the addition of external cofactor led to a considerable increase in enzyme activity resulting in a faster conversion of hexanal in comparison to the experiment under standard conditions without cofactor addition (figure 4). Surprisingly, the addition of 1 mM $NADP^+$ elevated the initial rate by factor 4.6 whereas the addition of 5 mM $NADP^+$ led to a lower improvement (2.9-fold) under standard conditions. This inactivation in the presence of higher cofactor concentrations can be explained by a substrate-excess inhibition of the GlyDH.

Effect of toluene treatment on whole-cell biotransformation

As a second parameter the permeabilization of the cells by toluene has been studied. Therefore, the cells were incubated with 1% (v/v) toluene for 1 h at 30°C under shaking at 800 rpm. The treatment was followed by the

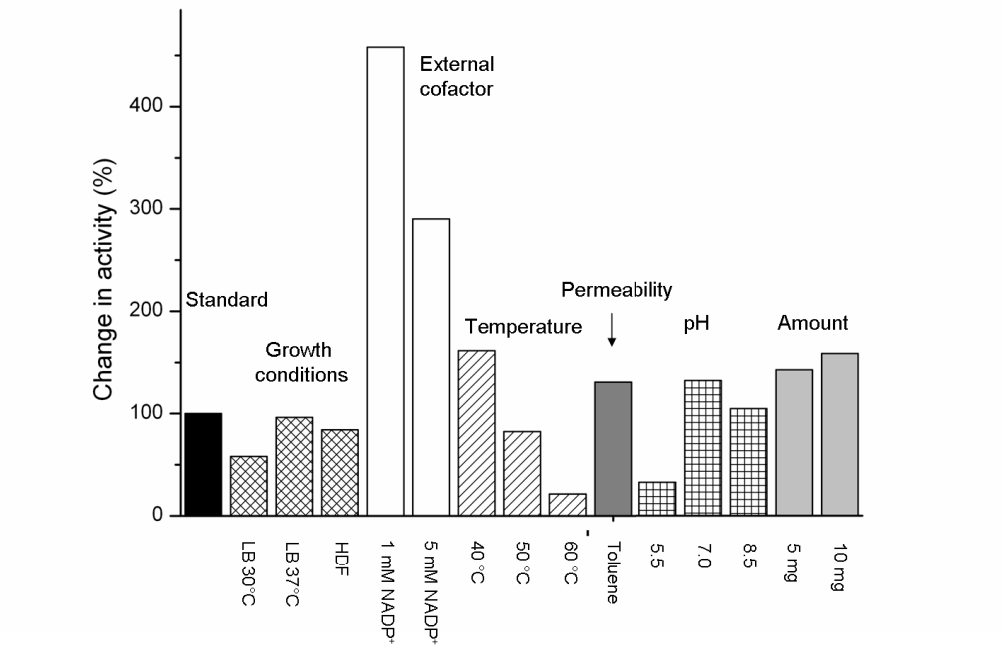

Figure 4. Influence of different parameters on the initial rate in the conversion of hexanal by the whole-cell catalyst. The initial rate under standard condition has been set to 100% (black). Alterations in initial rates by growth conditions (diamond), addition of external cofactor (white), variation of temperature (stripped), permeability (grey), pH (plaid) and amount of whole-cell catalyst (light grey) are displayed. All the data shown are the results of at least three independent measurements with standard deviations (>10%).

determination of initial rates. Figure 4 (grey) illustrates that a treatment with toluene increases the initial rate by factor 1.3. This demonstrates that a permeabilization of the cells results in an improved access of the substrate to the enzymes leading to an enhanced initial rate in the biotransformation of hexanal.

Dependence of temperature and pH on the activity and stability of the whole-cell catalyst

Since the influence of temperature and pH on enzyme activity and stability is often a limiting parameter in technical applications, studies concerning the dependence of temperature and pH on the whole-cell catalyst were performed. Furthermore, the temperature stability of the whole-cell catalyst and the cell-free system were examined comparatively.

Regarding temperature dependence, the whole-cell catalyst showed optimal activity at 40°C with a 1.6-fold higher initial rate compared to standard conditions (figure 4). Elevated temperatures decreased the activity of the whole-cell catalyst to approximately 80% residual activity at 50°C or 20% residual activity at 60°C, respectively. In addition, the stability under these elevated temperatures was reduced as well which can be seen as a result of the measurable inactivation of the catalyst after 10 min.

The pH dependence was investigated at three different pH values (pH 5.5, 7.0 and 8.5) and compared to the standard conditions at pH 6.8 (figure 4). At pH 7.0 the catalyst showed optimal activity (132.1%), whereas at pH 8.5 no improvement could be detected at all. Under slightly acidic conditions (pH 5.5) the whole-cell catalyst lost approximately 70% of its activity. Because of the importance of catalyst stability in technical applications, temperature-dependent inactivation over time of the whole-cell catalyst and the cell-free system were investigated.

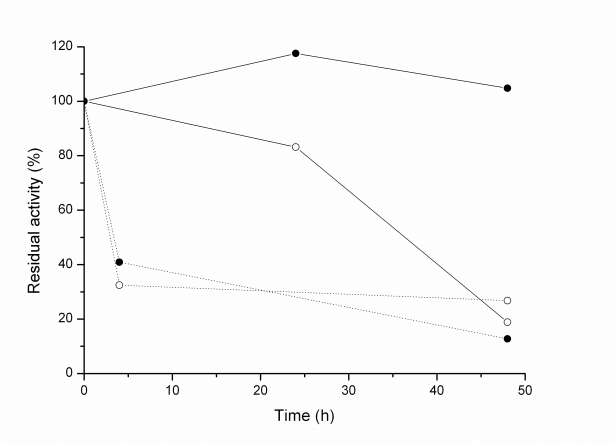

Figure 5. Thermal and operational stability of the whole-cell catalyst (●) in comparison with the cell-free system (○). The effect of temperature on both preparations stored in buffer (solid line) and under operational conditions (dotted line) over a period of 48 h at 30°C was investigated. Operational stability was measured under conditions where substrate (*rac*-glyceraldehyde) was converted by the catalyst over the investigated period. For the determination of the residual activity the initial rates were measured under standard conditions. All the data shown are the results of at least three independent measurements with standard deviations (<10%).

Studies were performed incubating both preparations at 30ºC and under shaking (800 rpm) in buffer (100 mM TEA, pH 7) and under conditions where *rac*-glyceraldehyde was converted over 48 h. For studies regarding the cell-free system the same amount cell free extract of the whole-cell catalyst was used. Residual activities after 4 h, 24 h and 48 h were determined using the standard assay for initial rates.

As shown in figure 5, after incubation in buffer the whole-cell catalyst is completely stable over the investigated period of time, whereas the cell-free system showed a significant inactivation, revealed by a residual activity of only 18.9% after 48 h. In contrast to the observed stabilities in buffer, both preparations show a significant decrease in activity when incubated under process conditions. After an incubation of 4 h residual activities of 32.4% using the cell free system and 40.9% with the whole-cell catalyst were determined. The residual activities further diminish over the 48 h incubation period. At that time the cell-free system shows a loss of 73.2% of its activity, while the whole-cell catalyst loses 83.3% of its activity, indicating that over time an inactivation in both enzyme preparations is visible while simultaneously converting *rac*-glyceraldehyde.

Comparing the observed results under process and storage conditions, both systems show a more vigorous decrease in residual activity under process conditions. Concerning the cell-free system, similar residual activities were observed under both investigated conditions while in contrast the activity of the whole-cell catalyst is drastically decreased under conditions where *rac*-glyceraldehyde is converted.

Nevertheless, after 48 h both systems still show activity, and due to the fact that enzyme stability is a very crucial parameter for technical applications and processes, any improvement in stability is important. Herein we could show that the whole-cell catalyst is significantly more stable for long-term applications than the cell-free system incubated in buffer. But regarding the stability while *rac*-glyceraldehyde is converted, both systems show residual activities of 26.8% for the cell-free system and 16.7% for the whole-cell catalyst operational stabilities in the same dimension.

Recycling of the whole-cell catalyst

Recycling of the whole-cell catalyst would generously facilitate technical applications in terms of efficiency and cost factors. For this reason we investigated the ability of using the whole-cell catalyst in repetitive batch conversions. Studies were performed by measuring the reduction of hexanal to hexanol as a model system over a period of 45 min. After this incubation time samples were withdrawn and the supernatant was discarded. By suspending the cells in fresh substrate solution the next cycle was started. In the reduction of hexanal the whole-cell catalyst showed 100% conversion of hexanal while simultaneously only 50% of product hexanol was formed. But due to the fact, that this reaction was chosen as model reaction the suboptimal product formation of the reaction was not further investigated.

First experiments showed that cells which were exposed to several freezing and unfreezing cycles were not recyclable. Indicating that this treatment led to a high level of permeabilization, this thesis was proven by studies where stored cells were used for recycling experiments. The results showed that the normal conversion in the first cycle was followed by a massive loss of activity in the second cycle and no detectable activity in the third (data not shown). According to this observation freshly harvested and washed cells have been used for the experimental setup to investigate the ability to recycle the whole-cell catalyst.

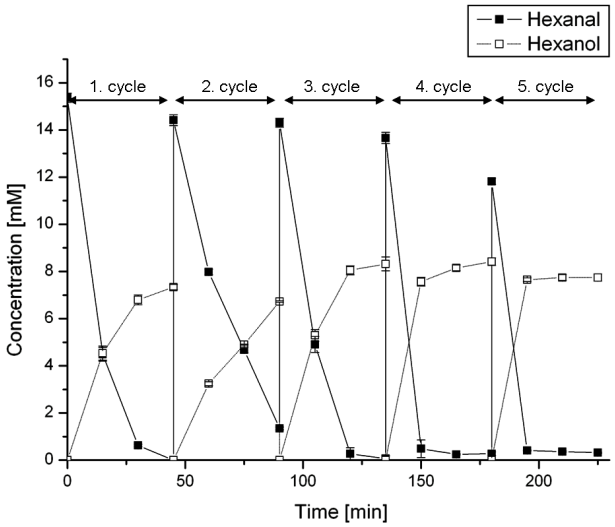

Figure 6. Result of a repetitive conversion of hexanal (15 mM) by the whole-cell catalyst. The figure shows the development of hexanal and hexanol concentrations over 225 min where 5 cycles were performed. After each conversion the samples were withdrawn, the supernatant was discarded and the whole-cell catalyst was suspended in fresh substrate solution. Standard deviations are indicated in the diagram.

Figure 6 illustrates that under these conditions a recycling of the whole-cell is possible for at least five times without any loss in activity. In the third cycle the reaction rate even increased and the maximal conversion was reached after a reaction time of approximately 30 min compared to the first cycle where a product formation of 50% was reached after 45 min. Further increase of activity was observed in cycle four and five where the reaction rate increases even more and the conversion was completed after only 15 min. The observed results lead to the suggestion that the increase in reaction rate is a result of the ongoing permeabilization of the catalyst caused by compounds in the reaction mixture. This thesis is emphasized by the observation that cells which are partially permeabilized by a toluene treatment showed a faster conversion than non permabilized ones. Along with the results, regarding the use of frozen cells, it becomes apparent that permeabilization leads to an increased reaction rate, but at a certain degree of permeabilization, a recycling of the whole-cell catalyst is not feasible anymore.

Table II. Comparison of the substrate specificity of the whole-cell catalyst and the purified enzyme. Activities are given in relation to hexanal (100%) (100% equates to 31.9 U/mg for the purified enzyme and 27.2 U/g). For the whole-cell catalyst initial rates with 20 mM substrate at 30°C were determined by means of gas chromatography.

Substrate	Structure	Relative activity whole-cell catalyst [%]	Relative activity purified enzyme [%]
Butanal	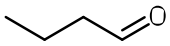	17.9	73.0
Hexanal	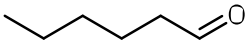	100	100
rac-Glyceraldehyde	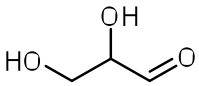	78.8	122.6
Benzaldehyde	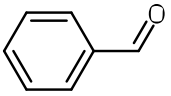	72.2	43.3

Substrate spectrum

For the purified GlyDH the activity towards a variety of different substrates was determined (Richter et al. 2009). From this substrate spectrum two aliphatic, one branched-chained and one aromatic substrate were chosen for the comparison of the substrate specificity in the reduction of purified enzyme and whole-cell catalyst (table 1).
For both preparations, activities were compared to the standard substrate hexanal (specific activity for the purified enzyme 31.9 U/mg). All selected substrates were accepted by the whole-cell catalyst and the purified enzyme, however revealing different relative activities towards the different substrates. For example, butanal was converted at a significantly lower activity by the whole-cell catalyst (17.9% related to hexanal) than using purified enzymes which showed an activity of 73.0% compared to hexanal. The reductions of benzaldehyde and glyceraldehyde were catalyzed with better activities using the whole-cell catalyst. These differences can be caused either by a different access to the enzyme by the diverse substrates due to the variable catalyst preparations or due to the existence of interfering enzymes in the crude extract catalysing unspecific reactions. In general there are some differences detectable regarding the activities towards the different substrates, but all in all the same substrates are accepted by the two different catalyst preparations.

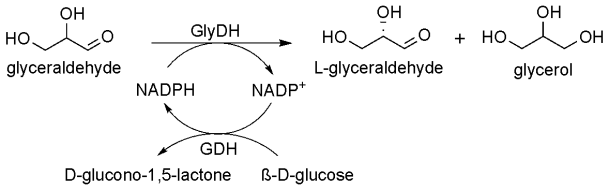

Figure 7. Scheme of the kinetic resolution of glyceraldehyde by the whole-cell catalyst combining GlyDH and GDH.

Application of the whole-cell catalyst in the kinetic resolution of glyceraldehyde

Enantiopure glyceraldehyde is an interesting chiral building block which can be used as starting material for the synthesis of a variety of different fine chemicals, pharmaceuticals and natural products (Areces et al. 2007; Bi and Aggarwal 2008; Bull et al. 2007; Kumar et al. 2007). Therefore, we tried to transfer results regarding the cell-free system (Richter et al. 2009) to a whole-cell system (figure 7). Thus, preparative scale kinetic resolution was performed using the whole-cell catalyst. Due to the obtained results regarding the externally added cofactor we performed the kinetic resolution of racemic glyceraldehyde in the presence of 0.5 mM $NADP^+$.
This concentration was chosen as a result of comparative conversions with 0.1 mM, 0.5 mM and 1 mM cofactor (data not shown). The results revealed that with an addition of 0.5 mM the conversion proceeds in reasonable time.
Figure 8 illustrates a typical time curve for the kinetic resolution of racemic glyceraldehyde using the whole-cell catalyst. The developments of the glyceraldehyde and glycerol concentrations are displayed in the diagram. Additionally the *ee* value of L-glyceraldehyde was measured over the investigated period of 60 min. A conversion of 54% and *ee* of 98% were achieved by using the whole-cell catalyst in the kinetic resolution of racemic glyceraldehyde. The reaction continues after a conversion of 50%. Therefore the reaction has to be stopped at a conversion of approximately 54%. Moreover, a conversion without cofactor addition was possible, resulting in comparable selectivity. Drawbacks of the cofactor-free application are the requirement of a higher amount of catalyst and longer incubation times (data not shown). Nevertheless, we succeeded in transferring the kinetic resolution of racemic glyceraldehyde to a whole-cell system.

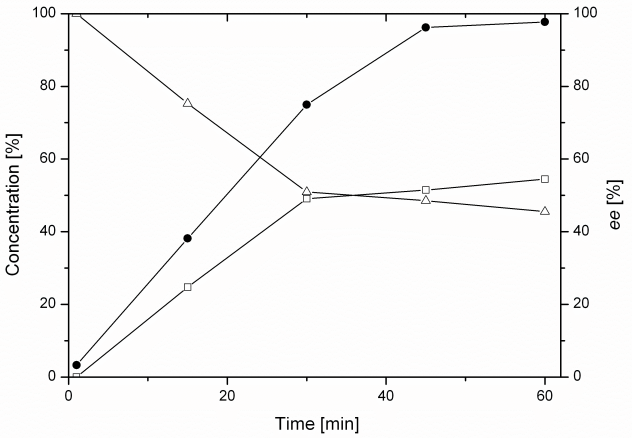

Figure 8. Kinetic resolution of racemic glyceraldehyde by the whole-cell catalyst. The development of glycerol (-□-) and glyceraldehyde (-Δ-) concentrations are measured over a period of 60 min; concentrations were determined by HPLC. The *ee* values were determined by means of chiral GC (-●-). The kinetic resolution was done using 2 g catalyst, 0.18 M *rac*-glyceraldehyde, 0.12 M glucose and 0.5 mM $NADP^+$ in 250 mL 100 mM TEA pH 7.0.

Discussion

In the present study, the successful construction and characterization of a whole-cell catalyst co-expressing GlyDH from *G. oxydans* and GDH from *B. subtilis* is presented. Moreover, the successful application of the whole-cell catalyst in the kinetic resolution of *rac*-glyceraldehyde producing enantiopure L-glyceraldehyde is reported in this paper.

An one plasmid strategy was applied cloning both genes into one plasmid for simultaneous expression of both proteins. We succeeded in generating a catalyst which showed activities in a similar range fulfilling an important issue regarding an efficient application of the catalyst (Gröger et al. 2006b; Menzel et al. 2004). Apart from the successful expression of both genes other parameters play an important role for the applicability of the catalyst. In terms of efficiency the need of external cofactor and the ability of catalyst recycling are of primary focus.

We could show that the presented catalyst stored in buffer is more stable than the cell-free system. Although both systems show significantly reduced long-time stabilities under operational conditions, the whole-cell system exhibits one main advantage over the cell free system. Namely the ability that the catalyst can be re-used for several biotransformation reactions without any loss of activity. The observed improved storage stability and rather similar operation stability compared to the cell-free system make the whole-cell catalyst better applicable for industrial processes than the cell-free system. Explanations for the faster inactivation of the cell-free system under storage conditions can be found in the temperature-dependent inactivation of the GlyDH over time. In former studies the purified GlyDH showed a loss of 60% of its activity over a period of 48 h at 30°C (Richter et al. 2009). Comparing these results to the 80% loss of activity using the crude extract in this study under same conditions, the results clearly show that in a cell-free system the GlyDH is responsible for loss of activity over time. Regarding the operational stability of both enzyme preparations the aldehyde, especially the investigated glyceraldehyde, might have a negative effect on both enzyme activity and permeabilization of the cells. These effects combined are potentially the reason why both preparations show comparable inactivation profiles under conditions where glyceraldehyde is converted to glycerol.

Regarding the use of external cofactor we could show that the reaction rate could be improved by factor 4.6 by the addition of a low $NADP^+$ concentration of 1 mM. Due to the fact that intact cells are not able to take up externally added cofactor efficiently, this effect can be explained by a slight permeabilization of the cells through the freezing procedure while storing the catalyst at -20°C. This kind of permeabilization causes a decrease of the internal cofactor level which leads to reduced enzyme activities, which can be counterbalanced by the addition of cofactor. This statement was underlined by the observed enhancement in the reaction rate when cofactor was externally added.

But even if the reaction rates are improved by the addition of external cofactor the conversion still proceeds in absence of externally added cofactor, indicating that the amount of intracellular cofactor is sufficient for a preparative conversion (Gröger et al. 2006a; Gröger et al. 2006b; Menzel et al. 2004). Therefore, in terms of applicability one has to decide whether to use high catalyst concentrations and longer incubation periods without cofactor addition or lower catalyst concentrations and shorter reaction times with cofactor addition.

Since pH and temperature are also crucial parameters, the dependence of the catalyst on pH and temperature has been investigated to perform conversions under optimal conditions.

A whole-cell system has many advantages compared to the cell free system. Gröger and co-workers have compared the economy of isolated enzymes and whole-cells. Due to the more extensive procedures and the need of adding expensive cofactor to the isolated enzymes, the biotransformation with whole-cells is a cost-attractive alternative (Gröger et al. 2006b). Since GlyDH showed excellent enantioselectivity in the reduction of racemic glyceraldehyde (Richter et al. 2009) our primary focus was to transfer the kinetic resolution of racemic glyceraldehyde to the whole-cell system. There are some kinetic resolutions with oxidoreductases in whole wild type cells published (Buisson et al. 2000; Eh and Kalesse 1995; Hioki et al. 2000; Stewart 2001) whereas the use of a recombinant whole-cell system is not so common (Kataoka et al. 2008). Fortunately, the use of the whole-cell system was possible catalysing the kinetic resolution of racemic glyceraldehyde with an *ee* of 98% and a conversion of 54% on preparative scale (4 g). Compared to the process using the cell-free system selectivity and conversion are in a similar range. But in terms of stability, recycling and addition of external cofactor the whole-cell process is significantly better than the cell-free process.

In conclusion we could demonstrate that the constructed whole-cell catalyst makes the valuable chiral building block L-glyceraldehyde accessible in a direct enzymatic one-step

transformation, even without the need of adding expensive cofactor.

Experimental Section

General: If not stated otherwise all chemicals were purchased from Sigma Aldrich. Centrifugations were carried out using the centrifuges RC5BPlus (Sorvall), Mikro22 and Rotina 35 R (Hettich). Restriction enzymes were purchased from Fermentas. The studied GlyDH and GDH are commercially available at evocatal GmbH (evo-1.1.190 and evo-1.1.060).

Construction of the whole-cell catalyst: For cloning of the *glydh* gene, the plasmid pNR-1 was used as template for PCR introducing the restriction sites *Nde*I and *Kpn*I (up: 5'-GGAATTCCATATGGCATCCGACACCATCCGC-3' down: 5'-GGGGTACCTCAGTCCCGTGCCGGGGG-3'). The amplification was performed using standard PCR techniques, the created *Nde*I-*Kpn*I fragment was subcloned into the vector pGDH1. This vector is based on the commercially available pETDuet-1. The *gdh* gene was amplified using genomic DNA from *B. subtilis* as template and primers with recognition sites for the restriction enzymes *Eco*RI and *Not*I (up: 5'-CCGGAATTCATGTATC CGGATTTAAAAGGAAAAGTCG-3', down: 5'-ATAGTTTA GCGGCCGCTTAACCGCGGCCTGCCTG-3'). The resulting construct was named pNR-2 (figure 1).

Cultivation of the whole-cell catalyst in shaking flasks: *E. coli* BL21(DE3) cells carrying the recombinant plasmid (pNR-2) were cultivated overnight at 37°C in 5 mL LB medium (Bertani 1951), containing 100 µg/mL ampicillin. These cultures were used to inoculate different amounts of LB medium, TB medium (24 g/L yeast extract, 12 g/L casein hydrolysate, 5 g/L glycerol in 100 mM KP_i buffer pH 7), autoinduction (AI) medium (TB medium, 2 g/L lactose, 0.5 g/L glucose) and M9 (4 g/l glucose, 0.05 g/L $MgSO_4 \cdot 7H_2O$, 0.02 g/L $CaCl_2 \cdot 2H_2O$, 70 g/L $Na_2HPO_4 \cdot 2H_2O$, 30 g/L KH_2PO_4, 5 g/L NaCl, 10 g/L NH_4Cl in distilled water) containing 100 µg/mL ampicillin for expression in shaking flasks at a final concentration of 0.05 optical density at 600 nm (OD_{600}). The cultures were grown at 37°C. When the OD_{600} reached a value between 0.5 and 0.7 the production of the recombinant GlyDH and GDH were induced by the addition of isopropyl thio-β-D-galactoside (IPTG) to a final concentration of 0.3 mM. The cultures were shaken for 4 h or 20 h at 25°C, 30°C or 37°C and harvested by centrifugation. For the detailed characterization of the whole-cell catalyst cells cultivated in LB medium at 25°C were used.

High density fermentation (HDF): Fermentation of *E. coli* BL21(DE3) cells carrying the recombinant plasmid (pNR-2) was performed in a 40 l bioreactor (Infors AG) in a 15 L scale. The components of the batch medium are as follows: 0.2 g/L NH_4Cl, 2 g/L $(NH_4)_2SO_4$, 13 g/L KH_2PO_4, 10 g/L K_2HPO_4, 6 g/L $NaH_2PO_4 \cdot H_2O$, 3 g/L yeast extract, 2 g/L glucose, 1 g/L $MgSO_4 \cdot 7H_2O$, 0.25% vitamin solution (0.1 g/L riboflavin, 10 g/L thiamine, 0.5 g/L nicotinic acid, 0.5 g/L pyridoxine, 0.5 g/L Ca-phanthotenate, 0.001 g/L biotin, 0.002 g/L folic acid, 0.01 g/L cyanocabalamine), 0.16% micronutrient solution (10 g/L $CaCl_2 \cdot 2H_2O$, 0.5 g/L $ZnSO_4 \cdot 7H_2O$, 0.25 g/L $CuCl_2 \cdot 2H_2O$, 2.5 g/L $MnSO_4 \cdot H_2O$, 1.75 g/L $CoCl_2 \cdot 6H_2O$, 0.125 g/L H_3BO_3, 2.5 g/L $AlCl_3 \cdot 6H_2O$, 0.5 g/L $Na_2MoO_4 \cdot 2H_2O$, 10 g/L $FeSO_4 \cdot 7H_2O$), 0.1g/L thiamine in distilled water. Additionally, a fed medium was used which consists of the same components as the batch medium but differs in the following concentrations: 18 g/L yeast extract, 600 g/L glucose, 10 g/L $MgSO_4 \cdot 7H_2O$, 1 g/L thiamine. After sterilization of the reactor including the batch medium the HDF was started by an inoculation of 1% (v/v) with pre-culture grown over night at 37°C. For optimal growth the cells were cultivated under glucose limiting conditions. The addition of fed medium was done according to an optimized protocol for *E. coli* cells at 30°C. H_3PO_4 was used to keep the pH at a constant level (pH 7.0), the oxygen feed was controlled by increasing agitation speed and airflow to keep it over 30%. The the protein expression was induced after 27 h by an IPTG concentration of 2 mM. After induction, the temperature was shifted from 30°C to 25°C. Temperature, pH and oxygen feed were controlled automatically by computer. After an incubation time of 41 h, the cells were harvested by centrifugation.

Preparation of cell-free extracts: The bacterial culture was harvested by centrifugation at 17,000 x g for 20 min at 4°C. A cell suspension (20%) was prepared in 100 mM triethanolamine buffer (TEA) pH 7.0. Cells were disrupted by two sonification cycles of two min (40% power output) with cooling periods in-between. The lysed cells were centrifuged at 17,000 x g for 30 min at 4°C, and the supernatant was used for determination of GlyDH and GDH activity. Protein concentrations were determined according to Bradford using BSA as a standard (Bradford 1976).

Real-time PCR: For RT-PCR analysis cells were cultivated as described; only the point of induction was shifted to an OD_{600} of 0.3 and cells were incubated at 25°C until a final OD_{600} of 0.9 was reached. Total RNA was isolated using the RNeasy Mini Kit including the optional DNA digestion step (Qiagen). An additional DNA digestion was performed with the RQ1 RNase-free DNase Set (Promega). RNA concentrations were determined using an Eppendorf BioPhotometer equipped with a Tray Cell 105.810 UVS (Hellma). 150 ng of total RNA in a reaction volume of 20 µL were used for reverse transcription and subsequent RT-PCR using the QuantiTect SYBR Green RT-PCR Kit (Qiagen). The temperature program was adjusted according to manufacturers' instructions (annealing temperature 58°C, 30 cycles) in a Mastercycler epgradient S with realplex^4 module (Eppendorf). For amplification the following primers were used: *glydh* (up: 5'-CCTGCTG ACAGGCAAGATGAAC-3' down: 5'-GAGGTACTTCTCG AAATTCGGCTTC-3'), *gdh* (up: 5'-GCTGACCCTAAACAG AAAGCTGATG-3' down: 5'-GAATAACGTGATGCCTGTGA CGTAG-3') and *bla* as internal standard (up: 5'-TAACTACG ATACGGGAGGGCTTACC-3' down: 5'-GGATAAAGTTGC AGGACCACTTCTG-3'). The given data are results of at least three measurements. Spectrophotometrical assays for the determination of the GDH and GlyDH activity. Continuous assays using UV absorbance at 340 nm were employed to monitor the NADPH concentration during reduction or oxidation catalyzed by GlyDH or GDH. One unit of activity was defined as the amount of enzyme which catalyzes the oxidation of 1 µmol NADPH per minute (GlyDH) or reduction of 1 µmol $NADP^+$ (GDH) under standard conditions (30°C, pH 7). For the determination of GlyDH activity racemic glyceraldehyde was used as standard substrate. The assay mixture contains 970 µL substrate solution (10 mM substrate in 100 mM TEA buffer pH 7), 20 µL NADPH (12.5 mM) in distilled water and 10 µL enzyme solution. For the determination of GDH activity D-glucose was used as substrate, standard conditions were 30°C and pH 7.0. The assay mixture contains 970 µL substrate solution (100 mM substrate in 100 mM TEA buffer pH 7), 20 µL $NADP^+$ (100 mM) and 10 µL enzyme solution. Reactions were started by addition of the enzyme solution and the amount of NADPH was measured over 1 min.

Determination of initial rates of the whole-cell catalyst: For the use in whole-cell biotransformations 5 mg cells (wet weight) were suspended per mL buffer (100 mM TEA, pH 7). 500 µL/mL of the cell solution and 500 µL/mL of substrate solution (20-40 mM substrate, 200 mM D-glucose in 100 mM TEA, pH 7.0) were mixed. Hexanal (40 mM) was used as standard substrate for determination of initial rates. Biotransformations were carried out at 30°C and 800 rpm. Samples of 100 µL were taken periodically and diluted with 100 µL of internal standard (2.3 mM octanol) and 800 µL ethyl acetate. After mixing and centrifugation the organic phases were analyzed for the production of hexanol using the gas chromatograph GC-17A (Shimadzu) equipped with the column CP-Chirasil-DEX (Varian, 25 m x 0.25 mm ID).

The temperature program included: 60°C for 2 min, 5°C/min to 105°C and 10°C/min to 130°C. To examine alterations in initial rates different parameters such as pH, temperature, cofactor concentration or permeability of the cells were varied and the initial rates were determined using standard conditions. The activity of the whole-cell catalyst was determined by measuring product formation at different times followed by calculation of the initial product formation rate per gram wet cells. The activity of whole-cell catalyst is expressed as U which means µmol product formed per minute and the cell specific activity is expressed as U/g cell wet weight.

Recycling of the whole-cell catalyst: For recycling studies of the whole-cell catalyst transformations with freshly harvested cells were performed. Cells (60 mg wet weight) per mL were suspended in substrate solution (20 mM hexanal, 200 mM D-glucose in 100 mM TEA buffer pH 7). Conversions were carried out at 30°C and 800 rpm. After 0 min, 15 min, 30 min and 45 min samples were taken and analysed by gas chromatography (GC) as described. After 45 min conversion the cells were separated by centrifugation and the supernatant was discarded. The cells were suspended in fresh substrate solution and the conversion over 45 min was determined again.

Whole-cell biotransformation: For the kinetic resolution of glyceraldehyde, the reaction mixture contained racemic glyceraldehyde (4 g, 0.18 M), glucose (5.28 g, 0.12 M), $NADP^+$ (0.1 g, 0.5 mM) in 250 mL of TEA buffer (100 mM, pH 7) and the whole-cell catalyst (2 g wet weight). Samples of 50 µL were taken periodically and diluted either with trifluoroacetic acid (950 µL) for HPLC analysis to determine the conversion or with ethyl acetate (75 µL) for GC analysis to determine the enantiomeric excess (*ee*). GC samples were derivatized for 30 min with dioxane (75 µL), acetic anhydride (50 µL) and pyridine (5 µL). Concentrations of glyceraldehyde and glycerol were determined by using an Agilent 1100 HPLC equipped with a CS organic acid resin column (300 mm·8 mm) with 5 mM trifluoroacetic acid (0.7 mL/ min) at room temperature. The enantiomeric ratio for glyceraldehyde was determined by using a HP 6890 GC with a Varian CP-Chirasil-Dex CB column (25 m x 0.32 mm). The temperature was kept constant at 108°C over a period of 20 min.

Acknowledgements

This project was supported by funds from the Deutsche Bundesstiftung Umwelt (DBU) Project number: Az13194. We would like to thank Ruslan Yuyev for helpful discussions and support. Additionally, we thank Dipl.-Ing. Holger Gieren for his support regarding the high density fermentation.

References

Andrews GC, Crawford TC, Bacon BE. 1981. Stereoselective, Catalytic Reduction of L-Ascorbic-Acid - a Convenient Synthesis of L-Gulono-1,4-Lactone. J Org Chem 46:2976-2977.

Areces P, Carrasco E, Light ME, Santos M, Plumet J. 2007. Synthesis of enantiopure 4-(dihydroxyalkyl)-b-lactams from D-mannitol using Ley's BDA-protected L-glyceraldehyde. Synlett:3180-3182.

Baer E, Fischer HOL. 1939. Studies on acetone-glyceraldehyde IV. Preparation of d(+)- acetone glycerol. J Biol Chem 128:463-473.

Bertani G. 1951. Studies on lysogenesis :1. the mode of phage liberation by lysogenic *Escherichia coli*. J Bacteriol 62:293-300.

Bi J, Aggarwal VK. 2008. Application of furyl-stabilized sulfur ylides to a concise synthesis of 8a-epi-swainsonine. Chem Commun:120-122.

Bommarius AS, Schwarm M, Drauz K. 1998. Biocatalysis to amino acid-based chiral pharmaceuticals - examples and perspectives. J Mol Catal B-Enzym 5:1-11.

Bradford MM. 1976. Rapid and sensitive method for quantitation of microgram quantities of protein utilizing principle of protein-dye binding. Anal Biochem 72:248-254.

Breuer M, Ditrich K, Habicher T, Hauer B, Keßeler M, Stürmer R, Zelinski T. 2004. Industrial methods for the production of optically active intermediates. Angew Chem-Int Edit 43:788-824.

Buisson D, Baucherel X, Levoirier E, Juge S. 2000. Baker's yeast reduction of a-alkyl-a-hydroxy-b-keto esters. Tetrahedron Lett 41:1389-1392.

Bull JA, Balskus EP, Horan RAJ, Langner M, Ley SV. 2007. Total synthesis of potent antifungal marine bisoxazole natural products bengazoles A and B. Chem-Eur J 13:5515-5538.

Chenault HK, Whitesides GM. 1987. Regeneration of nicotinamide cofactors for use in organic-synthesis. Appl Biochem Biotechnol 14:147-197.

Crocq V, Masson C, Winter J, Richard C, Lemaitre Q, Lenay J, Vivat M, Buendia J, Prat D. 1997. Synthesis of trimegestone: the first industrial application of bakers' yeast mediated reduction of a ketone. Org Process Res Dev 1:2-13.

Eh M, Kalesse M. 1995. Remarkable kinetic resolution of chiral b-keto-esters by bakers-yeast reduction. Synlett:837-838.

Ernst M, Kaup B, Müller M, Bringer-Meyer S, Sahm H. 2005. Enantioselective reduction of carbonyl compounds by whole-cell biotransformation, combining a formate dehydrogenase and a *(R)*-specific alcohol dehydrogenase. Appl Microbiol Biotechnol 66:629-634.

Fujita Y, Ramaley R, Freese E. 1977. Location and properties of glucose dehydrogenase in sporulating cells and spores of *Bacillus subtilis*. J Bacteriol 132:282-293.

Galkin A, Kulakova L, Yoshimura T, Soda K, Esaki N. 1997. Synthesis of optically active amino acids from a-keto acids with *Escherichia coli* cells expressing heterologous genes. Appl Environ Microbiol 63:4651-4656.

Geueke B, Riebel B, Hummel W. 2003. NADH oxidase from *Lactobacillus brevis*: a new catalyst for the regeneration of NAD. Enzyme Microb Technol 32:205-211.

Ghisalba O, Meyer HP, Wohlgemuth R. 2009. Industrial Biotransformation. In: Flickinger MC, editor.

Encyclopedia of Industrial Biotechnology. Hoboken, NJ: Wiley.

Goldberg K, Schroer K, Lütz S, Liese A. 2007. Biocatalytic ketone reduction - a powerful tool for the production of chiral alcohols - part I: processes with isolated enzymes. Appl Microbiol Biotechnol 76:237-248.

Gröger H, Chamouleau F, Orologas N, Rollmann C, Drauz K, Hummel W, Weckbecker A, May O. 2006a. Enantioselective reduction of ketones with "Designer cells" at high substrate concentrations: Highly efficient access to functionalized optically active alcohols". Angew Chem-Int Edit 45:5677-5681.

Gröger H, Hummel W, Rollmann C, Chamouleau F, Hüsken H, Werner H, Wunderlich C, Abokitse K, Drauz K, Buchholz S. 2004. Preparative asymmetric reduction of ketones in a biphasic medium with an *(S)*-alcohol dehydrogenase under in situ-cofactor-recycling with a formate dehydrogenase. Tetrahedron 60:633-640.

Gröger H, May O, Werner H, Menzel A, Altenbuchner J. 2006b. A "Second-Generation process" for the synthesis of L-neopentylglycine: Asymmetric reductive amination using a recombinant whole cell catalyst. Org Process Res Dev 10:666-669.

Hanson RL, Schwinden MD, Banerjee A, Brzozowski DB, Chen BC, Patel BP, McNamee CG, Kodersha GA, Kronenthal DR, Patel RN and others. 1999. Enzymatic synthesis of L-6-hydroxynorleucine. Bioorg Med Chem 7:2247-2252.

Hilt W, Pfleiderer G, Fortnagel P. 1991. Glucose dehydrogenase from *Bacillus subtilis* expressed in *Escherichia coli* .1: purification, characterization and comparison with glucose dehydrogenase from *Bacillus megaterium*. Biochim Biophys Acta 1076:298-304.

Hioki H, Hashimoto T, Kodama M. 2000. Efficient kinetic resolution of (+/-)-4-methyl-Hajos-Parrish ketone by baker's yeast reduction. Tetrahedron-Asymmetry 11:829-834.

Hubschwerlen C. 1986. A Convenient Synthesis of L-*(S)*-Glyceraldehyde Acetonide from L-Ascorbic-Acid. Synthesis:962-964.

Hubschwerlen C, Specklin JL, Higelin J. 1995. L-*(S)*-Glyceraldehyde Acetonide - (1,3-Dioxolane-4-Carboxaldehyde, 2,2-Dimethyl-, *(S)*-). Organic Syntheses 72:1-5.

Hummel W. 1999. Large-scale applications of NAD(P)-dependent oxidoreductases: recent developments. Trends Biotechnol 17:487-492.

Jurczak J, Pikul S, Bauer T. 1986. *(R)*-2,3-O-isopropylideneglyceraldehyde and *(S)*-2,3-O-isopropylideneglyceraldehyde in stereoselective organic-synthesis. Tetrahedron 42:447-488.

Kataoka M, Ishige T, Urano N, Nakamura Y, Sakuradani E, Fukui S, Kita S, Sakamoto K, Shimizu S. 2008. Cloning and expression of the L-1-amino-2-propanol dehydrogenase gene from *Rhodococcus erythropolis*, and its application to double chiral compound production. Appl Microbiol Biotechnol 80:597-604.

Kataoka M, Yamamoto K, Kawabata H, Wada M, Kita K, Yanase H, Shimizu S. 1999. Stereoselective reduction of ethyl 4-chloro-3-oxobutanoate by *Escherichia coli* transformant cells coexpressing the aldehyde reductase and glucose dehydrogenase genes. Appl Microbiol Biotechnol 51:486-490.

Kosjek B, Nti-Gyabaah J, Telari K, Dunne L, Moore JC. 2008. Preparative asymmetric synthesis of 4,4-dimethoxytetrahydro-2H-pyran-3-ol with a ketone reductase and in situ cofactor recycling using glucose dehydrogenase. Org Process Res Dev 12:584-588.

Kumar I, Bhide SR, Rode CV. 2007. Asymmetric synthesis of a 3,4-substituted pyrrolidine by L-proline catalyzed direct enolexo aldolization. Tetrahedron-Asymmetry 18:1210-1216.

Liese A, Zelinski T, Kula MR, Kierkels H, Karutz M, Kragl U, Wandrey C. 1998. A novel reactor concept for the enzymatic reduction of poorly soluble ketones. J Mol Catal B-Enzym 4:91-99.

Lilius EM, Multanen VM, Toivonen V. 1979. Quantitative extraction and estimation of intracellular nicotinamide nucleotides of *Escherichia coli*. Anal Biochem 99:22-27.

Menzel A, Werner H, Altenbuchner J, Gröger H. 2004. From enzymes to "designer bugs" in reductive amination: A new process for the synthesis of L-*tert*-leucine using a whole cell-catalyst. Eng Life Sci 4:573-576.

Moore JC, Pollard DJ, Kosjek B, Devine PN. 2007. Advances in the enzymatic reduction of ketones. Accounts Chem Res 40:1412-1419.

Patel RN. 2006. Biocatalysis: Synthesis of chiral intermediates for drugs. Curr Opin Drug Discov Dev 9:741-764.

Patel RN, Goswami A, Chu L, Donovan MJ, Nanduri V, Goldberg S, Johnston R, Siva PJ, Nielsen B, Fan JY and others. 2004. Enantioselective microbial reduction of substituted acetophenones. Tetrahedron-Asymmetry 15:1247-1258.

Pesti JA, DiCosimo R. 2003. Recent progress in enzymatic resolution and desymmetrization of pharmaceuticals and their intermediates. Curr Opin Drug Discov Dev 6:884-901.

Pollard D, Truppo M, Pollard J, Chen CY, Moore J. 2006. Effective synthesis of *(S)*-3,5-bistrifluoromethylphenyl ethanol by asymmetric enzymatic reduction. Tetrahedron-Asymmetry 17:554-559.

Richter N, Neumann M, Liese A, Wohlgemuth R, Eggert T, Hummel W. 2009. Characterisation of a Recombinant NADP-dependent glycerol dehydrogenase from *Gluconobacter oxydans* and its application in the production of L-glyceraldehyde. Chembiochem 10:1888-96.

Röthig TR, Kulbe KD, Bückmann F, Carrea G. 1990. Continuous coenzyme-dependent stereoselective

synthesis of sulcatol by alcohol-dehydrogenase. Biotechnol Letters 12:353-356.

Rouhi AM. 2004. Chiral chemistry. Chem Eng News 82:47-+.

Schmid CR, Bryant JD. 1995. D-*(R)*-Glyceraldehyde Acetonide - (1,3-Dioxolane-4-Carboxaldehyde, 2,2-Dimethyl-, *(R)*-). Organic Syntheses 72:6-13.

Schroer K, Mackfeld U, Tana IAW, Wandrey C, Heuser F, Bringer-Meyer S, Weckbecker A, Hummel W, Daußmann T, Pfaller R and others. 2007. Continuous asymmetric ketone reduction processes with recombinant *Escherichia coli*. J Biotechnol 132:438-444.

Schubert T, Hummel W, Kula MR, Müller M. 2001. Enantioselective synthesis of both enantiomers of various propargylic alcohols by use of two oxidoreductases. Eur J Org Chem 4181-4187.

Stewart JD. 2001. Dehydrogenases and transaminases in asymmetric synthesis. Curr Opin Chem Biol 5:120-129.

Uzura A, Nomoto F, Sakoda A, Nishimoto Y, Kataoka M, Shimizu S. 2009. Stereoselective synthesis of *(R)*-3-quinuclidinol through asymmetric reduction of 3-quinuclidinone with 3-quinuclidinone reductase of *Rhodotorula rubra*. Appl Microbiol Biotechnol 83:617-626.

Vasic-Racki D, Jonas M, Wandrey C, Hummel W, Kula MR. 1989. Continuous *(R)*-mandelic acid production in an enzyme membrane reactor. Appl Microbiol Biotechnol 31:215-222.

Walton AZ, Stewart JD. 2004. Understanding and improving NADPH-dependent reactions by nongrowing *Escherichia coli* cells. Biotechnol Prog 20:403-411.

Weckbecker A. 2005. Entwicklung von Ganzzellbiokatalysatoren zur Synthese von chiralen Alkoholen: Heinrich-Heine Universität Düsseldorf.

Weckbecker A, Gröger H, Hummel W. 2010. Regeneration of nicotinamide coenzymes: Principles and applications for the synthesis of chiral compounds. Adv Biochem Engin/ Biotechnol.

Weckbecker A, Hummel W. 2004. Improved synthesis of chiral alcohols with *Escherichia coli* cells co-expressing pyridine nucleotide transhydrogenase, $NADP^+$-dependent alcohol dehydrogenase and NAD^+-dependent formate dehydrogenase. Biotechnol Lett 26:1739-1744.

Weckbecker A, Hummel W. 2005. Glucose dehydrogenase for the regeneration of NADPH and NADH. In: Barredo JL, editor. Meth in Biotechnology. Totowa, NJ: Humana Press Inc. p 225-237.

Wills M, Hannedouche J. 2002. New methodology for the asymmetric reduction of ketones. Curr Opin Drug Discov Dev 5:881-891.

6 PREPARATIVE PRODUCTION OF L-GLYCERALDEHYDE

6.1 PREPARATIVE BIOCATALYTIC PRODUCTION AND ISOLATION OF L-GLYCERALDEHYDE

M. Neumann, N. Richter, T. Eggert, W. Hummel,
R. Wohlgemuth, A. Liese

Submitted

Preparative biocatalytic production and isolation of L-Glyceraldehyde

M. Neumann[1], N. Richter[2], T. Eggert[2], W. Hummel[3], R. Wohlgemuth[4], A. Liese[1]*

[1]Institute of Technical Biocatalysis, Hamburg University of Technology, 21073 Hamburg, Germany
[2]evocatal GmbH, 40225 Düsseldorf, Germany
[3] Institute of Molecular Enzyme Technology, Heinrich-Heine University Düsseldorf, Research Center Jülich, 52426 Jülich, Germany
[4]Research Specialties, Sigma-Aldrich Chemie GmbH, Buchs CH-9471, Switzerland

* corresponding author. Phone: +49-40-42878-3218, fax: +49-40-42878-2127
E-mail: liese@tuhh.de

A process for the biocatalytical production of L-glyceraldehyde has been developed. The catalytic system was based on NADPH-dependent Glycerol dehydrogenase Gox1615 from Gluconobacter oxydans coupled to glucose dehydrogenase for cofactor regeneration. In gram-scale productivities of 6.2 g L^{-1} d^{-1} and product concentrations of 4.3 g L^{-1} were reached. For downstream processing the establishment of a separation routine for an aqueous mixture of glycerol, glyceraldehyde, glucose and gluconic acid was necessary. Crude product was processed by centrifugation, preparative column chromatography and evaporation to yield L-glyceraldehyde with a purity of 85% and an ee of 94%.

Introduction

The synthesis of optically active compounds for the chemical or pharmaceutical industry is usually based on low-molecular building blocks with several functional groups [1]. Especially chiral alcohols are versatile intermediates for further transformations to valuable products. Synthetic routes to these compounds are usually based on chemical or biocatalytic reactions, like reduction of carbonyl moieties, oxidation of hydrocarbons or alcohols or hydrolysis of ester bonds [2].

Ketoses, aldoses or sugar acids are ideal candidates for the preparation of enantiopure products. Regioselective enzymatic redox reactions enable the direct conversion of carbonhydrates without complicated and cost intensive protection steps. For example, oxidoreductases catalyze stereoselective redox reactions with high chemo-, regio- and stereoselectivity [3]. The drawback of expensive nicotinamide cofactors associated with oxidoreductases in industrial processes can be overcome by effective regeneration systems [4].

A key chiral sugar molecule is L- and D-glyceraldehyde (GA). Both D- and L-enantiomers are ideal candidates as starting material for the preparation of complex structures. The preparative synthesis of optical pure GA was first published in 1934 [5]. It is based on a three step chemical synthesis starting from mannitol, which also comprises the chiral information. The oxidative cleavage of the hexose with sodium periodate demands the application of acetale protecting groups. As only D-mannitol is available from the chiral pool of nature, only the D-GA can be produced by this method at large scale. L-mannitol on the other side has to be synthesized by different multistep synthetic routes. One route starts from L-arabinose [6], but industrial production of L-GA by this lengthy route is not an economic and industrially viable option. A shorter route to L-glyceraldehyde starts from L-ascorbic acid, but the need to protect adjacent α - and β-hydroxy-groups despite the use of mild and rather selective oxidants for the conversion of the primary alcohol group in mutlifunctionalized alcohols to aldehydes leads to stoichiometric waste, many synthetic steps and significant organic solvent usage.

Few biocatalytic routes to enantiopure GA are described in literature. Most common is the selective oxidation of glycerol with oxidases or oxidoreductases. The galactose oxidase from *Dactylium dendroides* [EC 1.1.3.9] is able to oxidize aliphatic and aromatic primary alcohols like 1,2-propanediol, glycerol, dihydroxyacetone, hydroxypyruvate, hydroxyacetone, glycolaldehyde or hydroxyacetophenone stereoselectively [7]. The enzyme shows a very low activity towards glycerol and is only available as wild type enzyme. Another example is the use of methanol dehydrogenase from *Methylobacterium organophilum*

Tab. 1. Kinetic parameters.

GA reduction (Gox1615)		Glucose oxidation (GDH)	
v_{max}	50.1 ± 5.2 U/mL	v_{max}	111 ± 5.8 U/mL
$K_{m,GA}$	0.45 ± 0.37 mM	$K_{m,Glucose}$	8.8 ± 3.0 mM
$K_{m,NADPH}$	1.2 ± 2.4 µM	$K_{m,NADP}$	5.5 ± 1.8 µM
$K_{i,GLY}$	0.69 ± 0.83 mM		
$K_{i,GA}$	738 ± 261 mM		

[EC 1.1.99.8] [8]. The isolated enzyme needs an artificial electron carrier like phenazine methosulfate which can be regenerated by molecular oxygen. But in analogy to galactose oxidase, methanol dehydrogenase shows only low activity towards glycerol. Furthermore, no stereoselectivity is noted in literature. At last *horse liver* alcohol dehydrogenase [EC 1.1.1.1] can be applied for the oxidation of glycerol to GA [9]. In this case, the enzyme is coupled with an aldehyde dehydrogenase for the direct further oxidation of GA to glyceric acid.

We recently reported the characterization of a recombinant NADPH-dependent glycerol dehydrogenase from *Gluconobacter oxydans* [EC 1.1.1.72] and the potential of this enzyme for the production of L-GA [10]. In this contribution we describe the corresponding development of a biocatalytic process, including kinetic characterization of the used enzymes, optimization of reaction conditions and product separation.

Results and Discussion

The glycerol dehydrogenase Gox1615 [EC 1.1.1.72] from *Gluconobacter oxydans* is able to produce D-GA with high stereoselectivity [10]. The NADPH-dependent enzyme was cloned and overexpressed into *Escherichia coli* BL21(DE3) and is therefore available in recombinant form.

Kinetic analysis

The development of biocatalytic processes requires a deep knowledge of the kinetic properties of the considered enzymes. Therefore the influence of all reaction compounds on the activity of the Gox1615 and the cofactor regeneration enzyme glucose dehydrogenase was determined. The kinetic analysis was performed in initial rate measurements by monitoring the cofactor concentration at 340 nm.

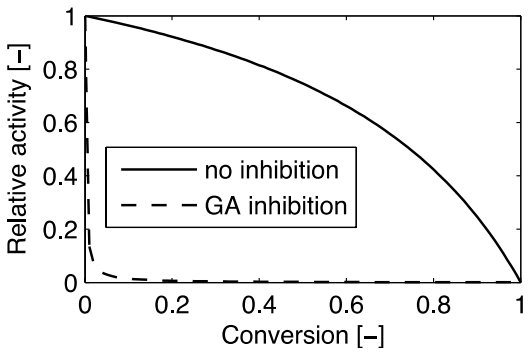

Fig. 1. Relative rate versus conversion with no inhibition or with inhibition by GA.

The activity of Gox1615 for the oxidation of glycerol is quite low. The determined v_{max} is 0.92 ± 0.12 U/mL of crude cell extract (0.4 g/mL). The affinity constant of the substrate glycerol $K_{m,GLY}$ is about 1.04 ± 0.36 M, for the cofactor $NADP^+$ a $K_{m,NADP}$ of 0.035 ± 0.008 mM was found. Unfortunately, the product D-GA shows a strong impact on the activity of the glycerol oxidation. The determined inhibition constant $K_{i,GA}$ was 1.07 ± 0.37 mM. For an industrial production the ration of K_i to K_m can be used to decide, whether a process would be economic on a large scale. At a ratio of $K_i/K_m > 1$, a reaction will proceed efficiently [11]. In this case the value of $K_{i,GA}/K_{m,GLY}$ is equal to 0.001. For visualization, the relative rate of the enzyme can be plotted versus the conversion (fig. 1).

With the assumption of a reaction with 2 M glycerol, 1 mM $NADP^+$ and no inhibition by the product D-GA, the relative rate would decrease slowly due to reduction of substrate concentration (solid line). But as a result of strong inhibition by the product, the relative activity decreases much stronger. At a conversion of 10%, the remaining activity is below 2%.

In comparison to the oxidation of glycerol, Gox1615 shows a much higher activity for the reverse direction. The reduction of D-GA is 50 times faster than the oxidation of glycerol. Therefore, another approach for the production of optical pure GA becomes beneficial: kinetic resolution of *rac*-GA to glycerol and L-GA. This leads to higher cost for the starting material *rac*-GA and limitation to a maximal conversion of 50% due to the nature of a kinetic resolution, but compared to chemical routes this single step procedure would still be competitive.

The reduction of *rac*-GA with Gox1615 requires NADPH as cofactor, so that an effective regeneration protocol is needed. For this, an enzyme-coupled approach utilizing glucose dehydrogenase was chosen. The required cosubstrate glucose is cheap and highly soluble in aqueous buffer systems. Furthermore, in aqueous solutions the coproduct glucono-γ-lactone is irreversibly hydrolyzed to gluconic acid, leading to a positive impact on the equilibrium and a maximization of the conversion. The enzyme is commercially available in recombinant form (evocatal, evo-1.1.060) and is therefore suitable for industrial applications.

The reaction system consists of three basic reactions, reduction of D-GA, oxidation of glycerol (back reaction) and oxidation of glucose (cofactor regeneration). Kinetic parameters of GA reduction and glucose oxidation were determined as follows (Tab. 1):

With this information batch experiments were conducted. Because of lower costs the oxidized cofactor $NADP^+$ was used. Due to effective cofactor regeneration, NADPH is formed directly to provide the enzyme with redox equivalents.

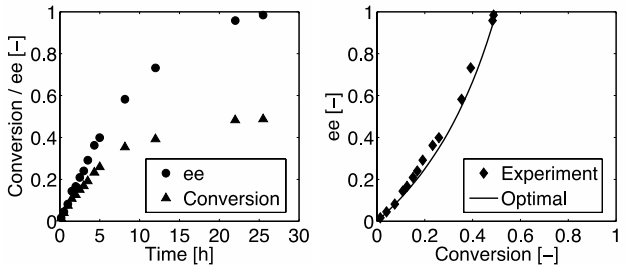

Fig. 2. Time course for conversion and *ee* (left). Enantiomeric excess as function of conversion (right).

The oxidation of glucose to gluconic acid leads to a pH shift. In experiments for the kinetic analysis of the system, buffer was used to achieve a constant value. On production scale high buffer salt concentration would be necessary and consequently cause higher costs and a more complicated product reprocessing. A technical approach to overcome this problem is the application of an automatic titration in combination with no or less buffer.

Racemic resolution of GA was accomplished in potassium phosphate buffer system (100 mM, pH 7) with *rac*-GA (150 mM), glucose (200 mM), ammonium sulfate (200 mM) and $NADP^+$ (1 mM). The pH was adjusted by controlled addition of potassium hydroxide solution (2 M). Conversion was followed by HPLC-determination of glycerol and GA concentrations. The enantiomeric excess of remaining L-GA was determined after derivation by gas chromatography.

In the reaction a conversion of 49% with an enantiomeric excess of 98% was reached after a reaction time of 25.5 hours (fig. 2). This corresponds to an E value of > 100 so that the enzyme shows a very good enantioselectivity. Regarding ee as function of conversion an almost ideal course was detected (fig. 2). Based on this feasibility study the reaction parameters were adapted for large scale application.

Preparative production of L-GA

For the preparative production of L-GA suitable reaction conditions have to be selected. For a maximal efficiency and cost-effectiveness the application of starting reagents and chemicals should be minimized.

The highest substrate concentration is limited by the solubility of *rac*-GA in the aqueous reaction medium. In literature a value of 30 g/L (0.33 M) is described [12], but by prolonged stirring higher values of > 10 M are possible. The reason for this phenomenon is most likely the high stability of the GA dimer in solid state and therefore the slow formation of the soluble monomer. Furthermore, glucose as cosubstrate has a solubility of 470 g/L (2.6 M), which limits the overall reaction to this value.

Standard reaction mixtures for the operation of glycerol dehydrogenases usually contain ammonia to increase the activity and stability of the enzyme. For Gox1615 both parameters were tested. The addition of up to 200 mM ammonium sulfate leads to an increase in activity of about 40%. Also the long time stability (reaction time > one week) can be enhanced significantly. But higher ammonium contents also lead to the occurence of side reactions with GA [13] and the formation of an intensive yellow color of the reaction mixture.

Preparative production of L-GA was accomplished in a batch reaction with pH regulation. *Rac*-GA dimer (10.0 g, 111 mmol) and glucose monohydrate (13.2 g, 66.6 mmol) were dissolved in triethanolamine buffer (40 mL, 100 mM, pH 7). After 16 hours a homogenous solution was obtained. The resulting yellowish solution was charged with Gox1615 crude cell extract (25 mL, 1.25 kU), glucose dehydrogenase (4 mL, 0.44 U) and $NADP^+$ (32 mg, 43 µmol). During the reaction progress the pH was constantly adjusted to a value of 7.0 by titration with potassium hydroxide (2.0 M). After 10 hours a final conversion of 57% with an ee of 96% was reached, corresponding to 4.3 g L-GA in solution. Precipitated proteins were centrifuged at 10000 rpm for 30 minutes. Alternatively, microfiltration can be applied for the separation of the precipitate.

Downstream Processing

For the isolation of the desired product L-GA the separation from aqueous solutions containing at the same time glycerol, glucose and gluconic acid is necessary. Due to unfavorable properties like very high boiling point, high polarity and structural similarity between the separate compounds suitable methods are limited. Furthermore, GA in solution is structural unstable. Epimerization of this simple aldose to the corresponding ketose, the Lobry de Bruyn-Alberda van Ekenstein transformation [14], may occur under certain condition forming dihydroxyacetone (DHA) or leading to racemization.

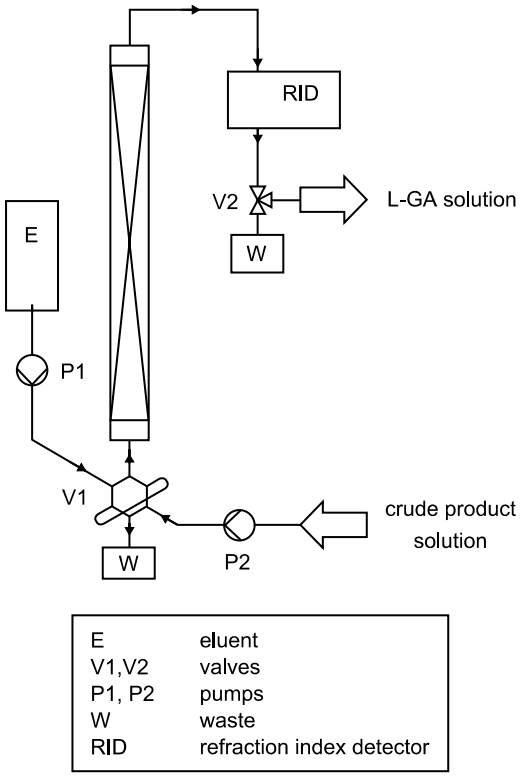

Fig. 3. Scheme of the automated chromatography system.

Different approaches were tested for the separation of L-GA. Extraction of aqueous media with organic solvents is an established tool in the biocatalytic production of chemicals and is easily scaleable. Ethyl acetate, butanone, tetrahydrofurane, tert-butyl methyl ester, dichloromethane, diethylether, toluene and isohexane were assayed by contacting with GA, glycerol or DHA-containing aqueous solutions. The change in concentration in the aqueous phase was in the range of measurement precision. An alternative route to the separation of the distinct compounds is preparative liquid chromatography. Silica gel as

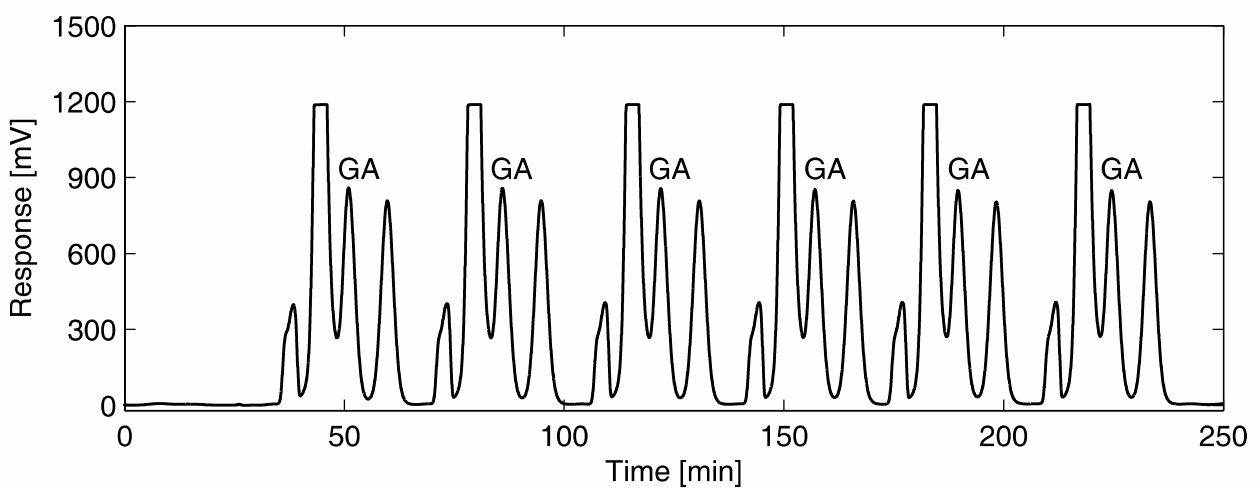

Fig. 4. RID response during the successive injection of crude L-GA.

stationary phase was tested with different eluents including water, trifluoro acetic acid, ethanol and 2-propanol in different compositions. No sufficient separation performance could be detected, meaning no difference in retention time or low solubility of crude mixture in the eluent, respectively.

To separate sugar derivatives by liquid chromatography ion exchange resins are used quite frequently. Based on the material from the analytical HPLC column, which is able to separate GA from the other compounds, a similar resin was chosen as the stationary phase. DOWEX 50WX8 (200-400 mesh) is based on a polystyrene divinylbenzene copolymer functionalized with sulfonic acid groups. By applying this resin in preparative column chromatography a successful separation of GA was accomplished.

Performing a single chromatography run, only limited amount of crude GA can be separated. Therefore an automated design of the downstream processing would be beneficial (fig. 3). A chromatography glass column (100 cm × 5 cm ø) was packed with 1.5 kg ion exchange resin and 5 mM trifluoroacetic acid at a flow rate of 1.15 L/h was used as mobile phase. Automated injection and peak collection was accomplished with valves and a fraction collector. Refractive index detection was applied for the monitoring of the separation performance.

The obtained supernatant after the biocatalysis step (115 mL) was subjected to the automated preparative liquid chromatography. For each run the column was loaded with 5 mL of the reaction mixture corresponding to 0.2 g L-GA. Under the established conditions the L-GA peak eluted from 48.5 to 56 min, but it was collected in the range of 49-54 min because of its partial overlap with excess glucose and the coproduct gluconic acid. To reduce purification time injection of the reaction mixture was done in sequence every 35 min (fig 4).

The collected eluate (2 L) was evaporated (18 mbar, 40°C) and finally dried in vacuum (0.02 mbar). L-GA product was yielded as odorless viscous colorless oil (4.24 g, 85%). HPLC-analysis of the product showed no glycerol and only traces of glucose and gluconic acid. About 7% of GA was isomerized to DHA, probably due to the acidic eluent and to high temperatures during evaporation. As the chromatographic separation is also possible with water as eluent, this drawback could be circumvented. The enantiomeric excess was equal to 94% which should also be optimized by changing the product separation conditions.

Further optimization of the downstream processing and product recovery part of the process development in the direction of reducing the crude L-GA to the two components glycerol and L-GA as a 50/50 mixture and increasing product yield per unit amount of the stationary phase in chromatography will allow the use of simulated moving bed chromatography at large scale.

Experimental Section

General. Chemicals were purchased from Sigma-Aldrich Inc., Buchs, Switzerland. The glycerol dehydrogenase Gox1615 (evo-1.1.190) and glucose dehydrogenase (GDH) (evo-1.1.060) are commercially available from evocatal GmbH, Düsseldorf, Germany.

Kinetic analysis. The activity assays for the kinetic analysis of Gox1615 and GDH were performed by photometric monitoring of NADPH-formation or consumption at 340 nm. The total volume of the single assays was 1 mL, consisting of potassium phosphate buffer (0.1 M, pH 7.0), substrate, cofactor and optionally other reaction compounds like product for inhibition studies. The activity was calculated from the absorbance change in one minute.

Analytics. The concentrations of GA and glycerol were determined by using an Agilent 1100 HPLC-system equipped with the organic acid resin column (300 x 8 mm, CS-Chromatographie Service) with 5 mM trifluoroacetic acid (0.7 ml/min, 25°C) and refractive index detection (RID). The enantiomeric ratio of GA was determined after derivatization with acetic anhydride and pyridine (100 µL sample, 300 µL ethyl acetate, 100 µl acetic anhydride, 10 µL pyridine, 15 min incubation at ambient temperature) by using a HP 6890 GC-system equipped with a Varian CP-Chirasil.Dex CB column (25 m x 0.32 mm) and hydrogen as carrier gas.

Batch reactions. Batch reactions were carried out as stirred tank reactions in flasks with a thermo-jacket. *Rac*-GA was first dissolved in water inside the reactor at 35 °C, while the reaction was performed at 25°C. Glucose and $NADP^+$ were added in solid form to the *rac*-GA solution. The reaction was started by addition of crude cell extracts containing Gox1615 and GDH. A pH-shift induced by the formation of the coproduct gluconic acid was regulated by automated addition of 2 M potassium hydroxide with a pH-stat (Metrohm Dosimat 665, Metrohm Impulsomat 614 and Metrohm pH-meter 632). For the monitoring of the conversion, samples for HPLC-analysis were taken periodically or the consumption of potassium hydroxide was observed, respectively.

Product separation. The separation of glyceraldehyde from the reaction mixture was achieved by automated preparative column chromatography using cation exchange resin DOWEX® 50WX8 (200-400 mesh). This resin is based on a styrene-divinylbenzene matrix functionalized with sulfonic acid groups. The chromatographic setup consists of an Amersham Bioscience P-500 pump, a Gilson 231 sample injection system with Gilson Dilutor 401 for automated sample charging and product collection and a Merck differential refractometer RI-71 for compound detection. Detector output was monitored with the software SCPA Chromstar 6.3.

Acknowledgements

This project was supported by funds from the Deutsche Bundesstiftung Umwelt (DBU), project number Az13194. We would like to thank Ruslan Yuyev for helpful discussions and support.

References

(1) (a) Santaniello, E.; Ferraboschi, P.; Grisenti, P.; Manzocchi, A. Chem. Rev. **1992** *92*, 1071.
(b) Burk, M. J.; Gross, M. F.; Harper, T. G. P.; Kalberg, C. S.; Lee, J. R.; Martinez, J. P. Pure & Appl. Chem. **1996**, *68*, 37.
(c) Hilterhaus, L.; Liese, A. Adv. Biochem. Engin./Biotechnol. **2007**, *105*, 133.

(2) (a) Liese, A.; Seelbach, C.; Wandrey, C. Industrial biotransformations, 2nd ed.; Wiley-VCH, **2006**.
(b) Goldberg, K.; Schroer, K.; Lütz, S.; Liese, A. Appl. Microbiol. Biotechnol. **2007**, *76*, 237.

(3) Wandrey, C. Chem. Rec. **2004**, *4*, 254.

(4) (a) Hummel, W. Trends Biotechnol. **1999**, *17*, 487.
(b) Weckbecker, A., Gröger, H., Hummel, W. Adv. Biochem. Engin./ Biotechnol. **2010**, early view, doi: 10.1007/10_2009_55.

(5) Fisher, H. O. L.; Baer E. Helv. Chim. Acta **1934**, *17*, 622.

(6) Baer, E.; Fischer, H. O. L. J. Am. Chem. Soc. **1939**, *61*, 761.

(7) Klibanov, A. M.; Alberti, B. N.; Marletta, M. A. Biochem. Biophys. Res. Commun. **1982**, *108*, 804.

(8) Wolf, H. J. U. S. Patent 4,353,987, **1982**.

(9) Wong, C.-H.; Matos, J. R. J. Org. Chem. **1985**, *50*, 1992.

(10) (a) Richter, N.; Neumann, M.; Liese, A.; Wohlgemuth, R.; Eggert, T.; Hummel, W. ChemBioChem **2009**, *10*, 1888.
(b) Richter, N.; Neumann, M.; Liese, A.; Wohlgemuth, R.; Weckbecker, A.; Eggert, T.; Hummel, W. Biotechnol Bioeng. **2010**, early view, doi: 10.1002/bit.22714.

(11) Lee, L. G., Whitesides, G. M. J. Am. Chem. Soc. **1985**, *107*, 6999.

(12) O'Neil, M. J.; Heckelman, P. E.; Koch, C. B.; Roman, K. J. The Merck Index, 14th ed.; Merck & Co., Inc, **2006**.

(13) Weber, A. L. J. Mol. Evol. **1985**, *21*, 351.

(14) Angyal, S. J. Top. Curr. Chem. **2001**, *215*, 1.

7 DISCUSSION

The application of biocatalytic approaches for the production of valuable chiral building blocks has gained increasing interest over the past few decades. Therefore, the demand for novel catalysts is very high, especially in the field of asymmetric synthesis. Based on this demand, the intention of this thesis was to identify and characterise novel oxidoreductases that can be applied in the production of chiral building blocks. A schematic overview of all steps that were performed in this thesis, from genome mining to process development, is shown in Figure 7.1.

The following chapter outlines a classification of the accomplished work in the general contents of this thesis and summarises the selected strategy of enzyme identification.

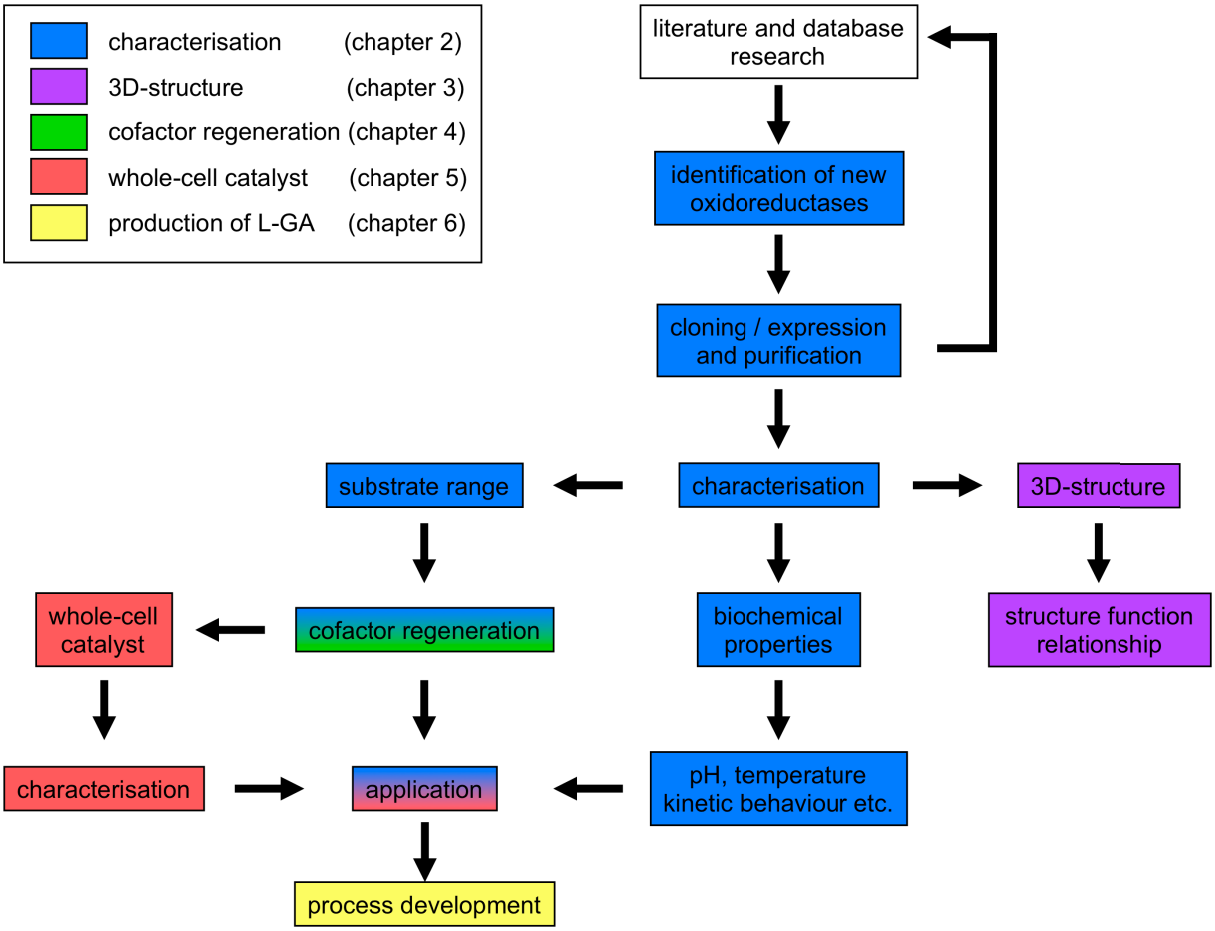

Fig. 7.1. Schematic overview of the overall strategy of this thesis. The colour code indicates the chapter where the corresponding results are shown.

7.1 IDENTIFICATION OF NEW OXIDOREDUCTASES - STRATEGIES AND CHALLENGES

Oxidoreductases comprise a large class of enzymes that catalyse various reactions of biotechnological interest, such as the reduction and oxidation of carbonyl and hydroxy moieties and the reduction of olefinic double bonds. This class of enzymes is ubiquitously distributed and has been found in approximately 4,170 different organisms throughout all kingdoms of life (BRENDA, www.brenda-enzymes.org). Among the oxidoreductases are members of a variety of different structural families. According to the fact that the asymmetric reduction of prochiral ketones, as well as the selective oxidation of alcohols, are of major interest within organic synthesis, these enzyme class has been extensively studied[1, 9, 23-27, 29]. Moreover, the demand for new oxidoreductases that are capable of catalysing asymmetric reactions of interest is growing tremendously.

There are multiple potential strategies available, as introduced in Section 1.4, to identify new enzymes. Principally, one can distinguish between sequence-based[108] and activity-based[30, 35, 103] methods. The activity-based approach enables the identification of new enzymes, independent from the sequence identity to other enzymes that catalyse the desired reaction. However, due to the use of wild-type strains, there are also some limitations to this approach, such as the time consuming subsequent identification of the responsible gene sequence. Even if activity-based screening is still one of the most powerful tools for identifying new biocatalysts, in this thesis, sequence-based approaches were mainly applied to identify new oxidoreductases. The major benefit of this method is the knowledge of the corresponding gene sequence, which provides easier access to the recombinant catalyst.

Based on the broad distribution of oxidoreductases, an enormous number of genes are annotated as putative oxidoreductases in databases, such as GenBank from NCBI (www.ncbi.nlm.nih.gov) and EMBL (www.ebi.ac.uk/embl). To identify new oxidoreductases, gene sequences of enzymes that catalyse related reactions are required as a starting point.

In this thesis, the sequence of GLD1 (DQ_422037), an $NADP^+$-dependent GlyDH from the mould *Hypocrea jecorina*, was chosen for DNA sequence analysis[193]. The amino acid sequence of GLD1 was used because it has been previously described to catalyse the conversion of D– and L-glyceraldehyde to glycerol (Fig. 7.2).

Fig. 7.2. General reaction scheme of the NADPH-dependent reduction catalysed by GLD1.

The described reaction is of major interest because it enables the production of glyceraldehyde, and both glyceraldehyde enantiomers are ideal chiral building blocks for the synthesis of complex compounds (Section 1.1)[13-16]. However, GLD1 is able to convert both enantiomers, as reflected by the similar K_M values (0.9 mM)[193], demonstrating that the reduction is catalysed in a non-stereoselective manner. In an attempt to identify new oxidoreductases that catalyse the reaction in a stereoselective manner, *in silico* screening of sequenced genomes based on the sequence of GLD1 was performed. The strategy applied is outlined in Figure 7.3.

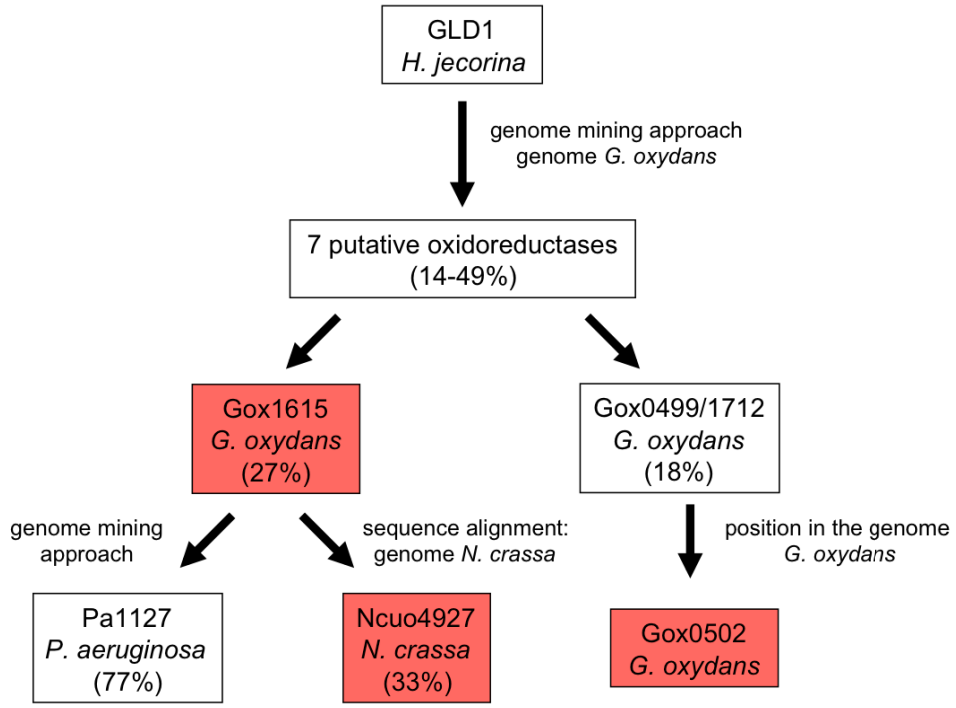

Fig. 7.3. Strategy employed to identify new oxidoreductases.

Due to the fact that acetic acid bacteria, such as *G. oxydans*, display a high capability to oxidise and reduce a variety of different compounds, the screening was restricted to the genome of *G. oxydans* 621 H, which was recently sequenced by Prust and co-workers[194] in a first approach.

The *in silico* screening uncovered seven genes that encode putative oxidoreductases that display considerable amino acid sequence similarities (14-49%) to GLD1. The corresponding genes were then subsequently cloned. Five of them were successfully expressed in *E. coli* and consequently screened for the desired activity. One of the

most promising enzymes was Gox1615, which exhibited high activity in the reduction of *rac*-glyceraldehyde in a preliminary activity screening. More detailed studies revealed that Gox1615 catalyses the reduction of glyceraldehyde in a stereoselective way. The reduction of the D-enantiomer is highly preferred by the enzyme (23-fold). This finding indicated that we successfully indentified a novel prokaryotic enzyme that catalyses the same reaction in a stereoselective manner, based on only 27% amino acid sequence identity with the eukaryotic non-selective enzyme. However, because the oxidation of glycerol is only catalysed with very low activity (0.2 U/mg), a second round of *in silico* screening was performed. This time, the amino acid sequence of Gox1615 was used to further identify similar enantioselective oxidoreductases that are also capable of catalysing the oxidation. As a result, two more enzymes were identified in the genome of *Neurospora crassa* (Ncuo4927) and *Pseudomonas aeruginosa* (Pa1127). The identified enzymes were then successfully cloned and expressed in *E. coli*.

Fig. 7.4. Reaction scheme of the NAD^+-dependent oxidation of glyceraldehyde to the corresponding acid as catalysed by aldehyde dehydrogenases (AldDH).

Another interesting strategy for the identification of new oxidoreductases was based on the position of the Gox0499 and Gox1712 genes in the *G. oxydans* genome. Both enzymes were annotated as aldehyde dehydrogenases (AldDH), which catalyse the oxidation of glyceraldehyde to the corresponding acid (Fig. 7.4). Due to the fact that the corresponding aldehyde must be produced by another enzyme whose gene is potentially located in the same operon, one putative oxidoreductase located in close proximity to the Gox0499 encoding gene was selected for further studies (Gox0502).
In general, the applied sequence-based approach led to the identification of a large number of different putative oxidoreductases. The main advantage of this method is that because gene sequences were available, the cloning of the corresponding genes into suitable expression vectors could be easily performed. Nevertheless, there were also limitations, such as the functional expression of the corresponding enzymes and screening for catalyst activity. However, the identification of a substrate accepted by the catalyst can be extensive or even impossible because a related protein sequence is no guarantee of similar or even related activity. Notably, compared to the classical approach of screening wild-type strains followed by an extensive identification of the

gene responsible for the desired activity, the *in silico*-screening strategy applied in this thesis is superior.

In summary, among all of the putative oxidoreductases identified, Gox1615 (glycerol dehydrogenase; GlyDH) and Gox0502 (enoate reductase, EnR) from *G. oxydans* and Ncuo4923 (carbonyl reductase; NcCR) from *N. crassa* were the most promising biocatalysts with respect to the reactions that they catalyse (Fig. 7.3, marked in red). Therefore, the biochemical characterisations of the three identified oxidoreductases and the evaluation for their applications were the focus of this thesis. General information in regard to the origin, catalysed reaction and classification of the studied oxidoreductases is summarised in Table 7.1.

Table 7.1. Overview of the general properties of the oxidoreductases investigated in this thesis.

Gene name	Origin	Reaction catalysed	Subfamily	Structure
Gox1615[194]	*G. oxydans*	Reduction of aldehydes oxidation of sugar alcohols	Glycerol dehydrogenase (GlyDH; EC 1.1.1.72)	AKR-family
Ncuo4923[195]	*N. crassa*	Reduction of α- and β-ketoesters	Carbonyl reductase (CR; EC 1.1.1.184)	AKR-family
Gox0502[194]	*G. oxydans*	Reduction of C=C double bonds	Enoate reductase (EnR; EC 1.3.1.31)	TIM barrel family

7.2 NEW ENZYMATIC ROUTES TO CHIRAL BUILDING BLOCKS

Aside from the biochemical characterisation of the identified oxidoreductases, an additional focus of this work was to analyse their potential for applications in the asymmetric synthesis of chiral building blocks. Based on the isolated enzymes, the range of enzymatically accessible chiral building blocks should be expanded. Therefore, the identified oxidoreductases were evaluated according to their ability to catalyse reactions, which led to valuable chiral synthons of biotechnological interest.

Figure 7.5 summarises the determined reactions catalysed by the identified glycerol dehydrogenase (GlyDH), enoate reductase (EnR) and carbonyl reductase (CR). In general, four different reactions can be performed using these three enzymes:

1. Asymmetric reduction of ketones, especially α- and β-ketoesters by CR from *N. crassa* (NcCR) (Section 2.3, red box).

2. Selective reduction of a variety of different activated alkenes by EnR from *G. oxydans* (Section 2.4, blue box).
3. Reduction of different aldehydes by GlyDH from *G. oxydans* (Section 2.1, yellow box).
4. Chemo-, regio- and enantioselective oxidation of various sugar alcohols by GlyDH (Section 2.2, purple box).

All types of reactions and biocatalysts have been described in this thesis and will be discussed in the following chapters.

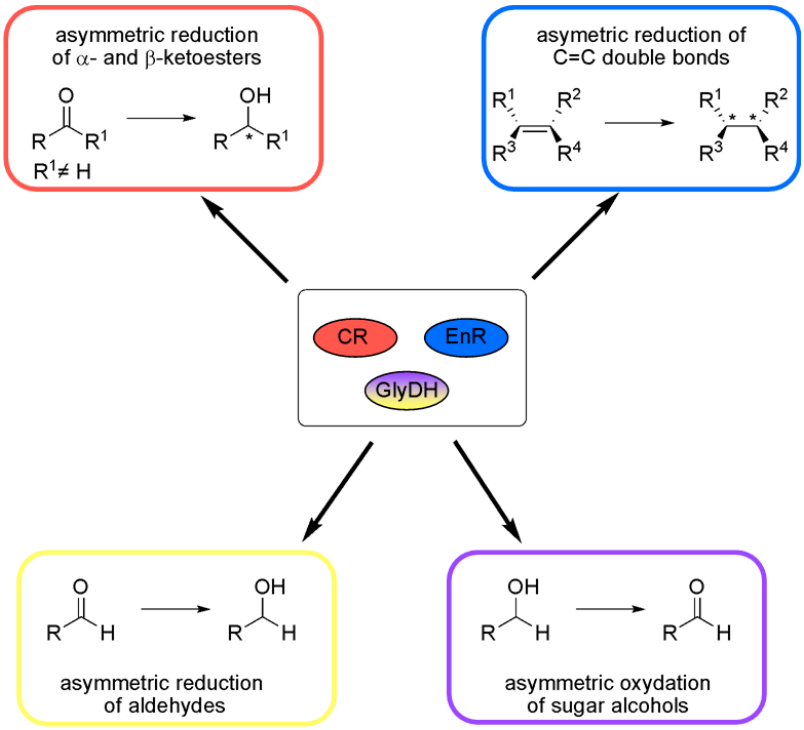

Fig. 7.5. Different reactions catalysed by carbonyl reductase (CR), enoate reductase (EnR) and glycerol dehydrogenase (GlyDH).

7.3 SELECTIVE ALDEHYDE REDUCTION USING GLYCEROL DEHYDROGENASE FROM *GLUCONOBACTER OXYDANS*

GlyDHs (EC 1.1.1.72) are $NADP^+$-dependent enzymes that catalyse the reduction of glyceraldehyde to glycerol. GlyDHs are common in moulds and filamentous fungi and can also be obtained from mammalian tissues[193, 196-198]. GlyDH from *G. oxydans* is a monomeric protein consisting of 332 amino acids, with a molecular mass of 37.213 kDa. Its amino acid sequence identifies GlyDH as a member of the aldo-keto reductase (AKR) family (Section 2.1).

A comparison of the properties of the GlyDH from *G. oxydans* with other described GlyDHs from different organisms[193, 196, 198] in regards to physical parameters (e.g., molecular weight and quaternary structure) was performed in Section 2.1.
A comparison of the regio- and enantioselectivities of different GlyDHs is given in Table 7.2. The most interesting feature of the identified GlyDH is its high regio- and enantioselectivity in contrast to previously described GlyDHs. A comparative analysis of the ratio between dihydroxyacetone (DHA; ketone) and glyceraldehyde (GA; aldehyde) reduction revealed that GlyDH from *G. oxydans* exhibits the highest regioselectivity. This enzyme prefers the reduction of glyceraldehyde over dihydroxyacetone, showing only 1% of the activity observed with D-glyceraldehyde when dihydroxyacetone was used as a substrate.

Table 7.2. Comparison of the regio- and enantioselectivities of the GlyDHs from *G. oxydans*, *H. jecorina, N. crassa* and rabbit skeletal muscle.

	GlyDH (*G. oxydans*)	GDL1[193] (*H. jecorina*)	GlyDH[196] (*N. crassa*)	GlyDH[198] (rabbit skeletal muscle)
DHA acceptance (D-GA/DHA)	100:1	100:20	100:43	100:4
Stereopreference	D-specific	No preference	D-specific	D-specific
D-GA/L-GA	100:4	100:93	100:36	100:36

Another important parameter is the enantioselectivity, as analysed by the ratio between the reductions of the D- and L-enantiomers of glyceraldehyde. A high enantioselectivity is required for the application of GlyDH from *G. oxydans* in the production of enantiopure glyceraldehyde. With an activity of only 4%, GlyDH from *G. oxydans* displayed a significantly lower activity compared to GlyDHs from *N. crassa* and rabbit skeletal muscle, which demonstrated an activity of 36% with L-glyceraldehyde. Consequently, among the GlyDHs published thus far, the GlyDH from *G. oxydans* is the only enzyme that shows the strong enantiopreference necessarily required for application in asymmetric synthesis, which was the object of this thesis and is discussed in greater detail in Section 7.4.

7.3.1 Structure of glycerol dehydrogenase from *Gluconobacter oxydans*

The detailed knowledge of the three-dimensional structure of an enzyme is of major importance with respect to the folding of the enzyme and its catalytic mechanism, including specific binding of the cofactor and substrate. Furthermore, the structure of

an enzyme can be used to obtain additional insight into structure-function relationships in terms of the substrate range, as well as the enantio- and regioselectivity of an enzyme. Such information can then be used to further optimise the catalytic activity of an enzyme via rational protein design. A prominent example is the structure-based alteration of the cofactor specificity of oxidoreductases, and various cases of such approaches have been published[122-133, 174, 199]. For instance, the cofactor preference of ADH from *L. brevis* was altered by a structure-based computational protein engineering approach. A single point mutation (Arg38Pro) was necessary for a fourfold increase in activity with NAD(H) as a cofactor[133].

In general, there are various ways to generate the molecular structure of an enzyme. First, the structure can be modelled based on an available structure that exhibits high homology at the structural level. This approach is beneficial for reducing lengthy time-consuming steps. However, one must be aware that the resulting structure is only a theoretical model. In contrast, there are time-consuming but far more reliable strategies to resolve the corresponding protein structure with methods such as X-ray crystallography or NMR spectroscopy.

In this thesis, crystals of GlyDH (AKR11B4) were grown, and data on the well-defracting crystals were collected via X-ray crystallography and utilised to solve the structure of GlyDH at a resolution of 2.0 Å (Chapter 3). GlyDH displayed the general structure of the aldo-keto reductase superfamily (AKR), consisting of the AKR-typical $(\beta/\alpha)_8$ TIM-barrel fold with three loops and a C-terminal tail that affects the protein's enzymatic properties. GlyDH belongs to family 11 of AKR superfamily and according to the systematic nomenclature within this family, the abbreviation AKR11B4 has been assigned to the enzyme[200].

Structure-function relationship – insights into the enantioselectivity of glycerol dehydrogenase

In general, AKR11B4 exhibited all of the typical features of bacterial AKRs[200-202]. Its close relative is AKR11B1 from *B. subtilis*[203], which has a sequence identity of 57.2%. The main differences between the structures of these two enzymes are found in the C-terminal segment and the active site cleft. While the C-terminus of AKR11B1 has the common conformation for AKRs that covers the active site and presumably plays a role in substrate binding[204], the C-terminus of AKR11B4 demonstrated a neighbour-anchoring conformation (Fig. 7.6). This difference may either be a result of the two different functional states (AKR11B1: binary complex with $NADP^+$; AKR11B4: apo-enzyme) or an inherent feature of the molecules arising from their specific sequences.

As mentioned above, the most unique feature of AKR11B4 is its high preference for reducing the D-enantiomer of glyceraldehyde. Therefore, based on the now available structure, the investigation of structure-function relationships was possible. The ternary complex with the cofactor and both glyceraldehyde enantiomers was modelled to elucidate the structural basis of the enzyme's enantiospecificity in the reduction of glyceraldehyde.

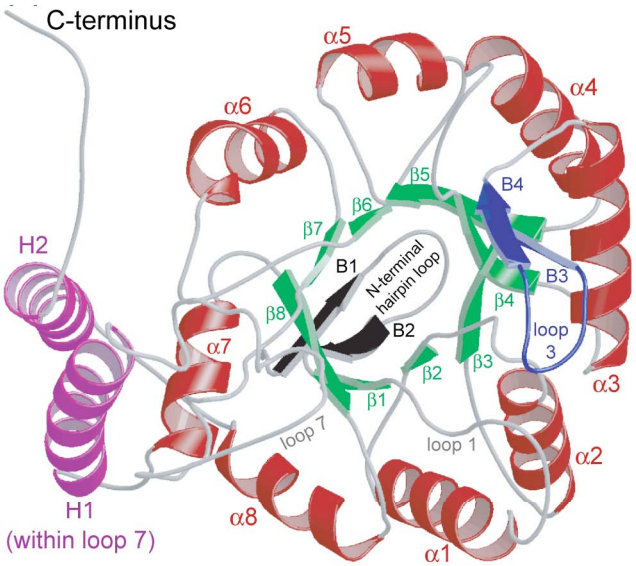

Fig. 7.6. Overview of the 3D-structure of GlyDH, exhibiting the $(\beta/\alpha)_8$ TIM-barrel fold typical of aldo-keto reductases (for more details, see Chapter 3).

Figure 7.7 shows the corresponding ternary complex. The substrate is surrounded by Trp^{23}, Tyr^{59}, His^{130}, Trp^{131} and Met^{326}. A comparison with the sequence of the non-selective GlyDH from *H. jecorina* demonstrated that with the exception of Met326, all residues are present in both enzymes.

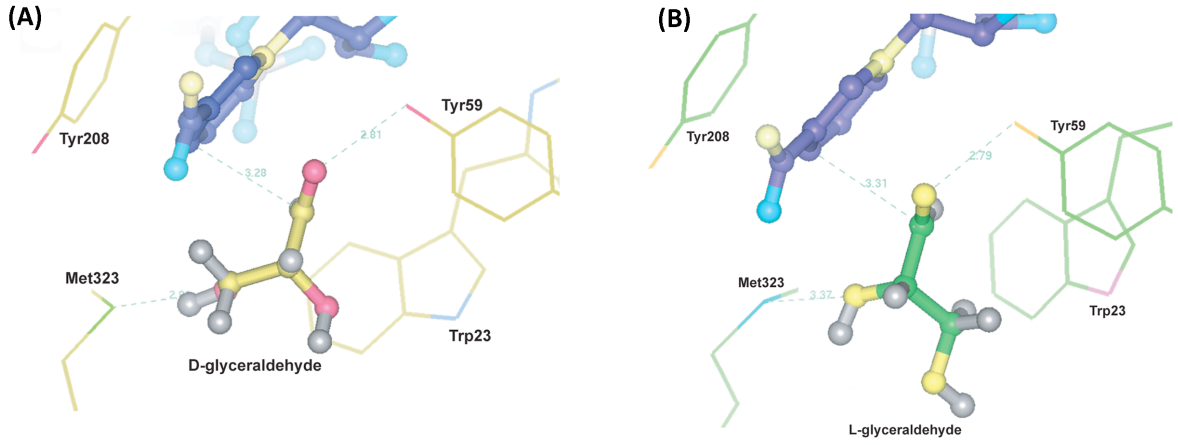

Fig. 7.7. Ternary complex model of AKR11B4 with NADP and either D-glyceraldehyde (A) or L-glyceraldehyde (B).

Furthermore, our studies revealed that Met^{326} is the most probable candidate to cause the enantiopreference of AKR11B4 via its ability to form a hydrogen bond to the terminal hydroxy group at the C3 atom of glyceraldehyde. Moreover, this hydrogen bond is only possible with D-glyceraldehyde as a substrate. This deduced mechanism confirms the observed biochemical data.
In summary, based on the three-dimensional structure of AKR11B, we were able to assign Met^{326} as the most important determinant for the enantiospecificity of GlyDH from *G. oxydans*.

7.4 PRODUCTION OF ENANTIOPURE GLYCERALDEHYDE – KINETIC RESOLUTION OF *RAC*-GLYCERALDEHYDE USING GLYCERCOL DEHYDROGENASE FROM *GLUCONOBACTER OXYDANS*

Because low-molecular chiral building blocks are versatile intermediates for further transformations into valuable products[11, 12, 205], one aim of this thesis was to establish a suitable selective route for the production of enantiopure glyceraldehyde. Due to its highly functionalised nature and asymmetry, glyceraldehyde is a good example of a chiral building block that can be used as a starting material for the synthesis of various complex structures (Section 1.1)[13-16]. The available chemical routes for the synthesis of both glyceraldehyde enantiomers are based on starting materials from the chiral pool, which comprise the chiral information. The fact that just D-mannitol is available only enables the synthesis of D-glyceraldehyde by applying a chemical route consisting of three steps, whereas the production of L-glyceraldehyde requires the synthesis of L-mannitol by a multi-step synthesis starting from L-arabinose[17]. Due to this drawback, the L-enantiomer is not easily accessible. Therefore, the demand for biocatalytic strategies to produce the L-enantiomer is high and was of major interest throughout this thesis.

7.4.1 Oxidative versus reductive production of enantiopure glyceraldehyde

To determine optimal reaction conditions, GlyDH was characterised with respect to its stability, as well as its oxidative and reductive potential and substrate range (Section 2.1).
GlyDH displayed the highest activity in the reduction reaction at a slightly acidic to neutral pH range, with optimal activity at pH 5.5. For oxidation reactions, GlyDH displayed a rather broad pH optimum, with the highest activity at pH 10.0.

However, the ability of GlyDH to catalyse the reduction of *rac*-glyceraldehyde and the oxidation of glycerol is far more important. According to the reversible character of the reaction, there are two possible enzymatic routes in applying GlyDH (Fig. 7.8).

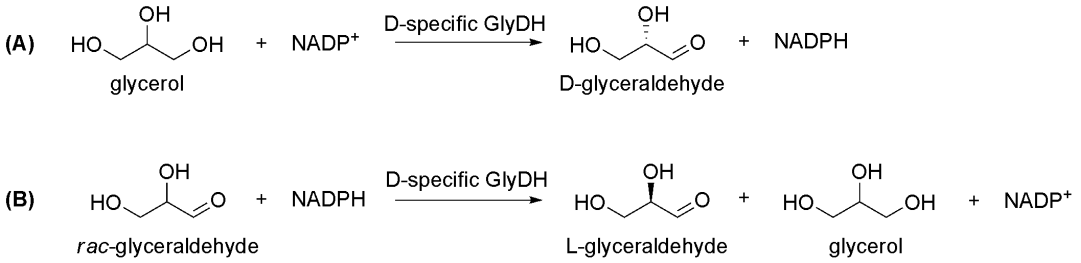

Fig. 7.8. Different enzymatic routes for the production of enantiopure glyceraldehyde *via* enzymatic oxidation (A) or kinetic resolution of the racemic mixture (B).

For biotechnological approaches, the favoured strategy is the enzymatic regioselective oxidation of glycerol because the theoretical yield of this route is 100%, and glycerol is a convenient starting material[206, 207]. The second route is the reduction of an enantiomer of glyceraldehyde that facilitates a resolution of the racemic mixture. The disadvantage of this reaction is the limited yield of only 50% and the rather expensive starting material.

To evaluate the optimal strategy, the specific activities of the oxidation of glycerol (0.17 U/mg) and the reduction of *rac*-glyceraldehyde (39.1 U/mg) were compared, the observed results differed remarkably. The reduction was catalysed with a 230-fold higher specific activity than the oxidation reaction, indicating that the equilibrium lies heavily in favour of the reduction of *rac*-glyceraldehyde. This observation is supported by similar results with other published GlyDHs. Indeed, all published enzymes show a low or absent oxidation activity[193, 208]. However, an exception can be found in GlyDH from *N. crassa*, which displays a rather high activity of 20.7 U/mg in the oxidation of glycerol. Unfortunately, the absolute configuration of the product was not determined. Regardless, it is highly unlikely that this enzyme is suited for the synthesis of enantiopure glyceraldehyde because the published biochemical data reveal only a weak stereochemical preference, with only a 2.7-fold higher activity in the stereoselective reduction of D-glyceraldehyde (Table 7.2)[209].

Interestingly, substrates such as sugar alcohols are oxidised by GlyDH with higher activities compared to glycerol (Section 2.1 and 2.2, and further discussed in Section 7.5). Detailed studies of the observed limitation revealed that the produced aldehyde has an inhibitory effect on the oxidation reaction. Therefore, the question arises whether this effect is caused by the formation of a Schiff base of the aldehyde and an active site lysine residue[210-212] or product inhibition[78]. Our results further

demonstrated that the inhibition is more pronounced when a free aldehyde moiety (e.g., glyceraldehyde) is formed by the enzyme. While the oxidation of a sugar alcohol leads to the formation of an aldose coupled with a spontaneous ring closure of the product (which diminishes the inhibitory effect (Section 2.2)), it is commonly known that lysine residues can form a Schiff bases in the presence of an aldehyde, especially at alkaline pH[210-212]. As a consequence, the lysine residue loses its positive charge, as well as the ability to form hydrogen bonds and electrostatic interactions, which can cause enzyme deactivation[210, 212].

Based on the three-dimensional structure of GlyDH, two conserved lysine residues (Lys^{84} and Lys^{219}) were identified that are involved in cofactor binding and the catalytic mechanism (Chapter 3). Thus, enzyme inactivation based on the formation of a Schiff base may be a possible explanation for the observed discrepancy between the reduction and oxidation activities. Furthermore, the fact that a pH value of approximately 10.0 is required for high oxidative activity supports this hypothesis. The effect of pH on the enzyme activity is further demonstrated by the fact that no inactivation of GlyDH by the same aldehyde at pH 7.0 was observed. Based on these inhibition, GlyDH cannot be used for the oxidation of glycerol. Therefore, the kinetic resolution of *rac*-glyceraldehyde was a major topic of this thesis because high specific activities and no inactivation effects were observed in the reduction of *rac*-glyceraldehyde. Moreover, different strategies were developed to establish a feasible kinetic resolution of *rac*-glyceraldehyde by GlyDH in combination with a suitable simultaneous regeneration system for the reduced cofactor. This aspect is discussed in the next chapter.

7.4.2 Production of L-glyceraldehyde – cell-free system versus whole-cell system

Oxidoreductases generally require cofactors such as NAD(P)H as donor of redox equivalents. Therefore, in terms of efficiency and economic issues, a regeneration system that can be used simultaneously is essential for biotechnological applications. The different methods to regenerate the reduced cofactor were introduced in Section 1.5. For the application of GlyDH in the kinetic resolution of *rac*-glyceraldehyde, GDH from *B. subtilis*[163, 213-215] was used for cofactor regeneration with D-glucose as the co-substrate (Fig. 7.9). GDH was selected because it has already been successfully applied in the regeneration of both reduced cofactors in cell-free and whole-cell systems[162, 163, 167]. Based on this strategy, two different systems for the production

of L-glyceraldehyde were created: a cell-free system with isolated enzymes (Section 2.1 and Chapter 6) and a recombinant whole-cell system (Chapter 5).

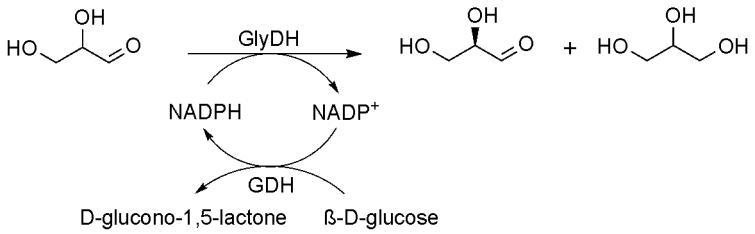

Fig. 7.9. Kinetic resolution of *rac*-glyceraldehyde by GlyDH with simultaneous cofactor regeneration by GDH and β-D-glucose as the co-substrate.

The general differences of the two used systems are summarised in Figure 7.10. While both enzymes must be expressed separately in the cell-free system, followed by disruption and centrifugation steps, the whole-cell catalyst only requires one fermentation and one separation step (Fig. 7.10)[188].

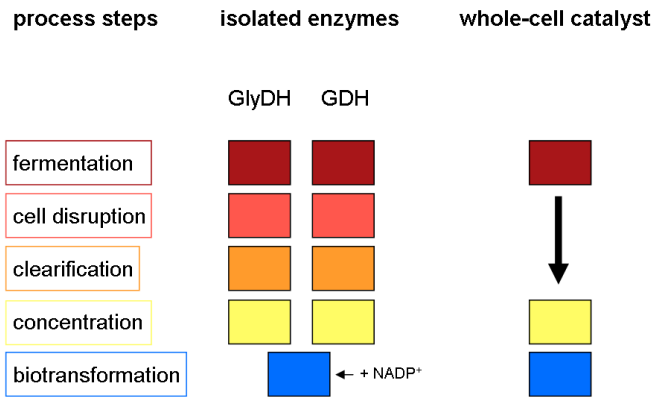

Fig. 7.10. Comparison of the application of isolated enzymes versus whole-cell catalysts for asymmetric synthesis. Figure modified according to Gröger *et al.* (2006)[188].

Another common advantage of whole-cell catalysts is that by using the intracellular amount of cofactor, the addition of an external cofactor is not necessarily required. Furthermore, whole cells can be used for several repetitive applications, while isolated enzymes can be used for only one reaction if no immobilisation of the catalyst is performed[216-218].

Table 7.3 provides an overview of the properties of the two applied systems. Both biotransformation systems show high activities in the selective reduction of *rac*-glyceraldehyde, resulting in efficient conversions with high *ee* values. However, a slightly lower selectivity of the whole-cell catalyst was observed compared to the cell-free system.

This effect may be caused by undesired side reactions catalysed by naturally occurring enzymes of the host organism. Indeed, such effects are very common when using whole-cell catalysts, especially in wild-type cells that only express low levels of the required enzymes[184]. According to this lower selectivity, a higher conversion was required (54%) to reach an appropriate enantiopurity of the L-glyceraldehyde product (98%).

Table 7.3. Comparison of the cell-free system and the whole cell catalyst.

System	Activity [U/mg]/	Conversion [%]	Selectivity [*ee*]	Cofactor addition	Recycling	pH-optimum	Temperature-optimum [°C]
Cell free	GlyDH 39[1)] GDH 295[2)]	50	>99%	yes	No	GlyDH: 5.5 GDH: 8.5	GlyDH: 55 GDH: 50
Whole-cell	21.4 U/g[1)] GlyDH 22.3[1);]* GDH 7.2[2)]*	54	98%	yes, but not required	Yes	7.0	40

[1)] Hexanal was used as substrate; [2)] D-glucose was used as substrate; and * measured in crude extract.

Because the selectivity of the whole-cell catalyst and the cell-free system were in a similar range, a transfer of the kinetic resolution was possible. Thus far, only the kinetic resolution of oxidoreductases using wild-type cells have been published[53, 219-221], whereas recombinant whole-cell systems have been used to a minor degree[190]. Comparing the preparative kinetic resolution of the *rac*-glyceraldehyde of both systems, the advantages of the whole-cell catalyst were confirmed. The whole-cell catalyst can be recycled up to five times without any loss of activity. Furthermore, an addition of the cofactor was not necessary, though the reaction rate can be accelerated by cofactor addition.

In addition to the advantages mentioned above, recombinant whole-cell catalysts also exhibit some limitations that must be overcome to facilitate a suitable application. The co-expression of the two genes can represent a challenge, particularly if the required enzymes exhibit large differences in specific activity. For example, the specific activities of leucine dehydrogenase (~400 U/mg) and formate dehydrogenase (~6 U/mg) differ by a factor of > 50. Menzel *et al.* (2004) applied a two-plasmid strategy using plasmids with different copy numbers to adjust the activity of the required enzymes. Consequently, the difference in activity was decreased to only a factor of 6.7 by recombinant DNA techniques[62]. Further strategies include the use of different promoters, as well as the variation of growth conditions and media. Both techniques were successfully applied to adjust the

different specific activities of GlyDH and GDH in the present study (Table 7.3; Chapter 4). Variations of growth conditions and media led to a GlyDH/GDH ratio in the range of 0.7 to 18.1. The results demonstrated that the use of different media had a phenomenal impact on the expression level of the co-expressed GlyDH and GDH. An optimal conversion was reached with cells cultivated at 25ºC in LB-medium (21.4 U/mg).

In contrast, with the cell-free system, the adjustment of the activity of the required enzymes was much easier because the application of different amounts of the catalysts is possible. Further limitations, which can occur with whole-cell catalysts, deal with the transport of substrate(s) into the cell and product(s) out of the cell. For a sufficient application, the substrate must be converted in the cytoplasm due to the localisation of the required enzymes, while for an easy separation, the product should ideally be located outside the cell.

The observations, based on the performed experiments, commonly approve the advantages of whole-cell systems compared to their cell-free pendant[62, 167, 188]. In the described example, the whole-cell system was superior to the cell-free system, which is not always the case. However, both systems are promising alternatives to traditional chemical methods.

In summary, we demonstrated that with whole-cell catalysts, no extensive disruption and separation procedures and no addition of external cofactors were required for a feasible reaction, and the catalyst can be recycled. These advantages make biotransformation with recombinant whole-cells a cost-attractive alternative to cell-free systems.

7.4.3 Preparative production of L-glyceraldehyde

There are different chemical and biocatalytic routes to synthesise enantiopure glyceraldehyde. The specific advantages and bottlenecks of the various published methods are summarised in Table 7.4 and are discussed in the following chapter.

Chemical routes to enantiopure glyceraldehyde

There are two traditional chemical strategies for the synthesis of enantiopure glyceraldehyde. The D-enantiomer can be easily produced based on a three-step chemical synthesis, starting with D-mannitol derived from the chiral pool of nature[17, 18].

In contrast, there are only a few efficient syntheses for the generation of the corresponding L-enantiomer because L-mannitol is not available from the chiral pool and must be synthesised by a multi-step method from L-arabinose[17, 222]. Therefore,

an alternative strategy has been described consisting of a four-step synthesis staring from L-ascorbic acid[19, 21]. For all chemical strategies, the starting material from the chiral pool is required, as well as a number of time consuming steps. Due to these difficulties in producing L-glyceraldehyde, its industrial production is not economically feasible. As a consequence, new suitable biocatalytic routes are in demand.

Biocatalytic routes to synthesise enantiopure glyceraldehyde

As described above, the chemical synthesis of both glyceraldehyde enantiomers is possible on a laboratory scale, but the procedures are extensive and expensive. Therefore, biocatalytic routes for the synthesis of L-glyceraldehyde are interesting alternatives to traditional chemistry, especially with respect to industrial-scale production.

Various enzymes have been reported to catalyse the asymmetric synthesis of enantiopure glyceraldehyde by selective oxidation[223-225], aldol addition[226] and kinetic resolution of *rac*-glyceraldehyde (Section 2.1 and Chapter 5; 6) (Table 7.4).

Table 7.4. Overview of different chemical and biocatalytic strategies for the production of enantiopure glyceraldehyde. The applied enzymes were as follows: galactose oxidase from *Dactylium dendroides,* ADH from horse liver, ADH from *Thermus thermophilus*, D-fructose-6-phosphate aldolase from *E. coli* and GlyDH from *G. oxydans*.

	Substrate	Product	Required steps	Time [h]	Scale [mmol]	Yield [%]
Chemical routes						
A[17, 222]	L-arabinose	L-GA	5	-	-	-
B[19, 21]	L-ascorbic acid	L-GA	4	-	-	-
C[17, 18]	D-mannitol	D-GA	3	-	-	-
Biocatalytic routes						
Galactose oxidase (*D. dendroides)*[224]	Glycerol	L-GA	1	48	0.25	17
Alcohol dehydrogenase (horse liver)[225]	Glycerol	GA (GA acid)	2	-	12-14	-
D-fructose-6-phosphate aldolase (*E. coli*)[226]	Formaldehyde + Glycolaldehyde	L-GA	1	-	0.024	-
Alcohol dehydrogenase (*T. thermophilus*)[223]	Glycerol	D-GA	1	14	32 mM*	-
GlyDH (*G. oxydans*)	*rac*-GA	L-GA	1	10	111	43

* no reaction volume is given.

All enzymatic strategies for the production of enantiopure glyceraldehyde require only a single catalytic step. Among the different routes, the best strategy is the asymmetric oxidation of glycerol catalysed by galactose oxidase from *Dactylium dendroides* (GOase)[224], ADH from horse liver (HLADH)[225] and the ADH from *Thermus thermophilus* (TtADH)[223]. TtADH produces the D-enantiomer, GOase is described to produce the L-enantiomer, while no configuration is given in the case of HLADH. Based on the described results, the GOase seems to be a promising catalyst due to the favourable starting material and the existing enantiopreference. However, with regard to scale (0.25 mmol), conversion (17%) and reaction time (48 h), the described example is not industrially feasible. Moreover, H_2O_2 is formed as a by-product of the enzymatic reaction, making the addition of a second enzyme (catalase) for the decomposition of H_2O_2 necessary.

A second route to enantiopure glyceraldehyde is the aldol addition catalysed by D-fructose-6-phosphate aldolase (FSA) from *E. coli*[226]. FSA catalyses the direct stereoselective cross-aldol addition of formaldehyde and glycolaldehyde, leading to L-glyceraldehyde formation. The published method is a promising approach but has only been reported on a 0.024 mmol scale.

Therefore, the strategy used in this thesis is currently the only efficient biocatalytic method applied on the 111 mmol scale. The production of L-glyceraldehyde was catalysed by the described GlyDH from *G. oxydans*. Due to the fact that the oxidation activity of the enzyme was inhibited by the produced aldehyde, asymmetric oxidation was not possible. Therefore, L-glyceraldehyde was produced *via* the kinetic resolution of *rac*-glyceraldehyde. As a result, a yield of 43% (111 mmol) L-glyceraldehyde was achieved by the applied strategy.

Chemical versus biocatalytic synthesis of L-glyceraldehyde

A comparative evaluation of the three chemical routes and five biocatalytic routes for the production of enantiopure L-glyceraldehyde reveals that with regard to the required steps, the biocatalytic strategies are favourable. Such a significant reduction of reaction steps is desirable due to improved production efficiency by a decreased number of workup and purification steps[46, 227, 228]. Furthermore, considering environmental issues, the biocatalytic route is preferred because toxic metal catalysts must be used for the chemical syntheses[17, 18, 222]. Therefore, with respect to environmental aspects and cost factors, short enzymatic routes are desirable.

In summary, among the different enzymatic routes, the process of applying GlyDH is most promising, though all have an immense potential for the production of L-glyceraldehyde (Chapter 6). Key benefits of the established process are the

production scale and the yield and the selectivity of the described process in comparison with the other enzymatic routes. By applying this method, 111 mmol enantiopure L-glyceraldehyde (*ee* 96%) was produced.

Apart from the enzymatic production, the downstream processing is also of major importance for the production of pure building blocks (Section 1.1). Thus, a suitable purification procedure was established within this thesis (Chapter 6). The separation of the produced L-glyceraldehyde from glycerol, glucose and gluconic acid was accomplished by preparative liquid chromatography using an ion exchange resin. The purification resulted in a yield of 85% (4.24 g L-glyceraldehyde) with an enantiopurity of 94%.

7.5 SELECTIVE OXIDATION OF SUGAR ALCOHOLS BY GLYCEROL DEHYDROGENASE FROM *GLUCONOBACTER OXYDANS*

As previously discussed in Section 7.4.1, GlyDH from *G. oxydans* catalyses the oxidation of various alcohols (Section 2.2). However, due to the appearance of massive product inhibition in the presence of linear free aldehyde, only the conversion of sugar alcohols was possible. An explanation can be found in the subsequent ring closure of the produced aldehyde. Therefore, the oxidation of L-arabitol and ribitol were investigated in this thesis.

Biotransformations were performed using GlyDH in combination with glutamate dehydrogenase (GluDH) from *E. coli* for cofactor regeneration (Section 2.2) (Fig. 7.11).

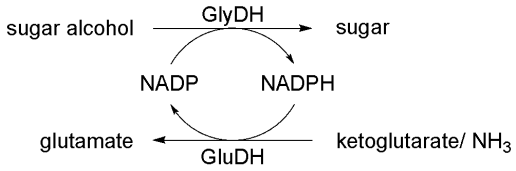

Fig. 7.11. General reaction scheme of the oxidation of sugar alcohols by GlyDH from *G. oxydans* with a simultaneous regeneration of $NADP^+$ using the GluDH from *E. coli* with ketoglutarate/NH_3 as a co-substrate.

In general, both substrates were fully converted by GlyDH. Ribitol was converted to ribose, and the transformation of L-arabitol yielded lyxose and arabinose. These results indicated that GlyDH exhibits a high regioselectivity because the primary hydroxyl group is specifically oxidised. Thus far, only a few dehydrogenases that catalyse the oxidation of primary hydroxy groups have been described in the literature[72, 229, 230]. Membrane-bound dehydrogenases that catalyse the oxidation of secondary alcohols are more common[72, 229-238], whereas a number of different oxidases are known to catalyse the oxidation of primary alcohols[72, 229, 239, 240].

Furthermore, the configuration of the carbon atom next to the terminal hydroxy group influenced the activity of GlyDH because only the L-enantiomers of the tested sugar alcohols were oxidised. For example, L-arabitol and L-threitol were converted to the corresponding sugars by GlyDH, while the corresponding D-enantiomers were not, indicating that GlyDH additionally exhibits enantioselectivity.

A further interesting observation was the formation of lyxose and arabinose during the biocatalytic oxidation of L-arabitol. This result can be explained by the hypothesis that both terminal hydroxy groups of L-arabitol are oxidised by GlyDH. The only requirement for this reaction is the L-configuration of the carbon atom next to the terminal hydroxy group. Therefore, in theory, the L-configuration of the arabinose and lyxose are synthesised, while during the oxidation of ribitol, the formation of D-ribose is proposed. Nevertheless, the determination of the absolute configuration of these molecules is essential to support this hypothesis.

In conclusion, according to its ability to catalyse the selective reduction of *rac*-glyceraldehyde, as well as the regio- and stereoselective oxidation of various sugar alcohols, GlyDH is a versatile catalyst with tremendous biotechnological potential. Based on its oxidative catalytic activity, a number of valuable sugars such as L-lyxose can be synthesised *via* a direct enzymatic route. L-lyxose is an unnatural sugar and is a versatile synthon for various applications in the food, pharmaceutical and nutrition industries[230]. A further example is L-ribose, which can be synthesised by chemical means from D-ribose (chiral pool) by five synthetic steps with an overall yield of 50%[232]. Therefore, a number of studies were performed to establish suitable enzymatic routes[231, 233] for L-ribose production. Thus, based on the high demand of new enzymatic routes, GlyDH is a novel enzyme with very promising properties for biotechnological applications.

7.5.1 Regeneration of the oxidised cofactor

The regeneration of the oxidised cofactor is of major importance for the efficient use of dehydrogenases for oxidation reactions because the equilibrium of dehydrogenases heavily favours the reduction reaction. Strategies that have been used for the regeneration of the oxidised cofactor are summarised in Section 1.5.3. Lactate dehydrogenases (LDHs) are enzymes that are frequently applied in the regeneration of NAD^+[81, 171-173, 241]. Their application is limited to NAD^+ based on the cofactor specificity of LDHs, because an $NADP^+$-dependent LDH has not yet been found in nature. Nevertheless, such a LDH variant would be very useful because it would facilitate the regeneration of the phosphorylated cofactor.

Therefore, one of the aims in this thesis was to enable the regeneration of $NADP^+$ by an LDH variant constructed by methods of structure-based protein design.

7.5.2 Alteration of the cofactor specificity of the lactate dehydrogenase from *Bacillus subtilis*

The LDH from *B. subtilis* (BsLDH) has been characterised with regard to its biochemical properties[242-244] and displays high homology to the LDH from *G. stearothermophilus* (GsLDH)[49, 122-124, 199, 245]. Based on this high homology and because the three-dimensional structure of GsLDH has been solved, a homology model of BsLDH was constructed (Chapter 4). This model was used for the prediction of several essential amino acid residues which might be involved in cofactor binding (positions 36-40) (Fig. 7.12).

The selected amino acids are located adjacent to Asp^{38}, which is known to be responsible for the NAD^+ preference of the enzyme due to its ability to form hydrogen bonds with the cofactor and to repulse the phosphorylated cofactor due to its negative charge[134]. Using this insight, a variety of groups investigating the alternation of the cofactor specificity of oxidoreductases have mutated amino acids located in this conserved fingerprint region[63, 246-248]. Most examples focus on the alteration of $NADP^+$-dependency of dehydrogenases[131, 133, 249] because NAD^+ is more stable, and its price is five- to tenfold lower compared to $NADP^+$.

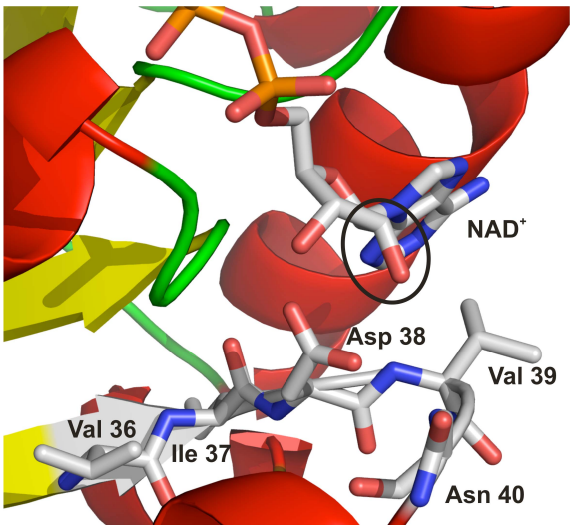

Fig. 7.12. Structure of the modelled binary complex of wild-type BsLDH in combination with NAD^+ using the structure of GsLDH (1LND) as a template. The protein backbone is coloured by secondary structure elements: α-helices (red), β-sheets (yellow) and single stands (green). The atoms are coloured according to type: oxygen (red), nitrogen (blue), carbon (grey) and phosphorus (orange). The NAD^+-binding region responsible for $NADP^+$ discrimination is displayed, showing the position of the selected amino acids for mutagenesis. The position of the additional phosphate group is circled.

With respect to enzymes applied in cofactor regeneration, the reverse direction has also been studied extensively to expand the scope of enzymes such as formate dehydrogenase (FDH)[126, 128, 132, 199] or LDH[63, 246, 247].

In this thesis, a structure-based site-directed saturation mutagenesis approach was performed, resulting in a BsLDH variant with a single point mutation (BsLDH_V39R). BsLDH_V39R showed a 100-fold higher specific activity with $NADP^+$ as the cofactor in comparison to the wild-type enzyme but still exhibited activity with NAD^+. Furthermore, BSLDH_V39R displayed a remarkable increase in catalytic efficiency (249-fold) compared to the wild-type BsLDH.

The alternation in cofactor specificity was caused by the substitution of valine (Val^{39}), a small neutral amino acid, to an arginine (Arg), a strongly positively charged bulky amino acid. The introduced Arg^{39} led to a rearrangement in which a positively charged amino acid is located next to a negatively charged one at this crucial position. Interestingly, the resulting variant accepted both cofactors as a consequence. This finding was unpredictable because one would assume that the introduced mutation may be incompatible with respect to electrostatic repulsion with the adjacent Asp^{38}. Furthermore, this arrangement suggests that according to charge of the two amino acids (Asp^{38} negative and Arg^{39} positive), both cofactors would be repulsed. However, BsLDH_V39R exhibited activity with both cofactors, indicating that neither the negative nor the positive charge at this crucial position causes a destabilisation of the two cofactors. In contrast, the introduction of two positively charged amino acids (D38R:V39R) led to dramatically decreased activity with NADPH, combined with rejection of NADH.

Comparing the observed results with other published LDH variants from *G. stearothermophilus* (GsLDH)[122-124] and *T. thermophilus* (TtLDH)[174], position 39 (BsLDH Val^{39}; GsLDH Ala^{39}, see alignment in Chapter 4) was interestingly never a target for mutagenesis. Therefore, herein, we showed for the first time the importance of the amino acids directly adjacent to Asp^{38} for the cofactor specificity of BsLDH.

Moreover, the published variants differ in the number of introduced mutations. While the investigated mutants BsLDH_V39R and GsLDH_D38S[124] only exhibited a single point mutation, GsLDH_I37K:D38S[122] contains two mutations, and Mut31 required the introduction of five different mutations (F16Q:C81S:N85R:I37K:D38S)[123]. Another strategy was the construction of a *T. thermophilus* (TtLDH) variant where the complete loop region of an $NADP^+$-dependent malate dehydrogenase was introduced into the cofactor binding site of TtLDH[174]. However, the necessity for the introduced mutations remains questionable. In addition, one must keep in mind that

a higher number of mutations enhances the occurrence of side effects, such as reduced stability or restricted substrate range, in the corresponding enzyme[250-253]. Regardless, the biochemical properties of the LDH variants are comparatively discussed below.

Biochemical properties of BsLDH_V39R and its application in the regeneration of the oxidised cofactor

BSLDH_V39R was characterised with respect to its biochemical properties, which are important for its application in the regeneration of $NADP^+$ (Chapter 4). In comparison to wild-type BsLDH and LDH variants from other sources, BSLDH_V39R displayed significantly improved kinetic properties. Table 7.5 provides an overview of the kinetic properties of BsLDH_V39R, two published GsLDH variants (D38S and I37K:D38S)[122, 124] and a variant of TtLDH[174]. In general, all of these mutants show a shift towards $NADP^+$, but only moderate improvements in catalytic efficiency were observed.

Table 7.5. Comparison of the biochemical properties of BsLDH_V39R and wild-type BsLDH with data from the literature on other LDH variants from *B. subtilis, G. stearothermophilus* and *T. thermophilus*.

	K_M (mM)		k_{cat} (s^{-1})		k_{cat}/K_M (µM s^{-1})		Alteration compared to wild-type [a)]
	NADH	NADPH	NADH	NADPH	NADH	NADPH	
B. subtilis Wild-type BsLDH	0.05	0.14	77.5	1.3	1.5	9.4 x 10^{-3}	-
BsLDH_V39R	0.06	0.06	291.6	140.4	4.9	2.2	249
BsLDH[243]	0.06	-	-	-	-	-	-
G. stearothermophilus D38S[124]	0.04	0.1	145	55	3.63	0.55	1.1
G. stearothermophilus I37K:D38S[122]	1.0	0.7	160	160	0.16	0.23	1.6
T. thermophilus Tt27 LDH-EX7[174]	1.19	0.35	11.2	127	0.03	0.11	2.4

a) NADPH compared to the wild-type values published together with the corresponding mutants.

Based on the mutation, the K_M value of BsLDH_V39R with NADPH was reduced from 0.14 mM to 0.06 mM, which is now in the same range with that observed for NADH as the cofactor. In comparison, the previously published mutants demonstrate higher K_M values in the range of 0.1 mM to 0.7 mM. Further, a main difference was found in the K_M value for NADH, which was significantly enhanced in the case of GsLDH (I37K:D38S) and TtLDH (Tt27 LDH-EX7) compared to their respective wild-type

enzymes, while the K_M of BsLDH_V39R was not altered by the introduced mutation. Therefore, the catalytic efficiency for NADPH in relation to the efficiency of the corresponding wild-type BsLDH was used as a degree for alteration by the corresponding mutant. The most significant alteration was observed with BSLDH_V39R, which displayed a 249-fold enhancement compared to a 1.1- to 2.4-fold enhancement observed with the other mutants (Table 7.5).

In addition to the summarised mutants, another interesting GsLDH mutant, Mut31, demonstrates a 36-fold improvement (compared to wild-type GsLDH) in cofactor specificity in the presence of fructose-1,6-bisphosphate as the activator[123]. In contrast, with respect to cofactor specificity, BSLDH_V39R displayed 100-fold improved activity. Furthermore, this enzyme does not require an expensive activator.

According to the excellent kinetic properties of BsLDH_V39R, the regeneration of $NADP^+$ was possible. In comparison to other established $NADP^+$ regeneration systems, such as glutamate dehydrogenases (GluDHs) (Section 2.2)[47, 81, 177, 178] and NAD(P)H-oxidases (NOXs)[47, 79, 175, 176], BSLDH_V39R is a promising alternative enzyme. BSLDH_V39R has higher specific activity than NOXs, as well as an economically favourable co-substrate and the pH constancy of the reaction mixture compared to GluDHs.

In conclusion, due to its biochemical properties, BsLDH_V39R is a promising candidate for biotechnological application in the regeneration of both oxidised cofactors (NAD^+ and $NADP^+$). Moreover, BsLDH_V39R was successfully used for the regeneration of $NADP^+$ in combination with LkADH for the oxidation of the (*R*)-enantiomer of *rac*-1-phenylethanol (Chapter 4). Because none of the other published mutants were applied in the regeneration of either NAD^+ or $NADP^+$, we were able to report the regeneration of $NADP^+$ using an LDH for the first time in this thesis.

7.6 SELECTIVE REDUCTION OF α- AND β-KETOESTERS BY CARBONYL REDUCTASE FROM *NEUROSPORA CRASSA*

An interesting reaction is the enantioselective reduction of carbonyl groups to produce chiral hydroxy compounds. Carbonyl reductases (CRs) are capable of catalysing this type of reaction and have been applied in various biotransformations over the past few decades[254]. Enantiomerically pure α- and β-hydroxyesters are valuable synthons.

The enzymatic production of optically pure 4-chloro-3-hydroxybutanoate (CHBE) derived from pro-chiral ethyl-4-chloro-oxobutanoate (COBE) is a prominent example[166, 246, 247, 255-257]. Both isomers are valuable synthons for important compounds[258-261]. In this thesis, the carbonyl reductase from *N. crassa* (NcCR) was cloned, heterologously expressed, purified, biochemically characterised and applied in the synthesis of various α- and β-hydroxyesters.

7.6.1 Biochemical properties of carbonyl reductase from *Neurospora crassa*

A comparative analysis of the biochemical properties of NcCR with the published carbonyl reductases (CR) is presented in Table 7.6. In general, CRs are widely distributed throughout various protein families. All CRs displayed in the table belong to either the short chain dehydrogenase family (SDR) or the aldo-keto reductase family (AKR). The amino acid sequence of NcCR identifies these enzymes, such as CmAR from *Candida magnoliae*[262] and ARI from *Sporobolomyces salmonicolor*[65, 263], as members of the AKR family. With the exception of KaCRI from *Kluyveromyces aestuarii*[256], all summarised enzymes are $NADP^+$-dependent.

Table 7.6. Biochemical properties of various carbonyl reductases. Their microbial sources are *S. salmonicolor, C. magnoliae, K. aestuarii, K. lactis, Pichia stipitis* and *N. crassa*.

Enzyme	ARI [65, 263]	S1 [256]	KaCRI [256]	CmAR [262]	KlCR [264]	PsCR [257, 265]	NcCR
Source	*S. salmonicolor*	*C. magnoliae*	*K. aestuarii*	*C. magnoliae*	*K. lactis*	*P. stipitis*	*N. crassa*
Molecular weight (kDa)	37	32	32	35	190	35	38
Protein family	AKR	SDR	SDR	AKR	-	SDR	AKR
Cofactor	$NADP^+$	$NADP^+$	NAD^+	$NADP^+$	$NADP^+$	$NADP^+$	$NADP^+$
pH optimum	7.0	5.5	5.0	7.0	6.5	6.0	7.0
Temperature optimum (°C)	60	55	45	40	45	30	45
Specific activity COBE (U/mg)	144	270	-	184	-	337	325
Stereopreference for COBE	>99% (*R*)	>99% (*S*)	>99% (*S*)	>99% (*R*)	>99% (*S*)	>99% (*S*)	>98% (*S*)

The temperature optima of the enzymes listed in the table are located between 30 and 60ºC, and the pH-optima range between pH 5.0 and 7.0.

With respect to substrate specificity, NcCR, PsCR from *Pichia stipitis*[257, 265] and KaCRI from *K. aestuarii*[256] (both members of the SDR superfamily), displayed a restricted substrate range. All three CRs are active in the reduction of α- and β-ketoesters, as well as α,β-diketones, whereas aliphatic and aromatic aldehydes and ketones are either not converted or reduced with low activity.

All displayed enzymes (Table 7.6) exhibit high activities in the selective reduction of COBE to produce either the (*R*)- or (*S*)-enantiomer with high enantiopurity. Interestingly, NcCR is the only member of the AKR family that produces (*S*)-CHBE. All other AKRs produce the (*R*)-enantiomer, and all of the SDRs produce the (*S*)-enantiomer.

Another interesting feature of NcCR is the observed strong correlation between enantioselectivity and temperature (Section 2.3). Such temperature effects are commonly known to influence the enantioselectivity of chemical, and in some cases, also enzymatic reactions[266-270]. Therefore, the conversion of COBE to (*S*)-CHBE was studied at different temperatures. At 40ºC, a poor *ee* of 78.8% was detected. However, the selectivity of NcCR was enhanced to >98% by shifting the temperature to -3ºC (Fig. 7.13). A sufficient reaction at this temperature was only possible by continued vigorous stirring and the addition of buffer salts (100 mM).

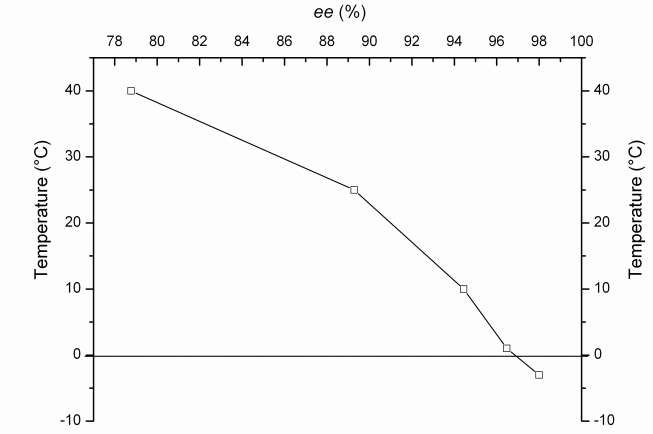

Fig. 7.13. Dependence of the enantioselectivity of NcCR on temperature (-□-).

Influencing the enantioselectivity of enzymes by altering the physical environmental parameters (e.g., temperature) has also been reported for other enzymes. A prominent example is the ADH from *Thermoanaerobater brockii* (TBADH), which was extensively studied[266, 271, 272]. TBADH catalyses the reduction of 2-pentanone with the highest enantioselectivity at a temperature of 7ºC. Further studies of TBADH were performed in detail by Keinan and co-workers (1986), who demonstrated a

drastically enhanced selectivity by shifting the temperature from 50 to 7ºC[273]. Another example is pig liver esterase, which shows the highest enantioselectivity in 20% aqueous methanol at -10ºC[274].

In summary, the reported results in this thesis demonstrate that the establishment of a feasible process for the production of important chiral synthons is possible by applying simple methods of reaction engineering. Therefore, a preparative conversion of COBE was performed using NcCR at -3ºC.

7.6.2. Preparative biotransformation of Ethyl 4-chloro-oxobutanoate (COBE)

Chiral α- and β- hydroxyesters are valuable synthons as key intermediates in the production of fine chemicals, pharmaceuticals and natural products[6, 25, 27, 30, 52]. Therefore, much attention has been paid to establish chemical and particularly enzymatic strategies to produce these building blocks[63-65].

One key building block is enantiopure CHBE. Therefore, the preparative reduction of COBE to yield (*S*)-CHBE was performed using NcCR. Table 7.7 provides an overview of different enzymatic approaches to produce enantiopure CHBE.

Table 7.7. Overview of different enzymatic routes for the production of enantiopure CHBE using enzymes from *S. salmonicolor, C. magnoliae, K. aestuarii, P. stipitis* and *N. crassa*.

Enzyme	Origin	Cofactor regeneration	Scale (g)	Yield (%)	*ee* (%)	Time (h)
NcCR	*N. crassa*	GDH	0.3	100	(S) >98	3
AldDH[166]	*S. salmonicolor*	GDH	15	94.1	(R) 91.7	50
S1[255]	*C. magnoliae*	GDH	3.75	87.5	(S) 100	30
menadione reductase[275]	*C. magnoliae*	GDH	15	92.2	(S) 91.6	8
PsCR[257]	*P. stipitis*	GDH	0.1	94.0	(S) 99	18
S1*[246]	*C. magnoliae*	GDH	15	85	(S) 100	16
KaCRI*[256]	*K. aestuarii*	GDH/FDH	1		(S) 99	6

* COBE was continuously fed into the reaction mixture.

In all cases, the coupled enzymatic routes use GDH for the enzymatic regeneration of NAD(P)H. Comparing NcCR-mediated conversion with the other enzymatic routes, it becomes obvious that the scale of the reaction using NcCR is considerable smaller than the previously published data. The best productivity (12.75 g) combined with an excellent enantioselectivity (100%) was reached using CR S1 from *C. magnoliae*[255]. Other approaches in the same range lacked in selectivity by exhibiting *ee* values of 91.7% (AldDH; *S. salmonicolor*) and 91.6% (menadione reductase; *C. magnoliae*)[166, 275]. Interestingly, despite the fact that a number of (*R*)-selective enzymes exist (Table 7.7), the use of (*S*)-selective enzymes prevails on a preparative scale.

Although there are better strategies in terms of productivity and efficiency for the production of enantiopure CHBE, we demonstrated that a sufficient process for the production of α- and β-hydroxyesters can be established with an enzyme (NcCR) that did not seems to be feasible at first sight.

7.7 SELECTIVE REDUCTION OF C=C DOUBLE BONDS

A further example of the use of oxidoreductases in asymmetric synthesis is the reduction of C=C double bonds, which creates up to two chiral centres (Section 1.3.2). Enoate reductases (EnR) [EC 1.3.1.31] are flavin-dependent enzymes that largely catalyse C=C double bond reduction in a chemo-, regio- and stereoselective manner. These flavin-containing enzymes and a growing number of discovered homologues are valuable tools for the asymmetric reduction of C=C double bonds. To date, various representatives of such enzymes have been found in yeast, bacteria and plants[276-284]. In this thesis, the EnR from *G. oxydans* was investigated for its ability to catalyse the asymmetric reduction of activated alkenes, such as ketoisophorone (KIP) and citral, which are valuable synthons for further synthesis[87-89, 91, 285].

7.7.1 Biochemical properties of enoate reductase from *Gluconobacter oxydans*

G. oxydans EnR was cloned, heterologously expressed and assessed for its ability to catalyse the reduction of activated alkenes (Section 2.4). This enzyme and its heterologous expression and purification have been previously published[93, 286-288]. However, the reported biochemical data differ, especially in regard to cofactor dependency, pH optimum and selectivity in the biotransformation of citral. In

addition, the influence of an N- or C-terminal modification of EnR has also been studied.

With respect to cofactor specificity, all published data commonly reveal that EnR is NADPH-dependent, while Yin *et al.* (2008) reported an NADH-dependency for this enzyme (Table 7.8)[93]. A further difference was found in the pH and temperature optima, and based on the fact that the same enzyme was characterised, the deviations in these parameters are remarkable.

Moreover, considerable differences in the biotransformation of citral, compared to the work of Yin *et al.* (2008), are present in the literature. Yin *et al.* report diastereoselectivity by EnR because it only reduced the *cis*-isomer neral, while the *trans*-isomer geranial was not converted. Our study confirmed a preference for neral, but geranial was also converted when the neral concentration was significantly reduced. This effect may either be caused by a moderate diastereoselectivity of the enzyme or by a common amino acid-catalysed isomerisation of the substrate[289].

Table 7.8. Comparison of the measured kinetic properties of the enoate reductase from *G. oxydans* with published data.

	Cofactor dependency	pH optimum	Temperature optimum	Biotransformation of citral
Yin *et al.*[93]	NADH	-	-	Diastereoselective (*cis*)-isomer
Shinagawa *et al.* [286]	NADPH	5.0	-	-
Schweiger et al. [287]	NADPH	7.0	RT	-
This study	NADPH	5.5	45°C	Diastereoselective (*cis*)-isomer

In addition, the influence of a N- or C-terminal modification on the activity of EnR was investigated. Our results revealed that a C- or N-terminal His-tag does not negatively influence the activity of EnR. Interestingly, the variant with the N-terminal His-tag showed even higher activity compared to the native enzyme. In general, such modifications have no influence on biological activity[290], but some exceptions have been published[291, 292]. One of the goals of this work was to investigate the scope of EnR with respect to an application in the asymmetric reduction of C=C double bonds. Furthermore, the reduction of citral and KIP was studied to investigate the use of EnR for organic syntheses.

7.7.2 Biotransformation of citral and ketoisophorone

The field of biocatalytic C=C double bond reductions is still poorly explored. This is due to the fact that whole cells approaches are plagued with numerous side reactions (e.g., carbonyl reduction catalysed by competing ADHs) and a limited number of stable available catalysts in a recombinant form. Therefore, the demand for additional stable enzymes that are capable of catalysing this important reaction is of growing interest. Furthermore, non-biological strategies are often limited by their lack of chemo-, regio- and enantioselectivity[293-296].

To investigate the biotechnological potential of EnR, citral and KIP (3,3,5-trimethyl-2-cyclohexen-1,4-dione, ketoisophorone) were chosen as model substrates, yielding chiral synthons with biotechnological and pharmaceutical applications (Section 1.3.2)[87-89, 91, 285]. Moreover, citral reduction is a challenging task in terms of regio- and chemoselectivity based on the existence of three different double bonds.

Table 7.9 summarises different enoate reductases and their ability to asymmetrically reduce KIP and citral. In general, different enzymes that catalyse the studied reactions with different conversions and selectivities are available. Interestingly, all enzymes preferentially produce (*R*)-levodione and (*S*)-citronellal. The *trans*-fashion is a more common feature of these enzymes, and thus far, only the EnR from *Nicotiana tabacum* catalyses C=C double bond formation in a *cis*-specific manner[299]. The selectivity and conversion of EnR are excellent in comparison to the other enzymes. Furthermore, the chemo-, regio- and stereoselectivity of EnR in the reduction of citral were also outstanding. Due to the occurrence of side reactions caused by numerous competing enzymes in the cells (e.g., ADHs depending on the same nicotinamide cofactors), purified enzyme was required to obtain pure products. Such side reactions are observed when using the whole cells of wild-type organisms. Indeed, in the reduction of compounds such as citral, non-chemoselective side-reactions occur by different enzymes[92, 300-303].

In conclusion, the EnR from *G. oxydans* exhibits excellent selectivity in the asymmetric reduction of KIP and citral. Furthermore, a number of other activated alkenes are also accepted by EnR. Therefore, the scope of EnR in the asymmetric bioreduction of additional compounds in a stereoselective manner is currently under investigation.

Table 7.9. Overview of different enoate reductases and their ability to reduce ketoisophorone and citral. Applying either whole cell or isolated enzymes from *Aspergillus niger, G. oxydans, Lycopersicon esculentum B. subtilis, Salmonella typhimurium, Zymomonas mobilis, Thermoanaerobacter pseudoethanolicus* and *C. macedoniensis.*

		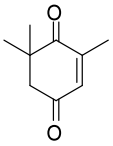 Ketoisophorone		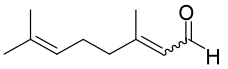 Citral	
Enzyme	Origin	Selectivity [*ee*]	Conversion [%]	Selectivity [*ee*]	Conversion [%]
Whole cells [297]	*A. niger*	(*R*)	6 products	-	-
GYE1 [93]	*G. oxydans*	-	-	n.d.	40
OPR1 [298]	*L. esculentum*	(*R*) > 51	> 98	(*S*) > 95	> 99
OPR3 [298]	*L. esculentum*	(*R*) >43	> 85	(*S*) >95	> 90
YqiM [298]	*B. subtilis*	(*R*) >42	> 95	(*S*) >95	> 70
NRSal [276]	*S. typhimurium*	(*R*) 87	12	-	No conversion
NCR-EnR [282]	*Z. mobilis*	(*R*) >95	>99	(*S*) >95	> 99
TOYE[284]	*T. pseudethanolicus E39*	(*R*) 26	74	-	-
EnR[87]	*C. macedoniensis*	(*R*)	n.d.	-	-
EnR (this study)	*G. oxydans*	(*R*) >99	>99	(*S*) >99	> 99

* n.d. = not determined

7.8 CONCLUSIONS

With the identification of three novel oxidoreductases (i.e., the carbonyl reductase from *N. crassa* (NcCR), as well as the enoate reductase (EnR) and glycerol dehydrogenase (GlyDH) from *G. oxydans*), the syntheses of various versatile chiral building blocks were facilitated within this thesis. Figure 7.14 summarises the scope of the investigated enzymes.

These new catalysts made it possible to produce different chiral alcohols, α- and β-hydroxyesters and, in particular, enantiopure L-glyceraldehyde. In addition, they also enabled the regio- and enantioselective oxidation of diverse sugar alcohols.
To facilitate conversions on a preparative scale, different strategies for the regeneration of either the reduced or the oxidised cofactor were applied. Furthermore, a $NADP^+$-dependent mutant of a bacterial lactate dehydrogenase was constructed, which can be applied in the regeneration of both nicotinamide cofactors.

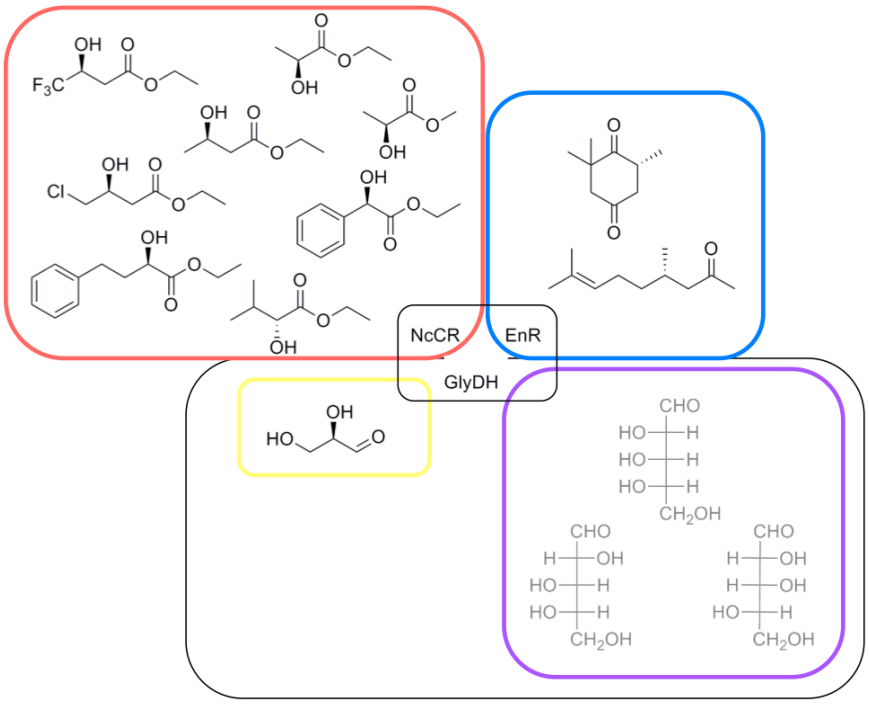

Fig. 7.14. Overview of the building blocks that can be produced by the three identified enzymes.

The production of L-glyceraldehyde was performed by using GlyDH in the kinetic resolution of *rac*-glyceraldehyde. For this purpose, a cell-free system and a novel recombinant whole-cell system were compared and successfully utilised for the synthesis of L-glyceraldehyde. Based on this enzymatic route, the first preparative scale biocatalytic production of L-glyceraldehyde was established within this thesis.
Moreover, the three-dimensional structure of GlyDH was also successfully solved during the course of this thesis. Based on this structure, molecular mechanisms that explain the substrate preference and the enantioselectivity of GlyDH were deduced.

Overall, the scope of biocatalytic routes for the production of chiral building blocks was expanded by the identification of new oxidoreductases in this thesis. Moreover, the biocatalytic access to L-glyceraldehyde, a key chiral building block, was facilitated.

8 REFERENCES

[1] **Faber, K.,** *Biotransformations in organic chemistry*, 5th Edn. Springer-Verlag, Berlin: 2004.

[2] **Crossley, R.** The relevance of chirality to the study of biological activity. *Tetrahedron* 1992. **48**: 8155-8178.

[3] **De Camp, W. H.** The FDA perspective on the development of stereoisomers. *Chirality* 1989. **1**: 2-6.

[4] Fda Policy Statement for the Development of New Stereoisomeric Drugs. *Chirality* 1992. **4**: 338-340.

[5] **Rouhi, A. M.** Chiral roundup *Chem. Eng. News* 2002. **80**: 43-50.

[6] **Rouhi, A. M.** Chiral chemistry. *Chem. Eng. News* 2004. **82**: 47-62.

[7] **Rouhi, A. M.** Chirality at work. *Chem. Eng. News* 2003. **81**: 56-61.

[8] **Agranat, I., Caner, H. and Caldwell, A.** Putting chirality to work: The strategy of chiral switches. *Nat. Rev. Drug. Discov.* 2002. **1**: 753-768.

[9] **Breuer, M., Ditrich, K., Habicher, T., Hauer, B., Keßeler, M., Stürmer, R. and Zelinski, T.** Industrial methods for the production of optically active intermediates. *Angew. Chem.-Int. Edit.* 2004. **43**: 788-824.

[10] **Ghanem, A. and Aboul-Enein, H. Y.** Application of lipases in kinetic resolution of racemates. *Chirality* 2005. **17**: 1-15.

[11] **Hilterhaus, L. and Liese, A.** Building blocks. *Adv. Biochem. Engin./Biotechnol.* 2007. **105**: 133-173.

[12] **Santaniello, E., Ferraboschi, P., Grisenti, P. and Manzocchi, A.** The biocatalytic approach to the preparation of enantiomerically pure chiral building blocks. *Chem. Rev.* 1992. **92**: 1071-1140.

[13] **Areces, P., Carrasco, E., Light, M. E., Santos, M. and Plumet, J.** Synthesis of enantiopure 4-(dihydroxyalkyl)-β-lactams from D-mannitol using Ley's BDA-protected L-glyceraldehyde. *Synlett* 2007: 3180-3182.

[14] **Bi, J. and Aggarwal, V. K.** Application of furyl-stabilized sulfur ylides to a concise synthesis of 8a-epi-swainsonine. *Chem. Commun.* 2008: 120-122.

[15] **Bull, J. A., Balskus, E. P., Horan, R. A. J., Langner, M. and Ley, S. V.** Total synthesis of potent antifungal marine bisoxazole natural products bengazoles A and B. *Chem. Eur. J.* 2007. **13**: 5515-5538.

[16] **Kumar, I., Bhide, S. R. and Rode, C. V.** Asymmetric synthesis of a 3,4-substituted pyrrolidine by L-proline catalyzed direct enolexo aldolization. *Tetrahedron Asymmetry* 2007. **18**: 1210-1216.

[17] **Jurczak, J., Pikul, S. and Bauer, T.** *(R)*-2,3-O-isopropylideneglyceraldehyde and *(S)*-2,3-O-isopropylideneglyceraldehyde in stereoselective organic-synthesis. *Tetrahedron* 1986. **42**: 447-488.

[18] **Baer, E. and Fischer, H. O. L.** Studies on acetone-glyceraldehyde IV. Preparation of D(+)- acetone glycerol. *J. Biol. Chem.* 1939. **128**: 463-473.

[19] **Andrews, G. C., Crawford, T. C. and Bacon, B. E.** Stereoselective, catalytic reduction of L-ascorbic acid: A convenient synthesis of L-gulono-1,4-lactone. *J. Org. Chem.* 1981. **46**: 2976-2977.

[20] **Schmid, C. R. and Bryant, J. D.** D-(*R*)-glyceraldehyde acetonide - (1,3-dioxolane-4-carboxaldehyde, 2,2-dimethyl-, (*R*)-). *Organic. Synth.* 1995. **72**: 6-13.

[21] **Hubschwerlen, C.** A convenient synthesis of L-(*S*)-glyceraldehyde acetonide from L-ascorbic acid. *Synthesis* 1986: 962-964.

[22] **Hubschwerlen, C., Specklin, J. L. and Higelin, J.** L-(*S*)-glyceraldehyde acetonide - (1,3-dioxolane-4-carboxaldehyde, 2,2-dimethyl-, (*S*)-). *Organic. Synth.* 1995. **72**: 1-5.

[23] **Patel, R. N.** Synthesis of chiral pharmaceutical intermediates by biocatalysis. *Coord. Chem. Rev.* 2008. **252**: 659-701.

[24] **Pollard, D. J. and Woodley, J. M.** Biocatalysis for pharmaceutical intermediates: the future is now. *Trends Biotechnol.* 2007. **25**: 66-73.

[25] **Patel, R. N.** Biocatalysis: Synthesis of chiral intermediates for drugs. *Curr. Opin. Drug. Discov. Dev.* 2006. **9**: 741-764.

[26] **Tao, J. H. and Xu, J. H.** Biocatalysis in development of green pharmaceutical processes. *Curr. Opin. Chem. Biol.* 2009. **13**: 43-50.
[27] **Daußmann, T., Hennemann, H. G., Rosen, T. C. and Dünkelmann, P.** Enzymatic technologies for the synthesis of chiral alcohol derivatives. *Chem. Ing. Tech.* 2006. **78**: 249-255.
[28] **Faber, K. and Kroutil, W.** New enzymes for biotransformations. *Curr. Opin. Chem. Biol.* 2005. **9**: 181-187.
[29] **Hudlicky, T. and Reed, J. W.** Applications of biotransformations and biocatalysis to complexity generation in organic synthesis. *Chem. Soc. Rev.* 2009. **38**: 3117-3132.
[30] **Nakamura, K., Yamanaka, R., Matsuda, T. and Harada, T.** Recent developments in asymmetric reduction of ketones with biocatalysts. *Tetrahedron Asymmetry* 2003. **14**: 2659-2681.
[31] **Straathof, A. J. J., Panke, S. and Schmid, A.** The production of fine chemicals by biotransformations. *Curr. Opin. Biotechnol.* 2002. **13**: 548-556.
[32] **Buchholz, K., Kasche, V. and Bornscheuer, U. T.,** *Biocatalysts and enzyme technology*. Wiley-VCH, Weinheim: 2005.
[33] **Rosenthaler, L.** Enzyme effected asymmetrical synthesis. *Biochem. Z.* 1908. **14**: 238-253.
[34] **Leggewie, C., Puls, M. and Eggert, T.** Identification and expression of new biocatalysts. *Chem. Ing. Tech.* 2010. **82**: 27-34.
[35] **Bornscheuer, U. T. and Buchholz, K.** Highlights in biocatalysis - Historical landmarks and current trends. *Eng. Life Sci.* 2005. **5**: 309-323.
[36] **Cohen, S. N., Chang, A. C. Y., Boyer, H. W. and Helling, R. B.** Construction of biologically functional bacterial plasmids *in vitro*. *Proc. Nat. Acad Sci. USA* 1973. **70**: 3240-3244.
[37] **Kirk, O., Borchert, T. V. and Fuglsang, C. C.** Industrial enzyme applications. *Curr. Opin. Biotechnol.* 2002. **13**: 345-351.
[38] **Hodgson, J.** The changing bulk biocatalyst market. *Biotechnology (N.Y.)* 1994. **12**: 789-790.
[39] **Schoemaker, H. E., Mink, D. and Wubbolts, M. G.** Dispelling the myths - Biocatalysis in industrial synthesis. *Science* 2003. **299**: 1694-1697.
[40] **Schmid, A., Dordick, J. S., Hauer, B., Kiener, A., Wubbolts, M. and Witholt, B.** Industrial biocatalysis today and tomorrow. *Nature* 2001. **409**: 258-268.
[41] **Müller, M., Wolberg, M., Schubert, T. and Hummel, W.** Enzyme-catalyzed regio- and enantioselective ketone reductions. *Adv. Biochem. Engin. / Biotechnol.* 2005. **92**: 261-287.
[42] **Wolberg, M., Filho, M. V., Bode, S., Geilenkirchen, P., Feldmann, R., Liese, A., Hummel, W. and Müller, M.** Chemoenzymatic synthesis of the chiral side-chain of statins: Application of an alcohol dehydrogenase catalysed ketone reduction on a large scale. *Bioprocess Biosyst. Eng.* 2008. **31**: 183-191.
[43] **Baer, K., Krausser, M., Burda, E., Hummel, W., Berkessel, A. and Gröger, H.** Sequential and modular synthesis of chiral 1,3-diols with two stereogenic centers: Access to all four stereoisomers by combination of organo- and biocatalysis. *Angew. Chem. Int. Ed.* 2009. **48**: 9355-9358.
[44] **Menger, F. M.** Enzyme reactivity from an organic perspective. *Acc. Chem. Res.* 1993. **26**: 206-212.
[45] **Eigen, M. and Hammes, G. G.** Elementary steps in enzyme reactions *Adv. Enzymol. Relat. Areas Mol. Biol.* 1963. **25**: 1-38.
[46] **Schäfer, T., Borchert, T. W., Nielsen, V. S., Skagerlind, P., Gibson, K., Wenger, K., Hatzack, F., Nilsson, L. D., Salmons, S., Pedersen, S., Heldt-Hansen, H. P., Poulsen, P. B., Lund, H., Oxenboll, K. M., Wu, G. F., Pedersen, H. H. and Xu, H.** Industrial enzymes. *Adv. Biochem. Engin./ Biotechnol.* 2007. **105**: 59-131.
[47] **Weckbecker, A., Gröger, H. and Hummel, W.** Regeneration of nicotinamide coenzymes: Principles and applications for the synthesis of chiral compounds. *Adv. Biochem. Engin./ Biotechnol.* 2010.

[48] **Wichmann, R. and Vasic-Racki, D.** Cofactor regeneration at the lab scale. *Adv. Biochem. Engin. / Biotechnol.* 2005. **92**: 225-260.

[49] **Allen, S. J. and Holbrook, J. J.** Production of an activated form of *Bacillus stearothermophilus* L-2-hydroxyacid dehydrogenase by directed evolution. *Protein Eng.* 2000. **13**: 5-7.

[50] **Yuryev, R. and Liese, A.** Biocatalysis: The Outcast. *ChemCatChem* 2010. **2**: 103-107.

[51] **Sarett, L. H.** Partial synthesis of pregnene-4-triol-17(β),20(β),21-dione-3,11 and pregnene-4-diol-17(β),21-trione-3,11,20 monoacetate. *J. Biol. Chem.* 1946. **162**: 601-631.

[52] **Wills, M. and Hannedouche, J.** New methodology for the asymmetric reduction of ketones. *Curr. Opin. Drug. Discov. Devel.* 2002. **5**: 881-891.

[53] **Stewart, J. D.** Dehydrogenases and transaminases in asymmetric synthesis. *Curr. Opin. Chem. Biol.* 2001. **5**: 120-129.

[54] **Goldberg, K., Schroer, K., Lütz, S. and Liese, A.** Biocatalytic ketone reduction - A powerful tool for the production of chiral alcohols - Part I: processes with isolated enzymes. *Appl. Microbiol. Biotechnol.* 2007. **76**: 237-248.

[55] **Patel, R. N.** Biocatalysis: Synthesis of chiral intermediates for pharmaceuticals. *Curr. Org. Chem.* 2006. **10**: 1289-1321.

[56] **Turner, N. J.** Applications of transketolases in organic synthesis. *Curr. Opin. Chem. Biol.* 2000. **11**: 527-531.

[57] **Andexer, J. N., Langermann, J. V., Kragl, U. and Pohl, M.** How to overcome limitations in biotechnological processes - Examples from hydroxynitrile lyase applications. *Trends Biotechnol.* 2009. **27**: 599-607.

[58] **Dean, S. M., Greenberg, W. A. and Wong, C. H.** Recent advances in aldolase-catalyzed asymmetric synthesis. *Adv. Synth. Catal.* 2007. **349**: 1308-1320.

[59] **Vasic-Racki, D., Jonas, M., Wandrey, C., Hummel, W. and Kula, M. R.** Continuous *(R)*-mandelic acid production in an enzyme membrane reactor. *Appl. Microbiol. Biotechnol.* 1989. **31**: 215-222.

[60] **Bommarius, A. S., Schwarm, M. and Drauz, K.** Biocatalysis to amino acid-based chiral pharmaceuticals - Examples and perspectives. *J. Mo.l Catal. B Enzym* 1998. **5**: 1-11.

[61] **Galkin, A., Kulakova, L., Yoshimura, T., Soda, K. and Esaki, N.** Synthesis of optically active amino acids from α-keto acids with *Escherichia coli* cells expressing heterologous genes. *Appl. Environ. Microbiol.* 1997. **63**: 4651-4656.

[62] **Menzel, A., Werner, H., Altenbuchner, J. and Gröger, H.** From enzymes to "designer bugs" in reductive amination: A new process for the synthesis of L-*tert*-leucine using a whole cell-catalyst. *Eng. Life. Sci.* 2004. **4**: 573-576.

[63] **He, C. M., Chang, D. L. and Zhang, J.** Asymmetric reduction of substituted α- and β-ketoesters by *Bacillus pumilus* Phe-C3. *Tetrahedron Asymmetry* 2008. **19**: 1347-1351.

[64] **Zhu, D. M., Stearns, J. E., Ramirez, M. and Hua, L.** Enzymatic enantioselective reduction of α-ketoesters by a thermostable 7 α-hydroxysteroid dehydrogenase from *Bacteroides fragilis*. *Tetrahedron* 2006. **62**: 4535-4539.

[65] **Zhu, D. M., Yang, Y., Buynak, J. D. and Hua, L.** Stereoselective ketone reduction by a carbonyl reductase from *Sporobolomyces salmonicolor*. Substrate specificity, enantioselectivity and enzyme-substrate docking studies. *Org. Biomol. Chem.* 2006. **4**: 2690-2695.

[66] **Gröger, H., Hummel, W., Rollmann, C., Chamouleau, F., Hüsken, H., Werner, H., Wunderlich, C., Abokitse, K., Drauz, K. and Buchholz, S.** Preparative asymmetric reduction of ketones in a biphasic medium with an *(S)*-alcohol dehydrogenase under in situ-cofactor-recycling with a formate dehydrogenase. *Tetrahedron* 2004. **60**: 633-640.

[67] **Liese, A., Zelinski, T., Kula, M. R., Kierkels, H., Karutz, M., Kragl, U. and Wandrey, C.** A novel reactor concept for the enzymatic reduction of poorly soluble ketones. *J. Mol. Catal. B Enzym* 1998. **4**: 91-99.

[68] **Pollard, D., Truppo, M., Pollard, J., Chen, C. Y. and Moore, J.** Effective synthesis of *(S)*-3,5-bistrifluoromethylphenyl ethanol by asymmetric enzymatic reduction. *Tetrahedron Asymmetry* 2006. **17**: 554-559.

[69] **Pollard, D. J., Telari, K., Lane, J., Humphrey, G., McWilliams, C., Nidositko, S., Salmon, P. and Moore, J.** Asymmetric reduction of α, β-unsaturated ketone to *(R)* allylic alcohol by *Candida chilensis*. *Biotechnol. Bioeng.* 2006. **93**: 674-686.

[70] **Röthig, T. R., Kulbe, K. D., Bückmann, F. and Carrea, G.** Continuous coenzyme-dependent stereoselective synthesis of sulcatol by alcohol-dehydrogenase. *Biotechnol. Letters* 1990. **12**: 353-356.

[71] **Schubert, T., Hummel, W., Kula, M. R. and Müller, M.** Enantioselective synthesis of both enantiomers of various propargylic alcohols by use of two oxidoreductases. *Eur. J. Org. Chem.* 2001: 4181-4187.

[72] **Kroutil, W., Mang, H., Edegger, K. and Faber, K.** Biocatalytic oxidation of primary and secondary alcohols. *Adv. Synth. Catal.* 2004. **346**: 125-142.

[73] **Matsuyama, A., Yamamoto, H., Kawada, N. and Kobayashi, Y.** Industrial production of *(R)*-1,3-butanediol by new biocatalysts. *J. Mol. Catal. B-Enzym* 2001. **11**: 513-521.

[74] **De Muynck, C., Pereira, C., Soetaert, W. and Vandamme, E.** Dehydrogenation of ribitol with *Gluconobacter oxydans*: Production and stability of L-ribulose. *J. Biotechnol.* 2006. **125**: 408-415.

[75] **Muniruzzaman, S., Tokunaga, H. and Izumori, K.** Isolation of *Enterobacter agglomerans* strain 221e from soil, a potent D-tagatose producer from galactitol. *J. Ferment. Bioeng.* 1994. **78**: 145-148.

[76] **Yamamoto, H., Kawada, K., Matsuyama, A. and Kobayashi, Y.** Cloning and expression in *Escherichia coli* of a gene coding for a secondary alcohol dehydrogenase from *Candida parapsilosis*. *Biosci. Biotechnol. Biochem.* 1999. **63**: 1051-1055.

[77] **Hummel, W. and Riebel, B.** Chiral alcohols by enantioselective enzymatic oxidation. *Enzyme Engin. XIII* 1996. **799**: 713-716.

[78] **Liese, A., Karutz, M., Kamphuis, J., Wandrey, C. and Kragl, U.** Enzymatic resolution of 1-phenyl-1,2-ethanediol by enantioselective oxidation: Overcoming product inhibition by continuous extraction. *Biotechnol. Bioeng.* 1996. **51**: 544-550.

[79] **Geueke, B., Riebel, B. and Hummel, W.** NADH oxidase from *Lactobacillus brevis*: A new catalyst for the regeneration of NAD. *Enzyme Microb. Technol.* 2003. **32**: 205-211.

[80] **Lemiere, G. L., Lepoivre, J. A. and Alderweireldt, F. C.** HLADH-catalyzed oxidations of alcohols with acetaldehyde as a coenzyme recycling substrate. *Tetrahedron Lett.* 1985. **26**: 4527-4528.

[81] **Lee, L. G. and Whitesides, G. M.** Preparation of optically active 1,2-diols and α-hydroxy ketones using glycerol dehydrogenase as catalyst: Limits to enzyme-catalyzed synthesis due to noncompetitive and mixed inhibition by product. *J. Org. Chem.* 1986. **51**: 25-36.

[82] **Carrea, G., Bovara, R., Cremonesi, P. and Lodi, R.** Enzymatic preparation of 12-ketochenodeoxycholic acid with NADP regeneration. *Biotechnol. Bioeng.* 1984. **26**: 560-563.

[83] **Hummel, W., Kuzu, M. and Geueke, B.** An efficient and selective enzymatic oxidation system for the synthesis of enantiomerically pure D-tert-leucine. *Org. Lett.* 2003. **5**: 3649-3650.

[84] **Blaser, H. U., Malan, C., Pugin, B., Spindler, F., Steiner, H. and Studer, M.** Selective hydrogenation for fine chemicals: Recent trends and new developments. *Adv. Synth. Catal.* 2003. **345**: 103-151.

[85] **Goswami, J., Bezbaruah, R. L., Goswami, A. and Borthakur, N.** A convenient stereoselective synthesis of (*R*)-(-)-denopamine and (*R*)-(-)-salmeterol. *Tetrahedron Asymmetry* 2002. **12**: 3343-3348.

[86] **Exner, C., Pfaltz, A., Studer, M. and Blaser, H. U.** Heterogeneous enantioselective hydrogenation of activated ketones catalyzed by modified Pt-

catalysts: A systematic structure-selectivity study. *Adv. Synth. Catal.* 2003. **345**: 1253-1260.

[87] **Kataoka, M., Kotaka, A., Hasegawa, A., Wada, M., Yoshizumi, A., Nakamori, S. and Shimizu, S.** Old Yellow Enzyme from *Candida macedoniensis* catalyzes the stereospecific reduction of the C=C bond of ketoisophorone. *Biosci. Biotechnol. Biochem.* 2002. **66**: 2651-2657.

[88] **Leuenberger, H. G. W., Boguth, W., Widmer, E. and Zell, R.** Synthesis of optically active natural carotenoids and structurally related compounds I. Synthesis of chiral key compound (4*R*,6*R*)-4-hydroxy-2,2,6-trimethylcyclohexanone. *Helv. Chim. Acta* 1976. **59**: 1832-1849.

[89] **Wegner, G., Kaibel, G., Therre, J., Aquila, W. and Fuchs, H.,** Citral preparation in high yield, for use e.g. as intermediate for perfumes or vitamins, by 6-stage process from isobutene and formaldehyde via isoprenol, prenal and prenol. BASF AG 2008.

[90] **Trasarti, A. F., Marchi, A. J. and Apesteguia, C. R.** Highly selective synthesis of menthols from citral in a one-step process. *J. Catal.* 2004. **224**: 484-488.

[91] **Goussevskaia, E. V., Robles Dutenhfner, P. A. and Da Silva Rocha, K. A.,** Catalytic production of isopulegol by cyclizing of citronelal comprises application of hetero polyacid as catalyst in menthol precursor preparation. Univ Federal Minas Gerais 2007.

[92] **Hall, M., Hauer, B., Stuermer, R., Kroutil, W. and Faber, K.** Asymmetric whole-cell bioreduction of an α,β-unsaturated aldehyde (citral): competing prim-alcohol dehydrogenase and C-C lyase activities. *Tetrahedron Asymmetry* 2006. **17**: 3058-3062.

[93] **Yin, B., Yang, X. P., Wei, G. D., Ma, Y. S. and Wei, D. Z.** Expression of two old yellow enzyme homologues from *Gluconobacter oxydans* and identification of their citral hydrogenation abilities. *Mol. Biotechnol.* 2008. **38**: 241-245.

[94] **Sambaiah, T., Fanwick, P. E. and Cushman, M.** Investigation of an unexpected addition reaction that occurs when 2,3: 4,5-di-O-isopropylidene-D-ribose diethyl dithioacetal is treated with mercuric oxide and mercuric chloride. *J. Org. Chem.* 2001. **66**: 4405-4408.

[95] **Pearson, M. S. M., Plantier-Royon, R., Szymoniak, J., Bertus, P. and Behr, J. B.** Synthesis of a 5-spirocyclopropyl deoxyrhamnojirimycin as a constrained naringinase inhibitor. *Synthesis* 2007: 3589-3594.

[96] **Banwell, M. G., De Savi, C., Hockless, D. C. R., Pallich, S. and Watson, K. G.** Syntheses of the D-aldopentoses from non-carbohydrate sources. *Synlett* 1999: 885-888.

[97] **Tang, C. J. and Wu, Y. K.** On the synthesis of cepacin A. *Tetrahedron* 2007. **63**: 4887-4906.

[98] **Sheldon, R. A. and Arends, I.** Organocatalytic oxidations mediated by nitroxyl radicals. *Adv. Synth. Catal.* 2004. **346**: 1051-1071.

[99] **Burton, S. G.** Oxidizing enzymes as biocatalysts. *Trends Biotechnol.* 2003. **21**: 543-549.

[100] **Kroutil, W., Mang, H., Edegger, K. and Faber, K.** Recent advances in the biocatalytic reduction of ketones and oxidation of *sec*-alcohols. *Curr. Opini. Chem. Biol.* 2004. **8**: 120-126.

[101] **Faber, K. and Patel, R.** Chemical biotechnology. A happy marriage between chemistry and biotechnology: Asymmetric synthesis *via* green chemistry *Curr. Opin. Biotechnol.* 2000. **11**: 517-519.

[102] **Ogawa, J. and Shimizu, S.** Industrial microbial enzymes: Their discovery by screening and use in large-scale production of useful chemicals in Japan. *Curr. Opin. Biotechnol.* 2002. **13**: 367-375.

[103] **Asano, Y.** Overview of screening for new microbial catalysts and their uses in organic synthesis - Selection and optimization of biocatalysts. *J. Biotechnol.* 2002. **94**: 65-72.

[104] **Lorenz, P., Liebeton, K., Niehaus, F., Schleper, C. and Eck, J.** The impact of non-cultivated biodiversity on enzyme discovery and evolution. *Biocat. Biotransf.* 2003. **21**: 87-91.

[105] **Beloqui, A., Pita, M., Polaina, J., Martinez-Arias, A., Golyshina, O. V., Zumarraga, M., Yakimov, M. M., Garcia-Arellano, H., Alcalde, M., Fernandez, V. M., Elborough, K., Andreu, J. M., Ballesteros, A., Plou, F. J., Timmis, K. N., Ferrer, M. and Golyshin, P. N.** Novel polyphenol oxidase mined from a metagenome expression library of bovine rumen - Biochemical properties, structural analysis, and phylogenetic relationships. *J. Biol. Chem.* 2006. **281**: 22933-22942.

[106] **Robertson, D. E., Chaplin, J. A., DeSantis, G., Podar, M., Madden, M., Chi, E., Richardson, T., Milan, A., Miller, M., Weiner, D. P., Wong, K., McQuaid, J., Farwell, B., Preston, L. A., Tan, X. Q., Snead, M. A., Keller, M., Mathur, E., Kretz, P. L., Burk, M. J. and Short, J. M.** Exploring nitrilase sequence space for enantioselective catalysis. *Appl. Environ. Microbiol.* 2004. **70**: 2429-2436.

[107] **Pottkämper, J., Barthen, P., Ilmberger, N., Schwaneberg, U., Schenk, A., Schulte, M., Ignatiev, N. and Streit, W. R.** Applying metagenomics for the identification of bacterial cellulases that are stable in ionic liquids. *Green Chem.* 2009. **11**: 957-965.

[108] **Wackett, L. P.** Novel biocatalysis by database mining. *Curr. Opin. Chem. Biol.* 2004. **15**: 280-284.

[109] **Labesse, G.** MulBlast 1.0: A multiple alignment of BLAST output to boost protein sequence similarity analysis. *Comput. Appl. Biosci.* 1996. **12**: 463-467.

[110] **Reetz, M. T.** Controlling the enantioselectivity of enzymes by directed evolution: Practical and theoretical ramifications. *Proc. Nat. Acad Sci. USA* 2004. **101**: 5716-5722.

[111] **Fox, R. J., Davis, S. C., Mundorff, E. C., Newman, L. M., Gavrilovic, V., Ma, S. K., Chung, L. M., Ching, C., Tam, S., Muley, S., Grate, J., Gruber, J., Whitman, J. C., Sheldon, R. A. and Huisman, G. W.** Improving catalytic function by ProSAR-driven enzyme evolution. *Nat. Biotechnol.* 2007. **25**: 338-344.

[112] **Labrou, N. E.** Random mutagenesis methods for in vitro directed enzyme evolution. *Curr. Protein Pept. Sci.* 2010. **11**: 91-100.

[113] **Woodyer, R., van der Donk, W. A. and Zhao, H. M.** Optimizing a biocatalyst for improved NAD(P)H regeneration: Directed evolution of phosphite dehydrogenase. *Comb. Chem. High Throughput Screen.* 2006. **9**: 237-245.

[114] **Bornscheuer, U. T. and Pohl, M.** Improved biocatalysts by directed evolution and rational protein design. *Curr. Opin. Chem. Biol.* 2001. **5**: 137-143.

[115] **Reetz, M. T., Bocola, M., Carballeira, J. D., Zha, D. X. and Vogel, A.** Expanding the range of substrate acceptance of enzymes: Combinatorial active-site saturation test. *Angew. Chem. Int. Ed.* 2005. **44**: 4192-4196.

[116] **Reetz, M. T., Carballeira, J. D., Peyralans, J., Hobenreich, H., Maichele, A. and Vogel, A.** Expanding the substrate scope of enzymes: Combining mutations obtained by CASTing. *Chem. Eur. J.* 2006. **12**: 6031-6038.

[117] **Reetz, M. T.** Directed evolution of enantioselective enzymes: An unconventional approach to asymmetric catalysis in organic chemistry. *J. Org. Chem.* 2009. **74**: 5767-5778.

[118] **Bougioukou, D. J., Kille, S., Taglieber, A. and Reetz, M. T.** Directed evolution of an enantioselective enoate reductase: Testing the utility of iterative saturation mutagenesis. *Adv. Synth. Catal.* 2009. **351**: 3287-3305.

[119] **Tee, K. L. and Schwaneberg, U.** Directed evolution of oxygenases: Screening systems, success stories and challenges. *Comb. Chem. High Throughput Screen.* 2007. **10**: 197-217.

[120] **Arnold, F. H. and Georgiou, G.,** *Directed evolution library creation*. Humana Press, Totowa, New Jersey: 2003.

[121] **Shivange, A. V., Marienhagen, J., Mundhada, H., Schenk, A. and Schwaneberg, U.** Advances in generating functional diversity for directed protein evolution. *Curr. Opin. Chem. Biol.* 2009. **13**: 19-25.

[122] **Holmberg, N., Ryde, U. and Bülow, L.** Redesign of the coenzyme specificity in L-lactate dehydrogenase from *Bacillus stearothermophilus* using site-directed mutagenesis and media engineering. *Protein Eng.* 1999. **12**: 851-856.

[123] **Flores, H. and Ellington, A. D.** A modified consensus approach to mutagenesis inverts the cofactor specificity of *Bacillus stearothermophilus* lactate dehydrogenase. *Protein Eng. Des. Sel.* 2005. **18**: 369-377.
[124] **Feeney, R., Clarke, A. R. and Holbrook, J. J.** A single amino acid substitution in lactate dehydrogenase improves the catalytic efficiency with an alternative coenzyme. *Biochem. Biophys. Res. Commun.* 1990. **166**: 667-672.
[125] **Rosell, A., Valencia, E., Ochoa, W. F., Fita, I., Pares, X. and Farres, J.** Complete reversal of coenzyme specificity by concerted mutation of three consecutive residues in alcohol dehydrogenase. *J. Biol. Chem.* 2003. **278**: 40573-40580.
[126] **Gul-Karaguler, N., Sessions, R. B., Clarke, A. R. and Holbrook, J. J.** A single mutation in the NAD-specific formate dehydrogenase from *Candida methylica* allows the enzyme to use NADP. *Biotechnol. Lett.* 2001. **23**: 283-287.
[127] **Chen, R. D., Greer, A. and Dean, A. M.** Redesigning secondary structure to invert coenzyme specificity in isopropylmalate dehydrogenase. *Proc. Natl. Acad. Sci. USA* 1996. **93**: 12171-12176.
[128] **Wu, W. H., Zhu, D. M. and Hua, L.** Site-saturation mutagenesis of formate dehydrogenase from *Candida bodinii* creating effective $NADP^+$-dependent FDH enzymes. *J. Mol. Catal. B-Enzymatic* 2009. **61**: 157-161.
[129] **Bubner, P., Klimacek, M. and Nidetzky, B.** Structure-guided engineering of the coenzyme specificity of *Pseudomonas fluorescens* mannitol 2-dehydrogenase to enable efficient utilization of NAD(H) and NADP(H). *FEBS Lett.* 2008. **582**: 230-234.
[130] **Leitgeb, S., Petschacher, B., Wilson, D. K. and Nidetzky, B.** Fine tuning of coenzyme specificity in family 2 aldo-keto reductases revealed by crystal structures of the Lys-274 -> Arg mutant of *Candida tenuis* xylose reductase (AKR2B5) bound to NAD^+ and $NADP^+$. *FEBS Lett.* 2005. **579**: 763-767.
[131] **Scrutton, N. S., Berry, A. and Perham, R. N.** Redesign of the coenzyme specificity of a dehydrogenase by protein engineering. *Nature* 1990. **343**: 38-43.
[132] **Andreadeli, A., Platis, D., Tishkov, V., Popov, V. and Labrou, N. E.** Structure-guided alteration of coenzyme specificity of formate dehydrogenase by saturation mutagenesis to enable efficient utilization of $NADP^+$. *Eur. J. Biochem.* 2008. **275**: 3859-3869.
[133] **Machielsen, R., Looger, L. L., Raedts, J., Dijkhuizen, S., Hummel, W., Hennemann, H. G., Daussmann, T. and Van der Oost, J.** Cofactor engineering of *Lactobacillus brevis* alcohol dehydrogenase by computational design. *Eng. Life Sci.* 2009. **9**: 38-44.
[134] **Clermont, S., Corbier, C., Mely, Y., Gerard, D., Wonacott, A. and Branlant, G.** Determinants of coenzyme specificity in glyceraldehyde-3-phosphate dehydrogenase: Role of the acidic residue in the fingerprint region of the nucleotide binding fold. *Biochemistry* 1993. **32**: 10178-10184.
[135] **Carugo, O. and Argos, P.** NADP-dependent enzymes 2. Evolution of the mono- and dinucleotide binding domains. *Proteins* 1997. **28**: 29-40.
[136] **Carugo, O. and Argos, P.** NADP-dependent enzymes 1: Conserved stereochemistry of cofactor binding. *Proteins* 1997. **28**: 10-28.
[137] **Andexer, J., Guterl, J. K., Pohl, M. and Eggert, T.** A high-throughput screening assay for hydroxynitrile lyase activity. *Chem. Commun.* 2006: 4201-4203.
[138] **Williams, G. J. and Thorson, J. S.** A high-throughput fluorescence-based glycosyltransferase screen and its application in directed evolution. *Nat. Protoc.* 2008. **3**: 357-362.
[139] **Reymond, J. L. and Babiak, P.,** Screening systems *White Biotechnology* 2007, pp 31-58.
[140] **Bustos-Jaimes, I., Hummel, W., Eggert, T., Bogo, E., Puls, M., Weckbecker, A. and Jaeger, K.-E.** A high-troughput sreening method for chiral alcohols and its application to determine enantioselectivity of lipases and esterases. *ChemCatChem* 2009. **1**: 445-448.

[141] **Felber, S.,** Optimierung der NAD-abhängigen Formiatdehydrogenase aus *Candida boidinii* für den Einsatz in der Biokatalyse. Heinrich Heine-Universität Düsseldorf 2001.

[142] **Henning, H., Leggewie, C., Pohl, M., Müller, M., Eggert, T. and Jaeger, K. E.** Identification of novel benzoylformate decarboxylases by growth selection. *Appl. Environ. Microbiol.* 2006. **72**: 7510-7517.

[143] **Zhu, L. L., Tee, K. L., Roccatano, D., Sonmez, B., Ni, Y., Sun, Z. H. and Schwaneberg, U.** Directed evolution of an antitumor drug (arginine deiminase PpADI) for increased activity at physiological pH. *ChemBioChem* 2010. **11**: 691-697.

[144] **Schliessmann, A., Hidalgo, A., Berenguer, J. and Bornscheuer, U. T.** Increased enantioselectivity by engineering bottleneck mutants in an esterase from *Pseudomonas fluorescens*. *ChemBioChem* 2009. **10**: 2920-2923.

[145] **Jones, J. B., Lewis, A. J., Sneddon, D. W. and Higgins, W.** Preparative-scale reductions of cyclic ketone and aldehyde substrates of horse liver alcohol dehydrogenase with *in situ* sodium dithionite bicycling of catalytic amounts of NAD. *J. Chem. Soc. Chem. Commun.* 1972: 856-857.

[146] **Nakamura, K. and Yamanaka, R.** Light-mediated regulation of asymmetric reduction of ketones by a cyanobacterium. *Tetrahedron Asymmetry* 2002. **13**: 2529-2533.

[147] **Nakamura, K. and Yamanaka, R.** Light mediated cofactor recycling system in biocatalytic asymmetric reduction of ketone. *Chem. Commun.* 2002: 1782-1783.

[148] **Aksu, S., Arends, I. W. C. E. and Hollmann, F.** A new regeneration system for oxidized nicotinamide cofactors. *Adv. Synth. Catal.* 2009. **351**: 1211-1216.

[149] **Komoschinski, J. and Steckhan, E.** Efficient indirect electrochemical *In situ* regeneration of NAD^+ and $NADP^+$ for enzymatic oxidations using iron bipyridine and phenanthroline complexes as redox catalysts. *Tetrahedron Lett.* 1988. **29**: 3299-3300.

[150] **Hollmann, F., Witholt, B. and Schmid, A.** $(Cp^*Rh(bpy)(H_2O))^{2+}$: A versatile tool for efficient and non-enzymatic regeneration of nicotinamide and flavin coenzymes. *J. Mol. Catal. B Enzym* 2002: 167-176.

[151] **Hollmann, F. and Schmid, A.** Electrochemical regeneration of oxidoreductases for cell-free biocatalytic redox reactions. *Biocatal. Biotransform.* 2004. **22**: 63-88.

[152] **Hummel, W.** Large-scale applications of NAD(P)-dependent oxidoreductases: Recent developments. *Trends Biotechnol.* 1999. **17**: 487-492.

[153] **Patel, R. N., Banerjee, A., McNamee, C. G., Brzozowski, D., Hanson, R. L. and Szarka, L. J.** Enantioselective microbial reduction of 3,5-dioxo-6-(benzyloxy) hexanoic acid, ethylester. *Enzyme Microb. Technol.* 1993. **15**: 1014-1021.

[154] **Tao, J. H. and McGee, K.** Development of a continuous enzymatic process for the preparation of (*R*)-3-(4-fluorophenyl)-2-hydroxy propionic acid. *Org. Process. Res. Dev.* 2002. **6**: 520-524.

[155] **Patel, R. N., McNamee, C. G., Banerjee, A., Howell, J. M., Robison, R. S. and Szarka, L. J.** Stereoselective reduction of β-Keto-Esters by *Geotrichum candidum*. *Enzyme Microb. Technol.* 1992. **14**: 731-738.

[156] **Yun, H., Yang, Y. H., Cho, B. K., Hwang, B. Y. and Kim, B. G.** Simultaneous synthesis of enantiomerically pure (*R*)-1-phenylethanol and (*R*)-α-methylbenzylamine from racemic α-methylbenzylamine using ω-transaminase/alcohol dehydrogenase/glucose dehydrogenase coupling reaction. *Biotechnol. Lett.* 2003. **25**: 809-814.

[157] **Bozic, M., Pricelius, S., Guebitz, G. M. and Kokol, V.** Enzymatic reduction of complex redox dyes using NADH-dependent reductase from *Bacillus subtilis* coupled with cofactor regeneration. *Appl. Microbiol. Biotechnol.* 2010. **85**: 563-571.

[158] **Kruse, W., Hummel, W. and Kragl, U.** Alcohol dehydrogenase-catalyzed production of chiral hydrophobic alcohols. A new approach leading to a nearly waste-free process. *Recl. Trav. Chim. Pays-Bas.* 1996. **115**: 239-243.

[159] **Wolberg, M., Hummel, W. and Müller, M.** Biocatalytic reduction of β,δ-diketo esters: A highly stereoselective approach to all four stereoisomers of a chlorinated β,δ-dihydroxy hexanoate. *Chem. Eur. J.* 2001. **7**: 4562-4571.

[160] **Wolberg, M., Ji, A. G., Hummel, W. and Müller, M.** Enzymatic reduction of hydrophobic β,δ-diketo esters. *Synthesis* 2001: 937-942.

[161] **Findrik, Z., Vasic-Racki, D., Lütz, S., Daußmann, T. and Wandrey, C.** Kinetic modeling of acetophenone reduction catalyzed by alcohol dehydrogenase from *Thermoanaerobacter* sp. *Biotechnol. Lett.* 2005. **27**: 1087-1095.

[162] **Hanson, R. L., Schwinden, M. D., Banerjee, A., Brzozowski, D. B., Chen, B. C., Patel, B. P., McNamee, C. G., Kodersha, G. A., Kronenthal, D. R., Patel, R. N. and Szarka, L. J.** Enzymatic synthesis of L-6-hydroxynorleucine. *Bioorg. Med. Chem.* 1999. **7**: 2247-2252.

[163] **Weckbecker, A. and Hummel, W.** Glucose dehydrogenase for the regeneration of NADPH and NADH. *Adv. Biochem. Engin. / Biotechnol.* 2005. **17**: 225-237.

[164] **Hanson, R. L., Schwinden, M. D., Banerjee, A., Brzozowski, D. B., Chen, B. C., Patel, B. P., McNamee, C. G., Kodersha, G. A., Kronenthal, D. R., Patel, R. N. and Szarka, L. J.** Enzymatic synthesis of L-6-hydroxynorleucine. *Bioorg Med Chem* 1999. **7**: 2247-2252.

[165] **Weckbecker, A. and Hummel, W.,** Glucose dehydrogenase for the regeneration of NADPH and NADH. In **Barredo, J. L.** (Ed.) *Meth in Biotechnology*. Humana Press Inc, Totowa, NJ 2005, pp 225-237.

[166] **Kataoka, M., Yamamoto, K., Kawabata, H., Wada, M., Kita, K., Yanase, H. and Shimizu, S.** Stereoselective reduction of ethyl 4-chloro-3-oxobutanoate by *Escherichia coli* transformant cells coexpressing the aldehyde reductase and glucose dehydrogenase genes. *Appl. Microbiol. Biotechnol.* 1999. **51**: 486-490.

[167] **Gröger, H., Chamouleau, F., Orologas, N., Rollmann, C., Drauz, K., Hummel, W., Weckbecker, A. and May, O.** Enantioselective reduction of ketones with "Designer cells" at high substrate concentrations: Highly efficient access to functionalized optically active alcohols. *Angew. Chem. Int. Ed.* 2006. **45**: 5677-5681.

[168] **Stampfer, W., Kosjek, B., Kroutil, W. and Faber, K.** On the organic solvent and thermostability of the biocatalytic redox system of *Rhodococcus ruber* DSM 44541. *Biotechnol. Bioeng.* 2003. **81**: 865-869.

[169] **Kosjek, B., Stampfer, W., van Deursen, R., Faber, K. and Kroutil, W.** Efficient production of raspberry ketone via 'green' biocatalytic oxidation. *Tetrahedron* 2003. **59**: 9517-9521.

[170] **Kosjek, B., Stampfer, W., Glueck, S. M., Pogorevc, M., Ellmer, U., Wallner, S. R., Koegl, M. F., Poessl, T. M., Mayer, S. F., Ueberbacher, B., Faber, K. and Kroutil, W.** Optimization of the organic solvent-stable asymmetric hydrogen transfer system of *Rhodococcus ruber* DSM 44541: an activity-growth study. *J. Mol. Catal. B Enzym* 2003. **22**: 1-6.

[171] **Monti, D., Ferrandi, E. E., Zanellato, I., Hua, L., Polentini, F., Carrea, G. and Riva, S.** One-pot multienzymatic synthesis of 12-ketoursodeoxycholic acid: Subtle cofactor specificities rule the reaction equilibria of five biocatalysts working in a row. *Adv. Synth. Catal.* 2009. **351**: 1303-1311.

[172] **Riva, S., Bovara, R., Zetta, L., Pasta, P., Ottolina, G. and Carrea, G.** Enzymatic α/β inversion of C-3 hydroxyl of bile acids and study of the effects of organic solvents on reaction rates. *J. Org. Chem.* 1988. **53**: 88-92.

[173] **Chenault, H. K. and Whitesides, G. M.** Lactate dehydrogenase-catalyzed regeneration of NAD from NADH for use in enzyme-catalyzed synthesis. *Bioorg. Chem.* 1989. **17**: 400-409.

[174] **Tomita, T., Kuzuyama, T. and Nishiyama, M.** Alteration of coenzyme specificity of lactate dehydrogenase from *Thermus thermophilus* by introducing the loop region of NADP(H)-dependent malate dehydrogenase. *Biosci. Biotechnol. Biochem.* 2006. **70**: 2230-2235.

[175] **Riebel, B. R., Gibbs, P. R., Wellborn, W. B. and Bommarius, A. S.** Cofactor regeneration of NAD^+ from NADH: Novel water-forming NADH oxidases. *Adv. Synth. Catal.* 2002. **344**: 1156-1168.

[176] **Hirano, J., Miyamoto, K. and Ohta, H.** Purification and characterization of thermostable H_2O_2-forming NADH oxidase from 2-phenylethanol-assimilating *Brevibacterium* sp KU1309. *Appl. Microbiol. Biotechnol.* 2008. **80**: 71-78.

[177] **Veronese, F. M., Nyc, J. F., Degani, Y., Brown, D. M. and Smith, E. L.** Nicotinamide adenine dinucleotide-specific glutamate dehydrogenase of *Neurospora J. Biol. Chem.* 1974. **249**: 7922-7928.

[178] **Sakamoto, N., Kotre, A. M. and Savageau, M. A.** Glutamate dehydrogenase from *Escherichia coli*: Purification and properties. *J. Bacteriol.* 1975. **124**: 775-783.

[179] **Haberland, J., Kriegesmann, A., Wolfram, E., Hummel, W. and Liese, A.** Diastereoselective synthesis of optically active (2*R*,5*R*)-hexanediol. *Appl. Microbiol. Biotechnol.* 2002. **58**: 595-599.

[180] **Braun, W., Calmuschi, B., Haberland, J., Hummel, W., Liese, A., Nickel, T., Stelzer, O. and Salzer, A.** Optically active phospholanes as substituents on ferrocene and chromium arene complexes. *Eur. J. Inorg. Chem.* 2004: 2235-2243.

[181] **Stampfer, W., Edegger, K., Kosjek, B., Faber, K. and Kroutil, W.** Simple biocatalytic access to enantiopure *(S)*-1-heteroarylethanols employing a microbial hydrogen transfer reaction. *Adv. Synth. Catal.* 2004. **346**: 57-62.

[182] **Stampfer, W., Kosjek, B., Faber, K. and Kroutil, W.** Biocatalytic asymmetric hydrogen transfer employing *Rhodococcus ruber* DSM 44541. *J. Org. Chem.* 2003. **68**: 402-406.

[183] **Patel, R. N., Goswami, A., Chu, L., Donovan, M. J., Nanduri, V., Goldberg, S., Johnston, R., Siva, P. J., Nielsen, B., Fan, J. Y., He, W. X., Shi, Z. P., Wang, K. W., Eiring, R., Cazzulino, D., Singh, A. and Mueller, R.** Enantioselective microbial reduction of substituted acetophenones. *Tetrahedron Asymmetry* 2004. **15**: 1247-1258.

[184] **Studier, F. W. and Moffatt, B. A.** Use of bacteriophage-T7 RNA-polymerase to direct selective high-level expression of cloned genes. *J. Mol.Biol.* 1986. **189**: 113-130.

[185] **Wilms, B., Wiese, A., Syldatk, C., Mattes, R. and Altenbuchner, J.** Development of an *Escherichia coli* whole-cell biocatalyst for the production of L-amino acids. *J. Biotechnol.* 2001. **86**: 19-30.

[186] **Ernst, M., Kaup, B., Müller, M., Bringer-Meyer, S. and Sahm, H.** Enantioselective reduction of carbonyl compounds by whole-cell biotransformation, combining a formate dehydrogenase and a *(R)*-specific alcohol dehydrogenase. *Appl. Microbiol. Biotechnol.* 2005. **66**: 629-634.

[187] **Weckbecker, A. and Hummel, W.** Improved synthesis of chiral alcohols with *Escherichia coli* cells co-expressing pyridine nucleotide transhydrogenase, $NADP^+$-dependent alcohol dehydrogenase and NAD^+-dependent formate dehydrogenase. *Biotechnol. Lett.* 2004. **26**: 1739-1744.

[188] **Gröger, H., May, O., Werner, H., Menzel, A. and Altenbuchner, J.** A "Second-Generation process" for the synthesis of L-neopentylglycine: Asymmetric reductive amination using a recombinant whole-cell catalyst. *Org. Process. Res. Dev.* 2006. **10**: 666-669.

[189] **Uzura, A., Nomoto, F., Sakoda, A., Nishimoto, Y., Kataoka, M. and Shimizu, S.** Stereoselective synthesis of *(R)*-3-quinuclidinol through asymmetric reduction of 3-quinuclidinone with 3-quinuclidinone reductase of *Rhodotorula rubra*. *Appl. Microbiol. Biotechnol.* 2009. **83**: 617-626.

[190] **Kataoka, M., Ishige, T., Urano, N., Nakamura, Y., Sakuradani, E., Fukui, S., Kita, S., Sakamoto, K. and Shimizu, S.** Cloning and expression of the L-1-amino-2-propanol dehydrogenase gene from *Rhodococcus erythropolis*, and its application to double chiral compound production. *Appl. Microbiol. Biotechnol.* 2008. **80**: 597-604.

[191] **Schroer, K., Mackfeld, U., Tana, I. A. W., Wandrey, C., Heuser, F., Bringer-Meyer, S., Weckbecker, A., Hummel, W., Daußmann, T., Pfaller, R., Liese, A. and Lütz, S.** Continuous asymmetric ketone reduction processes with recombinant *Escherichia coli*. *J. Biotechnol.* 2007. **132**: 438-444.

[192] **Girhard, M., Machida, K., Itoh, M., Schmid, R. D., Arisawa, A. and Urlacher, V. B.** Regioselective biooxidation of (+)-valencene by recombinant *E. coli* expressing CYP109B1 from *Bacillus subtilis* in a two-liquid-phase system. *Microb. Cell Fact.* 2009. **8**: Article No.: 36.

[193] **Liepins, J., Kuorelahti, S., Penttila, M. and Richard, P.** Enzymes for the NADPH-dependent reduction of dihydroxyacetone and D-glyceraldehyde and L-glyceraldehyde in the mould *Hypocrea jecorina*. *FEBS J.* 2006. **273**: 4229-4235.

[194] **Prust, C., Hoffmeister, M., Liesegang, H., Wiezer, A., Fricke, W. F., Ehrenreich, A., Gottschalk, G. and Deppenmeier, U.** Complete genome sequence of the acetic acid bacterium *Gluconobacter oxydans*. *Nat. Biotechnol.* 2005. **23**: 195-200.

[195] **Galagan, J. E., Calvo, S. E., Borkovich, K. A., Selker, E. U., Read, N. D., Jaffe, D., FitzHugh, W., Ma, L. J., Smirnov, S., Purcell, S., Rehman, B., Elkins, T., Engels, R., Wang, S. G., Nielsen, C. B., Butler, J., Endrizzi, M., Qui, D. Y., Ianakiev, P., Pedersen, D. B., Nelson, M. A., Werner-Washburne, M., Selitrennikoff, C. P., Kinsey, J. A., Braun, E. L., Zelter, A., Schulte, U., Kothe, G. O., Jedd, G., Mewes, W., Staben, C., Marcotte, E., Greenberg, D., Roy, A., Foley, K., Naylor, J., Stabge-Thomann, N., Barrett, R., Gnerre, S., Kamal, M., Kamvysselis, M., Mauceli, E., Bielke, C., Rudd, S., Frishman, D., Krystofova, S., Rasmussen, C., Metzenberg, R. L., Perkins, D. D., Kroken, S., Cogoni, C., Macino, G., Catcheside, D., Li, W. X., Pratt, R. J., Osmani, S. A., DeSouza, C. P. C., Glass, L., Orbach, M. J., Berglund, J. A., Voelker, R., Yarden, O., Plamann, M., Seller, S., Dunlap, J., Radford, A., Aramayo, R., Natvig, D. O., Alex, L. A., Mannhaupt, G., Ebbole, D. J., Freitag, M., Paulsen, I., Sachs, M. S., Lander, E. S., Nusbaum, C. and Birren, B.** The genome sequence of the filamentous fungus *Neurospora crassa*. *Nature* 2003. **422**: 859-868.

[196] **Viswanathreddy, M., Pyle, J. E. and Howe, H. B.** Purification and properties of $NADP^+$-linked glycerol dehydrogenase from *Neurospora crassa*. *J. Gen. Microbiol.* 1978. **107**: 289-296.

[197] **Sheys, G. H., Arnold, W. J., Watson, J. A., Hayashi, J. A. and Doughty, C. C.** Aldose reductase from *Rhodotorula* 1. purification and properties. *J. Biol. Chem.* 1971. **246**: 3824-3827.

[198] **Kormann, A. W., Hurst, R. O. and Flynn, T. G.** Purification and properties of an $NADP^+$-dependent glycerol dehydrogenase from rabbit skeletal muscle. *Biochim. Biophys. Acta* 1972. **258**: 40-55.

[199] **Karagüler, N. G., Sessions, R. B., Binay, B., Ordu, E. B. and Clarke, A. R.** Protein engineering applications of industrially exploitable enzymes: *Geobacillus stearothermophilus* LDH and *Candida methylica* FDH. *Biochem. Soc. Trans.* 2007: 1610-1615.

[200] **Hyndman, D., Bauman, D. R., Heredia, V. V. and Penning, T. M.** The aldo-keto reductase superfamily homepage. *Chem. Biol. Interact.* 2003. **143**: 621-631.

[201] **Jez, J. M., Bennett, M. J., Schlegel, B. P., Lewis, M. and Penning, T. M.** Comparative anatomy of the aldo-keto reductase superfamily. *Biochem. J.* 1997. **326**: 625-636.

[202] **Jez, J. M. and Penning, T. M.** The aldo-keto reductase (AKR) superfamily: An update. *Chem. Biol. Interact.* 2001. **130**: 499-525.

[203] **Ehrensberger, A. H. and Wilson, D. K.** Structural and catalytic diversity in the two family 11 aldo-keto reductases. *J. Mol. Biol.* 2004. **337**: 661-673.

[204] **Bohren, K. M., Grimshaw, C. E. and Gabbay, K. H.** Catalytic effectiveness of human aldose reductase. *J. Biol. Chem.* 1992. **267**: 20965-20970.

[205] **Burk, M. J., Gross, M. F., Harper, T. G. P., Kalberg, C. S., Lee, J. R. and Martinez, J. P.** Asymmetric catalytic routes to chiral building blocks of medicinal interest. *Pure Appl. Chem.* 1996. **68**: 37-44.

[206] **Zhou, C. H. C., Beltramini, J. N., Fan, Y. X. and Lu, G. Q. M.** Chemoselective catalytic conversion of glycerol as a biorenewable source to valuable commodity chemicals. *Chem. Soc. Rev.* 2008. **37**: 527-549.

[207] **Pagliaro, M., Ciriminna, R., Kimura, H., Rossi, M. and Della Pina, C.** From glycerol to value-added products. *Angew. Chem. Int. Ed.* 2007. **46**: 4434-4440.
[208] **Toews, C. J.** Kinetics and reaction mechanism of nicotinamide-adenine dinucleotide phosphate-specific glycerol dehydrogenase of rat skeletal muscle. *Biochem. J.* 1967. **105**: 1067-1073.
[209] **Viswanath-Reddy, M., Pyle, J. E. and Howe, H. B.** Purification and properties of $NADP^+$-linked glycerol dehydrogenase from *Neurospora crassa*. *J. Gen. Microbiol.* 1978. **107**: 289-296.
[210] **Dax, C., Coincon, M., Sygusch, J. and Blonski, C.** Hydroxynaphthaldehyde phosphate derivatives as potent covalent Schiff base inhibitors of fructose-1,6-bisphosphate aldolase. *Biochemistry* 2005. **44**: 5430-5443.
[211] **Cho, S. W., Yoon, H. Y., Ahn, J. Y., Lee, E. Y. and Lee, J.** Cassette mutagenesis of lysine 130 of human glutamate dehydrogenase *Eur. J. Biochem.* 2001. **268**: 3205-3213.
[212] **Weber, H. K., Zuegg, J., Faber, K. and Pleiss, J.** Molecular reasons for lipase-sensitivity against acetaldehyde. *J. Mol. Catal. B Enzym.* 1997. **3**: 131-138.
[213] **Hilt, W., Pfleiderer, G. and Fortnagel, P.** Glucose dehydrogenase from *Bacillus subtilis* expressed in *Escherichia coli* 1: purification, characterization and comparison with glucose dehydrogenase from *Bacillus megaterium*. *Biochim. Biophys. Acta* 1991. **1076**: 298-304.
[214] **Fujita, Y., Ramaley, R. and Freese, E.** Location and properties of glucose dehydrogenase in sporulating cells and spores of *Bacillus subtilis*. *J. Bacteriol.* 1977. **132**: 282-293.
[215] **Weckbecker, A.,** Entwicklung von Ganzzellbiokatalysatoren zur Synthese von chiralen Alkoholen *Institut für Molekulare Enzymtechnologie*. Heinrich-Heine Universität Düsseldorf 2005.
[216] **Bolivar, J. M., Wilson, L., Ferrarotti, S. A., Guisan, J. M., Fernandez-Lafuente, R. and Mateo, C.** Improvement of the stability of alcohol dehydrogenase by covalent immobilization on glyoxyl-agarose. *J. Biotechnol.* 2006. **125**: 85-94.
[217] **Jeromin, G. E.** Superabsorbed alcohol dehydrogenase - A new catalyst for asymmetric reductions. *Biotechnol. Lett.* 2009. **31**: 1717-1721.
[218] **Jiang, Y., Jiang, Y. J., Mang, Y. F., Li, R., Zhang, L. and Jiang, Z. Y.** Biosilica-coated κ-carrageenan microspheres for yeast alcohol dehydrogenase encapsulation. *J. Biomater. Sci. Polymer Edn.* 2007. **18**: 1517-1526.
[219] **Hioki, H., Hashimoto, T. and Kodama, M.** Efficient kinetic resolution of (+/-)-4-methyl-Hajos-Parrish ketone by baker's yeast reduction. *Tetrahedron Asymmetry* 2000. **11**: 829-834.
[220] **Buisson, D., Baucherel, X., Levoirier, E. and Juge, S.** Baker's yeast reduction of α-alkyl-α-hydroxy-β-keto esters. *Tetrahedron Lett.* 2000. **41**: 1389-1392.
[221] **Eh, M. and Kalesse, M.** Remarkable kinetic resolution of chiral β-keto-esters by bakers-yeast reduction. *Synlett* 1995: 837-838.
[222] **Baer, E. and Fischer, H. O. L.** Studies on acetone-glyceraldehyde. VII. Preparation of L-glyceraldehyde and L(-)acetone glycerol. *J. Am. Chem. Soc.* 1939. **61**: 761-765.
[223] **Raghava, S. and Gupta, M. N.** Purification and characterization of an alcohol dehydrogenase with an unusual specificity towards glycerol from *Thermus thermophilus*. *Bioresour. Technol.* 2010. **101**: 2554-2557.
[224] **Franke, D., Machajewski, T., Hsu, C. C. and Wong, C. H.** One-pot synthesis of L-fructose using coupled multienzyme systems based on rhamnulose-1-phosphate aldolase. *J. Org. Chem.* 2003. **68**: 6828-6831.
[225] **Wong, C. H. and Matos, J. R.** Enantioselective oxidation of 1,2-diols to L-α-hydroxy acids using coimmobilized alcohol and aldehyde dehydrogenases as catalysts. *J. Org. Chem.* 1985. **50**: 1992-1994.
[226] **Garrabou, X., Castillo, J. A., Guerard-Helaine, C., Parella, T., Joglar, J., Lemaire, M. and Clapes, P.** Asymmetric self- and cross-aldol reactions of glycolaldehyde catalyzed by D-fructose-6-phosphate aldolase. *Angew. Chem. Int. Ed.* 2009. **48**: 5521-5525.

[227] **Weiß, M. and Gröger, H.** Practical, highly enantioselective chemoenzymatic one-pot synthesis of short-chain aliphatic β-amino acid esters. *Synlett* 2009: 1251-1254.
[228] **Burda, E., Hummel, W. and Gröger, H.** Modular chemoenzymatic one-pot syntheses in aqueous media: combination of a palladium-catalyzed cross-coupling with an asymmetric biotransformation. *Angew. Chem. Int. Ed. Engl.* 2008. **47**: 9551-9554.
[229] **Schmid, R. D. and Urlacher, V. B.,** *Modern biooxidation*. Wiley-VCH, Weinheim: 2007.
[230] **Ahmed, Z.** Production of natural and rare pentoses using microorganisms and their enzymes. *Electron. J. Biotechnol.* 2001. **4**: 1-9.
[231] **Angyal, S. J.** L-Ribose: An easily prepared rare sugar. *Aust. J. Chem.* 2005. **58**: 58-59.
[232] **Yun, M., Moon, H. R., Kim, H. O., Choi, W. J., Kim, Y. C., Park, C. S. and Jeong, L. S.** A highly efficient synthesis of unnatural L-sugars from D-ribose. *Tetrahedron Lett.* 2005. **46**: 5903-5905.
[233] **Ahmed, Z., Shimonishi, T., Bhuiyan, S. H., Utamura, M., Takada, G. and Izumori, K.** Biochemical preparation of L-ribose and L-arabinose from ribitol: A new approach. *J. Biosci. Bioeng.* 1999. **88**: 444-448.
[234] **Kylmä, A. K., Granstrom, T. and Leisola, M.** Growth characteristics and oxidative capacity of *Acetobacter aceti* IFO 3281: implications for L-ribulose production. *Appl. Microbiol. Biotechnol.* 2004. **63**: 584-591.
[235] **Moonmangmee, D., Adachi, O., Shinagawa, E., Toyama, H., Theeragool, G., Lotong, N. and Matsushita, K.** L-erythrulose production by oxidative fermentation is catalyzed by PQQ-containing membrane-bound dehydrogenase. *Biosci. Biotechnol. Biochem.* 2002. **66**: 307-318.
[236] **Adachi, O., Fujii, Y., Ghaly, M. F., Toyama, H., Shinagawa, E. and Matsushita, K.** Membrane-bound quinoprotein D-arabitol dehydrogenase of *Gluconobacter suboxydans* IFO 3257: A versatile enzyme for the oxidative fermentation of various ketoses. *Biosci. Biotechnol. Biochem.* 2001. **65**: 2755-2762.
[237] **Whistler, R. L. and Underkofler, L. A.** The production of L-erythrulose by the action of *Acetobacter suboxydans* upon erythritol. *J. Am. Chem. Soc.* 1938. **60**: 2507-2508.
[238] **Adachi, O., Fujii, Y., Ano, Y., Moonmangmee, D., Toyama, H., Shinagawa, E., Theeragool, G., Lotong, N. and Matsushita, K.** Membrane-bound sugar alcohol dehydrogenase in acetic acid bacteria catalyzes L-ribulose formation and NAD-dependent ribitol dehydrogenase is independent of the oxidative fermentation. *Biosci. Biotechnol. Biochem.* 2001. **65**: 115-125.
[239] **van Hellemond, E. W., Vermote, L., Koolen, W., Sonke, T., Zandvoort, E., Heuts, D., Janssen, D. B. and Fraaije, M. W.** Exploring the biocatalytic scope of alditol oxidase from *Streptomyces coelicolor*. *Adv. Synth. Catal.* 2009. **351**: 1523-1530.
[240] **Heuts, D., van Hellemond, E. W., Janssen, D. B. and Fraaije, M. W.** Discovery, characterization, and kinetic analysis of an alditol oxidase from streptomyces coelicolor. *J. Biolo. Chem.* 2007. **282**: 20283-20291.
[241] **Wong, C.-H. and Whitesides, G. M.** Enzyme-catalyzed organicsynthesis: NAD(P)H cofactor regeneration using ethanol alcohol dehydrogenase/ aldehyde dehydrogenase and methanol/ alcohol dehydrogenase/ aldehyde dehydrogenase/ formate dehydrogenase. *J. Org. Chem.* 1982. **47**: 2816-2818.
[242] **Yoshida, A. and Freese, E.** Purification and chemical characterization of lactate dehydrogenase of *Bacillus subtilis*. *Biochim. Biophys. Acta* 1965. **99**: 56-65.
[243] **Yoshida, A.** Enzymic properties of lactate dehydrogenase of *Bacillus subtilis*. *Biochim. Biophys. Acta* 1965. **99**: 66-77.
[244] **Hediger, M. A., Frank, G. and Zuber, H.** Structure and function of L-lactate dehydrogenases from thermophilic and mesophilic bacteria IV. The primary structure of the mesophilic lactate dehydrogenase from *Bacillus subtilis*. *Biol.l Chem. Hoppe-Seyler* 1986. **367**: 891-903.

[245] **Wigley, D. B., Gamblin, S. J., Turkenburg, J. P., Dodson, E. J., Piontek, K., Muirhead, H. and Holbrook, J. J.** Structure of a ternary complex of an allosteric lactate dehydrogenase from *Bacillus stearothermophilus* at 2.5 A resolution. *J. Mol. Biol.* 1992. **223**: 317-335.

[246] **Kizaki, N., Yasohara, Y., Hasegawa, J., Wada, M., Kataoka, M. and Shimizu, S.** Synthesis of optically pure ethyl (*S*)-4-chloro-3-hydroxybutanoate by *Escherichia coli* transformant cells coexpressing the carbonyl reductase and glucose dehydrogenase genes. *Appl. Microbiol. Biotechnol.* 2001. **55**: 590-595.

[247] **Xu, Z. N., Liu, Y., Fang, L. M., Jiang, X. X., Jing, K. J. and Cen, P. L.** Construction of a two-strain system for asymmetric reduction of ethyl 4-chloro-3-oxobutanoate to (*S*)-4-chloro-3-hydroxybutanoate ethyl ester. *Appl. Microbiol. Biotechnol.* 2006. **70**: 40-46.

[248] **Rao, S. T. and Rossmann, M. G.** Comparison of super-secondary structures in proteins. *J. Mol. Biol.* 1973. **76**: 241-256.

[249] **Khoury, G. A., Fazelinia, H., Chin, J. W., Pantazes, R. J., Cirino, P. C. and Maranas, C. D.** Computational design of *Candida boidinii* xylose reductase for altered cofactor specificity. *Protein Sci.* 2009. **18**: 2125-2138.

[250] **Fasan, R., Chen, M. M., Crook, N. C. and Arnold, F. H.** Engineered alkane-hydroxylating cytochrome $P450_{BM3}$ exhibiting nativelike catalytic properties. *Angew. Chem. Int. Ed.* 2007. **46**: 8414-8418.

[251] **Bloom, J. D., Labthavikul, S. T., Otey, C. R. and Arnold, F. H.** Protein stability promotes evolvability. *Proc. Natl. Acad. Sci. U.S.A.* 2006. **103**: 5869-5874.

[252] **Bloom, J. D., Silberg, J. J., Wilke, C. O., Drummond, D. A., Adami, C. and Arnold, F. H.** Thermodynamic prediction of protein neutrality. *Proc. Natl. Acad. Sci. U.S.A.* 2005. **102**: 606-611.

[253] **Guo, H. H., Choe, J. and Loeb, L. A.** Protein tolerance to random amino acid change. *Proc. Natl. Acad. Sci. U.S.A.* 2004. **101**: 9205-9210.

[254] **Kataoka, M., Kita, K., Wada, M., Yasohara, Y., Hasegawa, J. and Shimizu, S.** Novel bioreduction system for the production of chiral alcohols. *Appl. Microbiol. Biotechnol.* 2003. **62**: 437-445.

[255] **Yasohara, Y., Kizaki, N., Hasegawa, J., Wada, M., Kataoka, M. and Shimizu, S.** Molecular cloning and overexpression of the gene encoding an NADPH-dependent carbonyl reductase from *Candida magnoliae*, involved in stereoselective reduction of ethyl 4-chloro-3-oxobutanoate. *Biosci. Biotechnol. Biochem.* 2000. **64**: 1430-1436.

[256] **Yamamoto, H., Mitsuhashi, K., Kimoto, N., Matsuyama, A., Esaki, N. and Kobayashi, Y.** A novel NADH-dependent carbonyl reductase from *Kluyveromyces aestuarii* and comparison of NADH-regeneration system for the synthesis of ethyl (*S*)-4-chloro-3-hydroxybutanoate. *Biosci. Biotechnol. Biochem.* 2004. **68**: 638-649.

[257] **Ye, Q., Yan, M., Xu, L., Cao, H., Li, Z., Chen, Y., Li, S. and Ying, H.** A novel carbonyl reductase from *Pichia stipitis* for the production of ethyl (*S*)-4-chloro-3-hydroxybutanoate. *Biotechnol. Lett.* 2009. **31**: 537-542.

[258] **Zhou, B. N., Gopalan, A. S., Vanmiddlesworth, F., Shieh, W. R. and Sih, C. J.** Stereochemical control of yeast reductions 1. Asymmetric-synthesis of L-carnitine. *J. Am. Chem. Soc.* 1983. **105**: 5925-5926.

[259] **Wang, G. J. and Hollingsworth, R. I.** Synthetic routes to L-carnitine and L-gamma-amino-beta-hydroxybutyric acid from (*S*)-3-hydroxybutyrolactone by functional group priority switching. *Tetrahedron Asymmetry* 1999. **10**: 1895-1901.

[260] **Santaniello, E., Casati, R. and Milani, F.** Chiral synthesis of a component of amanita-muscaria, (-)-4-hydroxypyrrolidin-2-one, and assessment of its absolute-configuration. *J. Chem. Res.* 1984: 132-133.

[261] **Karanewsky, D. S., Badia, M. C., Ciosek, C. P., Robl, J. A., Sofia, M. J., Simpkins, L. M., Delange, B., Harrity, T. W., Biller, S. A. and Gordon, E. M.** Phosphorus-containing inhibitors of Hmg-CoA reductase 1. 4-[(2-arylethyl)hydroxyphosphinyl]-3-hydroxybutanoic acids - A new class of cell-

selective inhibitors of cholesterol-biosynthesis. *J. Med. Chem.* 1990. **33**: 2952-2956.

[262] **Wada, M., Kawabata, H., Kataoka, M., Yasohara, Y., Kizaki, N., Hasegawa, J. and Shimizu, S.** Purification and characterization of an aldehyde reductase from *Candida magnoliae*. *J. Mol. Catal. B Enzym.* 1999. **6**: 333-339.

[263] **Kita, K., Matsuzaki, K., Hashimoto, T., Yanase, H., Kato, N., Chung, M. C. M., Kataoka, M. and Shimizu, S.** Cloning of the aldehyde reductase gene from a red yeast, *Sporobolomyces salmonicolor*, and characterization of the gene and its product. *Appl. Environ. Microbiol.* 1996. **62**: 2303-2310.

[264] **Yamamoto, H., Kimoto, N., Matsuyama, A. and Kobayashi, Y.** Purification and properties of a carbonyl reductase useful for production of ethyl (*S*)-4-chloro-3-hydroxybutanoate from *Kluyveromyces lactis*. *Biosci. Biotechnol. Biochem.* 2002. **66**: 1775-1778.

[265] **Ye, Q., Yan, M., Yao, Z., Xu, L., Cao, H., Li, Z. J., Chen, Y., Li, S. Y., Bai, J. X., Xiong, J., Ying, H. J. and Ouyang, P. K.** A new member of the short-chain dehydrogenases/reductases superfamily: Purification, characterization and substrate specificity of a recombinant carbonyl reductase from *Pichia stipitis*. *Bioresour. Technol.* 2009. **100**: 6022-6027.

[266] **Secundo, F. and Phillips, R. S.** Effects of pH on enantiospecificity of alcohol dehydrogenases from *Thermoanaerobacter ethanolicus* and horse liver. *Enzyme Microb. Technol.* 1996. **19**: 487-492.

[267] **Wiegers, A. and Scharf, H. D.** The influence of electronic effects and temperature on the enantioselective reductions of acetophenone derivatives with (-)-diisopinocampheylchloroborane - A dynamic model of enantioselection. *Tetrahedron Asymmetry* 1996. **7**: 2303-2312.

[268] **Phillips, R. S., Zheng, C., Pham, V. T., Andrade, F. A. C. and Andrade, M. A. C.** Effects of temperature on stereochemistry of enzymatic-reactions. *Biocatalysis* 1994. **10**: 77-86.

[269] **Phillips, R. S.** Temperature modulation of the stereochemistry of enzymatic catalysis: Prospects for exploitation. *Trends Biotechnol.* 1996. **14**: 13-16.

[270] **Buschmann, H., Scharf, H. D., Hoffmann, N. and Esser, P.** The isoinversion principle - A general-model of chemical selectivity. *Angew. Chem. Int. Ed. Engl* 1991. **30**: 477-515.

[271] **Pham, V. T. and Phillips, R. S.** Effects of substrate structure and temperature on the stereospecificity of secondary alcohol-dehydrogenase from *Thermoanaerobacter ethanolicus*. *J. Am. Chem. Soc.* 1990. **112**: 3629-3632.

[272] **Burdette, D. S., Secundo, F., Phillips, R. S., Dong, J., Scott, R. A. and Zeikus, J. G.** Biophysical and mutagenic analysis of *Thermoanaerobacter ethanolicus* secondary alcohol dehydrogenase activity and specificity. *Biochem. J.* 1997. **326**: 717-724.

[273] **Keinan, E., Hafeli, E. K., Seth, K. K. and Lamed, R.** Thermostable enzymes in organic-synthesis 2. asymmetric reduction of ketones with alcohol-dehydrogenase from *Thermoanaerobium brockii*. *J. Am. Chem. Soc.* 1986. **108**: 162-169.

[274] **Lam, L. K. P., Hui, R. and Jones, J. B.** Enzymes in organic-synthesis 35. stereoselective pig-liver esterase catalyzed hydrolyzes of 3-substituted glutarate diesters - optimization of enantiomeric excess *via* reaction conditions control. *J. Org. Chem.* 1986. **51**: 2047-2050.

[275] **Kataoka, M., Hoshino-Hasegawa, A., Thiwthong, R., Higuchi, N., Ishige, T. and Shimizu, S.** Gene cloning of an NADPH-dependent menadione reductase from *Candida macedoniensis*, and its application to chiral alcohol production. *Enzyme Microb. Technol.* 2006. **38**: 944-951.

[276] **Yanto, Y., Hall, M. and Bommarius, A. S.** Nitroreductase from *Salmonella typhimurium*: Characterization and catalytic activity. *Org. Biomol. Chem.* 2010. **8**: 1826-1832.

[277] **Strassner, J., Furholz, A., Macheroux, P., Amrhein, N. and Schaller, A.** A homolog of old yellow enzyme in tomato - Spectral properties and substrate specificity of the recombinant protein. *J. Biol. Chem.* 1999. **274**: 35067-35073.

[278] **Rohdich, F., Wiese, A., Feicht, R., Simon, H. and Bacher, A.** Enoate reductases of *Clostridia J. Biol. Chem.* 2001. **276**: 5779-5787.

[279] **Miranda, M., Ramirez, J., Guevara, S., Ongaylarios, L., Pena, A. and Coria, R.** Nucleotide sequence and chromosomal localization of the gene encoding the old yellow enzyme from *Kluyveromyces lactis*. *Yeast* 1995. **11**: 459-465.

[280] **Kitzing, K., Fitzpatrick, T. B., Wilken, C., Sawa, J., Bourenkov, G. P., Macheroux, P. and Clausen, T.** The 1.3 A crystal structure of the flavoprotein YqjM reveals a novel class of old yellow enzymes. *J. Biol. Chem.* 2005. **280**: 27904-27913.

[281] **Hirata, T., Matsushima, A., Sato, Y., Iwasaki, T., Nomura, H., Watanabe, T., Toyoda, S. and Izumi, S.** Stereospecific hydrogenation of the C=C double bond of enones by *Escherichia coli* overexpressing an enone reductase of *Nicotiana tabacum*. *J. Mol. Catal. B Enzym.* 2009. **59**: 158-162.

[282] **Hall, M., Stueckler, C., Hauer, B., Stuermer, R., Friedrich, T., Breuer, M., Kroutil, W. and Faber, K.** Asymmetric bioreduction of activated C=C bonds using *Zymomonas mobilis* NCR enoate reductase and old yellow enzymes OYE 1-3 from yeasts. *Eur. J. Org. Chem.* 2008: 1511-1516.

[283] **Burda, E., Kraußer, M., Fischer, G., Hummel, W., Müller-Uri, F., Kreis, W. and Gröger, H.** Recombinant $\Delta^{4,5}$-steroid 5 β-reductases as biocatalysts for the reduction of activated C=C-double bonds in monocyclic and acyclic molecules. *Adv. Synth. Catal.* 2009. **351**: 2787-2790.

[284] **Adalbjörnsson, B. V., Toogood, H. S., Fryszkowska, A., Pudney, C. R., Jowitt, T. A., Leys, D. and Scrutton, N. S.** Biocatalysis with thermostable enzymes: Structure and properties of a thermophilic 'ene'-reductase related to old yellow enzyme. *Chembiochem* 2010. **11**: 197-207.

[285] **Scott, D. C., Sanker, L. A. and Goulbourne, E. A.,** Blend of essential oil components useful in personal care products e.g. skin lotion, and in oral care compositions e.g. chewable tablet for treating caries, comprises acyclic components e.g. citral, and cyclic components e.g. eugenol. Scott D C; Sanker L a; Goulbourne E a; Procter & Gamble Co 2008.

[286] **Shinagawa, E., Ano, Y., Adachi, O. and Matsushita, K.** The occurrence of a novel NADH dehydrogenase, distinct from the old yellow enzyme, in *Gluconobacter* strains. *Biosci. Biotechnol. Biochem.* 2008. **72**: 260-264.

[287] **Schweiger, P., Gross, H., Wesener, S. and Deppenmeier, U.** Vinyl ketone reduction by three distinct *Gluconobacter oxydans* 621H enzymes. *Appl. Microbiol. Biotechnol.* 2008. **80**: 995-1006.

[288] **Adachi, O., Matsushita, K., Shinagawa, E. and Ameyama, M.** Occurrence of old yellow enzyme in *Gluconobacter suboxydans*, and the cyclic regeneration of NADP. *J. Biochem.* 1979. **86**: 699-709.

[289] **Wolken, W. A. M., ten Have, R. and van der Werf, M. J.** Amino acid-catalyzed conversion of citral: Cis-trans isomerization and its conversion into 6-methyl-5-hepten-2-one and acetaldehyde. *J. Agric. Food Chem.* 2000. **48**: 5401-5405.

[290] **Kenig, M., Peternel, S., Gaberc-Porekar, V. and Menart, V.** Influence of the protein oligomericity on final yield after affinity tag removal in purification of recombinant proteins. *J. Chromatogr. A* 2006. **1101**: 293-306.

[291] **Rumlova, M., Benedikova, J., Cubinkova, R., Pichova, I. and Ruml, T.** Comparison of classical and affinity purification techniques of mason-pfizer monkey virus capsid protein: The alteration of the product by an affinity tag. *Protein Expr. Purif.* 2001. **23**: 75-83.

[292] **Pietzsch, M., Wiese, A., Ragnitz, K., Wilms, B., Altenbuchner, J., Mattes, R. and Syldatk, C.** Purification of recombinant hydantoinase and L-N-carbamoylase from *Arthrobacter aurescens* expressed in *Escherichia coli*: Comparison of wild-type and genetically modified proteins. *J. Chromatogr. B* 2000. **737**: 179-186.

[293] **Ohta, T., Miyake, T., Seido, N., Kumobayashi, H. and Takaya, H.** Asymmetric hydrogenation of olefins with aprotic oxygen functionalities catalyzed by BINAP-Ru(II) complexes. *J. Org. Chem.* 1995. **60**: 357-363.

[294] **Dobbs, D. A., Vanhessche, K. P. M., Brazi, E., Rautenstrauch, V., Lenoir, J. Y., Genet, J. P., Wiles, J. and Bergens, S. H.** Industrial synthesis of (+)-*cis*-

methyl dihydrojasmonate by enantioselective catalytic hydrogenation; Identification of the precatalyst [Ru((-)-Me-DuPHOS)(H)-(η^6-1,3,5-cyclooctatriene)] (BF_4). *Angew. Chem. Int. Ed.* 2000. **39**: 1992-1995.

[295] **Lipshutz, B. H. and Servesko, J. M.** CuH-catalyzed asymmetric conjugate reductions of acyclic enones. *Angew. Chem. Int. Ed.* 2003. **42**: 4789-4792.

[296] **Lipshutz, B. H., Servesko, J. M., Petersen, T. B., Papa, P. P. and Lover, A. A.** Asymmetric 1,4-reductions of hindered β-substituted cycloalkenones using catalytic SEGPHOS-ligated CuH. *Org. Lett.* 2004. **6**: 1273-1275.

[297] **Yamazaki, Y., Hayashi, Y., Hori, N. and Mikami, Y.** Microbial conversion of 4-oxoisophorone by *Aspergillus niger*. *Agric. Biol. Chem.* 1988. **52**: 2919-2920.

[298] **Hall, M., Stueckler, C., Ehammer, H., Pointner, E., Oberdorfer, G., Gruber, K., Hauer, B., Stuermer, R., Kroutil, W., Macheroux, P. and Faber, K.** Asymmetric bioreduction of C=C bonds using enoate reductases OPR1, OPR3 and YqjM: Enzyme-based stereocontrol. *Adv. Synth. Catal.* 2008. **350**: 411-418.

[299] **Shimoda, K., Ito, D. I., Izumi, S. and Hirata, T.** Novel reductase participation in the *syn*-addition of hydrogen to the C=C bond of enones in the cultured cells of *Nicotiana tabacum*. *J. Chem. Soc. Perkin Trans. I* 1996: 355-358.

[300] **Müller, A., Hauer, B. and Rosche, B.** Enzymatic reduction of the α,β-unsaturated carbon bond in citral. *J. Mol. Catal. B Enzym.* 2006. **38**: 126-130.

[301] **Müller, A., Sturmer, R., Hauer, B. and Rosche, B.** Stereospecific alkyne reduction: Novel activity of old yellow enzymes. *Angew. Chem. Int. Ed.* 2007. **46**: 3316-3318.

[302] **Stuermer, R., Hauer, B., Hall, M. and Faber, K.** Asymmetric bioreduction of activated C=C bonds using enoate reductases from the old yellow enzyme family. *Curr. Opin. Chem. Biol.* 2007. **11**: 203-213.

[303] **Servi, S.** Baker yeast as a reagent in organic synthesis. *Synthesis* 1990: 1-25.

ACKNOWLEDGEMENTS

I deeply thank my supervisor Prof. Dr. Werner Hummel for his great support and guidance throughout my doctoral thesis and for the interesting subject that I enjoyed working on.

Furthermore, I would like to thank Prof. Dr. Karl-Erich Jaeger for the opportunity to perform my doctoral thesis at his institute. Many thanks also to Prof. Dr. Vlada Urlacher for her kind acceptance of the co-referee.

I would also like to thank the Deutsche Bundesstiftung Umwelt (DBU) and evocatal GmbH for financial support of my work and Dr. Thorsten Eggert for many helpful discussions

Moreover, I would like to thank all my partners and collaborators for their continuous dedication. Among these, I would like to thank Prof. Dr. Andreas Liese, Institute of Technical Biocatalysis, Hamburg University of Technology, for the fruitful collaboration and the possibility carry out experiments in his institute. In this context I would especially like to thank Dr. Markus Neumann and Dr. Ruslan Yuryev for introducing me to the methods of process engineering.

Furthermore, many thanks to Dr. Roland Wohlgemuth (Sigma Aldrich GmbH) for very helpful discussions and his critical review of our mutual manuscripts.

Many thanks also to PD Dr. Karsten Niefind from the Institute of Biochemistry, University of Cologne and his diploma student Klaus Breicha for the very successful cooperation, and for giving me the opportunity to get an insight into the field of crystallography.

I would like to thank Prof. Dr. Harald Gröger, Department Chemie und Pharmazie, Friedrich-Alexander-Universität Erlangen-Nürnberg, for helpful discussions and the successful cooperation.

Further thanks I would like to give as well to Prof. Dr. Lothar Elling, Department of Biotechnology and Helmholz-Institute for Biomedical Engineering, RWTH Aachen, for fruitful discussions and insights into sugar chemistry.

I would like to extend thanks to my colleagues at evocatal GmbH, at the Institute of Bioorganic Chemistry and at the Institute of Molecular Enzyme Technology. especially Dr. Thomas Drepper for endless support and his helpful advices.
Moreover, I thank Mark Bertram, Jennifer Andexer, Stephanie Serci, Jannina Knorr, Ulrich Krauss, Achim Heck, Vera Svenson, Astrid Wirtz and all members of lab 411. In particular, I would like to thank Anke Zienert for spending her diploma thesis with me.
Special thanks to Beatrix Paschold for her great technical support and her commitment.
Furthermore, I like to thank Andrea Weckbecker and Michael Puls for their help and support, as well as all other colleagues at evocatal GmbH.
Very special thanks also to Prof. Dr. Martina Pohl and Dr. Dörte Gocke for helpful advices and always keeping their door open.

Very special thanks go to Robert Simon for his ongoing support with respect to all chemical issues, and so much more…

Last but not least, I would like to express deep thanks to my friends for supporting me throughout this thesis, especially during the last rough weeks. Very special thanks to my family for giving me the strength and support to accomplish this work [<(")].

Die hier vorgelegte Dissertation habe ich eigenständig und ohne unerlaubte Hilfe angefertigt. Die Dissertation wurde in der vorgelegten oder in ähnlicher Form noch bei keiner anderen Institution eingereicht. Ich habe bisher keine erfolglosen Promotionsversuche unternommen

Jülich, den 17.05.2010